UNIVERSITA' DEGLI STUDI DI PADOVA

SEDE AMMINISTRATIVA: UNIVERSITÀ DEGLI STUDI DI PADOVA

DIPARTIMENTO DI SCIENZE FARMACEUTICHE

SCUOLA DI DOTTORATO DI RICERCA IN SCIENZE MOLECOLARI

INDIRIZZO SCIENZE FARMACEUTICHE

XXII CICLO

Synthesis and characterization of natural compounds derivatives for biological systems analysis: Topoisomerase I-DNA-camptothecin and protein kinase A-cyclic AMP complexes as case studies

Direttore della Scuola: Ch.mo Prof. Maurizio Casarin

Supervisore: Ch.mo Prof. Giuseppe Zagotto

Dottorando: Ricci Antonio

01 Febbraio 2010

1.1 Abstract vii
1.1a Riassunto xv
1.2 Abbreviation xxxixv

A. TOPO I-DNA-CPT COMPLEX

2. Introduction .....

2.1 DNA and Topoisomerase enzymes 1
2.2 Topoisomerase inhibitor 11
2.3 Camptothecin and its analogues 13

3. Aim of the work 22

4. Experimental part 27

4.1 Materials and instrumentation 29

5. Discussion of the results 63

B. PKA-cAMP COMPLEX

2'. Introduction 123

2'.1 Cyclic Adenine 3',5'-monophosphate (cAMP) cascade 125
2'.2 Protein Kinase A (PKA) 130

3'. Aim of the work 135

4'. Experimental part 139

5'. Discussion of the results 155

1.1 Abstract

TopoisomeraseI-DNA-CPT complex

Topoisomerase I (Topo I) is one of the enzyme involved into the control of the replication of the cell through the management of the topology of DNA, in particular the DNA supercoiling. Top1 relax supercoiled DNA operating a break in only one strand of the DNA duplex; the mechanism of action doesn't require energy (ATP) and is catalyzed by the phenolic group of the tyrosine (Tyr723) which attack a DNA phophodiester bond situated inside the the cleavage site. The resulting DNA–3' phosphotyrosine complex (called "covalent binary complex") allows the shift of the uncutted strand through the nick prior to undergoes the attack of the 5'-hydroxyl group of the nicked DNA strand. The whole process result in the relaxation of the DNA, a fundamental step in the replicative process of the DNA.

Due to its crucial role, great efforts were made to obtain inhibitors of this enzime in order to obtain potential anticancer drug.

Camptothecin (CPT, see figure below), a natural pentacyclic alkaloid firstly exctracted from the bark of the *Camptotheca acuminata* tree, and its derivatives are one of the more representative class of inhibitors of Topo I.

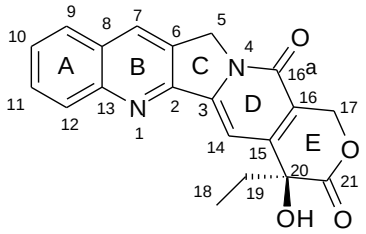

These molecules are able to intercalate inside the covalent binary complex Top1-DNA forming a reversible "ternary complex" Top1-DNA-CPT more stable respect to the previous one. This enhanced stability lead to a dimished possibility to religate the open strand and to the begin of the apoptotic

process, when the replicative fork arrives in proximity of the complex. For this indirect antiproliferative action, the camptothecin family are called Topo I poisons.

Camptothecin was early shown to be clinically problematic because, in addition to its negligible water solubility, its active "ring-closed" a-hydroxylactone form is rapidly converted under physiological conditions to the "open" carboxylate form, which is inactive and readily binds to human serum albumin, making it inaccessible for cellular uptake. To date, only two semisynthetic analogs of Camptothecin (Topotecan and Irinotecan) have been approved by FDA for the clinical treatment of the ovarian, small cell-lung and colorectal cancers.

Although all these drawbacks, camptothecin still cover a great role in the anticancer research due to its specific selectivity for the ternary complex, since it seems not interact with the Topoisomerase I alone and it doesn't intercalate into the DNA alone.

Once again, several efforts were made to better understand the mechanism of action of the camptothecin. Staker and his collaborators obtained a crystal of the ternary complex Topo I-DNA-Topotecan and, later, of Topo I-DNA-camptothecin; from the analysis of these crystals several details were elucidated around the position of the different components forming the ternary complex.

A further look inside this system could be achieved with other technique such as electron paramagnetic resonance (EPR), by which is possible to register the behaviour of a paramagnetic probe placed inside the system under investigation, in particular its different mobility.

In particular, a technique called site-directed spin labelled (SDSL) was used in this work to insert a paramagnetic probe inside the different components of the ternary complex Topo I-DNA-CPT.

First of all, several camptothecin derivatives bringing the nitroxide moiety were synthetized

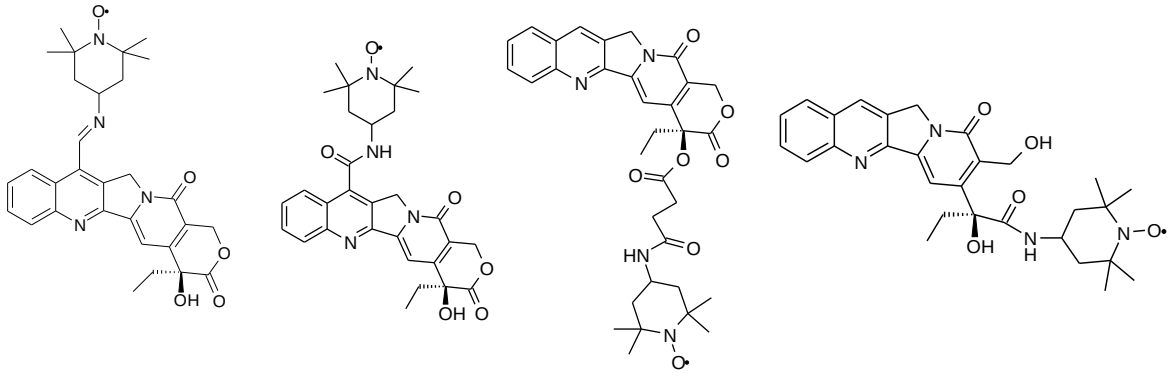

The substitutions were placed in different positions of the alkaloid in order to observe the different environments of the catalytic site. Biological tests showed good inhibitions properties for the first two derivatives, in particular for the first one which was used for the EPR experiment.

Subsequently, spin-labeled derivatives of the DNA oligonucleotides were further synthesized:

5' A A A A A A G A **X** T T G G **Y** A A A A T T T T T 3'

3' T T T T T C T G A A C C T T T T T A A A A A 5'

X	**Y**
C	**t-A**
t-C	A
t-C	**t-A**

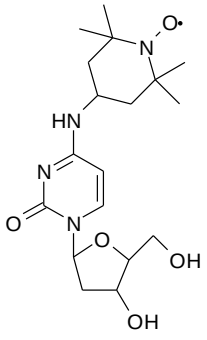

t-C

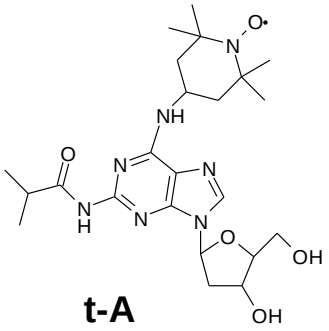

t-A

This 22-mer sequence (and its complementary one) was chosen for this experiment since it brings an high affinity cleavage site for the Topo I enzyme.

Unfortunately, biological tests demonstrated that Topo I can partially process only the TEMPOadenine derivative while it cannot process the other two oligonucleotide strands at all.

EPR first experiment was conducted to confirm the incapacity of the camptothecin to intercalate inside the DNA

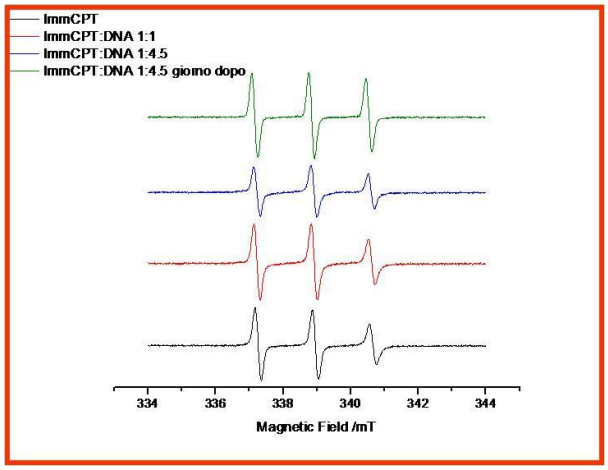

As could be appreciate from the picture showed above, no great differences could be observed between the different spectrum, indicating no intercalation of the CPT in the DNA.

A second experiment in presence of the Topo I, DNA and the most active CPT derivative (in a 1:5:1 ratio) gave the following result

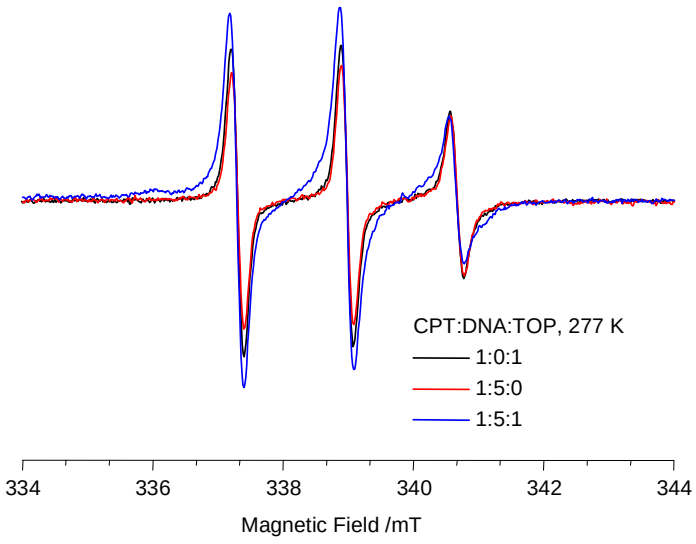

where a broadened signal and the presence of another peak was observed. Simulation of this spectrum gave the approximative value of CPT hindered in the ternary complex which was of the order of 40%.

PKA-cAMP complex

The Protein Kinase A (PKA) is a four-membered structure with two regulatory (R) and two catalytic (C) subunits which control a wide number of biological processes of the cell, such as lipid and sugar metabolism, gene expression, cell replication and apoptosis. It controls all these processes through the phosphorilation of other substrates, such as proteins, which in turn activate other substrate until the biological response is produced (such kind of domino reaction are called enzymatic "cascade"). The activity of the PKA is controlled by the cyclic adenosine monophosphate (cAMP), a second messenger produced from adenosine triphosphate (ATP) in response of the activation of the Adenylate Cyclase enzyme (AC) by another great class of membrane protein: the G-proteins (Gs)

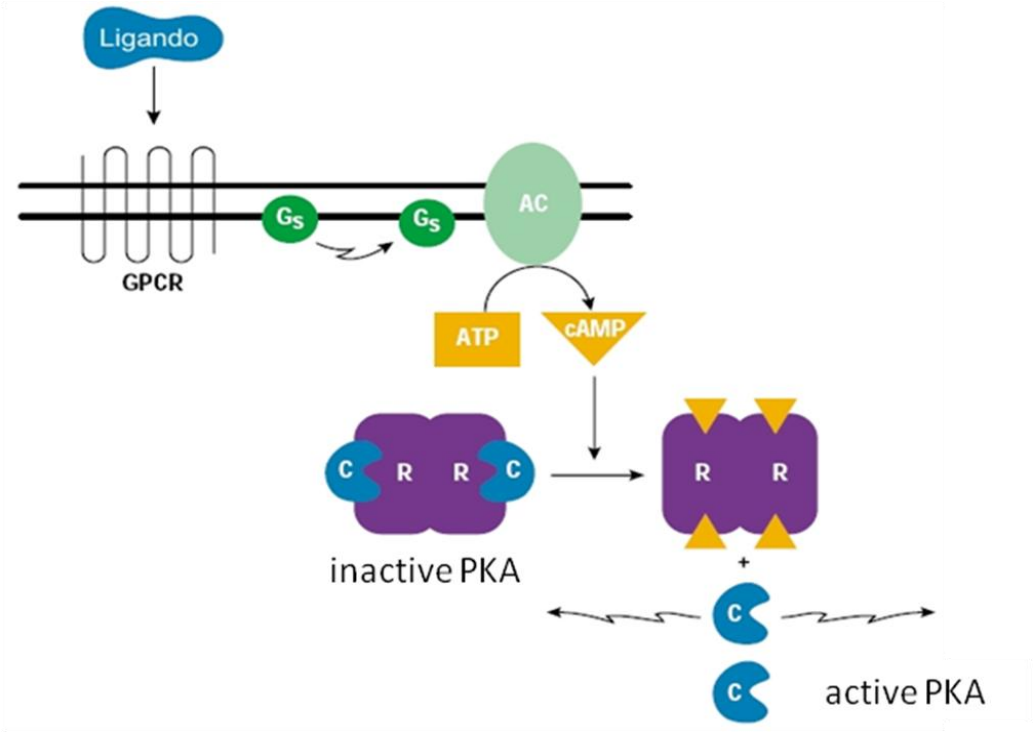

To regulate the PKA, two molecules of cAMP link each regulatory subunit of the enzyme as to release the two catalytic subunits which are active as single monomers.

Failure to keep PKA under control can have disastrous consequences, including diseases such as cancer; in fact, an abnormal distribution of one of the regulatory subunit was found in cells affected with glioma, a devastant cancer that hits the glia cells. Thus, to rapidly recognize the over expression of this protein inside the cells, a fluorescent-labeled marker was realized starting from cAMP

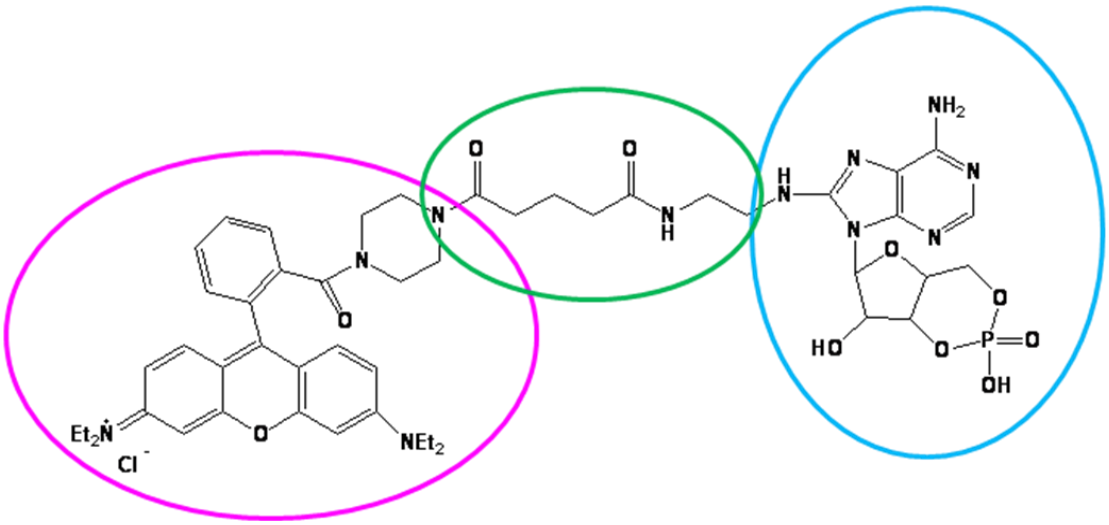

It was realized through a convergent synthesis of two synthons, one bearing the fluorescent moiety, the other bearing the cAMP function.

Firstly biological tests

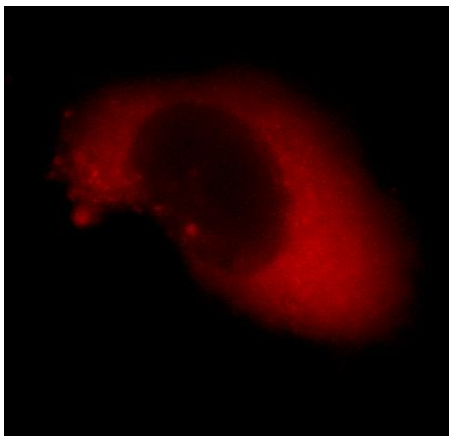

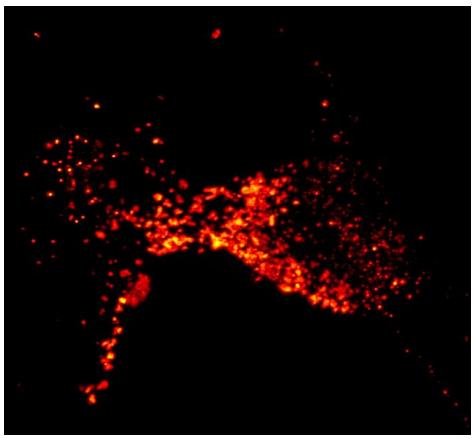

Showed how the marker (figure on the right) is able to penetrate inside the cells and to distribute in particular site of the cytoplasm (compared to the rhodamine alone, figure on the left), which could be associated with PKA concentrated spots. Immunohystochemical tests are under development to validate this hypothesis.

1.1a Riassunto

Complesso TOPO I-DNA-CPT

Le topoisomerasi sono un gruppo di enzimi deputati al controllo del superavvolgimento del DNA durante la fase di replicazione cellulare.
La topoisomerasi I (sottoclasse B) espressa nell'uomo e' in grado di rilassare il DNA attraverso il taglio di un singolo filamento ed il successivo scorrimento del filamento intatto senza consumo di ATP.

Il meccanismo di rilassamento può essere diviso in quattro fasi alle quali corrispondono due diverse conformazioni dell'enzima: una prima fase dove l'enzima, nella sua conformazione aperta, interagisce con il DNA grazie ad interazioni specifiche tra diversi aminoacidi e le basi azotate del DNA. A questa prima fase succede la seconda dove l'enzima interconverte nella conformazione chiusa ed opera il taglio del filamento di DNA (attraverso la formazione di un legame fosfodiestereo tra il DNA e la tirosina 723, vedi *fig.1b*) producendo cosi' il *complesso binario Topoisomerasi1-DNA (TOP1cc)*.

Dopo la rottura del filamento si ha la reazione di "topoisomerizzazione" attraverso un meccanismo di "rotazione controllata" in cui la porzione di doppia elica non legata covalentemente all'enzima ruota attorno al legame fosfodiestereo. Lo stadio finale consiste nella saldatura del filamento e nel rilascio del DNA con il numero di legame più basso di una unità (*fig. 1a*).

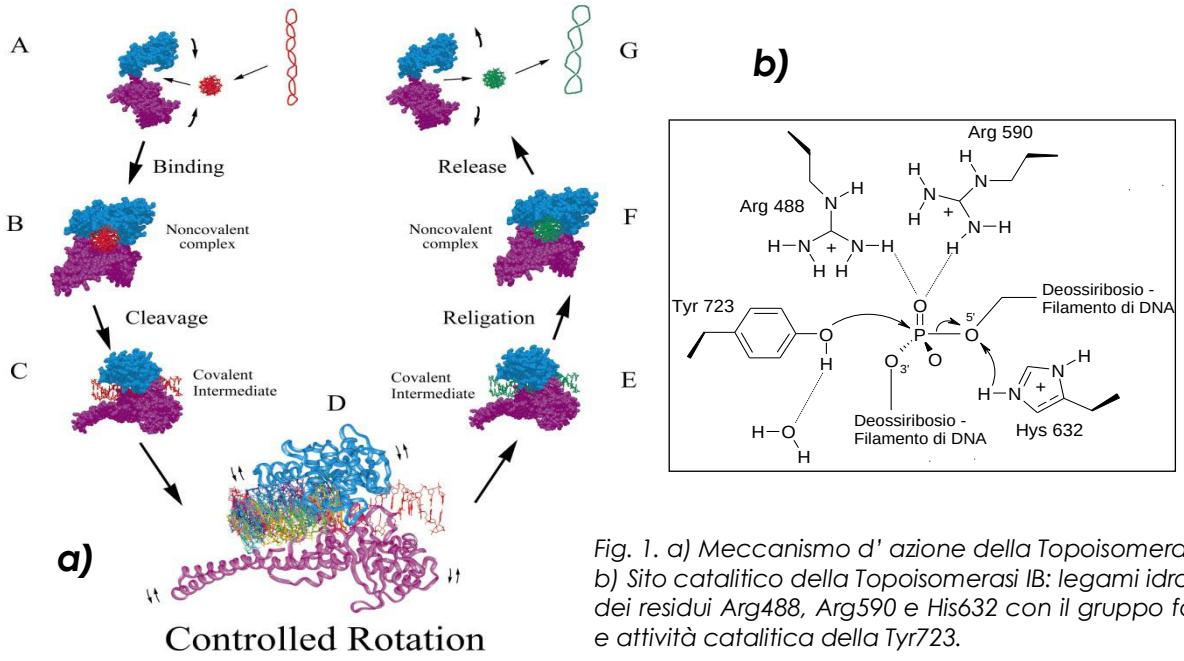

Fig. 1. a) Meccanismo d' azione della Topoisomerasi I b) Sito catalitico della Topoisomerasi IB: legami idrogeno dei residui Arg488, Arg590 e His632 con il gruppo fosfato e attività catalitica della Tyr723.

Per il suo ruolo chiave nel controllo della replicazione cellulare la topoisomerasi e' stata presa in considerazione come possibile bersaglio per la cura di patologie implicanti una rapida (ed incontrollata) replicazione, quali le neoplasie.

Tra le varie strategie sviluppate in questi anni merita attenzione l'utilizzo di molecole naturali interagenti con il meccanismo di azione dell'enzima, in particolare la camptotecina (*fig. 2*), alcaloide naturale estratto dalla *Camptotheca acuminata*.

Questa molecola, che presenta un centro chirale sul carbonio 20 (orientato nella configurazione assoluta *S*), svolge la propria azione stabilizzando il complesso binario DNA-enzima attrraverso la formazione di un *complesso ternario DNA-enzima-camptotecina*. Il danno subentra quando avviene la collisione tra la forcella replicativa e il complesso ternario: il mancato riconoscimento tra i due sistemi sfocia nella successiva attivazione del

programma di apoptosi. Per questo meccanismo d'azione questa molecola rientra nella classe di molecole chiamata veleni delle topoisomerasi.

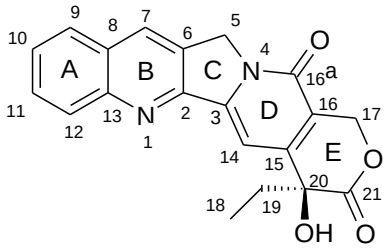

Fig. 2: Struttura chimica della camptotecina

Il grande vantaggio della camptotecina risiede nella sua selettività verso il complesso binario: essa, infatti, non è in grado di intercalare nel DNA da solo e non interagisce con la Topoisomerasi I da sola.

Uno studio interessante può essere effettuato sul meccanismo di azione del complesso ternario, in maniera tale da raccogliere nuove informazioni potenzialmente utili per la progettazione di nuovi inibitori.

Per questo studio è necessario disporre di una tecnica analitica che sia in grado di "registrare" l'attivita' della camptoecina in presenza del complesso binario e la sua capacità di convertire quest'ultimo nel complesso ternario.
La tecnica utilizzata per questo progetto è stata la spettroscopia di risonanza di spin elettronico (ESR od EPR), dove viene eccitato e successivamente registrato lo spin dell'elettrone.
Utlizzando la tecnica del "site directed spin labeling" (SDSL), dove viene inserita una sonda paramagnetica (probe) in una precisa posizione del sistema da analizzare, si è cercato di realizzare un complesso ternario opportunamente marcato in grado di rispondere al nostro scopo.
La metodica di marcatura dei derivati ha innanzitutto richiesto la realizzazione di un probe che rispondesse alle richieste di stabilita' e di

reattivita' chimica. La scelta e' caduta sul 4-aminotetrametilpiperidin-1-oxile (TEMPOamina, *Fig. 3*):

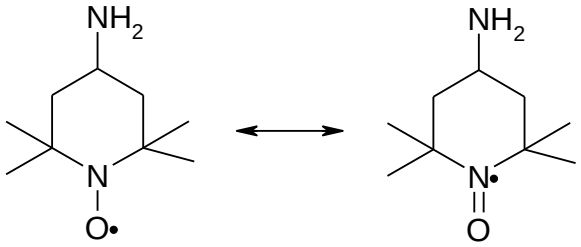

Fig. 3: Formule di risonanza della TEMPOamina

La sua sintesi e' partita dalla triacetoneamina, reagente commercialmente disponibile e molto economico, che e' stata convertita nella TEMPOamina in 5 steps:

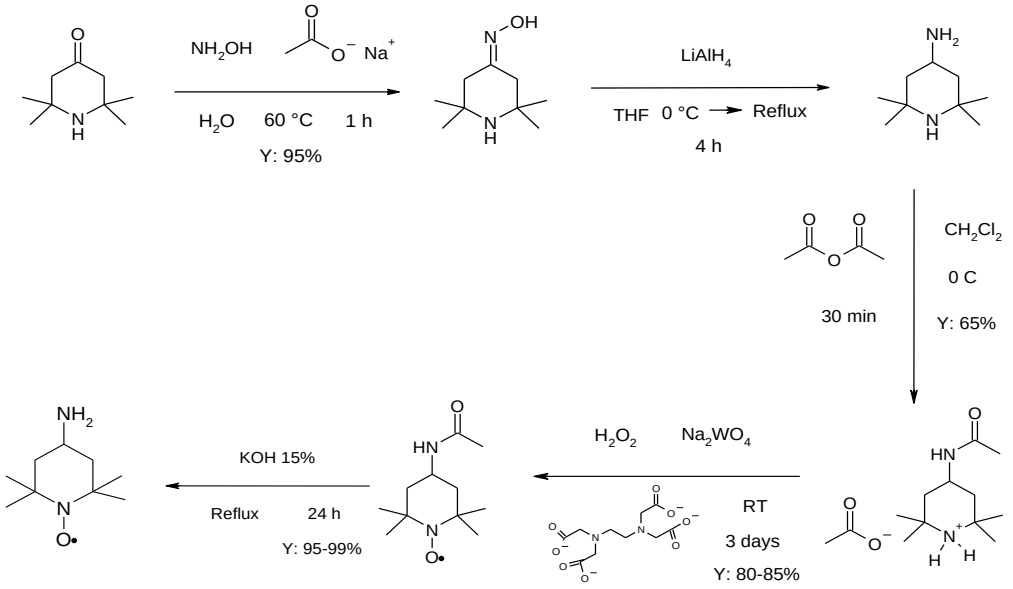

A questo punto la TEMPOamina e' stata utilizzata per la sintesi di diversi derivati marcati. Innanzitutto sono stati realizzati derivati della camptotecina recanti la funzione nitrossido in diverse posizioni (*Fig. 4*), in maniera tale da poter osservare diversi comportamenti nel complesso ternario. In particolare il derivato 7-TEMPOimminoCPT e' stato realizzato sulla base di precedenti studi

condotti dal prof. Merlini sull'attivita' di diversi derivati della camptotecina sostituiti in posizione 7

.

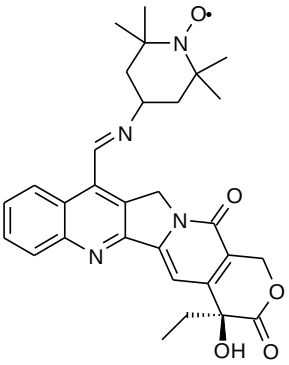

7-TEMPOimminoCPT

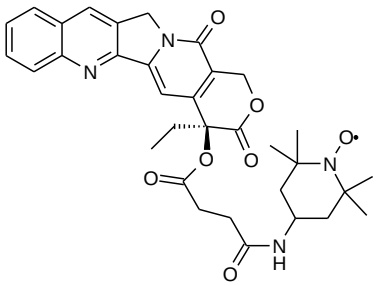

7-TEMPOsuccinimidoCPT

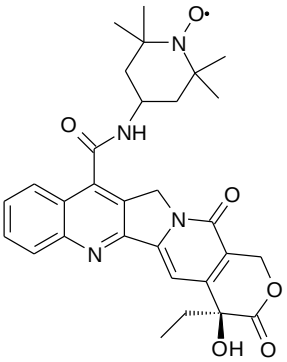

7-TEMPOammidoCPT

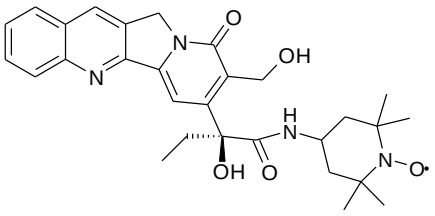

21-TEMPOammidoCPT

Fig. 4: Strutture molecolari dei derivati TEMPOmarcati della camptotecina

Tutti questi composti sono stati ottenuti per via semisintetica partendo dalla camptotecina:

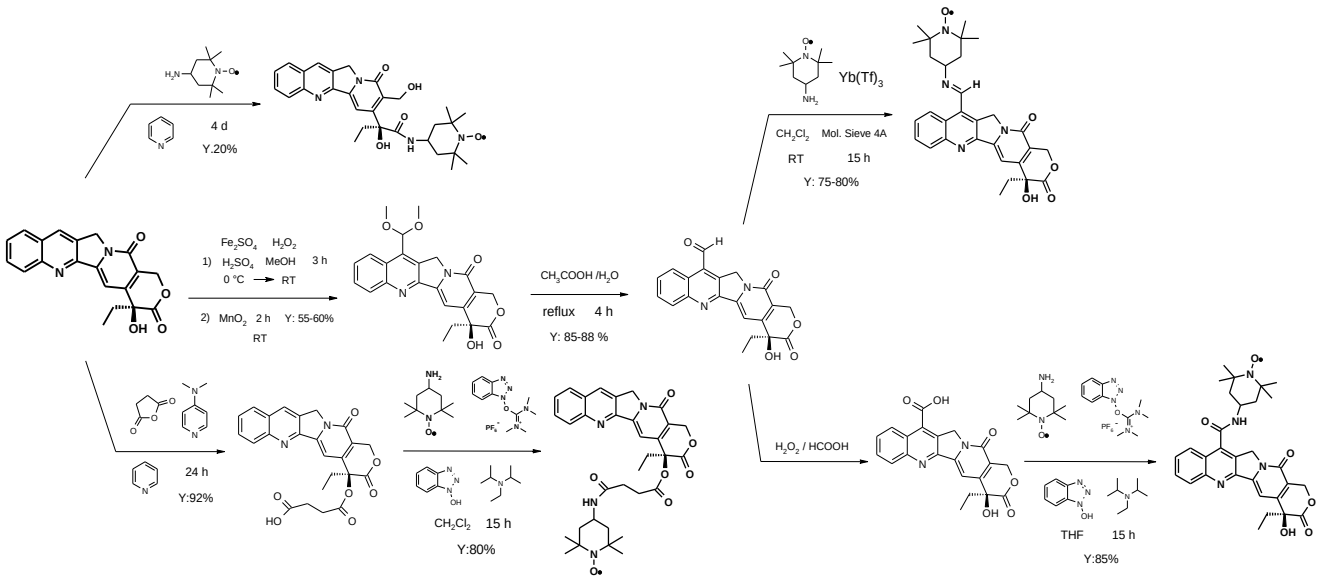

I prodotti ottenuti sono stati analizzati tramite metodica ESR per confermare l'avvenuta condensazione e per valutare la natura del suo spettro. L'analisi e' stata effettuata nell laboratorio della prof.ssa Maniero presso il Dipartimento di Chimica Fisica dell'Universita' di Padova. Come aspettato, il segnale di ogni esperimento consta di tre linee strette tipiche di un nitrossido in soluzione a temperatura ambiente (*Fig. 8*).

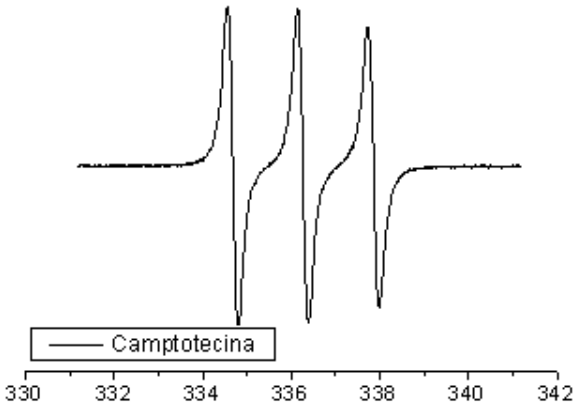

Fig. 5: Spettro ESR della 7-TEMPOiminocamptotecina.

Solvente $CHCl_3$;
Temperatura 294 K
MA: 1G
CT/TC: 10/20 ms
PW: 13mW/12dB
N_{scans}: 3

Successivamente sono stati effettuati test biologici per valutare le attivita' inibitorie dei derivati nei riguardi della rilegazione del DNA. Questi test sono stati svolti presso il laboratorio di Biologia Molecolare del Professor Capranico nell' Universita' di Bologna:

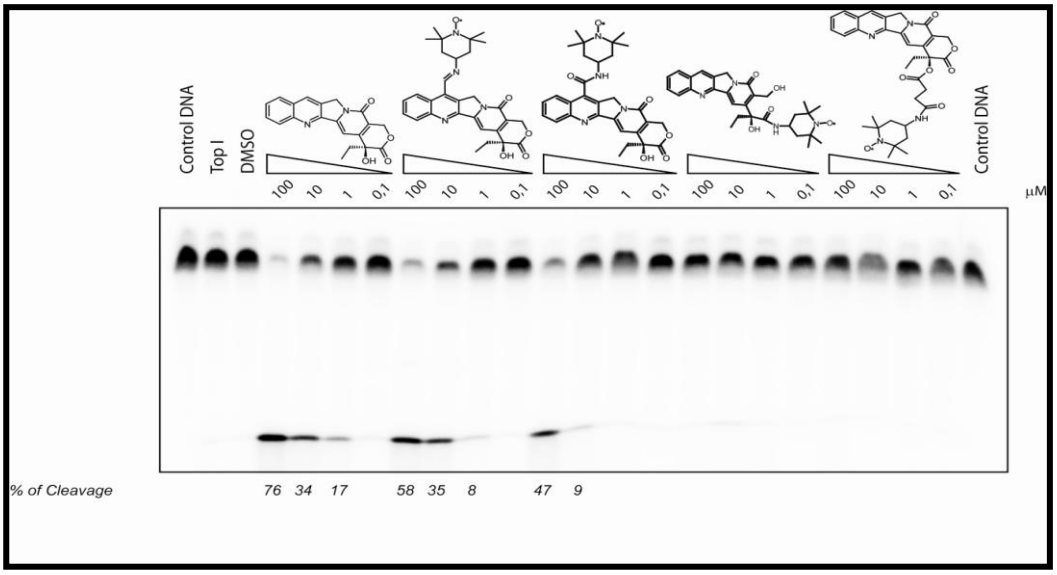

I risultati mostrano come il derivato 7-TEMPOimminoCPT ed il derivato 7-TEMPOamidoCPT abbiano un'attività rispettivamente comparabile e leggermente minore rispetto alla CPT. Si nota inoltre la completa inattività degli altri due derivati, in accordo con i dati di relazione struttura-attività (l'ossidrile in posizione 20 e l'anello lattonico sono infatti fondamentali per l'attività inibitoria).

Un dato interessante emerge da un secondo test volto a misurare la capacità di questi composti di stabilizzare il complesso ternario (il test viene chiamato "test di reversibilità"): i due derivati più attivi della serie sono inoltre in grado di stabilizzare il complesso ternario più efficacemente rispetto alla CPT:

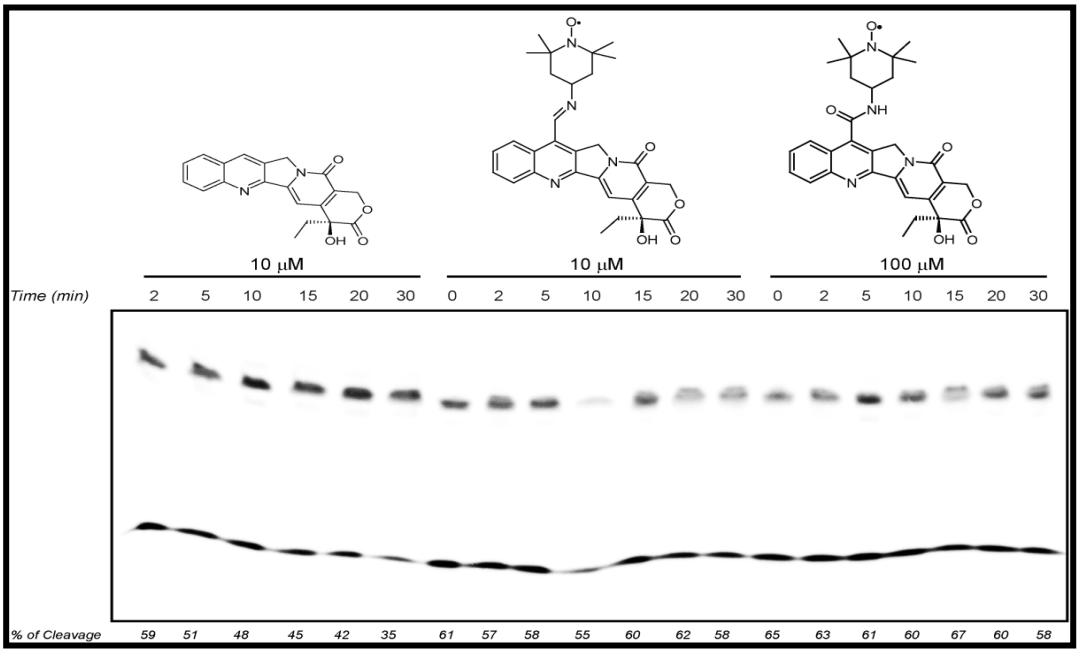

Per comprendere meglio il ruolo del radicale nella stabilizzazione del complesso ternario è stato quindi realizzato un derivato della CPT recante la catena laterale della 7-TEMPOimminoCPT (il più attivo della serie) in cui la funzione nitrossido è stata rimpiazzata con una funzione amminica:

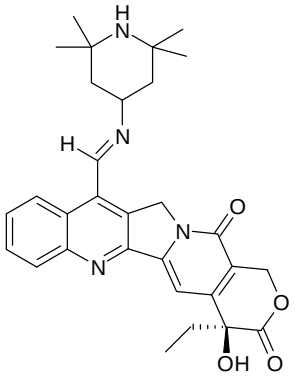

Fig. 6: Struttura del derivato 7-(4-ammino-2,2,6,6-tetrametipiperidnilimmno)camptotecina

La sintesi di questo derivato è stata effettuata in maniera analoga alla 7-TEMPOimminoCPT facendo però reagire nell'ultimo step la 7-formilCPT con il gruppo 4-amino-2,2,6,6-tetrametilpiperidinico in luogo della TEMPOamina.

Per ottenere informazioni sul complesso ternario è stato necessario inoltre cercare una sequenza oligonucleotidica che fosse riconosciuta e processata dall'enzima. Precedenti studi hanno mostrato come la sequenza:

5' A A A A A G A C T T/G G A A A A A T T T T T 3'

3' T T T T T C T G A A C C T T T T T A A A A A 5'

risulti essere altamente affine all'enzima (il taglio avviene preferenzialmente tra la timina$_{10}$ e la guanosina$_{11}$ nel filamento 5'-3').
Cercando inoltre di ampliare le possibili informazioni ricavabili dall'esperimento si è deciso di marcare tale sequenza con la sonda nitrossido. La marcatura è avvenuta nelle seguenti posizioni:

5' A A A A A G A C T T/G G A A A A A T T T T T 3'

3' T T T T T C T G A A C C T T T T T A A A A A 5'

poichè sostituzioni effettuate su nucleotidi piu' vicini al sito di taglio avrebbero potuto interferire con il meccanismo d'azione della topoisomerasi. Sono stati sintetizzati due filamenti recanti ciascuno uno dei due nucleotidi marcati ed un filamento contenente entrambi i nucleotidi.

Le strutture dei due derivati della 2'-deossicitidina e 2'-deossiadenosina recanti l'unita' TEMPOaminica sono le seguenti:

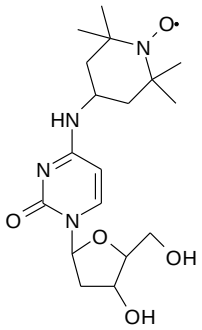

TEMPO-Citidina

Fig. 7: Strutture chimiche dei due nucleotidi marcati

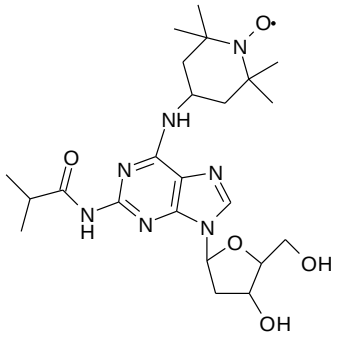

TEMPO-Adenina

Partendo dai rispettivi 2-deossinucleotidi, sono state protette le due funzioni idrossiliche in 3' e 5' attraverso la formazione di esteri isobutirrici in maniera tale da poter attivare il carbonio carbonilico (in posizione 4 e 6 rispettivamente) per l'attacco nucleofilo della TEMPOamina. I gruppi protettori sono stati successivamente rimossi ed infine l'idrossile terminale in 5' è stato protetto con il gruppo dimetossitritile (DMT) mentre l'idrossile terminale in 3' è stato attivato con il gruppo 2-cianoetil-N,N-diisopropilfosforamiditico (nello schema viene riportata la sintesi di uno solo dei due nucleotidi poichè la via di sintesi è similare):

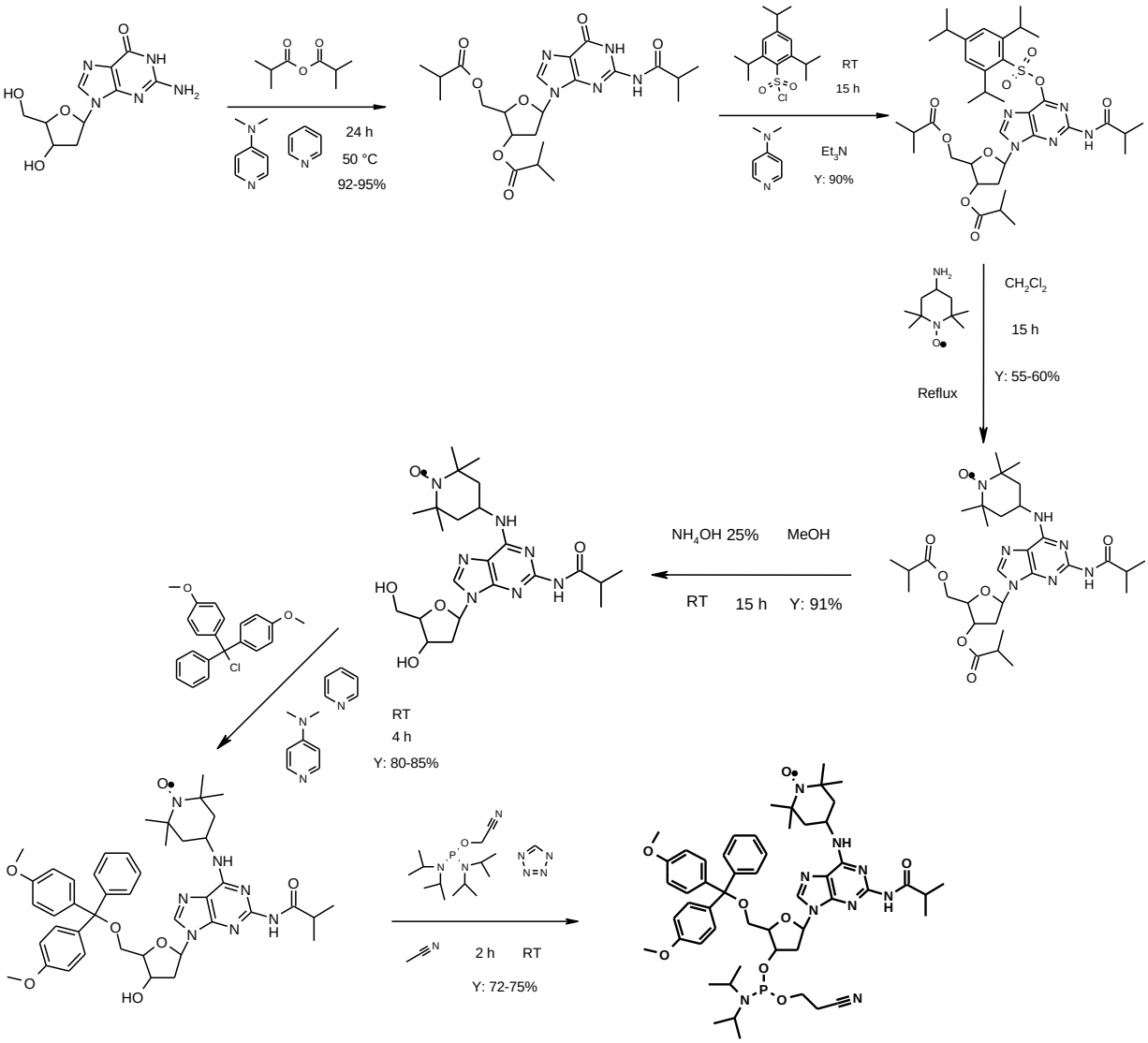

Tali derivati nucleotidici sono stati inclusi nella sequenza oligonucleotidica precedentemente descritta. La sintesi automatizzata degli oligonucleotidi può essere riassunta in tre step: una prima sostituzione della funzione diisopropilaminica (catalizzata dal tetrazolo) da parte del gruppo ossidrilico in 5' della catena oligonucleotidica (legata ad un supporto solido).

Il secondo passaggio consta di una protezione dei gruppi ossidrilici in 5' che non sono stati legati (per evitare la formazione di sequenze troncate) e dall'ossidazione della funzione fosfito a fosfato con iodio in una miscela di acqua e piridina.

L'ultimo step consta nella rimozione del gruppo protettore DMT; si libera cosi' l'ossidrile in 5' il quale potra' successivamente attaccare il fosfito di un secondo nucleotide e continuare l'elongazione della catena oligonucleotidica.

Questi passaggi sono riassunti nel seguente schema (e' riportato solo il derivato citidinico):

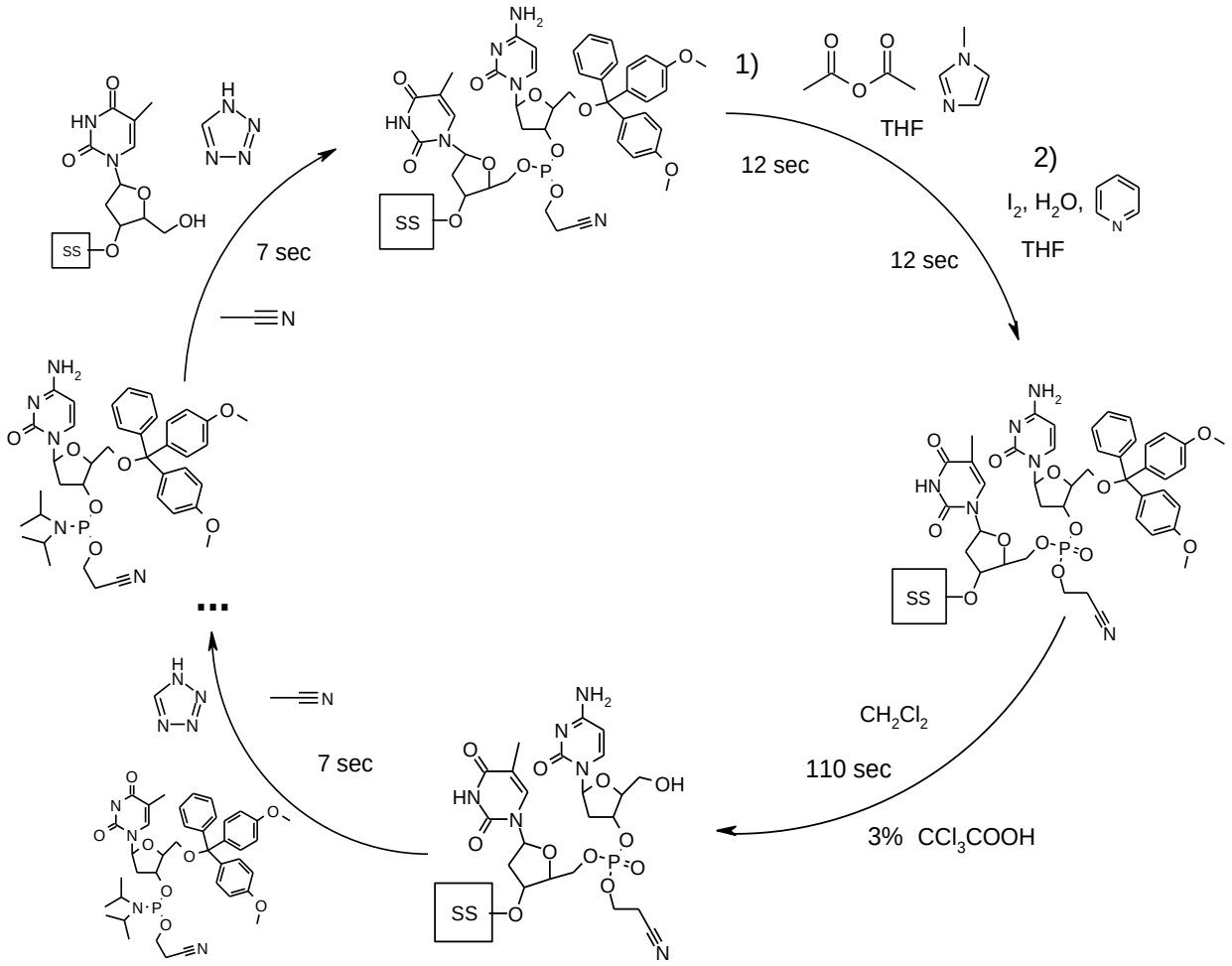

Nel caso dei nucleotidi marcati, la procedura è stata modificata in risposta alla reattività del radicale nitrossido nei confronti dell'agente ossidante (infatti

si è preferito usare ^{tert}butilidroperossido al posto dello iodio) e degli acidi (la scelta in questo caso è caduta sull'acido dicloroacetico):

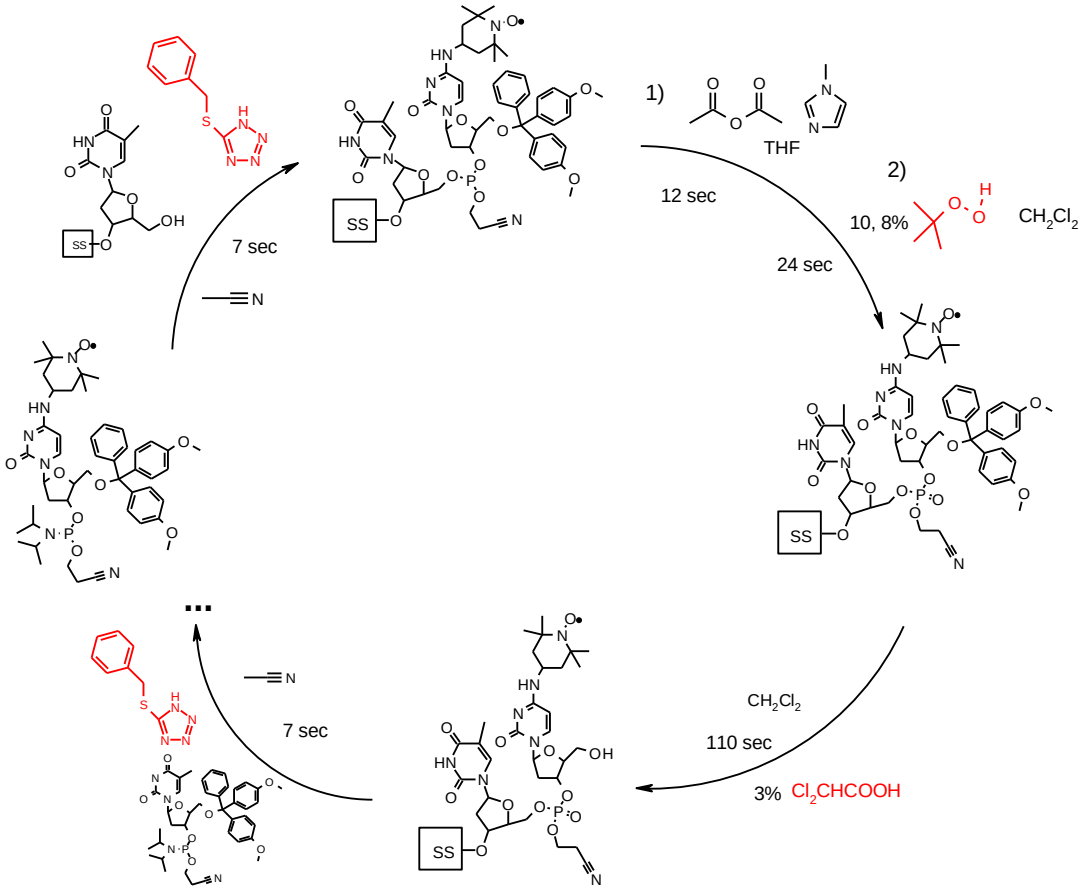

Nonostante queste modificazioni, non è stata ottenuta l'inserzione dei nucleotidi nella sequenza scelta. Per questo motivo si è infine ricorsi al coupling manuale dei suddetti nucleotidi: per monitorare l'effettiva riuscita della reazione è stata misurata l'assorbanza del gruppo tritale (liberato nello step di deprotezione dell'ossidrile in 5') a 499nm. I risultati sono stati i seguenti:

OLIGONUCLEOTIDE		Abs_{499}	mg weighted	YIELD (%)
TEMPO-Adenine Single-modification		0,4682	1,5	95,5
TEMPO-Cytidine Single-modification		0,396	1	88
TEMPO-Adenine Double-modification		0,3864	1,3	92,1
TEMPO-Cytidine double-modification		0,2546	0,9	87,7

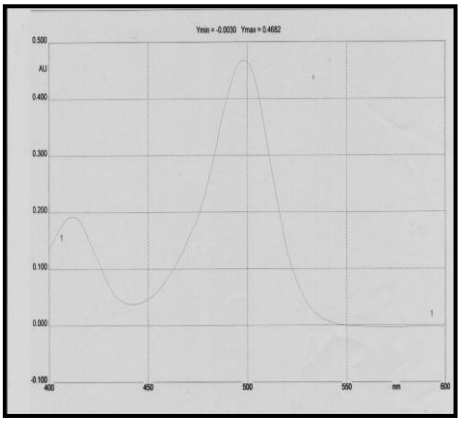

Le modificazioni effettuate per la sintesi automatica sono state comunque applicate per completare i filamenti oligonucleotidici.

L'oligonucleotide cosi' prodotto viene infine separato dal supporto polimerico (SS nello schema) in ambiente basico e purificato attraverso cromatografia liquida a media pressione (MPLC).

Sono stati effettuati test biologici per valutare se tali oligonucleotidi fossero processati dall'enzima Topoisomerasi I:

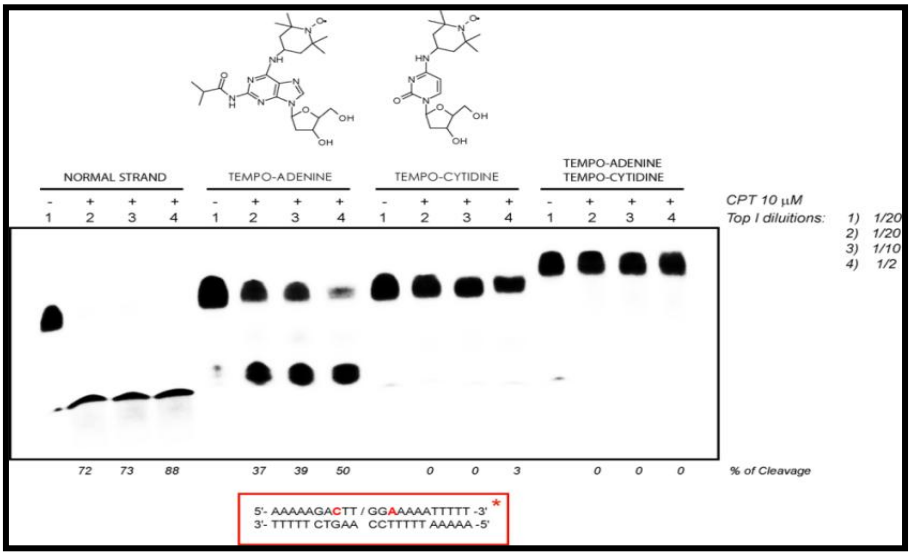

Purtroppo nessuno degli oligonucleotidi marcati viene processato in maniera comparabile rispetto allo strand non marcato.

Sono stati effettuati i primi esprimenti per valutare l'eventuale capacità della camptotecina di intercalare il DNA

Per avere un confronto positivo è stata sintetizzata una molecola a nucleo antrachinonico che fosse stata in grado di intercalare con il DNA:

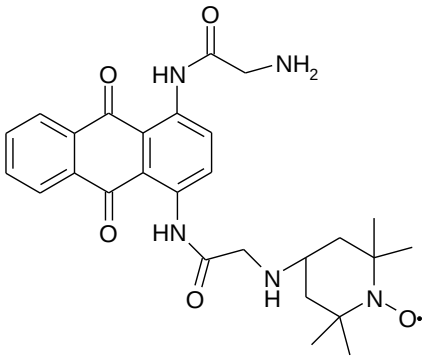

Fig 8: Struttura dell'1-glicinil 4-TEMPOammido antrachinone

Per la sintesi della molecola antrachinonica si è proceduto in questo modo:

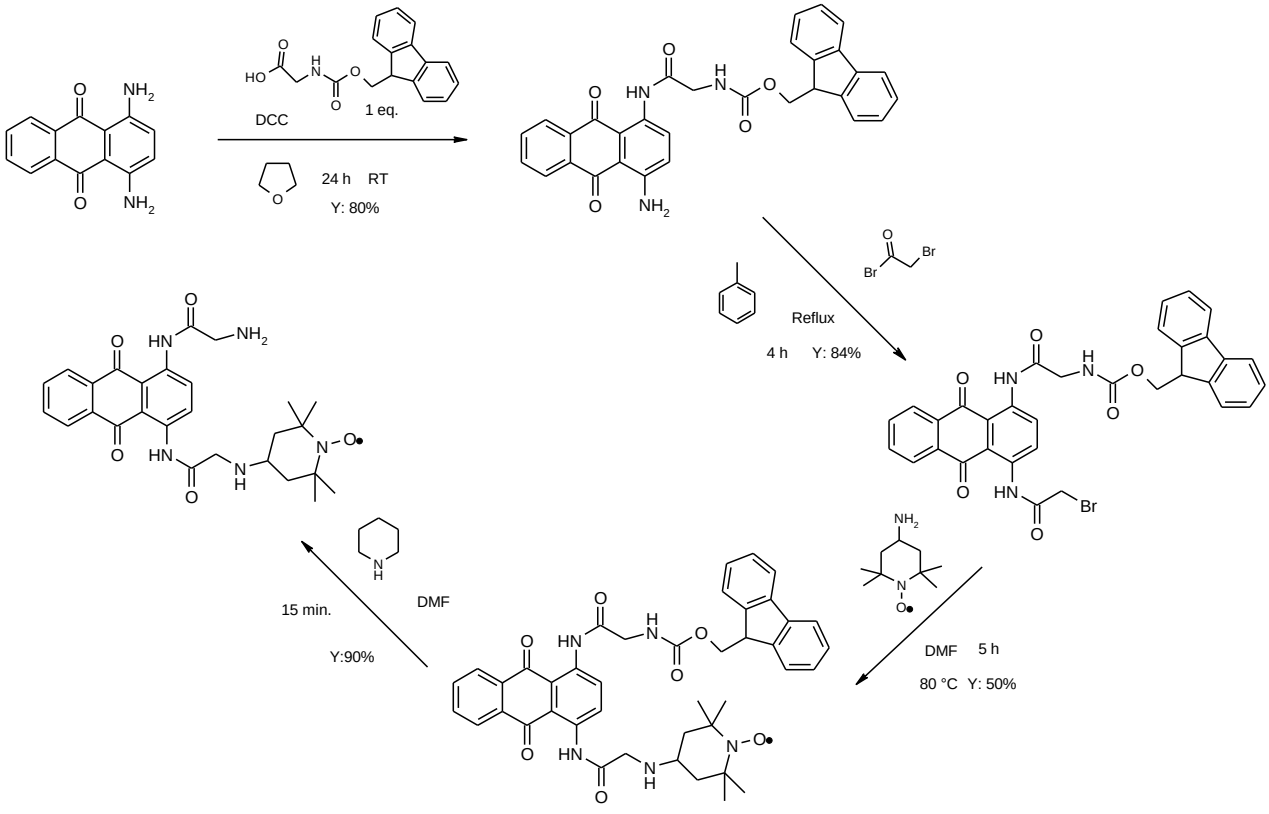

Il nucleo di partenza scelto è l'1,4-diamminoantrachinone che è stato monosostituito, controllando la stechiometria della reazione, con una molecola di glicina protetta sul gruppo amminico. La seconda funzione amminica dell'antrachinone è stata successivamente sostituita con un a-bromoacil bromuro affinché il bromo in a potesse essere successivamente sostituito con la TEMPOamina. L'ultimo step è la deprotezione del gruppo 9-fluorenilmetilossicarbonilico legato all'ammina glicinica.

L'esperimento EPR è stato eseguito realizzando una soluzione 50 umol di 7-TEMPOimminoCPT in un tampone a pH neutro in concentrazioni crescenti di DNA non marcato. Per confronto è stato realizzata una soluzione 50 umol dell'antrachinone marcato in presenza di 2 equivalenti di DNA:

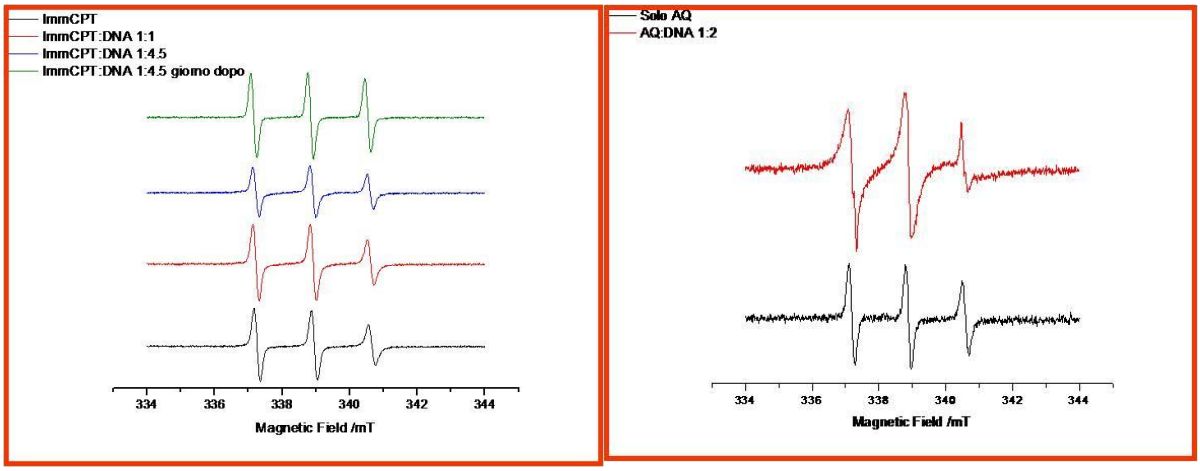

L'analisi non mostra alcun cambiamento nel segnale EPR, confermando l'incapacità della camptotecina di intercalare nel DNA in assenza del complesso binario.

E' stato infine seguito l'ultimo esperimento con il derivato 7-TEMPOiminoCPT (il più attivo tra i composti marcati), l'enzima Topoisomerasi I e il DNA non marcato (quest'ultimo in concentrazione maggiore rispetto agli altri due componenti):

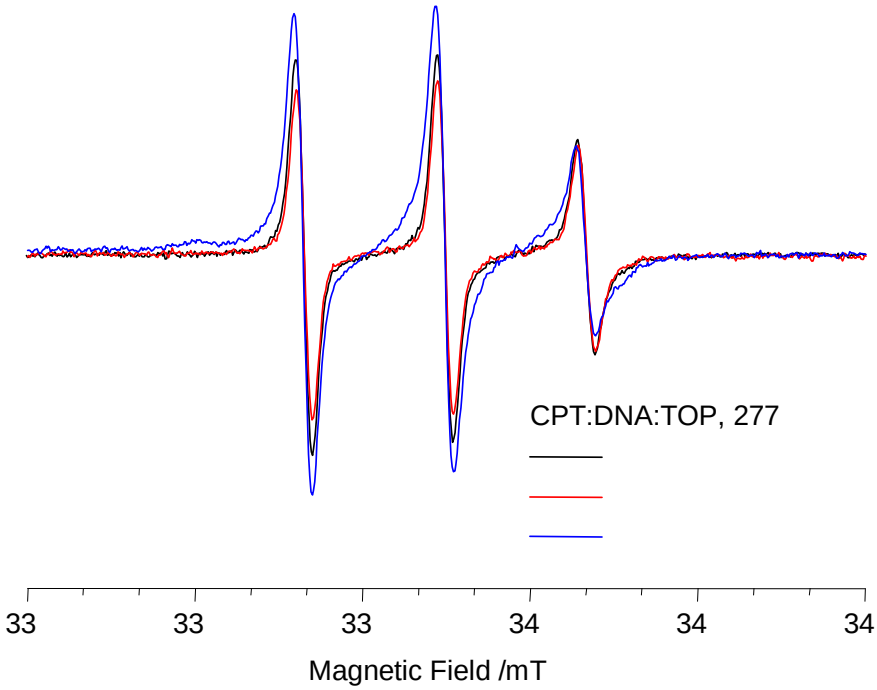

L'esperimento mostra una piccola differenza rispetto al controllo con solo il derivato della CPT ed il DNA (tale differenza è stata confermata anche nel secondo esperimento, dove è stata dimezzata la concentrazione della CPT marcata), probabilmente dovuta ad una minore mobilità dello spin all'interno del complesso ternario. Tuttavia questa differenza è troppo piccola per poter essere caratterizzata: la possibile causa di questo comportamento può essere dovuta alla cinetica della reversibilità del complesso ternario, troppo rapida per poter essere misurata nel tempo necessario per l'esperimento EPR. Una seconda possibile causa può essere attribuita all'inadeguata stechiometria utilizzata per questa reazione: il rapporto tra la proteina e l'inibitore potrebbe essere troppo basso. In questo caso, purtroppo, la difficile reperibilità della Topoisomerasi I umana in concentrazioni utili impedisce la possibilità di ripetere l'esperimento aumentando tale rapporto.

Complesso PKA-cAMP

Le proteine chinasi rappresentano una tra le più grandi e influenti classi di enzimi degli organismi eucarioti. Le protein chinasi cAMP dipendenti (PKA) sono enzimi dipendenti dal secondo messaggero, il cAMP (3'-5'-adenosina monofosfato ciclico). Il cAMP o adenosina 3'-5' monofosfato ciclico è un nucleotide presente in modo ubiquitario nelle cellule eucariotiche e indispensabile in numerosi processi biologici. Esso viene prodotto nella via dell'adenilato ciclasi (AC): una prima stimolazione per via endogena o esogena di recettori extracellulari legati a proteine G di membrana portano all'attivazione dell'AC che converte l'ATP in cAMP.

Il cAMP prodotto lega le subunità regolatorie delle PKA e converte quest'ultima nella conformazione attiva grazie alla quale è in grado di trasferire gruppi fosfato da una molecola donatrice quale l'ATP (adenosin-5'-trifosfato) a specifici substrati. Questo processo, definito fosforilazione, è alla base di numerosi processi metabolici cellulari, quali la trascrizione, il metabolismo, il ciclo cellulare, la differenziazione, la crescita, lo sviluppo e l'apoptosi.

Il cAMP o adenosina 3'-5' monofosfato ciclico è un nucleotide presente in modo ubiquitario nelle cellule eucariotiche e indispensabile in numerosi processi biologici.

a)

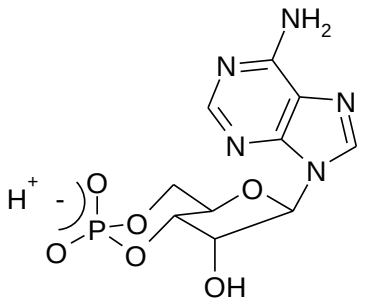

Fig 9a: Struttura molecolare del cAMP

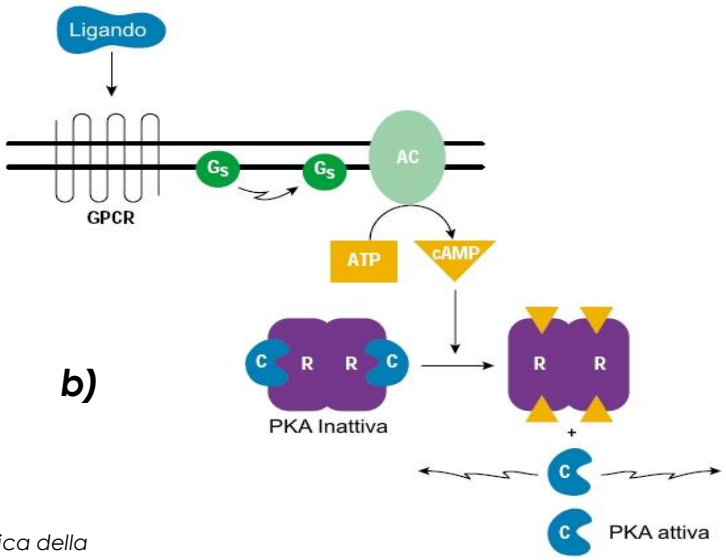

Fig 9b: Rappresentazione schematica della via dell'adenilato ciclasi

L'importanza delle PKA in numerosi processi metabolici e la sua peculiare distribuzione nei diversi tessuti hanno condotto la ricerca verso il possibile coinvolgimento della PKA in diversi tipi di neoplasie ottenendo risultati interessanti anche se di complessa interpretazione.

Per questo motivo può risultare interessante realizzare un marker diagnostico interagente con l'attività della PKA per la caratterizzazione in vitro ed ex-vivo di cellule somatiche o cancerose.

Per ottenere questo scopo è possibile legare alla struttura nucleotidica una sonda fluorescente in grado di comportarsi da tracciante all'interno delle cellule interessate. La sintesi di questa sonda parte dall'osservazione che derivati dell'AMP ciclico sostituiti in posizione 8 non perdono attività (Muneyama Biochemistry 1971- attività inibitoria dell'8-bromo-cAMP).

Su questa base è stata realizzata una prima sonda dal professor Caretta del dipartimento di Fisiologia dell'Università di Padova. Dagli ulteriori risultati ottenuti con questo composto è stato sintetizzato tale derivato:

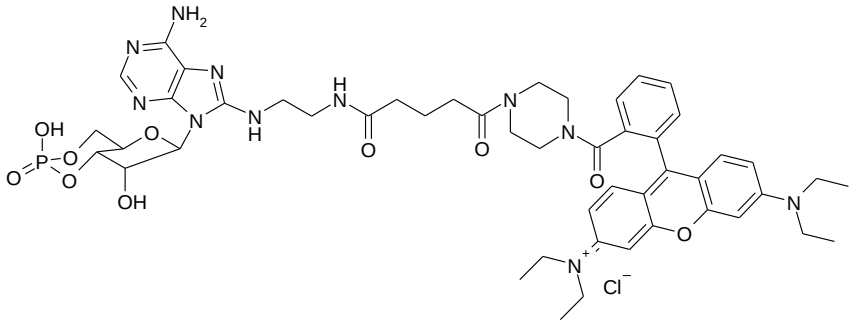

dove la struttura nucleotidica è stata sostituita in posizione 8 da uno spaziatore recante nell'altra estremità una molecola fluorescente (in questo caso rodamina). Lo spaziatore è stato sintetizzato cercando di separare il fluoroforo dal cAMP (impedendone l'interferenza sull'attività) ed allo stesso tempo di non renderlo troppo flessibile (impedendone così la possibilità di ripiegarsi sul cAMP).

La sintesi è stata effettuata per convergenza di due intermedi:

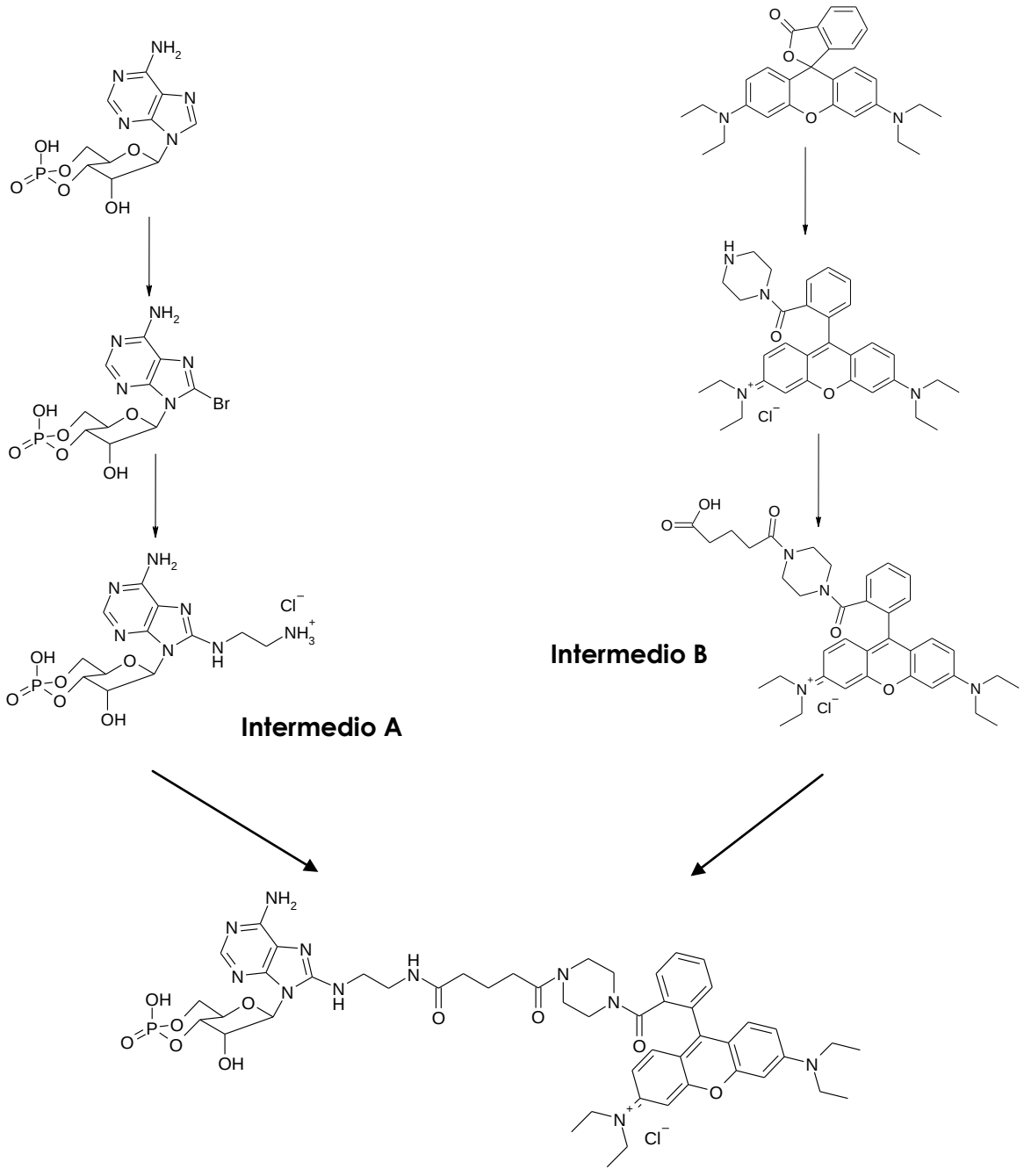

L'intermedio A è stato ottenuto partendo dal ciclico AMP il quale è stato inizialmente bromurato in posizione 8:

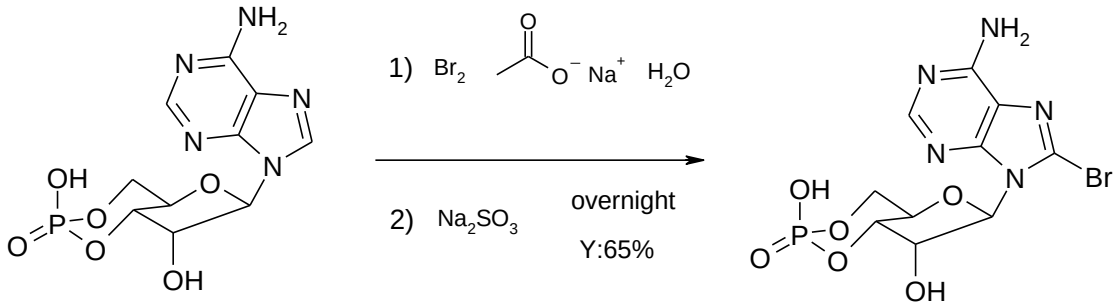

Il prodotto ottenuto è stato successivamente convetito nell'intermedio desiderato tramite sostituzione nucleofila operata dall'etilendiammina (che in questo caso funge anche da solvente):

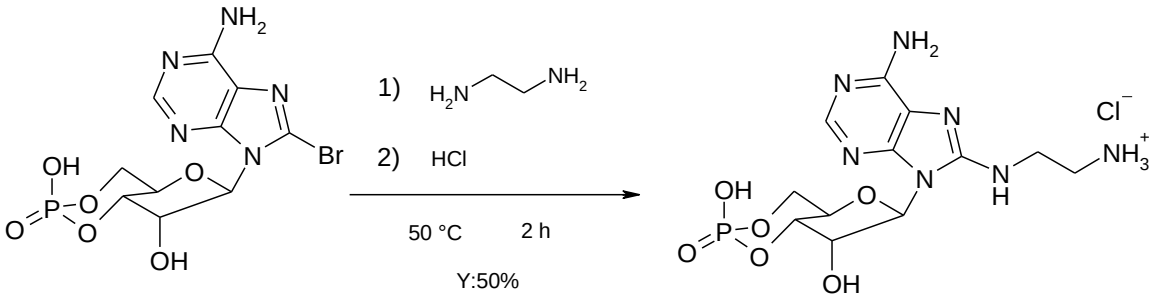

L'intermedio B è stato invece ottenuto attraverso una prima attivazione della Rodamina B base con piperazina in presenza di un acido di Lewis quale trimetilalluminio:

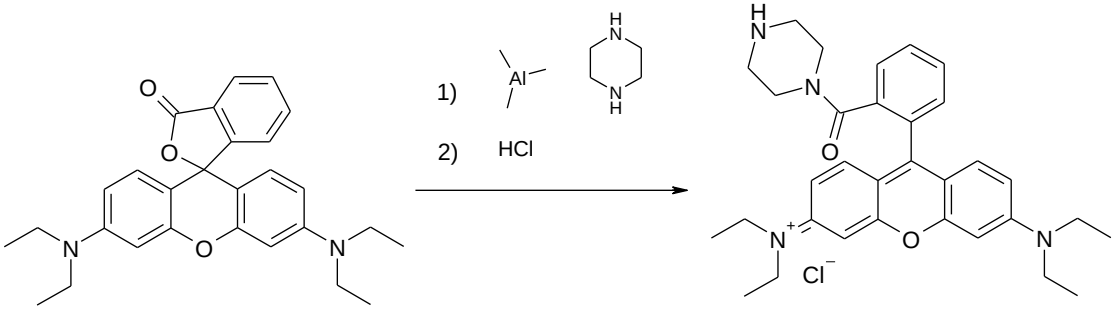

Il gruppo amminico secondario così formato può attaccare l'anidride glutarica portando alla formazione dell'intermedio B:

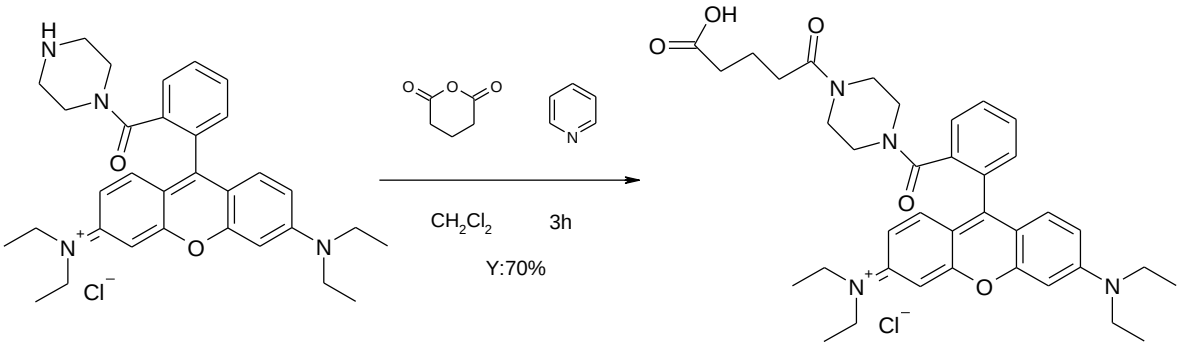

L'ultimo step è la sintesi del prodotto desiderato attraverso la formazione di un legame ammidico in presenza di TBTU:

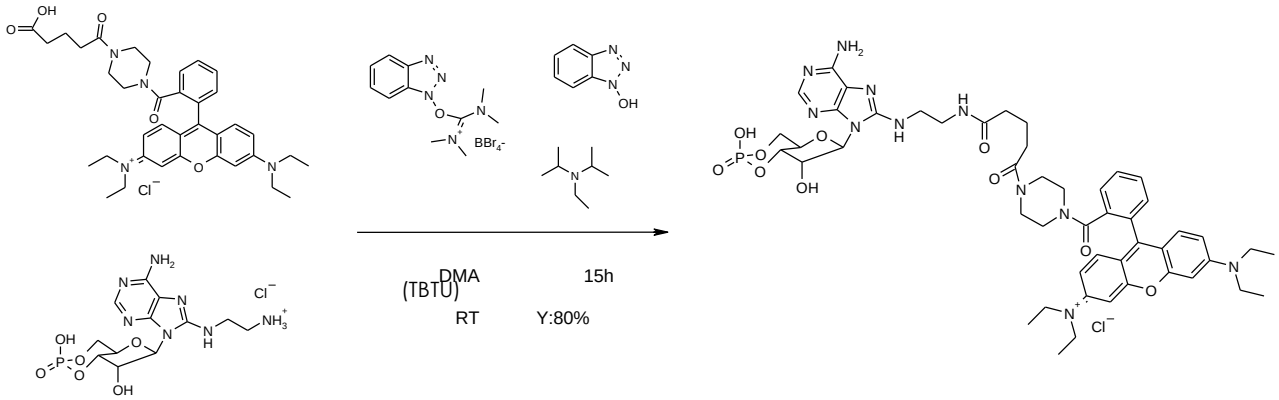

Il marker così ottenuto è in fase di test presso il laboratorio di Fisiologia della prof.ssa Mucignat. Prime immagini eseguite su colture cellulari di glioma di ratto (F98), trattate per 2 ore alla concentrazione 500 μM, mostrano come il composto sia capace di attraversare la membrana cellulare distribuendosi in maniera disomogenea all'interno del citoplasma, accumulandosi in particolari zone del citoplasma:

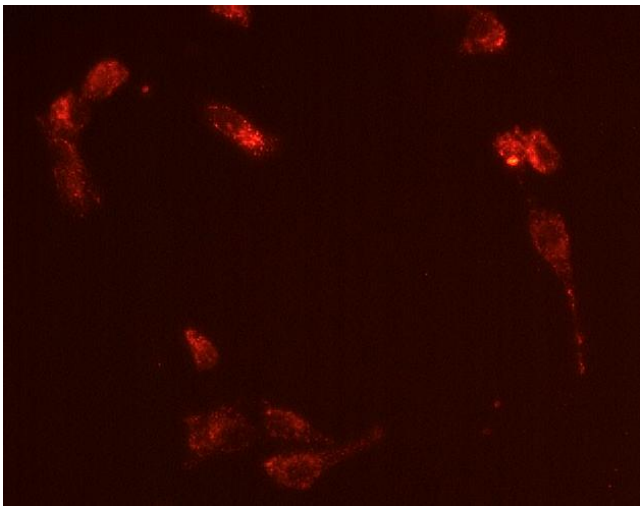

Il derivato fluorescente è stato testato anche su cellule di glia di ratto in assenza ed in presenza di un altro colorante in grado di raggiungere il nucleo cellulare, il 4',6-diamidino-2-fenilindolo (DAPI); le immagini mostrano come i due marker possono essere utilizzati contemporaneamente nello stesso campione cellulare, poiché essi non interferiscono tra loro:

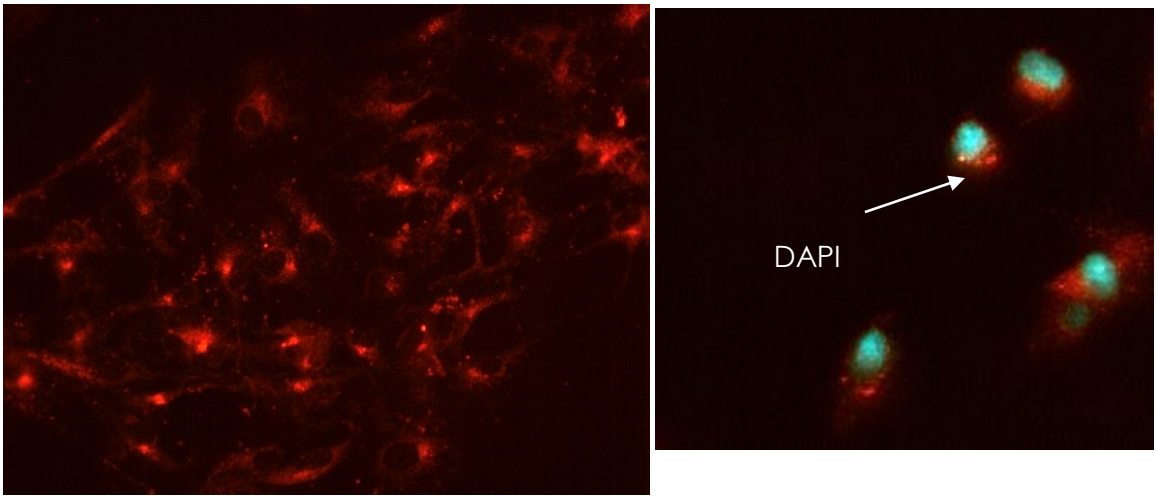

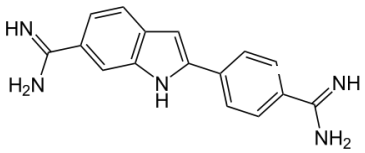

DAPI

Gli esperimenti successivi saranno focalizzati nella caratterizzazione dell'interazione del marcatore fluorescente all'interno della cellula; per ottenere ciò verranno eseguiti test immunoistochimici volti a comprendere meglio la natura delle zone dove il tracciante si accumula.

1.2 Abbreviations

Ac_2O	Acetic anhydride
$AlCl_3$	Aluminium chloride
Ba_2O	Barium oxide
CaH_2	Calcium hydride
$CDCl_3$	Deuterated chloroform
CPT	Camptothecin
AcCOOH	Acetic acid
bs	Broaded singolet
bm	Broaded multiplet
$CHCl_3$	Chloroform
CH_2Cl_2	Dichloromethane
d	Doublet
d(g/mL)	Density(g/mL)
dd	Doublet of doublets
dt	Doublet of triplets
DCC	Dicyclohexylcarbodiimide
DIEA	Diisopropylethylamine
DMAP	Dimethylaminopyridine
DMA	Dimethylacetamide
DMF	Dimethylformamide
DMSO	Dimhetylsulphoxide
DMT	Dimethoxytrityl
EPR	Electron paramagnetic resonance
ESR	Electronic spin resonance
Et_2O	Diethylether
EtOAc	Ethyl acetate
g	Grams
h	Hour
HCl	Hydrochloric acid
HOBt	Hydroxybenzotriazole
HBTU	Hydroxybenzotriazole hexafluorophosphate
H_2SO_4	Sulphuric acid
KOH	Potassium hydroxide
J	Coupling constant (Hz)
IR	Infrared spectroscopy
K_2CO_3	Potassium carbonate
LC	Liquid chromatography
m	Multiplet
M(mol/L)	Molarity(mol/L)
MeOH	Methanol
MHz	Megahertz
min	Minute
mg	Milligram

ml	Milliliter
mol	Mol
mmol	Millimol
NaCl	Sodium chloride
NMR	Nuclear magnetic resonance
PM	Molecular weight
ppm	Parts per milion
RT	Room temperature
s	Singolet
t	Triplet
tt	Triplet of triplets
TBTU	Hydroxybenzotriazole tetrafluoroborate
TPS-Cl	Triisopropylphenylsulphonyl chloride
TEA	Triethylamine
THF	Tetrahydrofuran
TLC	Thin Layer Chromatography
Ac_2O	Acetic anhydride
$AlCl_3$	Aluminium chloride
$CDCl_3$	Deuterated chloroform
CPT	Camptothecin
AcCOOH	Acetic acid

A. TOPO I-DNA-CPT COMPLEX

2. Introduction

2.1 DNA and Topoisomerase enzymes

The human genome is roughly composed of $3 \cdot 10^9$ base pair, separated each other by 3.4 Å[1]. The helical structure of duplex DNA allows for the faithful duplication and transmission of genetic information from one generation to the next, at the same time maintaining the integrity of the polynucleotide chains. The complementary nature of the two antiparallel DNA strands enables each to serve as a template for the synthesis of the respective daughter DNA strands. The intertwining of these polynucleotide chains in duplex DNA further ensures the integrity of the DNA helix by physically linking the individual strands in a structure stabilized by hydrogen bonding and stacking interactions between the hydrophobic bases. A further compression of the of the whole system is required because the whole extension of the human genome measure around 1 meter and it must be completely located inside the μm^3 cellular nucleus volume. To reach this goal, DNA duplex should be compacted around itself and around several structural proteins called hystons. These proteins form an octameric structure where the DNA could wrap around creating a 11 nm long structure called nucleasome.

When the DNA is arranged into this structure, it is *supercoiled*. This supercoil is superimposed to the coils formed between single DNA strands (in the double helix); the direction of the supercoil twist could be *positive* if it has the same direction of the double helix turns and *negative* if it has opposite directions.

[1] Adams, R. L. P.; Knowler, J. T.; Leader, D. P. *The Biochemistry of the Nucleic Acids.* Chapman&Hall, Ed. **1992**.

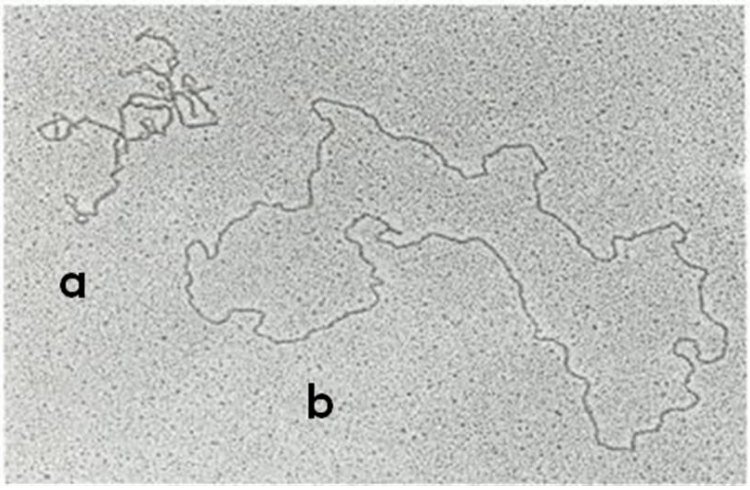

a) Negatively supercoiled DNA and **b)** relaxed DNA

The supercoiling topology of the DNA is expressed by the *linking number* equation Lk = Tw + Wr where:

- Lk (linking number) is the total number of the crosses of the DNA strands
- Tw (twist number) is the total number of the helix turns of the duplex; it could be calculated with the equation Tw = n/A where n is the number of the nucleotides and A is the number of nucleotides for each turn
- Wr (writhing number or supercoiling number) is the total axe folds number

However, these same features pose a number of topological constraints that affect most processes involving DNA, such as replication, transcription, and nucleosome assembly.

During semiconservative DNA replication, for example, the progressive unwinding of the DNA template requires a swivel in the DNA duplex to alleviate the overwinding of the strands ahead of the moving replication fork.

The replication fork is the complex responsible of the DNA replication[2]. It is constituted of 4 enzymes: the *helicase*, which separates the single strands of the duplex, the *poliymerase*, which creates a complementary copy of each

[2] Wastson, J. D.; Baker, A. T.; Bell, P. S.; Gann, A.; Levine, M.; Losick, R. Molecoular Biology of the Gene. *Cold spring Harbour Laboratory Press* **(2003)**, 5° edition

single strand (directly in the case of the leading 3'-5' strand), the *primase* and the *ligase* which help the polymerase to copy the lagging 5'-3' strand.

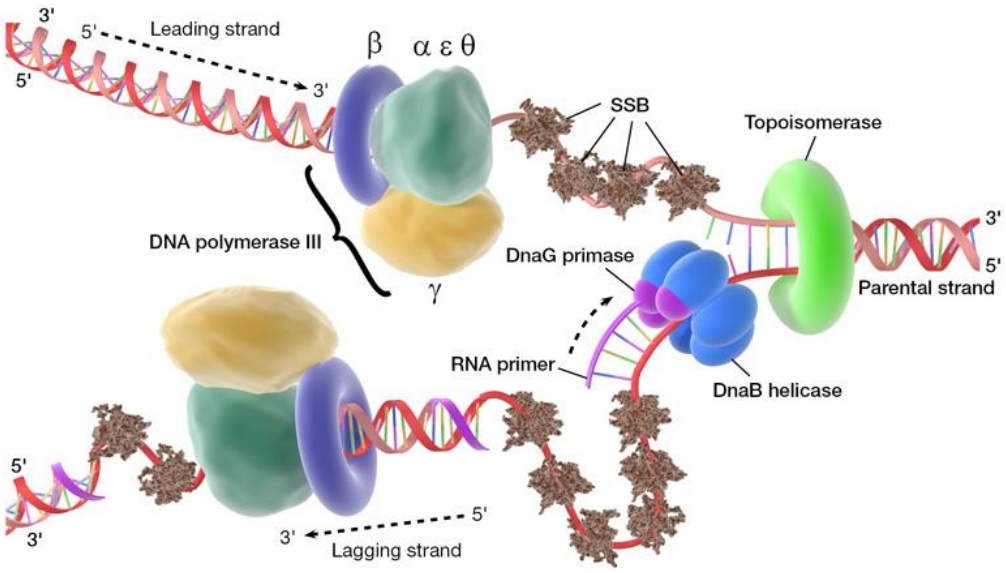

Of course, the replication apparatus may simply follow the helical path of the DNA template strands. However, this soon leads to a second problem of how to unlink the interwound DNA helices following the completion of DNA synthesis. This decatenation of daughter molecules is absolutely required in the case of circular genomes and plasmids, in which the template strands are physically linked circles. Similar considerations apply to the process of transcription, where the movement of a transcription complex along the DNA template may also produce a local unwinding of the DNA behind and overwinding of the DNA ahead. This may be viewed as the formation of local domains of negatively and positively supercoiled DNA, respectively[3]. Indeed, the translocation of any complex that forms between the two strands of a

[3] Liu, L. F.; Wang, J. C. Supercoiling of the DNA template during transcription. *Proc. Natl. Acad. Sci. USA* **(1987)**; 7024-7027

DNA duplex (such as a helicase or a recombination intermediate) has the potential to generate such local changes in DNA topology.

It is relatively straightforward to imagine the consequences of these events. Without a "swivel" in the DNA, the overwinding of the DNA strands would eventually prohibit the further movement of the complex along the DNA, resulting in the inhibition of DNA replication, transcription, recombination, and so forth. Along similar lines, the inability to unlink or decatenate replicated sister chromatids would produce an extremely high rate of chromosomal breakage and/or nondisjunction during mitosis. In the case of chromatin assembly, the wrapping of DNA around the histones stabilizes negative supercoils. Because the linking number of a topologically constrained DNA molecule is conserved, this would result in the accumulation of positive supercoils in the unconstrained DNA with potentially profound effects on gene expression and DNA replication.

One solution to the topological problem lies in a family of enzymes called DNA topoisomerases[4]. These enzymes catalyze changes in DNA topology by altering the linkage of DNA strands. This is accomplished via a mechanism of transient DNA strand breakage and religation. During an initial transesterification reaction, these enzymes form a covalent linkage between their active site tyrosyl residues and one end of cleaved DNA strand. This conserves the energy of the original phosphodiester backbone bond and creates a protein-linked break in the DNA. A second transesterification reaction between the free hydroxyl terminus of the noncovalently bound DNA strand and the phosphotyrosine linkage reseals the break in the DNA. Usually, this second reaction restores the original phosphodiester bond; however, under certain conditions, DNA topoisomerases may be induced to transfer one end of a DNA to a different DNA end.

[4] Wang, J. C. DNA Topoisomerases. *Ann. Rev. Biochem.* **(1996)**; 635-692

DNA topoisomerases constitute an ever-increasing family of enzymes that can be distinguished on the basis of the number of DNA strands that they cleave and the covalent linkage formed in the enzyme-DNA intermediate[5]. Type II DNA topoisomerases[6] cleave and religate both strands of the DNA duplex and form covalent intermediates with a 5' phosphate. This enzyme is essential and is required to resolved the multiply intertwined sister chromatids during mitosis. In all cases, a significant body of work suggests that these enzymes bind DNA as an ATP-dependent protein clamp *(26-28)*. Both strands of the bound DNA are cleaved to yield staggered protein-linked nicks. A second DNA strand is then passed through this gate in the DNA, and the nicks are religated. The hydrolysis of ATP is required to drive allosteric changes in enzyme structure, rather than the cleavage or religation of the DNA[7].

Type I enzymes, otherwise, cleave a single strand of a DNA duplex and produce changes in linking number in steps of one. One important feature of this process is the ability of this protein to work without the use of energy (ATP); the energy required for the whole process is actually obtained from the energy of the phosphoester bond[8].

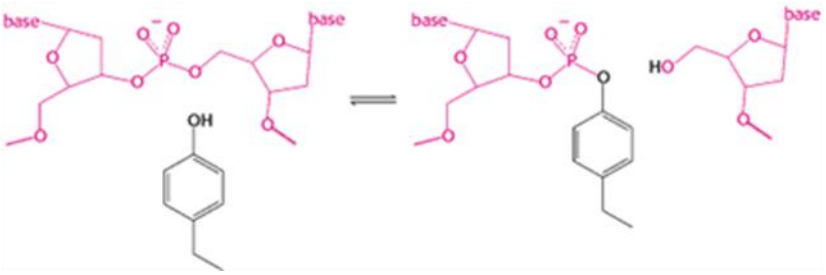

[5] Berger, J. M. Structure of DNA topoisomerases. *Biochimica et Biophysica Acta (BBA) - Gene Structure and Expression* **(1998),** 1400; 3-18

[6] Berger, J. M.; Gamblin, S. J.; Harrison, S. C.; Wang, J. C. Structure and Mechanism of DNA topoisomerases II. *Nature* **(1996),** 379; 225-232

[7] Wei, H.; Ruthenberg, A. J.; Bechis, S. K.; Verdine, G. L. Nucleotide-dependent domain movement in the ATPase domain of a human type IIA DNA topoisomerase. *J Biol Chem* **2005,** 280, 37041-7

[8] Stewart, L.; Redinbo, M. R.; Qiu, X.; Hol, W. G. J.; Champoux, J. J. A Model for the Mechanism of Human Topoisomerase I. *Science* **(1998),** 279; 1534-1541

The type IA enzymes, as exemplified by bacterial DNA topoisomerases I and III, and eukaryotic DNA topoisomerase III, encoded by the *topA, topB* and *TOP3* genes respectively, form a tyrosyl linkage with a 5' phosphate. The recent discovery of DNA topoisomerase III in humans attests to the universality of this enzyme. In *Escherichia coli,* DNA topoisomerase I (TopA) catalyzes the relaxation of negatively supercoiled. Since the changes in DNA linking number catalyzed by bacterial DNA gyrase are opposite to that observed with TopA, there appears to be homeostatic mechanism regulating the levels of expression of these enzymes to maintain the level of DNA supercoiling within a fairly narrow range. The function of DNA topoisomerase III in bacteria and in eukaryotes is less clear. These enzymes are highly related and appear to possess a potent decatenase activity. In yeast, the Top3 enzyme plays a role in suppressing recombination between repeated DNA sequences, is required during meiosis, and has been implicated in telomere maintenance. However, the enzyme does not appear to constitute a major DNA relaxation activity in the cell. Genetic studies suggest an association between Top3p and a helicase, Sgsip, a homolog of the Bloom's and Wemer's syndrome genes in human.

Reverse gyrase constitutes an additional member of the type IA family. This ATP-dependent enzyme catalyzes the positive supercoiling of DNA. Moreover, this enzyme appears to have a bipartite structure consisting of a helicase domain and a type IA topoisomerase.

Type IB enzymes include eukaryotic DNA topoisomerase I, the product of the *TOP1* gene.

The human Topoisomerase I enzime[9] (it will be abbreviated as TopoI in the text) is a 765 aminoacid monomer (100-120 kDa) subdivided into four domain:

[9] Redinbo, M. R.; Stewart, L.; Kuhn, P.; Champoux, J. J.; Hol, W. G. J. Crystal Structures of Human Topoisomerase I in Covalent and Noncovalent Complexes with DNA. *Science* **(1998),** 279; 1504-1513

NH2-terminal, linker, "core" (also subdivived in three different subdomains) and COOH-terminal (which contain the catalytic tyrosine).

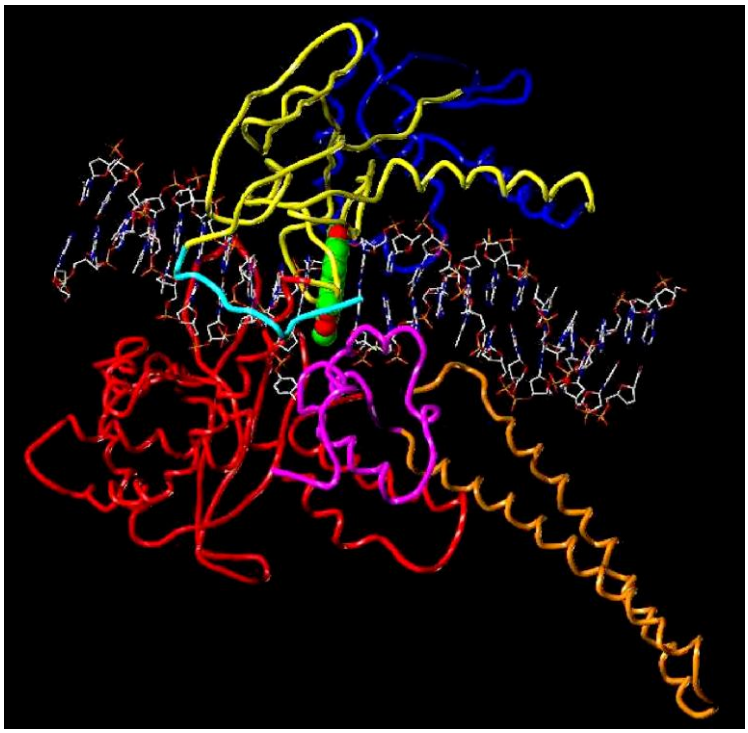

The nick of the DNA strand is operated by the tyrosine723 through the formation of a phosphodiesteric bond with the 3' portion of the DNA (the whole swivelase process, described above, is represented in the figure represented below). The bond formation is catalized by other aminoacids (Arg 488; Arg 590; Hys 632) that allow correct positions of both the phosphate and the tyrosine, a crucial step for the whole catalytic action.

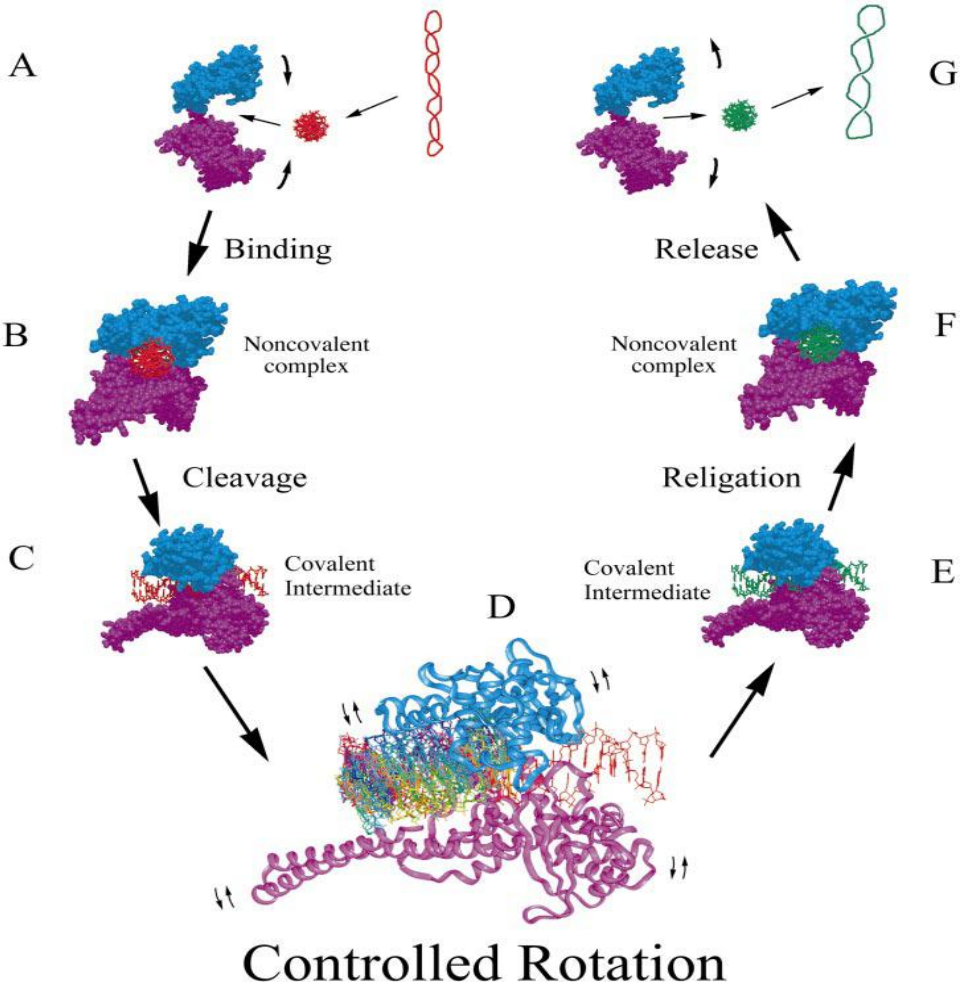
A
Binding
B
Noncovalent complex
Cleavage
C
Covalent Intermediate
D
Controlled Rotation
Covalent Intermediate
E
Religation
Noncovalent complex
F
Release
G

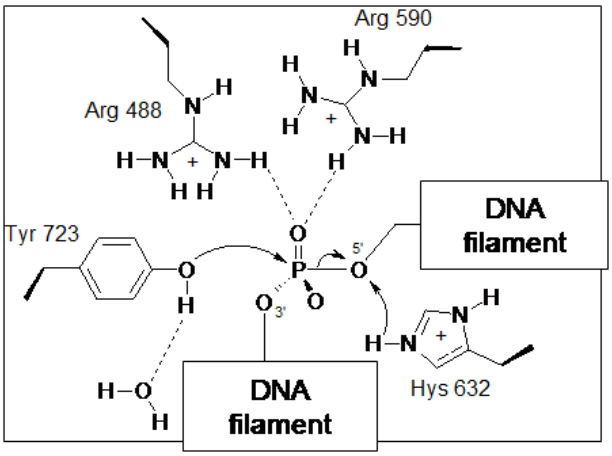
Arg 590
Arg 488
Tyr 723
DNA filament
DNA filament
Hys 632

Crystal structure[8] of the non-covalent binary complex DNA-Topoisomerase I, as well as the crystal of the covalent binary complex, played a primary role in understanding these interactions inside the catalytic pocket. They also showed an incredible number of secondary interactions between aminoacids belong to different domains and several components of the DNA, such as the nucleobases and the sugar backbone. Using these information, biologists were able to create a considerable number of mutants of Topoisomerase I revealing which of these aminoacids are fundamental for the correct catalytic process of the enzyme.

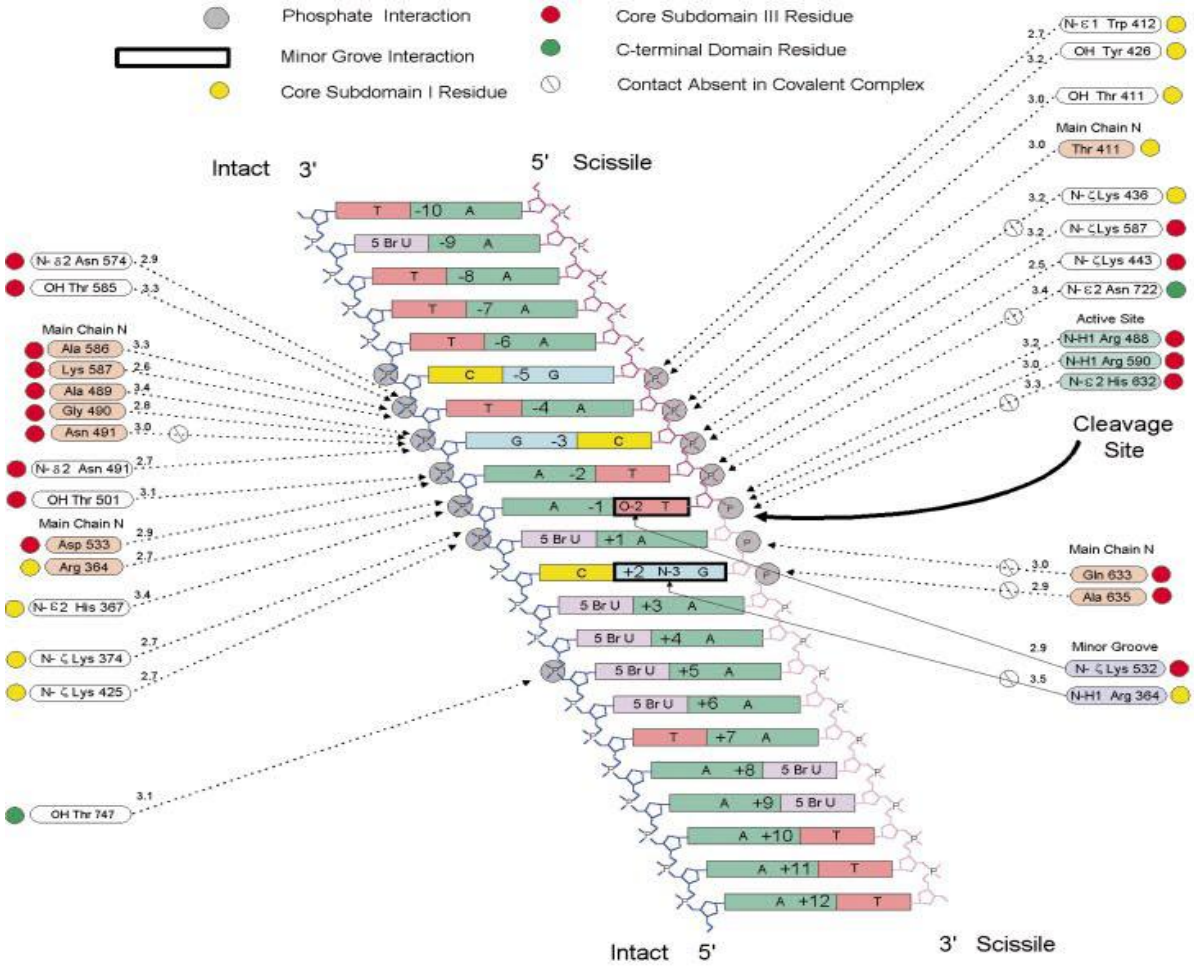

After that, Topoisomerase I changes its conformation in order to allow the correct shift of the intact strand into the nick. The passage is often referred as the *controlled rotation*[10] of the enzyme. Only after the correct shift the enzime sews up the strand through the reattack of the phopshotyrosine bond and escape from the binary complex. A remarkable aspect that must be underlined is the faster releasing speed rather than the nicking speed; this feature guarantees a low concentration of the binary complex inside the cell.

The key role of the Topoisomerase I in the replication process of the cell was rapidly considered by the scientific community as a possible target for therapeutic strategies[11,12].

In fact malignant cells, such as tumoral ones, are characterized by an uncontrolled replication process which collapse to a fast replication cycle. To correctly replicate, however, the DNA must be properly relaxed before the action of the replication fork.

Thus, the possibility to inhibit the Topoisomerase activity could bring to the forced stop of the replication process.

In the next chapter we could see the different strategies followed to interfere with the Topoisomerase action.

[10] Koster, D. A.; Croquette, V.; Dekker, C; Shuman, S; Dekker, N. H. Friction and torque govern the relaxation of DNA supercoils by eukaryotic topoisomerase IB *Nature* **(2005)**, 434; 671-4
[11] Li, T. K.; Liu, L. F. Tumor Cell Death Induced by Topoisomerase-Targheting Drugs. *Annual Reviews Pharmacol. Toxicol.* **(2001)**, 41; 53-77
[12] Pindur, U.; Lenster, T. Antitumor drug Design: DNA-binding ligands, which inhibit the topoisomerase I *Pharmazie* **(1998)**, 53; 79-86

2.2 Topoisomerase inhibitor

All the molecules known for their anti-Topoisomerase (class I and II) activity are divided into two great class, due to their mechanism of action[13]:

- Drugs of class I: they are able to stabilize the DNA-Topoisomerase reversiblecomplex

leading to the formation of a new DNA-Topoisomerase-inhibitor ternary complex. This complex is also reversible but it is not able to to religate the nicked strand. The antiproliferative effect start when the replicative fork collides with this complex; in fact the latter is not recognized by the previous, which stop the replication process and start the apoptotic procedure. For this indirect inhibition of the enzime, this class of drugs is called *Topoisomerase poisons*.

- Drugs of class II: they directly interfere with the catalitic site of the enzime, rather than the binary complex. The proliferative damage is due to the presence of unrelaxed DNA that could not be processed by the replicative fork. For their direct interferation with the protein, this class is also called *Topoisomerase suppressors.*

In the following table are listed the different molecules representative of these two classes.

[13] Topcu, Z. DNA Topoisomerases as targets for anticancer drugs. *J. Clin. Pharm. Therap.* **(2001)**, 26; 405-416.

Class	*Group*	*Examples*	*Target*
I	Acridine	Amsacrine	Topo II
	Alcaloids	Camptothecin, Topotecan, Irinotecan	Topo I
	Anthracyclin	Adriamycin, Daunomycin	Topo II
	Actinomycin	Actinomycin D	Topo II
	Quinolones	Nalidissic acid,	Girase
		Norfloxacine, Ciprofloxacine	
	Ellipticine	Ellipticine	Topo II
	Epipodofillotoxins	Etoposide	Topo II
	Isoflavodine	Genisteine	Topo II
	Other	Mitoxantrone, Bisantrene	Topo II
II	Coumarine	Novobiocine, Chlorobiocine	Topo II
	Other	Fostriecine	Topo II
		β-Lapacone	Topo I
		Velutine	Topo I
		Chebulagic acid	Topo I
		Alkannine, Shikonine	Topo I

A deeper description of all these classes of molecules would require too much time and is outside our direct interest but, for those who want to know more about them, some books could be consulted[14].

In this work we will describe one of the most important poisons of the Topoisomerase I enzyme: the camptothecin alkaloid. This molecule and its mechanism of action are the heart of the next chapter.

[14] Foye, W. O.; Williams, D. A.; Lemke, T. L. Foye's Principi di Chimica Farmaceutica. *Piccin* **(2005)**. See also ref **15** and **16**

2.3 Camptothecin and its analogues[15,16]

Camptothecin (CPT, **1**, Figure 1) is a potent antineoplastic molecule isolated for the first time by Wall and collaborators in 1958 from extracts of the bark of the Chinese tree *Camptotheca acuminata*, known as the "happy tree" in its native country.

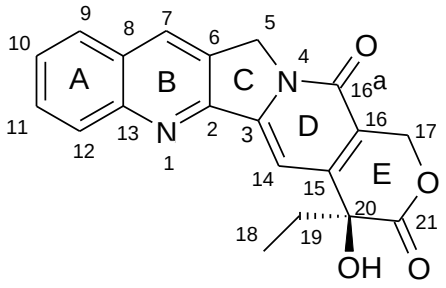

CPT is a pentacyclic alkaloid which structure was determined by X-ray crystallography in 1966[17]. More deeply, it is characterized by:

- a quinoline ring (rings A and B),
- a piperidine function (ring C) fused with a pyrazoline ring (ring D),
- a 6-member lactone (ring E),
- a chiral carbon at the 20 position with the *S* absolute configuration.

The importance of the 20(*S*)-chiral carbon for activity was immediately confirmed after the discovery of the inactivity of the *R* enantiomer to inhibit the Topoisomerase I action. The dynamic equilibrium between the closed-ring

[15] Pommier, Y. Topoisomerase I inhibitors: camptothecins and beyond. *Nat Rev Cancer* **2006,** 6; 789-802.
[16] Pommier Y. DNA Topoisomerase I Inhibitors: Chemistry, Biology, and Interfacial Inhibition. *Chem Rev* **(2009)**, 109; 2894-2902
[17] Wall M. E.; Wani M. C.; Cook C.E.; Palmer K. H.; McPhail A.T.; Sim G. A. Plan antitumor agents. I. The isolation and structure of Camptothecin, a novel alkaloid leukemia and tumor inhibitor, from Camptotheca acuminata. *J Am Chem Soc* **(1966)**,88; 3888-90

lactone and the open-ring carboxylic forms of CPT is another striking point. In physiological condition, CPT convert to its open lactone sodium salt derivative[18]:

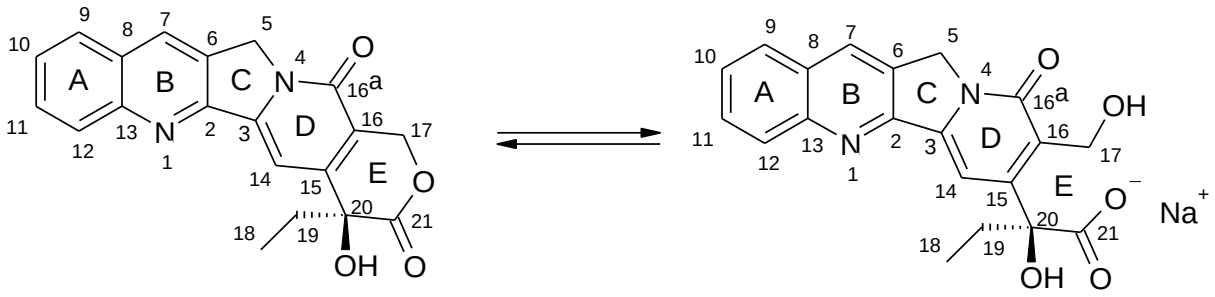

First preclinical studies on CPT were encouraging, showing efficacy in tumors of both colon and gastric origin. One of the major problems associated with CPT was its poor water solubility. For this reason, a sodium salt was made opening the lactone ring. Although this increased the molecule solubility, it was determined in first clinical trials that this also greatly reduced the corresponding anticancer activity. Moreover, CPT was found responsible for unacceptable side effects, in particular hemorrhagic cystitis and severe myelosuppression. Due to the loss of antitumor activity of the carboxylate form and to the high toxicity, clinical development of CPT in the 1970s was discontinued. In 1985 the enzyme Type I DNA Topoisomerase was discovered to be the primary cellular target of CPT[19]. As this unique mechanism of action was determined, the interest in CPT was renewed and the development of

[18] Mi, Z; Burke, T.G. Marker Interspecies Variations concerning the Interactions of Camptothecin with Serum Albumin: A Frequency-Domain fluorescence Spectroscopic Study *Biochemistry* **(1994)**, 33; 10325-6

[19] Hsiang Y.H.; Hertzberg R.; Hecht S.; Liu L. F. Camptothecin induces protein-linked DNA breaks via mammalian DNA topoisomerase I. *J Biol Chem* **(1985)**, 260(27);14873-8

CPTs as anticancer drugs reinitiated. This resulted in the development of a large number of CPT analogs during the last twenty years[20].

Nowadays, two CPT derivatives are in approved by the Food and Drug Administration (FDA) for cancer therapy: *Topotecan hydrochloride* (trade name Hycamtin®) a water-soluble derivative used to treat ovarian cancer and lung cancer and *Irinotecan* (trade name Camptosar®), a bis-piperidine water-soluble prodrug converted by an enzyme into its active metabolite SN-38 and used in metastatic colorectal cancer cases.

Several other compounds bearing modifications in different position of the CPT structure are also in clinical trial; a particular mention must be given to the *Diflomotecan* and *S39625*, a non-lactone CPT derivatives and to *Gimatecan*[21], a 7-oxime water soluble derivative of CPT.

The huge amount of information extracted from these derivative allowed the possibility to create a robust structure-activity relationship (SAR) criteria that was very useful for the develop of other CPT derivatives[22].

Moreover, following these SAR data supported by theoretical model of the possible interaction of CPT inside the ternary complex, other Topoisomerase I poisons with a non CPT structure were also recognized[12]. Right now, three classes of molecules were chosen a good candidates for possible FDA approval: the indolocarbazoles, the 5, 11-diketoindenoisoquinolines and the phenanthridines.

[20] Li, Q.; Zu, Y; Shi, R.; Yao. L. Review Camptothecin: current Perspectives. *Current Medicinal Chemistry* **(2006)**, 13; 2021-2039

[21] Sorbera L. A.; Serradel N.; Bolos J.; Rosa E.; Bozzo J. Gimatecan. *Drugs of the Future* **(2007)**, 32(10); 859

[22] Zunino F.; Dallavalle S.; Laccabue D.; Beretta G.; Merlini L.; Pratesi G. Current status and perspectives in the development on Camptothecin. *Current Pharmaceutical Design* **(2002)**, 8; 2505-20

CPT-like Inhibitor:

Modification of the A e B rings:

FDA approved drugs

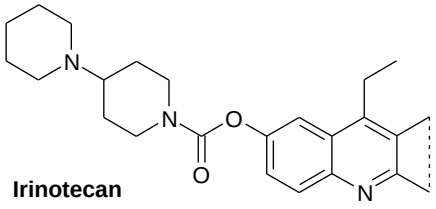

Irinotecan

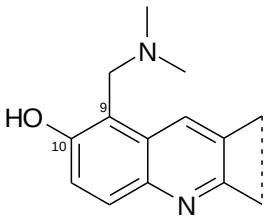

Topotecan

Clinical trial drugs

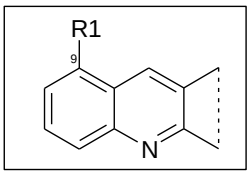

9-amminoCPT R1 = NH_2
Rubitecan R1 = NO_2

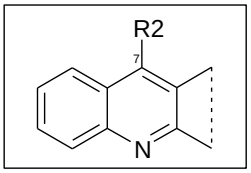

Gimatecan R = $-CH_2CH{=}NOC(CH_3)_3$
Kareniticin R = $-CH_2CH_2Si(CH_3)_3$
Silatecan R = $-CH_2Si(CH_3)_2C(CH_3)_3$

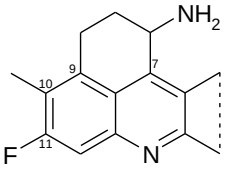

Exatecan

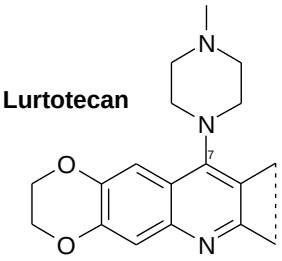

Lurtotecan

Modification of the E ring:

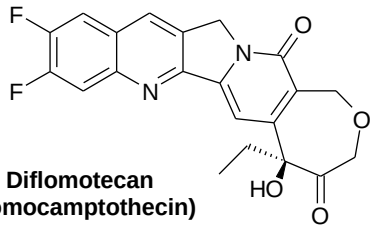

Diflomotecan
(Homocamptothecin)

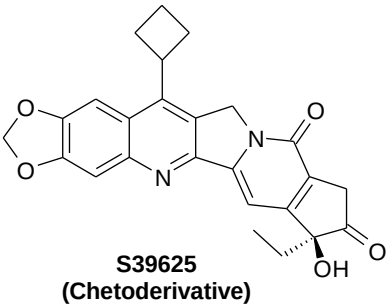

S39625
(Chetoderivative)

non CPT-like Inhibitor:

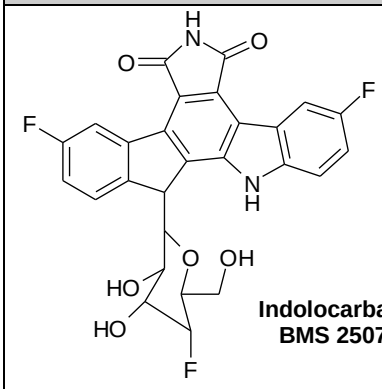

Indolocarbazole
BMS 250749

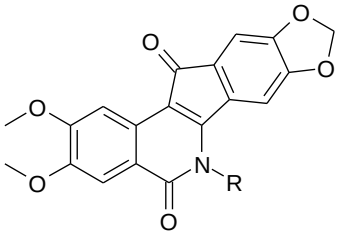

5, 11-Diketoindenoisoquinolines

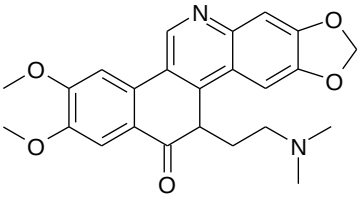

Phenanthridines
ARC-111 (topovale)

Under normal conditions, the cleavage intermediates are transient because religation is favoured over cleavage. CPT and its analogues interact with the cleavable intermediate forming a ternary complex. In presence of the drug, the initial cleavage action of TopoI is not affected, but the relegation step is inhibited (or significantly slowed down) because of a misalignment of the 5'-hydroxyl group and the scissile tyrosine-DNA bond due to the presence of the drug. This leads to the accumulation of single-stranded breaks in the DNA. These lesions are not in themselves toxic to the cell, because the strands rapidly religate after drug removal. However, the collision of the DNA replication fork with the ternary complex produces an irreversible double-strand break that ultimately leads to cell death. As already mentioned, this molecule is commonly referred to as TopoI *poison*, since it transforms TopoI into a damaging agent for the cell.

The CPTs are S-phase specific drugs, because ongoing DNA synthesis is a necessary condition to induce the above sequence of facts leading to cytotoxicity. Even the mechanisms of cellular response to Topoisomerase I poisons have been recently reviewed[23], the precise sequence of events which follow the drug-induced DNA damage are still not clear.

The first experimental information on the structure of the ternary complex were extracted from the 2.1 Å structure of Topotecan bound to the human TopoI-DNA covalent complex[24]. Analyzing the electronic density map, Topotecan seems to bind to the complex by intercalating between DNA base pairs of both DNA strands at the site of TopoI-induced cleavage. Topotecan interaction is stabilized by base-stacking interactions with both the -1 (upstream) and +1 (downstream) base pairs, mimicking a DNA base pair. Moreover, Topotecan binding is stabilized by a hydrogen bond contact with

[23] Beretta, G. L.; Perego, P.; Zunino, F. Targeting topoisomerase I: molecular mechanisms and cellular determinants of response to topoisomerase I inhibitors. *Expert Opin Ther Targets* **(2008)**, 12(10); 1243-56

[24] Staker, B. L.; Hjerrild, K.; Feese, M. D.; Behnke, C. A.; Burgin, A. B., Jr.; Stewart, L. The mechanism of topoisomerase I poisoning by a camptothecin analog. *PNAS* **(2002)**, 99; 15387-15392.

Asp533, a water-bridged contacts to the active site phosphotyrosine and Asn722 and another hydrogen bond contact between Arg364 and the nitrogen of the quinoline ring . These features are in accord with the complete inactivity of the N-oxide derivative and of the R enantiomer of the CPT. Subsequently, crystal structures of CPT bound to the human TopoI-DNA covalent complex[25] was published showing similar interaction respect to the previous one.

All the structures confirm that TopoI poisons can be defined as interfacial inhibitors, as they bind at the interface of the TopoI-DNA complex.

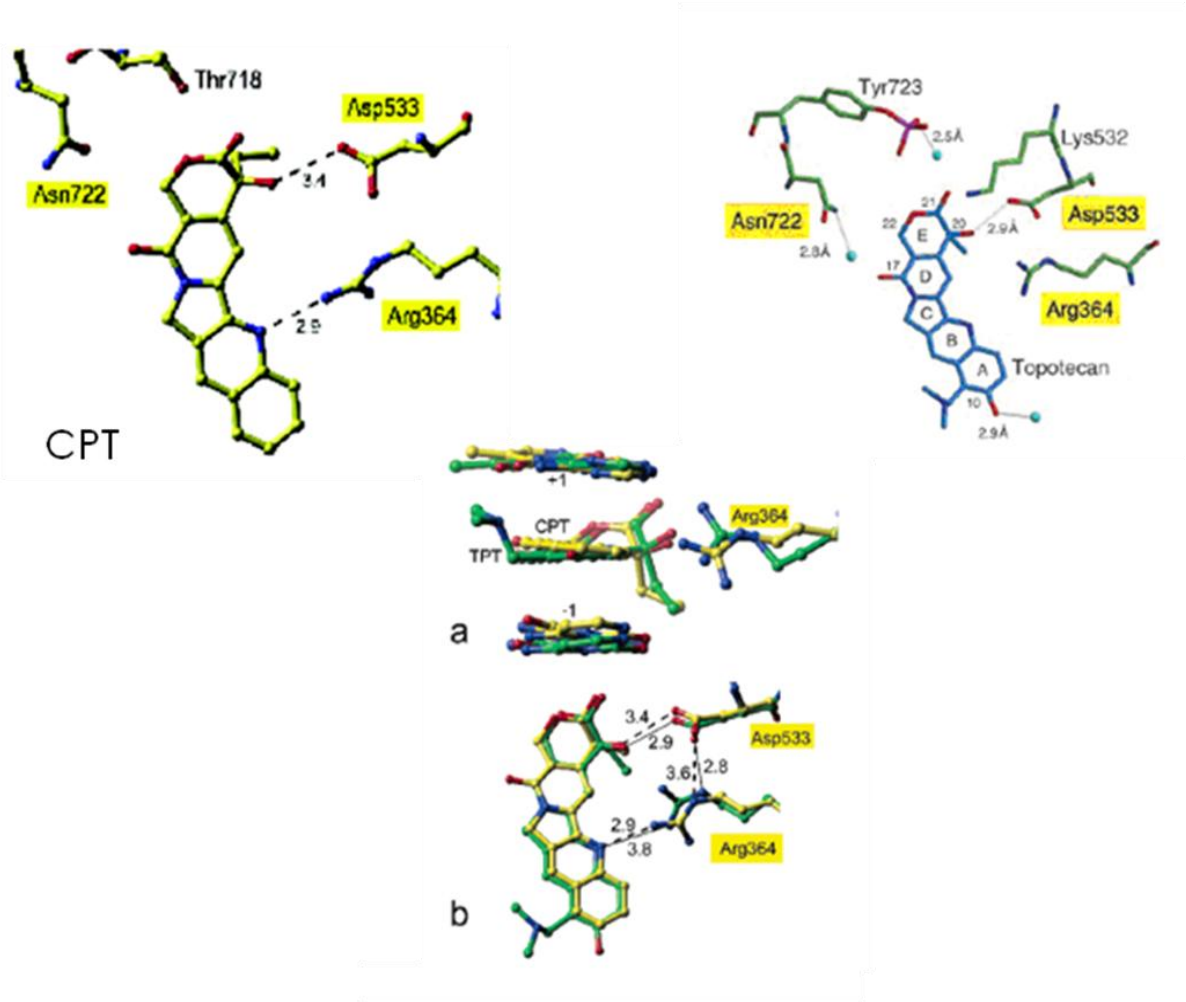

[25] Staker, B. L.; Feese, M. D.; Cushman, M.; Pommier, Y.; Zembower, D.; Stewart, L.; Burgin, A. B. Structures of Three Classes of Anticancer Agents Bound to the Human Topoisomerase I-DNA Covalent Complex. *Journal of Medicinal Chemistry*, **(2005)**, 48; 2336-2345.

Recently, another experiment, conduced in synergy between American and Holland researcher, seems to better clarify another crucial aspect of the CPT mechanism of action[26].

Following a previous work conducted on the Topoisomerase I-DNA interaction[27], these researchers fixed one of the two DNA double strand extremities to a magnetic bead (1µm of diameter) and the other one to a solid support.

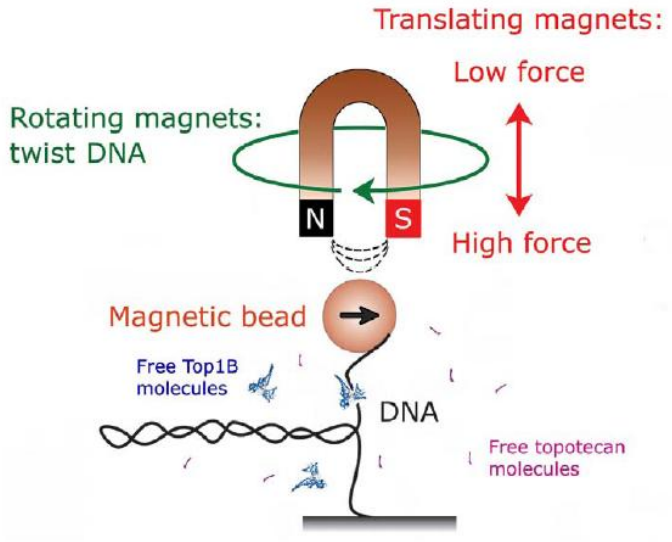

All this apparatus, called "magnetic tweezer" was placed firstly into a solution containing only the TopoI enzyme and, subsequently, into a solution containing TopoI and Topotecan.

In the first solution the DNA is mechanically coiled in the presence of TopIB, introducing multiple plectonemes that reduce the DNA extension. Looking at the figure showed above, a plateau (here from 25 to 100 s) is observed; this could correspond with the indication of a DNA in a supercoiled and unnicked state. The DNA is subsequently (at 100 s) rapidly uncoiled by the enzyme. An

[26] Koster, D. A.; Palle, K.; Bot, E. S.; Bjornsti, M. A.; Dekker, N. H. Antitumour drugs impede DNA uncoiling by topoisomerase I. *Nature* **(2007)**, *448*, 213–7
[27] See ref **10**

interesting feature that must be underlined concern the plectoneme removal: it occurs either in a single enzymatic event or in multiple steps depending of the TopoI concentration.

When the DNA is added to the second solution, a very different signature is observed. First, topotecan-mediated uncoiling occurs slowly compared with uncoiling in the absence of drug. Slow uncoiling is observed immediately following mechanical coiling and no plateau is observed, suggesting that religation does not take place. Moreover, this proceeds in a fashion that seems to be continuous (it can be fitted by a linear relation) and seems to continues for a longer periods of time.

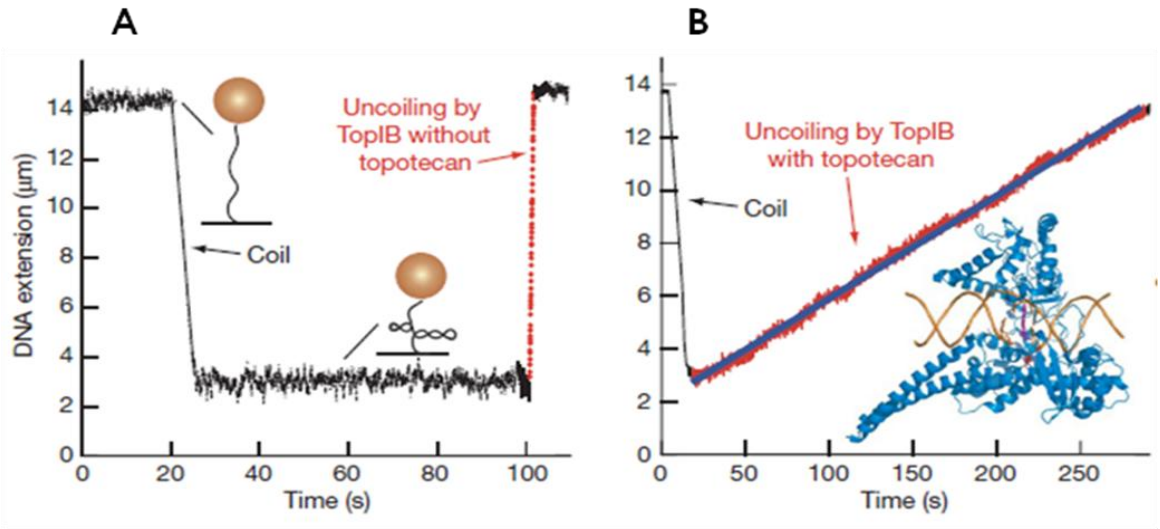

A further step was done. Analysing the data, the researcher were able to calculate that:

- topotecan-mediated uncoiling by TopoI occurs roughly 20-fold slower than uncoiling by TopoI alone (*4.1 µm/s*$^{-1}$ uncoiling speed of TopoI alone versus *0.2 µm/s*$^{-1}$ of TopoI involved into the ternary complex)

- in the presence of topotecan, TopoI remains trapped on the DNA for at least *121 s*. This timescale is about 400 times longer than the religation time in the absence of topotecan.

The experiment gave also precious information about enzymatic uncoiling rate of positive versus negative supercoils. In fact, in the absence of topotecan, no significant difference in this rate was detected. However, in the presence of drug, a clear and unexpected difference in supercoil removal rate could be appreciate: the uncoiling of positive supercoils is significantly slower than the uncoiling of negative supercoils.
This lead to the hypothesis that positive supercoils generated ahead of the fork (which cannot be efficiently removed by other topoisomerase enzymes, like the wild-type TopoII) may hamper fork progression. This mechanism, if correct, will replace the previous theory of the CPT mechanism of action based on the hindrance of the ternary complex to the replicative fork activity. Once again, the stalling of the replication machinery could result in fork collapse and in the formation of potentially lethal DNA lesions that induce apoptosys.

3. Aim of the work

Since the discover of the antiproliferative effect of the camptothecin, great efforts were made to understand the intimate nature of its mechanism of action. Biological studies were able to unravel the puzzle, finding its affinity with the binary complex estabilished between DNA and Topoisomerase I while several synthetic strategy underlined the structure-action relationship (SAR) of the molecule. However, all the details of this interaction remained obscure for years since the achievement of the first crystal of a ternary complex between Topotecan and binary complex (followed by a second crystal of the ternary complex with the camptothecin). These data were further extended by a second experiment devoted to the study of the dynamic properties of the ternary complex with the aid of a "magnetic tweezer".

Anyway, even with these precious information, lots of details are still unclear. Thus, to further investigate the molecular details of the poisoning mechanism of the camptothecin, we decided to study this system with the aid of another technique still unused for this kind of application.

From the wide spectrum of analytical technique available, we chose the electron paramagnetic spectroscopy (EPR).

Electron spin resonance (ESR) or electron paramagnetic resonance (EPR, a more general definition) spectroscopy is a technique for studying chemical species that have one or more unpaired electrons, such as organic and inorganic free radicals or inorganic complexes possessing a transition metal ion. The EPR technique guarantees great specificity, since ordinary chemical solvents and matrices do not give rise to EPR spectra.

The basic physical concepts of EPR are analogous to those of nuclear magnetic resonance (NMR), but it is electron spins that are excited instead of spins of atomic nuclei. A full explanation of the EPR theory is beyond the aim of this work (for those interested, a good EPR introduction could be found in

this book[28]). Nevetheless, some point must be explained, as to comprehend the EPR sprectra of the ternary complex. We will encounter only an organic paramagnetic species in this work, which is the tetramethylnitroxide moiety:

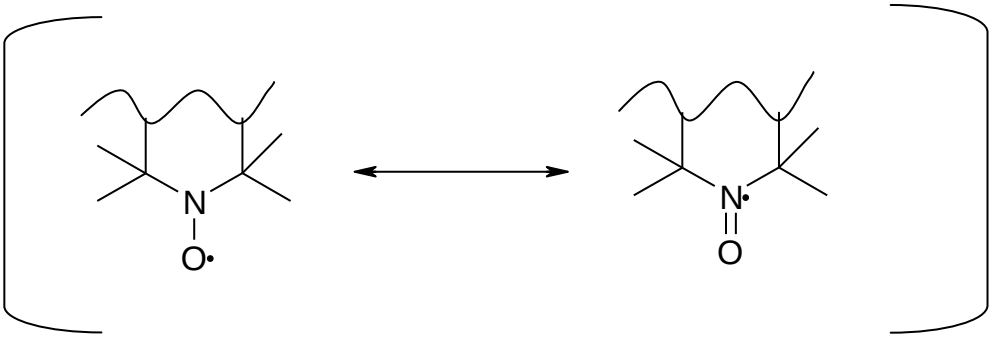

This radical is very stabilized by the hyperconjugation effect of the 4 methyl groups.

In a classical EPR experiment, the paramagnetic probe is dipped into a constant electric field; a variable magnetic field, meanwhile, scans the previous system for a desired range of Gauss (the magnetic field unity). When the magnetic field reaches the resonance value of the particular probe investigated, a signal is detected.

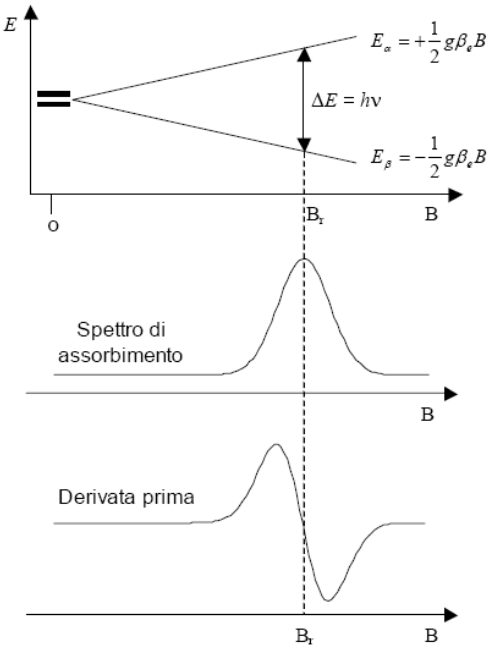

[28] Weil, J. A.; Bolton, J. R. Electron Paramagnetic Resonance: Elementary theory and Practical Application. *Wiley,* **(2007)**, 2° edition

To improve the signal/noise ratio, a derivation of the original signal is performed; the resonance value of the paramegnetic specie is thus found in the middle of the saddle of this first derivative. Moreover, when the paramagnetic probe is a nitroxide (for example, in our case) this signal is splitted into three similar peaks.

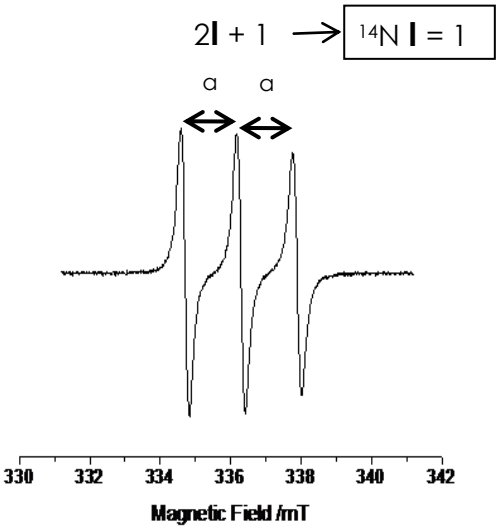

The splitting is caused by the interaction of the unpaired electron magnetic moment with the nuclear spin magnetic moment (the splitting rule is 2**I**+1, where **I** is the nuclear spin value). The number of the peaks and the distance between them gives direct information about the nature of the paramagnetic probe. In the nitroxide case, the unpaired electron seems to interact mainly with the nitrogen nucleus (which posses a nuclear spin magnetic moment of 1).

To reach our goal we used a technique called "site directed spin labeling" (SDSL), where a stable paramagnetic moiety is placed inside a specific site of the system investigated as to record its behavior. The most useful information arise from the mobility of the probe which deeply changes the spectrum aspect. As we will see later, in the discussion part, slowing down of the

nitroxide moiety lead to the broadned of the signal and the apparition of other components which superimpose the first spectrum. The diminished mobility could be due to a thermal condition (cooling the sample) or to a change in the hyndrance of the probe (if it interact with larger molecules).

The probe used for SDSL was the 4-amino-tetramethylpiperidin-1-oxyl (4-aminoTEMPO) which carries the stable nitroxide function and a reactive primary amine.
The TEMPO probe was then inserted into different components of the Topol-DNA-CPT ternary complex as to increase the number of potential interesting data.

4. Experimental part

4.1 Materials and Instruments

Materials

Reagents

All the reagents were purchased from Sigma-Aldrich, Fluka and Glen Reasearch (for oligonucleotide synthesis) and were used without further purifications.

Solvents

All solvents were purchased from Normapur Prolabo, Sigma-Aldrich, Riedel-De Haën and Glen Research. The pyridine was distilled over anhydrous KOH, the DMF was distilled under reduced pressure over BaO, the THF was distilled in presence of metallic sodium and benzophenone and the CH_2Cl_2 was distilled over CaH_2.

Deuterated solvents

All the deuterated solvents were purchased from Sigma-Aldrich.

TLC plates

A Merck Silica Gel 60 F_{254} glass plates were used for TL chromatography.

Stationary phase for LC

A Fluka Silica Gel 60 (220-440 Mesh) was used for liquid chromatography.

Instruments

Nuclear Magnetic Resonance (NMR)

A Bruker AMX 300 was used to record NMR experiments.

Infrared Spectroscopy (IR)

The IR experiments were performed with a Perkin-Elmer 1760 Infrared Fourier Trasformation Spectrometer.

Mass Spectrometry (MS)

The HRMS were obtained with a Mariner™ API-TOF System 5220 (ESI ionizer) spectrometer..

SYNTHESIS SCHEME I

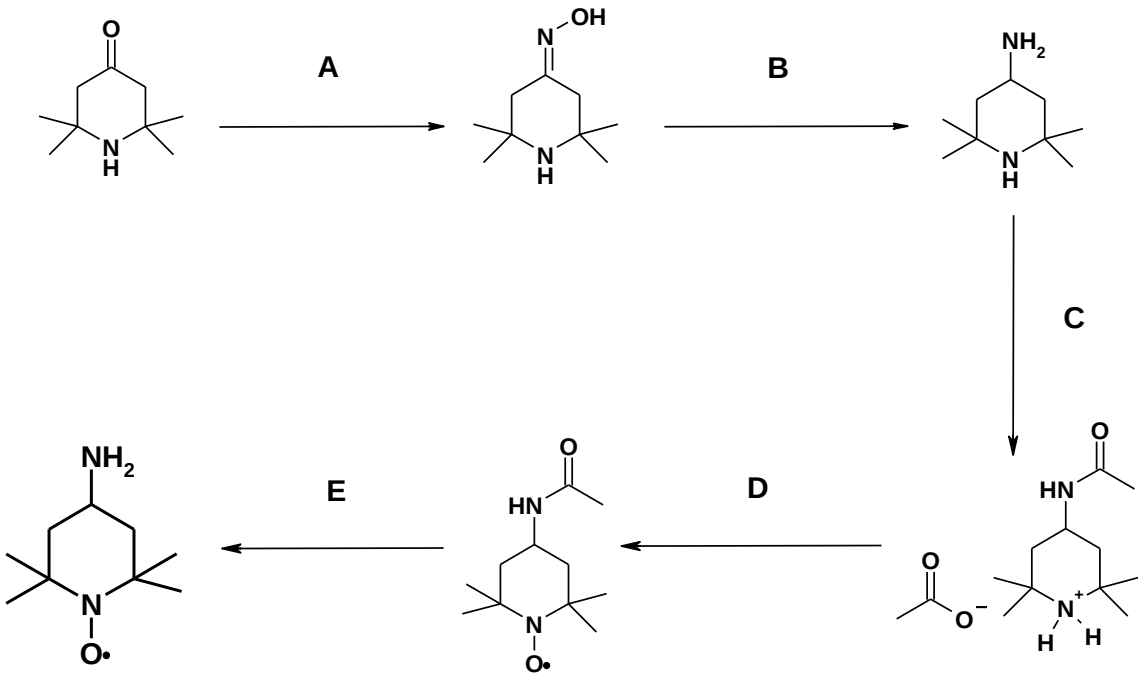

A) Hydroxylamine hydrochloride, sodium acetate, H_2O, 60 °C, 30 min (Yield 96%); **B)** $LiAlH_4$, THF, RT then reflux for 2h (Yield 98%); **C)** Acetic anhydride, Et_2O, 0 °C, 15 min (Yield 49%); **D)** Na_2CO_4, Na_2WO_4, EDTA•$4Na^+$, H_2O_2 30%,H_2O, 3 d, RT (Yield 89.5%); **E)** KOH 15%, H_2O, 24 h, reflux (Yield 92%)

Synthesis of **2,2,5,5-tetramethylpiperidin-4-oxime**

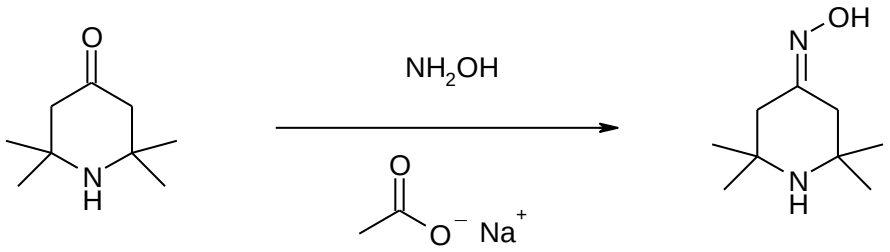

Components	Molecular formula	Molecular Weight	Volume	Weight	Density	n° of Mols
Triacetoneamine	$C_9H_{17}NO$	155 g/mol		10 g		64,52 mmol
Hydroxylamine hydrochloride	NH_2OH	69,5 g/mol		6,71 g		96,53 mmol
Sodium acetate	$C_2H_3O_2Na$	82.03 g/mol		15,84 g		193,06 mmol

6,71 g of hydroxylamine hydrochloride were added to a solution of 15,84 g of sodium acetate in H_2O (50 ml) and the whole was heated to 60 °C. Ten grams of triacetonamine was after added to the solution and the reaction mixture was kept at this temperature for 30 minutes. The reaction was cooled and the precipitate was filtered and dried to obtain 14 g of 2,2,5,5-tetramethylpiperidin-4-oxime acetate (Yield 96%). To obtain the free base the salt was solved in water; the solution was saturated with Na_2CO_3, extracted with EtOAc, dried with Na_2SO_4 and evaporated in vacuo.

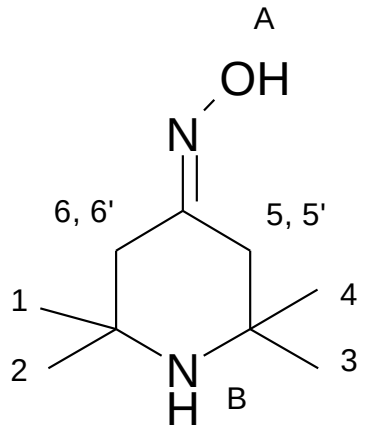

Molecular Weight	**Molecular Formula**
170.25 g/mol	$C_9H_{18}N_2O$

^{1}HNMR (Acetone-*d6*; 300MHz,) δ (ppm): 9,51 (s, 1H; H^A), 2,96 (s, 1H; H^B), 2,34 (s, 2H; $H^{5,6}$), 2,15 (s, 2H; $H^{5',6'}$), 1,113 (s, 6H; $H^{1,4}$), 1,11 (s, 6H; $H^{2,3}$)

HRMS (ESI): calcd for $C_9H_{19}N_2O$ ($M+H^+$) 171.1392, found 171.1276

Synthesis of **4-amino-2,2,5,5-tetramethylpiperidine**

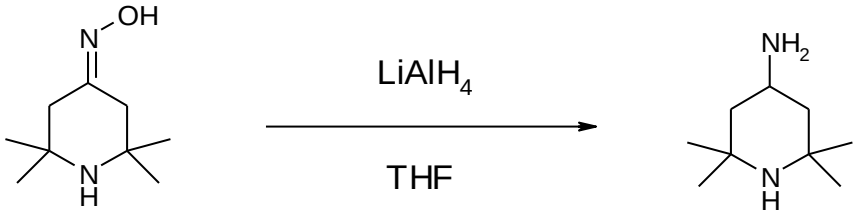

Components	Molecular formula	Molecular Weight	Weight	Density	n° of Mols
2,2,5,5-tetramethylpiperidin-4-oxime	$C_9H_{18}N_2O$	170 g/mol	2 g		11,76 mmol
Lithium Aluminium Hydride	$LiAlH_4$	37,95 g/mol	1,34 g		35,3 mmol

In a three neck flask fitted with a bubble condenser was placed 2 grams of 2,2,5,5-tetramethylpiperidin-4-oxime in 25 ml of THF and nitrogen was bubbled into the mixture. The mixture was cooled to 0 °C and 35,3 ml of a 1,0 M solution of $LiAlH_4$ in THF was slowly added to the suspension. After the formation of hydrogen the suspension was heated to reflux for 3h (the reaction was monitored with TLC eluent EtOAc : methanol 1:1). After the formation of the product (observed using an ethanolic solution of ninhydrin) the reaction was cooled to RT, quenched with 635 µl of H_2O, 635 µl of a 5% NaOH acqueous solution and 1,5 ml of H_2O and filtered. The solution filtered was anhydrified with Na_2SO_4 and dried in vacuo to obtain an oil (1,8 g) which was used in the next step without further purification.

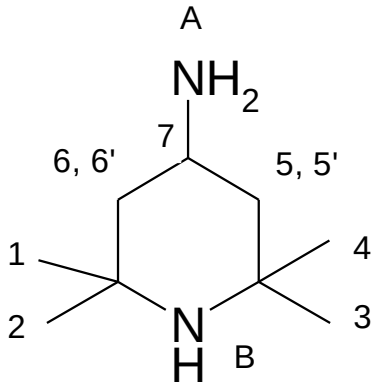

Molecular Weight	**Molecular Formula**
156.27 g/mol	$C_9H_{20}N_2$

^{1}HNMR (Acetone-*d6*; 300MHz,) δ (ppm): 4,30-4,15 (tt, 1H, J_1 = 12.5 Hz, J_2 = 3.7 Hz; H^7), 3.05 (s, 1H; H^B), 2.50 (s, 2H; H^A), 2.10 (s, 2H, *J* = 3.7 Hz; $H^{5,6}$), 2,06 (s, 2H, *J* = 3.7 Hz; $H^{5',6'}$), 1,20 (s, 6H; $H^{1,4}$), 1,15 (s, 6H; $H^{2,3}$)

HRMS (ESI): calcd for $C_9H_{21}N_2$ ($M+H^+$) 157.1699 found 158.1579

Synthesis of **4-acetamido-2,2,5,5-tetramethylpiperidine acetate**

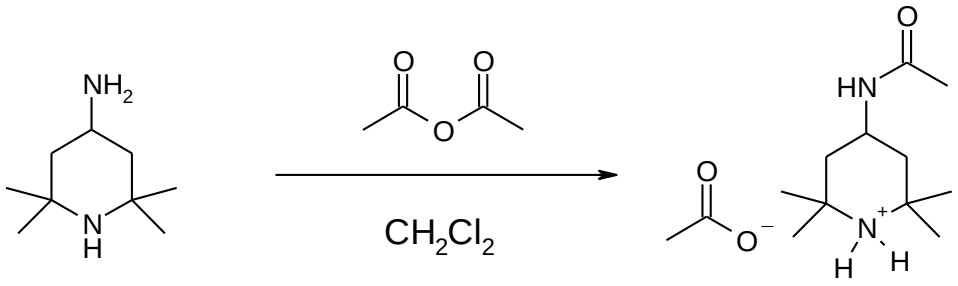

Components	Molecular formula	Molecular Weight	Weight	Density	n° of Mols
4-amino-2,2,5,5-tetramethylpiperidine	$C_9H_{20}N_2$	151 g/mol	1,8 g		11,92 mmol
Acetic anhydride	$C_4H_6O_3$	102,1 g/mol	2,43 g	1,08 g/mol	23,84 mmol

A round bottomed flask was charged with 1,8 g of 4-amino-2,2,5,5-tetramethylpiperidine and 10 ml of $(Et)_2O$. The solution was cooled to 0 °C and 2,25 ml of acetic anhydride were slowly dropped in order to keep the temperature under 20 °C. The mixture was allowed to stand at room temperature for 2h after which a with precipitate is formed. The solvent was removed and the precipitate was washed with acetone and dried to obtain 1,5 g of pure 4-acetamido-2,2,5,5-tetramethylpiperidine acetate (Yield 49%)

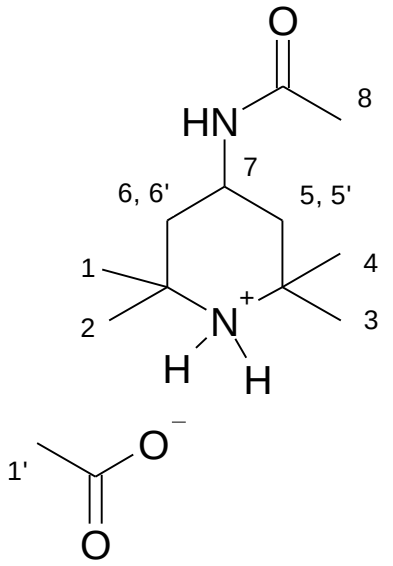

Molecular Weight	**Molecular Formula**
258.35 g/mol	$C_{13}H_{25}N_2O_3$

^{1}HNMR (D2O, 300MHz) δ (ppm): 4,18-4,29 (tt, 1H, J_1 = 12.3 Hz, J_2 = 3.5 Hz; H^7), 2,05-2,06 (d, 2H, J = 3.5 Hz; $H^{5,6}$), 2,00-2,02 (d, 2H, J = 3.5 Hz; $H^{5',6'}$), 1,96 (s, 3H; $H^{1'}$), 1,89 (s, 3H; H^8), 1,50 (s, 6H; $H^{1,4}$), 1,40 (s, 6H; $H^{2,3}$)

HRMS (ESI): calcd for $C_{11}H_{22}N_2O$ ($M+H^+$) 199.1805 found 199.1931

Synthesis of **4-acetamido-2,2,5,5-tetramethylpiperidine-1-oxyl (4-acetamidoTEMPO)**

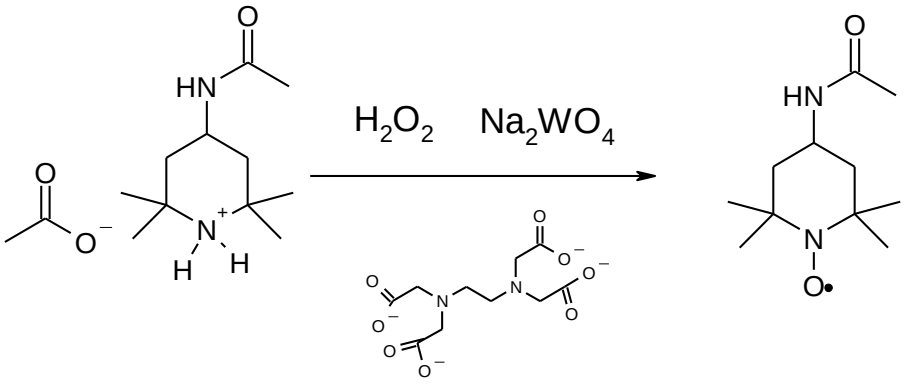

Components	Molecular formula	Molecular Weight	Weight	Density	n° of Mols
4-acetamido-2,2,5,5-tetramethylpiperidine acetate	$C_{13}H_{26}N_2O_3$	258 g/mol	500 mg		1,92 mmol
Sodium Carbonate	Na_2CO_3	106 g/mol	989 mg		9,33 mmol
Sodium Tungstate dihydrate	Na_2WO_4	329,85 g/mol	79 mg		0,24 mmol
EDTA-4Na	$C_{10}H_{12}N_2O_8Na_4$	360 g/mol	79 mg		0,219 mmol
Hydrogen peroxide	H_2O_2	34 g/mol	1,58 ml		

In a 250 ml round-bottomed flask 500 mg of 4-acetamido-2,2,5,5-tetramethylpiperidine acetate were solved in 20 ml of a 5% sodium carbonate water solution (in order to free the amino function). 79 mg of EDTA-4Na and 79 mg of sodium tungstate were further added before cooling the solution to 0-4 °C (ice bath).

At this point 1,58 ml of cold hydrogen peroxide was dropped into the clear solution and then the mixture was allowed to warm at RT and leaved at this temperature for 72 h (you will observe a first turn of the solution from clear to yellow and then to orange; after one day you will observe the formation of a

orange precipitate). The suspension thus obtained was filtered and the solution separated was saturated with sodium carbonate. The new orange precipitate formed was again filtered, collected with the previous one and dried to obtain 370 mg of 4-acetamidoTEMPO as orange crystals. Yield 89,5% [you can also solve the orange precipitate in ethyl acetate, remove the watery phase in a separation funnel, dry the organic phase with Na_2SO_4 and evaporate the solvent to obtain the product free of water impurities]

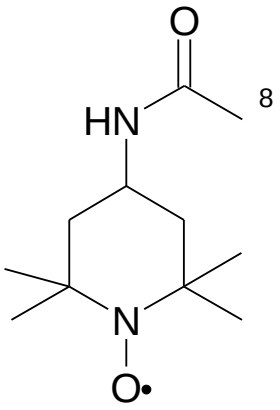

Molecular Weight	**Molecular Formula**
213.30 g/mol	$C_{11}H_{21}N_2O_2$

^{1}HNMR (Acetone-*d6*, 300MHz) δ (ppm): 1,90 (bs, 3H; H^8), from -15 to -35 (bm, 16H; H^{TEMPO})

HRMS (ESI): calcd for $C_{11}H_{22}N_2O_2$ ($M+H^+$) 214.1676 found 214.1458

Synthesis of **4-amino-2,2,5,5-tetramethylpiperidine-1-oxyl (4-aminoTEMPO, TEMPOamine)**

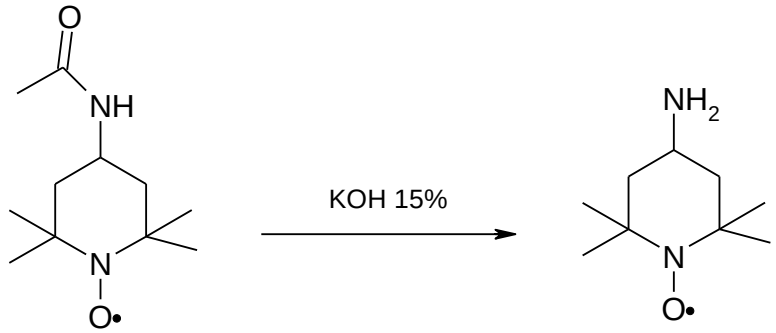

Components	Molecular formula	Molecular Weight	Weight	Density	n° of Mols
4-acetamido-2,2,5,5-tetramethylpiperidine acetate	$C_{13}H_{26}N_2O_3$	258 g/mol	500 mg		1,92 mmol
Sodium Carbonate	Na_2CO_3	106 g/mol	989 mg		9,33 mmol

200 mg of 4-acetamidoTEMPO were suspended into 12,5 ml of a 15%KOH aqueous solution and the whole was heated to reflux. The reaction was monitored by TLC (eluent EtOAc, Rf 0,1) until the complete disappear of the starting material. After 36 h the solution obtained was cooled to RT, saturated with potassium carbonate and extracted with diethyl ether. The organic phase was anhydrified over Na_2SO_4 and dried to obtain 147 mg of 4-aminoTEMPO as a red liquid that crystallize at 4 °C. Yield: 92,0 %

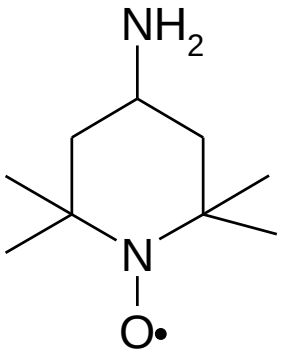

Molecular Weight	**Molecular Formula**
171.26 g/mol	$C_9H_{19}N_2O$

^{1}HNMR (Acetone-*d6*, 300MHz) δ (ppm): from -15 to -35 (bm, 16H; H^{TEMPO})

HRMS (ESI): calcd for $C_9H_{20}N_2O$ ($M+H^+$) 172.1570 found 172.1344

IR (KBr): 2973 (ν_{as} $^{TEMPO}CH_3$), 2936 (ν_s $^{TEMPO}CH_3$), 1459-1363 (δ $^{TEMPO}CH_3$)

SYNTHESIS SCHEME II

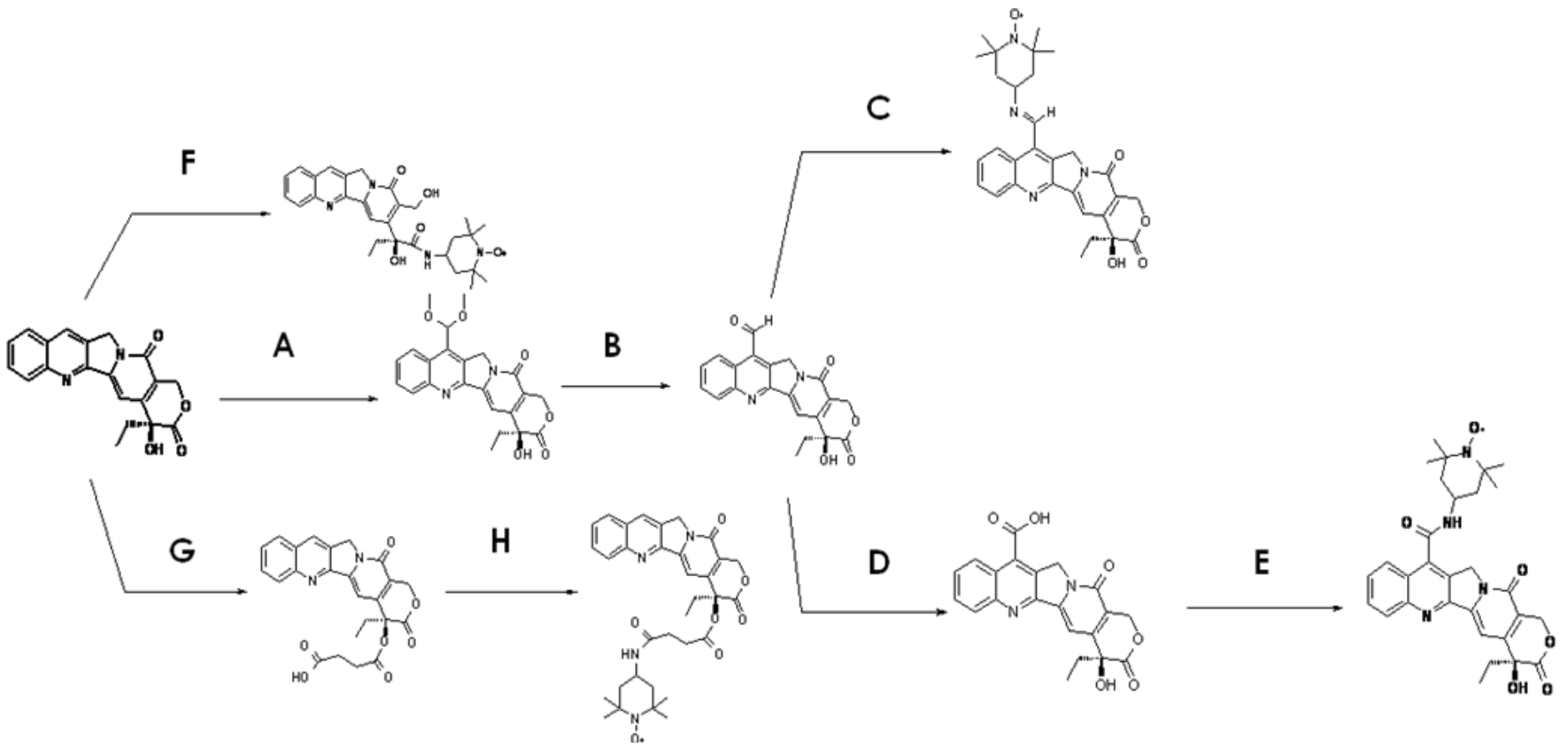

A) H_2SO_4, MeOH, $FeSO_4$,, H_2O_2 30%, then Mn_2O, RT, 2 h (Yield 20%); **B)** CH_3COOH, H_2O, reflux, 1 h (Yield 75%); **C)** TEMPOamine,Ytterbium triflate, molecular sieve 4Å, CH_2Cl_2, RT, 16 h (Yield 22%); **D)** HCOOH, H_2O_2 30%, 0 °C, 16 h (Yield 75%); **E)** TEMPOamine, HBTU, HOBt, DIPEA, THF, RT, 16 h (Yield 67%); **F)** TEMPOamine, pyridine, 60 °C, 4 d (Yield 20%); **G)** Succinic anhydride, DMAP, pyridine, 80 °C, 24 h (Yield 92%); **H)** TEMPOamine, HBTU, HOBt, DIPEA, CH_2Cl_2, RT, 16 h (Yield 75%)

Synthesis of **7-dimethoxymethylcamptothecin**

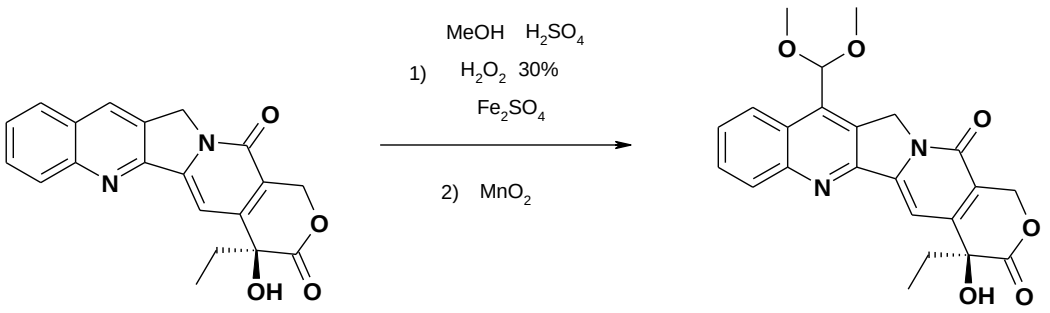

Components	Molecular formula	Molecular Weight	Volume	Weight	Density	n° of Mols
Camptothecin	$C_{20}H_{16}N_2O_4$	347 g/mol		347 mg		1 mmol
Sulphuric acid	H_2SO_4	56 g/mol	2.1 ml			
Ferrous sulphate	Fe_2SO_4			278 mg		1 mmol
Hydrogen peroxide 30%	H_2O_2	34 g/mol	215 µl	312 mg	1.46 g/ml	9.19 mmol
Manganese dioxide	MnO_2			130 mg		1.49 mmol

To a suspension of 347 mg of camptothecin in 21 ml of methanol, 2.1 ml of conc. H_2SO_4 and 278 mg of ferrous sulphate were added. The yellow solution obtained was heated to 50° afterwhich 215 µl of hydrogen peroxide (30% in water) was dropped into it. The reaction was monitored by TLC (eluent CH_2Cl_2:MeOH 95:5) until the disappear of the starting material; 130 mg (1.49 mmol) of manganese dioxide were then added to the mixture.. The black suspension was stirred for 2h at RT, filtered and concentrated to 1/3 of the starting volume. Water (25 ml) was added to the residue and the acid solution was neutralized with a 35% solution of NaOH. The yellow precipitated thus formed was collected, washed with water (three times) and dried to obtain 300 mg of 7-formylcampotecin which was used in the next step without

further purification. A sample was purified by silica gel chromatography (eluent CH_2Cl_2:MeOH 97:3) in order to characterize it.

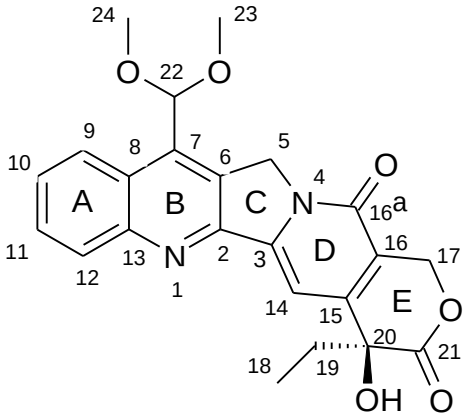

Molecular Weight	Molecular Formula
422.44 g/mol	$C_{23}H_{22}N_2O_6$

^{1}HNMR (CD_3Cl, 300MHz) δ (ppm): 8.31 (m, 2H; H^{9-12}), 7.80 (t, 1H, *J* = 8.3 Hz; H^{11}), 7.66 (m, 2H; H^{10-14}), 6.24 (s, 1H; H^{22}), 5.47 (s, 2H; H^{17}), 5.28-5.78 (dd, *J* = 15.8 Hz; 2H; H^5), 3.43 (s, 3H; H^{24}), 3.40 (s, 3H; H^{23}), 1.92 (m, 2H; H^{19}), 1.03 (t, 3H, *J* = 7.2; H^{18})

HRMS (ESI): calcd for $C_{23}H_{23}N_2O_6$ ($M+H^+$) 423.1551, found 423.1558.

Synthesis of **7-formylcamptothecin**

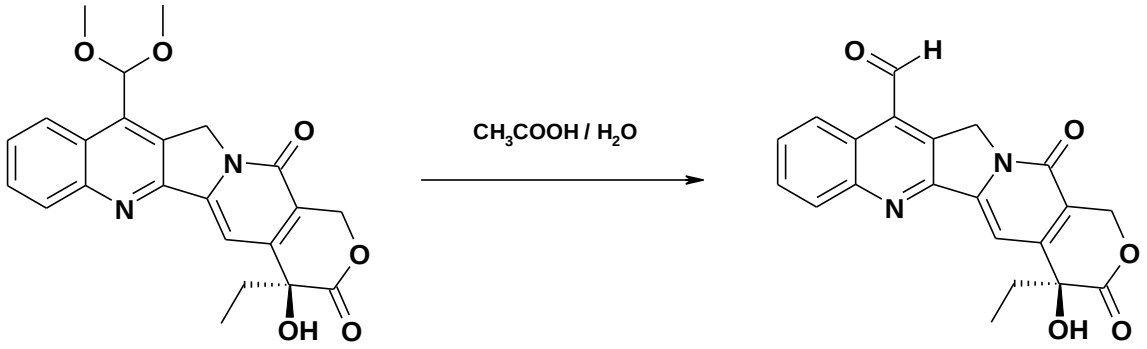

Components	Molecular formula	Molecular Weight	Volume	Weight	Density	n° of Mols
7-Camptothecin dimethoxyacetal	$C_{23}H_{22}N_2O_6$	422,4 g/mol		300 mg		0,71 mmol
Acetic Acid	$C_2H_4O_2$	56 g/mol	6 ml			

300 mg (0,71 mmol) of 7-dimethoxymethylcamptothecin were solved into 10 ml of an acetic acid/water mixture (3:2 ratio) and the solution was heated to reflux (you can observe the formation of a yellow precipitate after 15 min that solves again after 30 min and suddenly reappear after 5 min). After 1 h the suspension was allowed to cool to RT, the precipitate formed was filtered, washed with water and purified by silica gel chromatography (eluent CH_2Cl_2: MeOH 97: 3). 200 mg of 7-formylcamptothecin were obtained as a yellow solid. Yield 75%

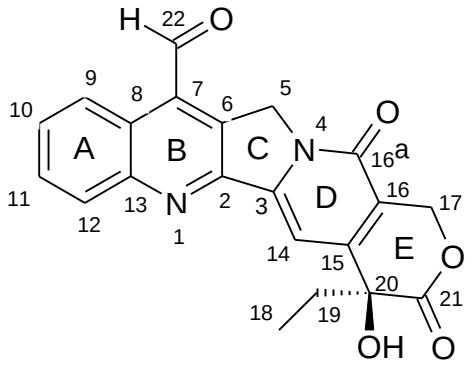

Molecular Weight	Molecular Formula
376.37 g/mol	$C_{21}H_{16}N_2O_5$

^{1}HNMR (CD_3Cl, 300MHz) δ (ppm): 11.20 (s, 1H; H^{22}), 8.77 (d, 1H, *J* = 8,1 Hz; H^9), 8.38 (d, 1H, *J* = 8,3 Hz; H^{12}), 7.90 (m, 2H; $H^{10\text{-}11}$) 7.33 (s, 1H; H^{14}), 5.62 (s, 2H; H^{17}), 5.20-5.70 (dd, 2H, *J* = 16 Hz; H^5), 1.90 (m, 2H; H^{19}), 1.05 (t, 3H, *J* = 7,3 Hz; H^{18})

HRMS (ESI): calcd for $C_{21}H_{17}N_2O_5$ ($M+H^+$) 377.1132, found 377.1121.

Synthesis of **7-(1-oxyl-2,2,5,5-tetramethylpiperidin-4-aminyl)-iminomethylcamptothecin (7-TEMPOiminocamptothecin)**

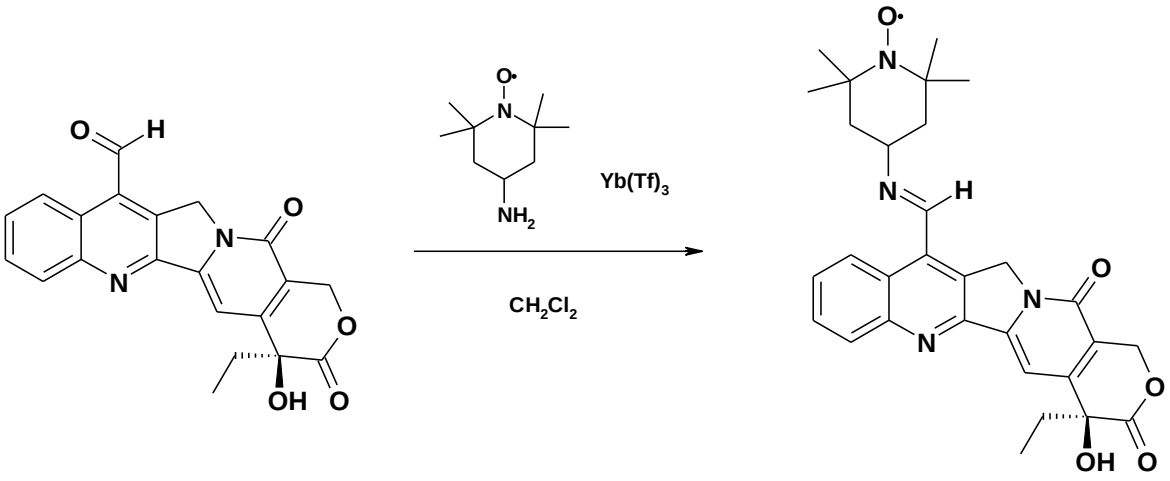

Components	Molecular formula	Molecular Weight	Volume	Weight	Density	n° of Mols
7-formylcamptothecin	$C_{21}H_{16}N_2O_5$	376,3 g/mol		50 mg		0,133 mmol
Ytterbium Trifluoromethansulphonate	$C_3O_9S_3F_9Yb$	620,25 g/mol		8 mg		0,013 mmol
TEMPOamine	$C_9H_{19}N_2$	171,26 g/mol		26,87 mg		0,22 mmol

In a round bottomed flask fitted with molecular sieves 4Å, 50 mg of 7-formylcamptothecin were suspended into 5 ml of dry CH_2Cl_2. 8 mg of $Yb(OTf)_3$ and 26 mg of 4-aminoTEMPO were further added. The mixture was allowed to react for 48 h afterwhich the sieves where removed by filtration. The solid was solved in CH_2Cl_2, washed with water (two times), anhydrified over Na_2SO_4 and finally purified by silica gel chromatography (eluent CH2Cl2: MeOH: $(Et)_2O$

96:2:2). 15 mg of 7-TEMPO-iminocamptothecin were obtained as a yellow solid. Yield 22%.

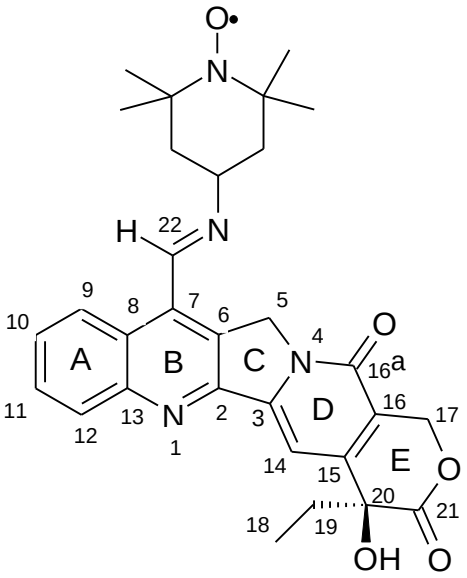

Molecular Weight	Molecular Formula
529.62 g/mol	$C_{30}H_{33}N_4O_5$

^{1}HNMR (CD_3Cl, 300MHz) δ (ppm): 9.69 (bs, 1H; H^{22}), 8.73 (bs, 1H; H^9), 8.26 (bs, 1H; H^{12}), 7.93 (m, 1H; H^{10}), 7.78 (m, 1H, H^{11}), 7.50 (s, 1H; H^{14}), 5.60 (s, 2H; H^{17}), 5.20-5.70 (m, 2H; H^5), 1.90 (m, 2H; H^{19}), 1.04 (bs, 3H; H^{18}), from -15 to -35 (bm, 16H; H^{TEMPO})

IR (KBr): 2973 (ν_{as} $^{TEMPO}CH_3$), 2936 (ν_s $^{TEMPO}CH_3$), 1746 (ν C=O, lactone), 1658 (ν C=O, amide), 1606 (ν C=N, immine), 1459-1363 (δ $^{TEMPO}CH_3$)

HPLC PURITY: 97%

Synthesis of **7-carboxycamptothecin**

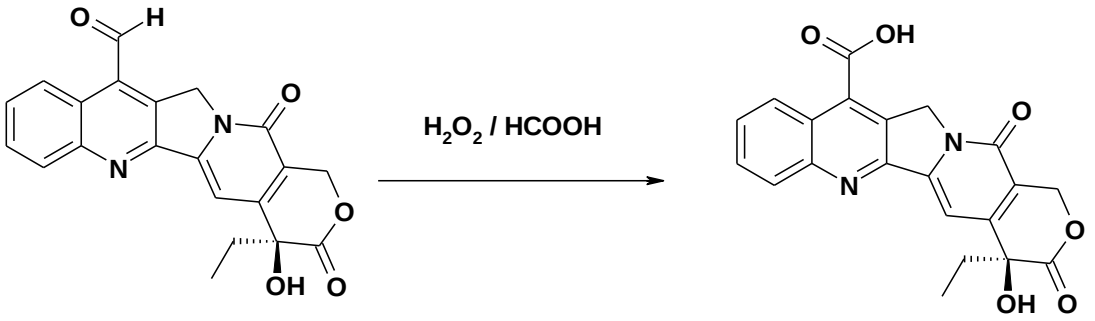

Components	Molecular formula	Molecular Weight	Volume	Weight	Density	n° of Mols
7-formyl camptothecin	$C_{21}H_{16}N_2O_5$	376,3 g/mol		100 mg		0,27 mmol
Formic Acid	CH_2O_2	46 g/mol	1,3 ml		1,22 g/ml	34,48 mmol
Hydrogen peroxide	H_2O_2	34 g/mol	41 µl	45,9 mg	1,12 g/ml	1,35 mmol

100 mg of 7-formylcamptothecin (0,13 mmol) were solved into 1,3 ml of formic acid (the solution obtained is red). The mixture was cooled to 0-4 °C (ice bath), added of 41 µl of hydrogen peroxide (the solution turns to yellow after few minutes) and leaved at the previous temperature overnight.

The yellow suspension thus obtained was filtered from the solvent, washed with water (to eliminate the formic acid) and dried to obtain 80 mg (0,20 mmol) of 7-carbossicamptothecin as a bright yellow solid. Yield 75,6 %.

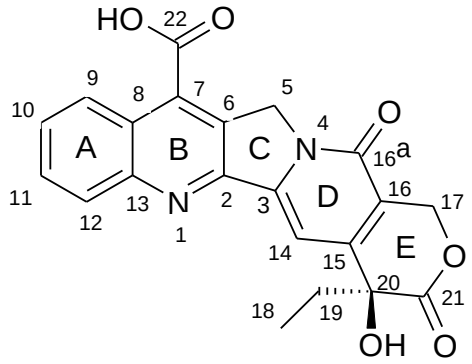

Molecular Weight	Molecular Formula
392.37 g/mol	$C_{21}H_{16}N_2O_6$

^{1}HNMR (CD_3Cl, 300MHz) δ (ppm): 13.8 (bs, 1H; H^{COOH}), 8.90 (bs, 1H; H^9), 8.30 (bs, 1H; H^{12}), 7.92 (m, 1H; H^{10}), 7.70 (m, 1H; H^{11}), 7.53 (s, 1H; H^{14}), 5.60 (s, 2H; H^{17}), 5.71 (d, 1H, *J* = 16.2 Hz; H^5), 5.23 (d, 1H, *J* = 16.2 Hz; H^5), 1.96 (m, 2H; H^{19}), 1.08 (bs, 3H; H^{18})

HRMS (ESI): calcd for $C_{21}H_{16}N_2O_6$ ($M\text{-}H^+$) 391.0935, found 391.0936.

Synthesis of **7-(1-oxyl-2,2,5,5-tetramethylpiperidin-4-aminyl)-amidocamptothecin (7-TEMPOamidocamptothecin)**

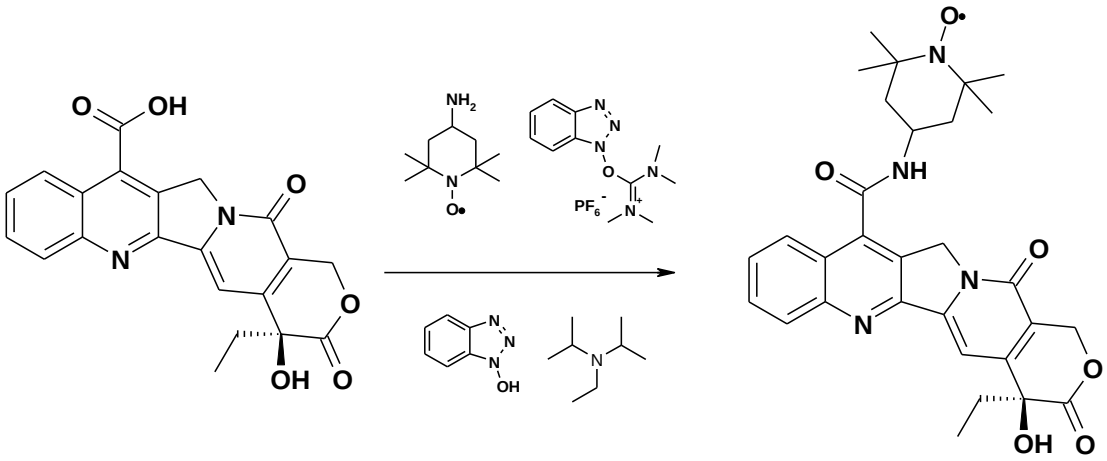

Components	Molecular formula	Molecular Weight	Volume	Weight	Density	n° of Mols
7-carboxy-camptothecin	$C_{21}H_{16}N_2O_6$	391 g/mol		15 mg		0,038 mmol
Hydroxybenzotriazole hexafluorophosphate (HBTU)	$C_{11}H_{16}F_6N_5OP$	379.30 g/mol		17 mg		0,045 mmol
Hydroxybenzotriazole (HOBt)	$C_6H_5N_3O$	135.12 g/mol		6 mg		0.045 mmol
Diisopropyletylamine (DIEA)	$C_8H_{19}N$	129.25 g/mol	15.67 µl		0.755 g/ml	0.09 mmol
TEMPOamine	$C_9H_{19}N_2O$	171 g/mol		19,50 mg		0,114 mmol

In a round bottomed flask was placed a suspension of 15 mg (0,038 mmol) 7-carboxycamptothecin in 5 ml of freshly distilled THF. To the mixture were added firstly 17 mg of HBTU, 6.08 mg of HOBt and 15.67 µl of DIEA; then, after 10 min, 19,5 mg of of TEMPOamine (the suspension turn its colour to a darker yellow). The reaction was stirred at RT overnight during that the formation of a

solution was observed (the reaction was also monitored by TLC using CH_2Cl_2:MeOH 97:3 as eluent). After 18 h this solution was dried and the yellow solid solved again in CH_2Cl_2, washed two times with a 10 % $NaHCO_3$ aqueous solution (to remove the unreacted carboxylic acid), two times with a 0,3 M solution of citric acid in H_2O (in order to remove the unreacted TEMPOamine) and finally with brine. The organic phase was anhydrified with Na_2SO_4 and dried in vacuo to obtain 14 mg of 7-TEMPOamidocamptothecin as a yellow solid. Yield 67,6 %.

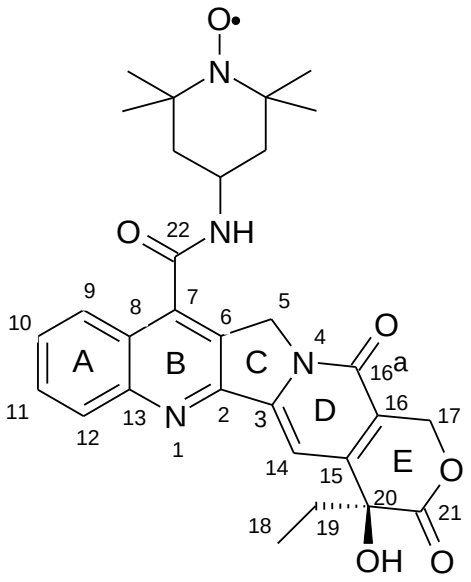

Molecular Weight	Molecular Formula
545.62 g/mol	$C_{30}H_{33}N_4O_6$

^{1}HNMR (CD_3Cl, 300MHz) δ (ppm): 8.73 (bs, 1H; H^9), 8.26 (bs, 1H; H^{12}), 7.93 (m, 1H; H^{10}), 7.78 (m, 1H, H^{11}), 7.50 (s, 1H; H^{14}), 5.60 (s, 2H; H^{17}), 5.20-5.70 (m, 2H; H^5), 1.90 (m, 2H; H^{19}), 1.04 (bs, 3H; H^{18}), from -15 to -35 (bm, 16H; H^{TEMPO})

HRMS (ESI): calcd for $C_{30}H_{34}N_4O_6$ ($M+H^+$) 546.2473, found 546.2487

IR (KBr): 2963 (ν_{as} $^{TEMPO}CH_3$), 2864 (ν_s $^{TEMPO}CH_3$), 1744 (ν C=O, lactone), 1655 (ν C=O, amide 3ª), 1603 (ν C=O, TEMPOamide), 1458-1363 (δ $^{TEMPO}CH_3$)

HPLC PURITY: ~99 %

Synthesis of **camptothecin-O-succinylester**

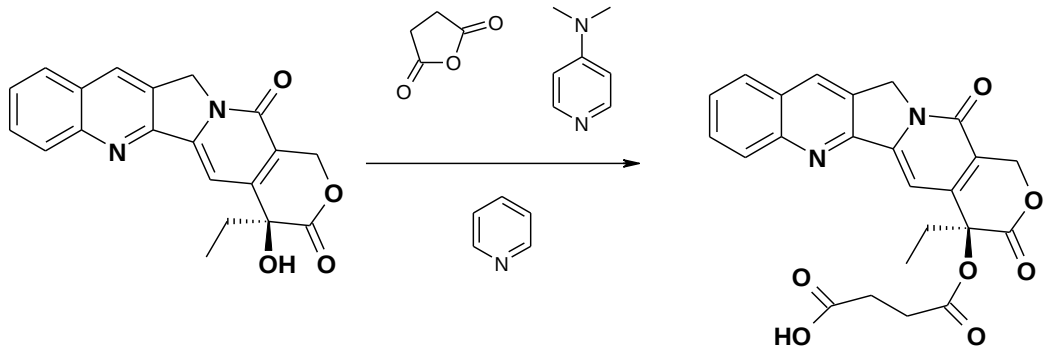

Components	Molecular formula	Molecular Weight	Volume	Weight	Density	n° of Mols
Camptothecin	$C_{20}H_{16}N_2O_4$	347 g/mol		600 mg		1,72 mmol
Succinic anhydride	$C_4H_4O_3$	100 g/mol		3,45 g		34,48 mmol
Dimethylaminopyridine (DMAP)	$C_7H_{10}N_2$	171 g/mol		83 mg		0,68 mmol

600 mg of camptothecin, 3.45 g of succinic anhydride and 171 mg of DMAP were suspended into 10 ml of dry pyridine. The suspension was heated to 80°C under stirring and monitored by TLC (eluent CH_2Cl_2:MeOH 97:3) until complete disappear of the starting material (around 24 h). The solvent was removed under vacuum and the residue was suspended into methanol (50ml). The suspension was heated to reflux for 2h, cooled to 0 °C, the white pearl precipitate filtered, washed with methanol and dried. Yield 92%.

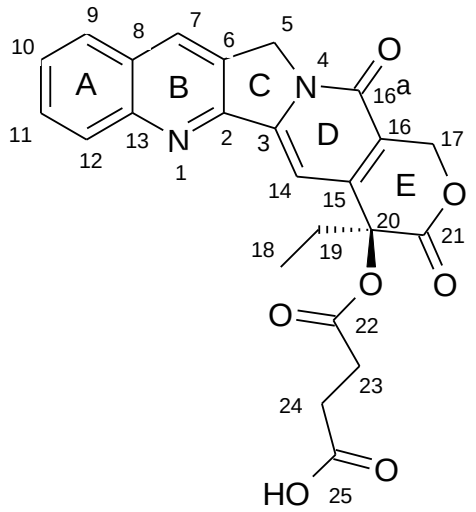

Molecular Weight	Molecular Formula
448.44 g/mol	$C_{24}H_{20}N_2O_7$

^{1}HNMR (DMSO-*d6*, 300MHz) δ (ppm): 12.20 (bs, 1H; H^{COOH}), 8.60 (d, 1H, *J* = 7,1 Hz; H^9), 8.09 (m, 2H; H^{12}), 7.82 (m, 1H; H^{10-11}), 7.65 (m, 1H; H^{14}), 7.07 (s, 1H; H^7), 5.43 (s, 2H; H^{17}), 5.21 (d, 2H, *J* = 8.5 Hz; H^5), 2.75 (m, 2H; H^{24}), 2.43 (m, 2H; H^{23}), 2.10 (q, 2H, *J* = 7 Hz; H^{19}), 0.90 (t, 3H, *J* = 7 Hz; H^{18})

HRMS (ESI): calcd for $C_{24}H_{19}N_2O_7$ ($M\text{-}H^+$) 447.1198, found 447.1187.

Synthesis of **camptothecin-O-succinyl-(1-oxyl-2,2,5,5-tetramethylpiperidin-4-aminyl)-amide**

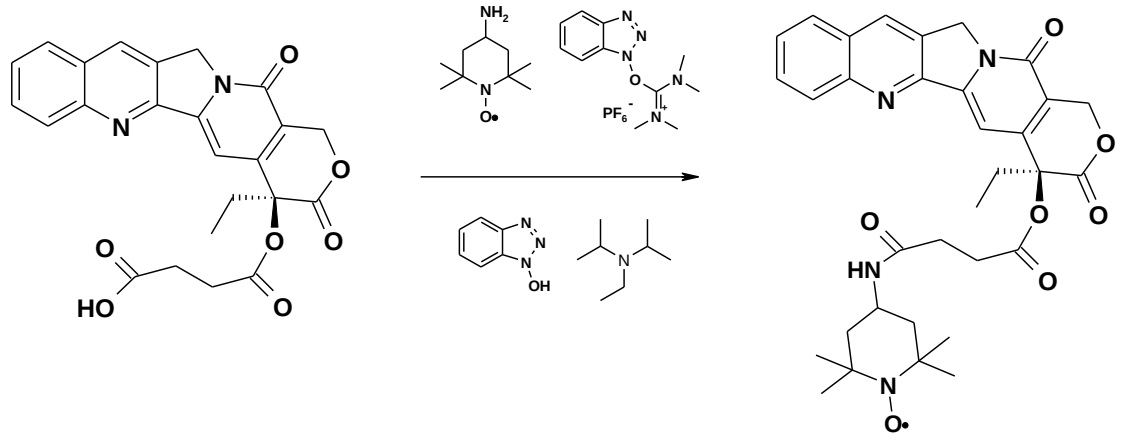

Components	Molecular formula	Molecular Weight	Volume	Weight	Density	n° of Mols
camptothecin-O-succinylester	$C_{24}H_{18}N_2O_7$	447 g/mol		45 mg		0,10 mmol
Hydroxybenzotriazole hexafluorophosphate (HBTU)	$C_{11}H_{16}F_6N_5OP$	379.30 g/mol		41.72 mg		0,11 mmol
Hydroxybenzotriazole (HOBt)	$C_6H_5N_3O$	135.12 g/mol		14.86 mg		0.11 mmol
Diisopropyletylamine (DIEA)	$C_8H_{19}N$	129.25 g/mol	38.32 µl		0.755 g/ml	0.22 mmol
TEMPOamine	$C_9H_{19}N_2O$	171 g/mol		31.20 mg		0,20 mmol

A suspension of 45 mg of 7-carboxy-camptothecin in 5 ml of freshly distilled CH_2Cl_2 was mixed firstly with 41.72 mg of HBTU, 14.86 mg of HOBt and 38.32 µl of DIEA then, after 10 min, with 31.20 mg of TEMPOamine. The reaction was stirred at RT overnight after which it was washed two times with a 10 % $NaHCO_3$ aqueous solution (to remove the unreacted carboxylic acid), two times with a 0,3 M solution of citric acid (in order to remove the unreacted

TEMPOamine) in H_2O and with brine. The organic phase was anhydrified with Na_2SO_4 and dried in vacuo to obtain 14 mg of camptothecin-O-succinyl-(1-oxyl-2,2,5,5-tetramethylpiperidin-4-amminyl)-amide with a 75% yield.

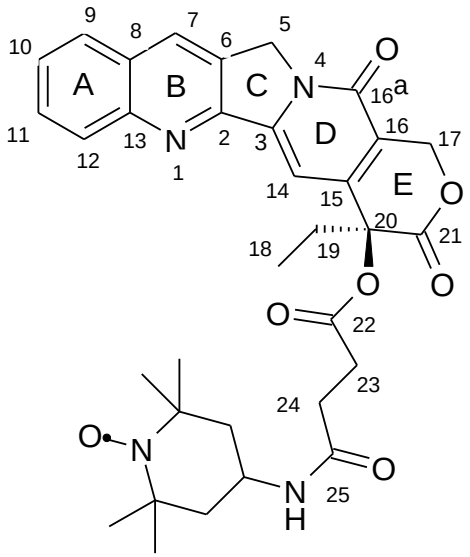

Molecular Weight	Molecular Formula
601.68 g/mol	$C_{33}H_{37}N_4O_7$

^{1}HNMR (CD_3Cl, 300MHz) δ (ppm): 8.41 (bs, 1H; H^9), 8.29 (bs, 1H; H^{12}), 7.94 (bs, 1H;), 7.84 (bs, 1H; $H^{10\text{-}11}$), 7.68 (bs, 1H; H^{14}), 7.30 (s, 1H; H14), 5.71-5,41 (m, 2H; H^5), 5.30 (d, 2H; H^{17}), 2.91 (bs, 2H; H^{23}), 2.50 (bs, 2H; H^{24}), 2.23 (bs, 2H; H^{19}), 1.01 (bs, 3H; H^{18}), from -15 to -35 (bm, 16H; H^{TEMPO})

HRMS (ESI): calcd for $C_{33}H_{38}N_4O_7$ ($M+H^+$) 602.2735, found 602.2584

HPLC PURITY: 96 %

Synthesis of **21-(1-oxyl-2,2,5,5-tetramethylpiperidin-4-aminyl)-amide camptothecin (21-TEMPOamidocamptothecin)**

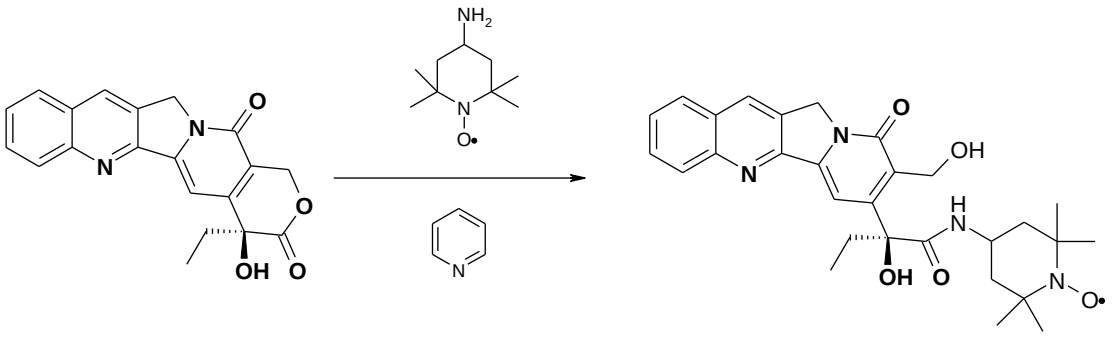

Components	Molecular formula	Molecular Weight	Volume	Weight	Density	n° of Mols
Camptothecin	$C_{20}H_{16}N_2O_4$	347 g/mol		100 mg		0.29 mmol
TEMPOamine	$C_9H_{19}N_2O$	171 g/mol		256.25 mg		1.5 mmol

100 mg of camptothecin was suspended into 5 ml of pyridine before the addition of 256.25 mg of TEMPOamine. The whole red mixture was allowed to react at 60 °C for 4 days under N_2 atmosphere. The solvent was then removed under vacuum and the crude product was purified by preparative TLC (eluent CH_2Cl_2:MeOH 98:2) to obtain 30 mg of 21-TEMPOamidocamptothecin with a 20% yield.

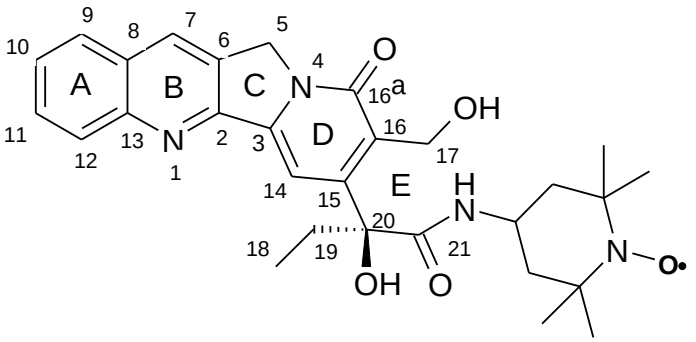

Molecular Weight	Molecular Formula
519.63 g/mol	$C_{29}H_{35}N_4O_5$

^{1}HNMR (CD_3Cl, 300MHz) δ (ppm): 8.41 (bs, 1H; H^9), 8.29 (bs, 1H; H^{12}), 7.94 (bs, 1H;), 7.84 (bs, 1H; H^{10-11}), 7.68 (bs, 1H; H^{14}), 7.30 (s, 1H; H14), 5.71-5,41 (m, 2H; H^5), 4.75 (m, 2H; H^{17}), 2.91 (bs, 2H; H^{23}), 2.50 (bs, 2H; H^{24}), 2.23 (bs, 2H; H^{19}), 1.01 (bs, 3H; H^{18}), from -15 to -35 (bm, 16H; H^{TEMPO})

HRMS (ESI): calcd for $C_{29}H_{36}N_4O_5$ ($M+H^+$) 520.2680, found 520.2705

IR (KBr): 2965 (ν_{as} $^{TEMPO}CH_3$), 2936 (ν_s $^{TEMPO}CH_3$), 1658 (ν C=O, amide 3°), 1591 (ν C=N, TEMPOamide), 1459-1363 (δ $^{TEMPO}CH_3$)

HPLC PURITY: 97 %

SYNTHESIS SCHEME III

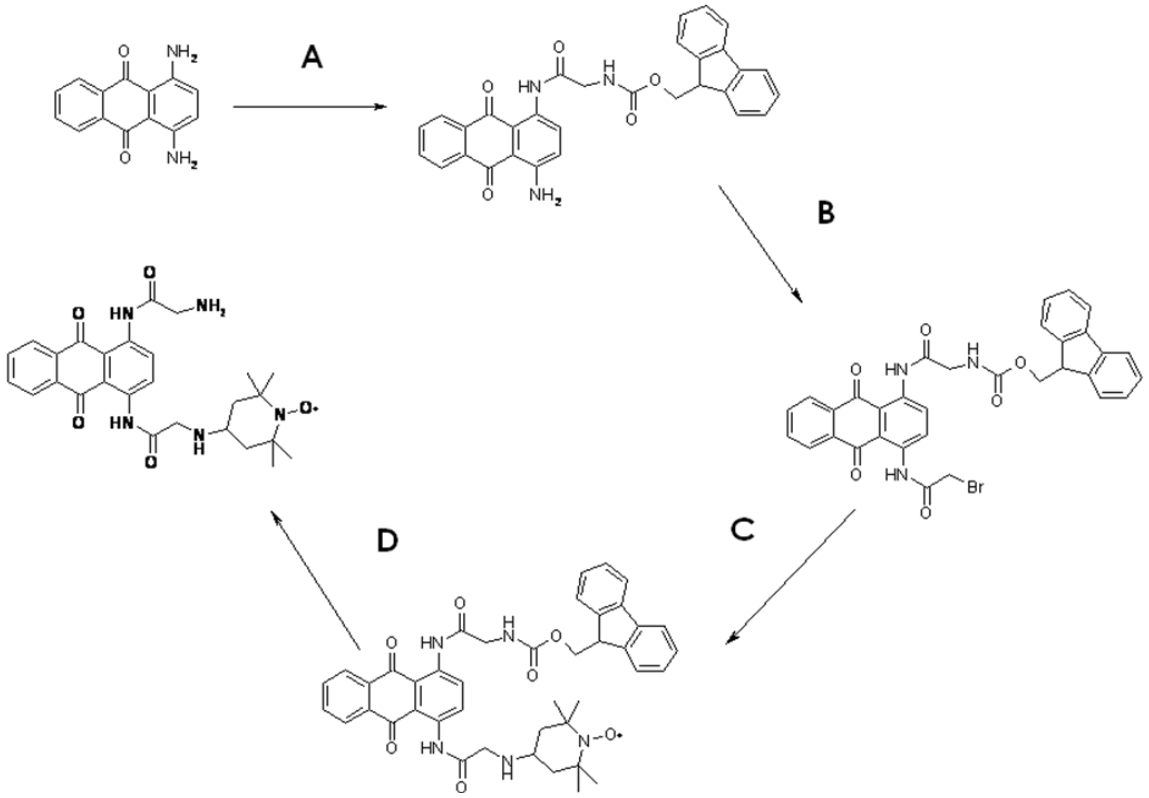

A) FMOC-glycine, DCC, THF, RT, 24 h (Yield 68%); **B)** Bromoacetyl bromide, pyridine, toluene, reflux, 4 h (Yield 84%); **C)** TEMPOamine, pyridine, DMF, 70 °C, 6 h (Yield 60%) **D)** Piperidine, DMF, RT, 30 min (Yield 85%)

Synthesis of **1-(N-FMOC-glycinamido)-4-aminoanthracene-9,10-dione**

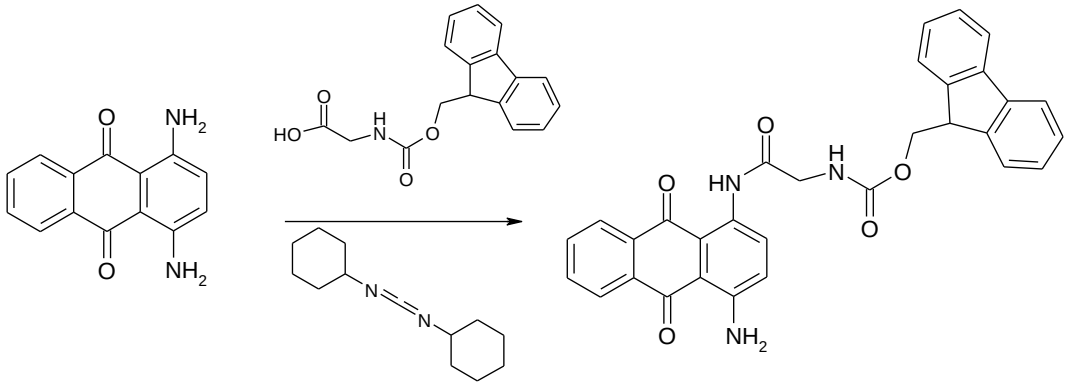

Components	Molecular formula	Molecular Weight	Volume	Weight	Density	n° of Mols
1,4-diaminoantraquinone	$C_{14}H_{10}N_2O_2$	234 g/mol		1 g		4,27 mmol
Dicyclohexylcarbodiimide (DCC)	$C_{12}H_{22}N_2$	360 g/mol		984 mg		4,75 mmol
9-fluorenyl-methylencarbamoyl-glycine (FMOC-glycine)	$C_{17}H_{15}NO_4$	297 g/mol		1,27 g		4.27 mmol

984 mg of DCC were solved in 50 ml of freshly distilled THF; 1.27 g of N-FMOC-glycine and 1 gram of 1,4-diaminoanthraquinone were later introduced to the solution. The whole mixture was stirred at RT for 18h (the formation of a precipitate and the shift of the colour to fucsia are observed) after which the suspension was filtered. The solid obtained was further extracted with THF; the solvent was removed in vacuo to obtain 1.5 g of 1-(FMOC-glycinamido)-4-aminoanthracene-9,10-dione as a fucsia solid with a sufficient degree of purity for the next reaction step. Yield 68%.

NOTE: In an attempt to recover the product from the first filtration, the solution was dried in

vacuo and the solid was crystallized from $CHCl_3$ but the solid thus obtained was still too impure to be accepted.

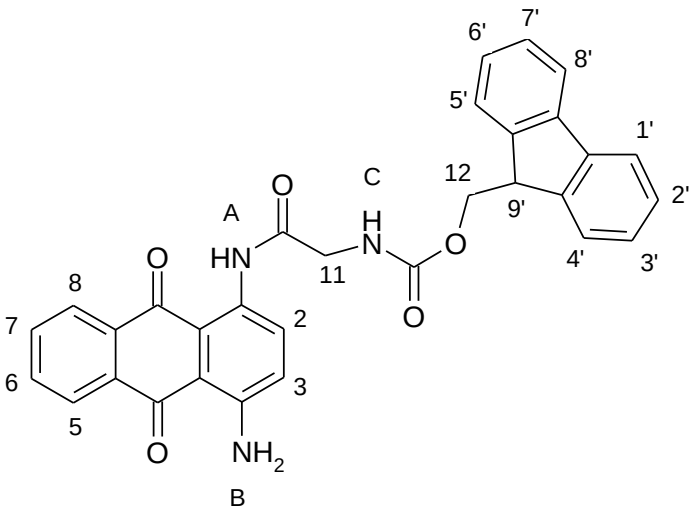

Molecular Weight	Molecular Formula
517.55 g/mol	$C_{31}H_{23}N_3O_5$

^{1}HNMR (CD_3Cl, 300MHz) δ (ppm): 12.84 (s, 1H; H^A), 8.82 (d, 1H, *J* = 9.6 Hz; H^2), 8.61 (s, 2H; H^B), 8.25 (m, 1H; H^7), 8.17 (d, 1H, *J* = 9.6 Hz; H^3), 7.94-7.79 (m, 5H; $H^{6,1',4',5',8'}$), 7.65 (m, 1H; H^C), 7.54-7.30 (m, 6H; $H^{5,8,2',3',6',7'}$), 6.54 (s, 2H; H^B), 4.43-4.35 (m, 3H; $H^{12,9'}$), 3.85 (d, 2H, J = 5.6 HZ; H^{11})

HRMS (ESI): calcd for $C_{31}H_{24}N_3O_5$ ($M+H^+$) 518.1710, found 518.1835

Synthesis of **1-(FMOC-glycinamido)-4-(bromoacetylamido)anthracene-9,10-dione**

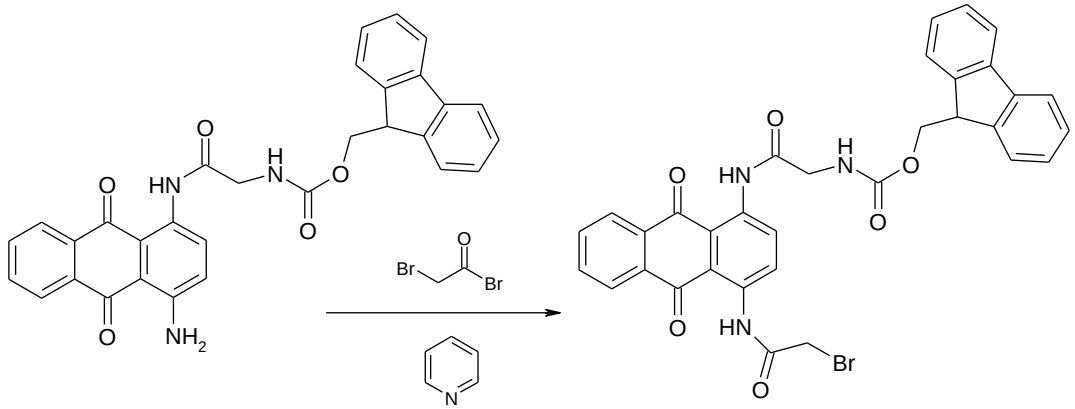

Components	Molecular formula	Molecular Weight	Volume	Weight	Density	n° of Mols
1-(FMOC-glycinamido)-4-aminoanthracene-9,10-dione	$C_{31}H_{23}N_3O_5$	517.55 g/mol		600 mg		1.16 mmol
2-Bromoacetyl bromide	$C_2H_2OBr_2$	201.85 g/mol	380 µl	878.05 mg	2.31 g/ml	4.,35 mmol
Pyridine	C_5H_5N	79.10 g/mol	351 µl	344 mg	0.98 g/ml	4.35 mmol

600 mg of 1-(Glycinamido)-4-aminoanthracene-9,10-dione were suspended in 600 ml of dry toluene. The mixture was added with 4,35 mmol of pyridine and finally with 380 µl of bromoacetylbromide. The mixture was heated to reflux and keeped at this temperature for 12h (the kinetic of this reaction is faster; in a second attempt the product was completely formed after 4h). The orange mixture obtained was cooled and the solvent was reduced to small volume (~15-25 ml). Ethanol (~150 ml) was added to the suspension and all was left to crystallize at -20°C. The precipitated was filtered, washed with water (in order to eliminated the pyridine bromohydrate salt) and again with ethanol to obtain 620 mg of pure 1-(FMOC-glycinamido)-4-

(bromoacetylamido)anthracene-9,10-dione as an orange solid. Yield 84%.

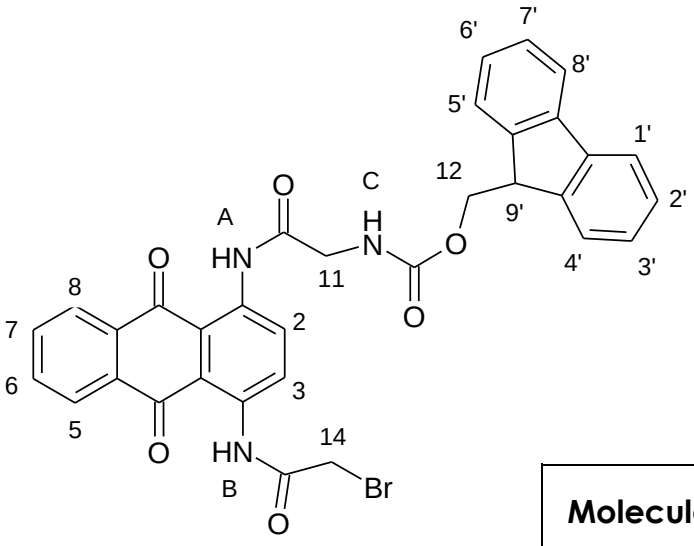

Molecular Weight	Molecular Formula
638.48 g/mol	$C_{33}H_{24}N_3O_6Br$

^{1}HNMR (CD_3Cl, 300MHz) δ (ppm): 12.77 (s, 1H; H^A), 12.56 (s, 1H; H^B), 9.04 (d, 1H, *J* = 9.5 Hz; H^2), 8.86 (d, 1H, *J* = 9.5 Hz; H^3), 8.27 (d, 1H, *J* = 7.4 Hz; H^8), 8.15 (d, 1H, *J* = 7.4 Hz; H^5), 7.94-7.80 (m, 5H; $H^{6,1',4',5',8'}$), 7.70 (m, 1H; H^C), 7.54-7.20 (m, 5H; $H^{7,2',3',6',7'}$), 4.43-4.35 (m, 3H; $H^{12,9'}$), 3.85 (m, 4H; $H^{11,14}$)

HRMS (ESI): calcd for $C_{33}H_{25}N_3O_6$ ($M+H^+$) 638.0921, 640.0907, found 638.0968, 640.0910

Synthesis of **1-(FMOC-glycinamido)-4-(2'-TEMPOaminoacetylamido)anthracene-9,10-dione**

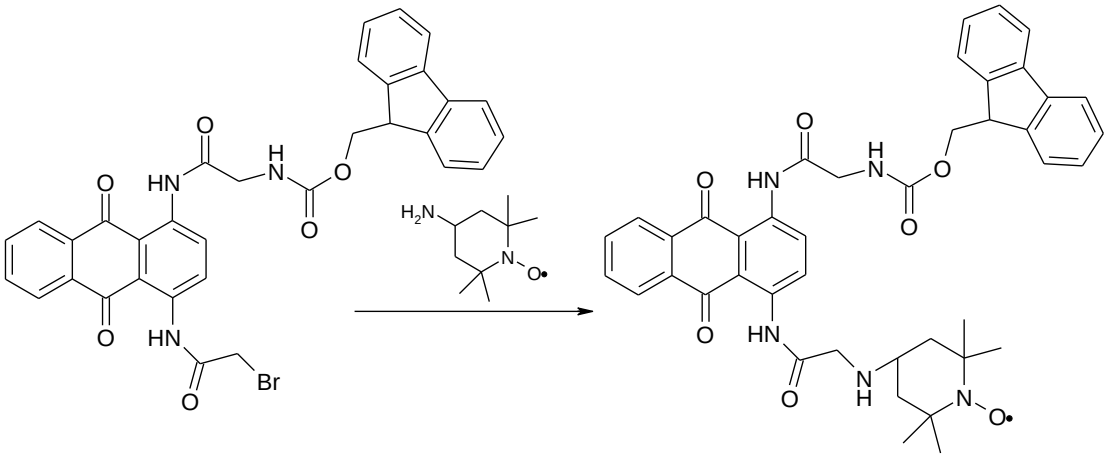

Components	Molecular formula	Molecular Weight	Volume	Weight	Density	n° of Mols
1-(FMOC-glycinamido)-4-(bromoacetylamido) anthracene-9,10-dione	$C_{33}H_{24}N_3O_6Br$	638.5 g/mol		50 mg		0.08 mmol
TEMPOamine	$C_9H_{19}N_2O$	171 g/mol		33.3 mg		0.19 mmol
Pyridine	C_5H_5N	79 g/mol	9.43 µl	9.22 mg	0.978 g/ml	0.12 mmol

A solution of 50 mg of 1-(FMOC-glycinamido)-4-(bromoacetylamido) anthracene-9,10-dione in 10 ml of amine-free DMF was added with 9.43 µl of pyridine and with 33.3 mg of TEMPOamine; the whole was heated to 70 °C for 6 h (the reaction was monitored by TLC with EtOAc as eluent until the disappear of the starting reagent. The solvent was subsequently evaporated and the orange solid obtained was suspended in EtOH, filtered and washed

again with H_2O (to eliminate the organic salts) and EtOH to obtain 35 mg of 1-(FMOC-glycinamido)-4-(2'-TEMPOaminoacetylamido) anthracene-9,10-dione as a brilliant orange solid.

NOTE: If the reaction is heated for more that 8 h the reaction mixture turns to a darker yellow and the product is harder to purify.

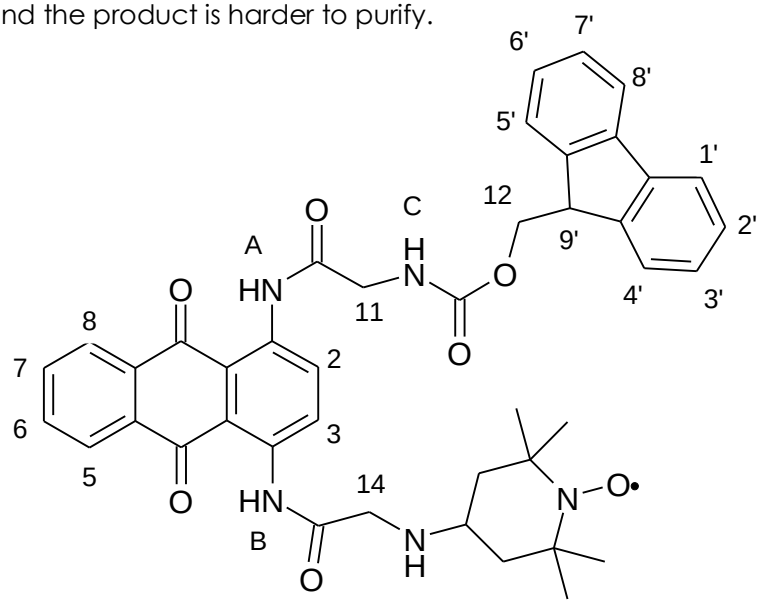

Molecular Weight	Molecular Formula
728.83 g/mol	$C_{42}H_{42}N_5O_7$

^{1}HNMR (CD_3Cl, 300MHz) δ (ppm): 12.60 (bs, 2H; $H^{A,B}$), 9.10 (bs, 1H; H^2), 8.90 (bs, 1H; H^3), 8.20 (bs, 2H; $H^{5,8}$), 7.90-7.70 (m, 5H; $H^{6,1',4',5',8'}$), 7.50-7.10 (m, 5H; $H^{7,2',3',6',7'}$), 4.40-4.25 (m, 3H; $H^{12,9'}$), 3.80 (m, 4H; $H^{11,14}$)

HRMS (ESI): calcd for $C_{42}H_{43}N_5O_7$ ($M+H^+$) 729.3157, found 729.3197

Synthesis of **1-(glycinamido)-4-(2'-TEMPOaminoacetylamido)anthracene-9,10-dione**

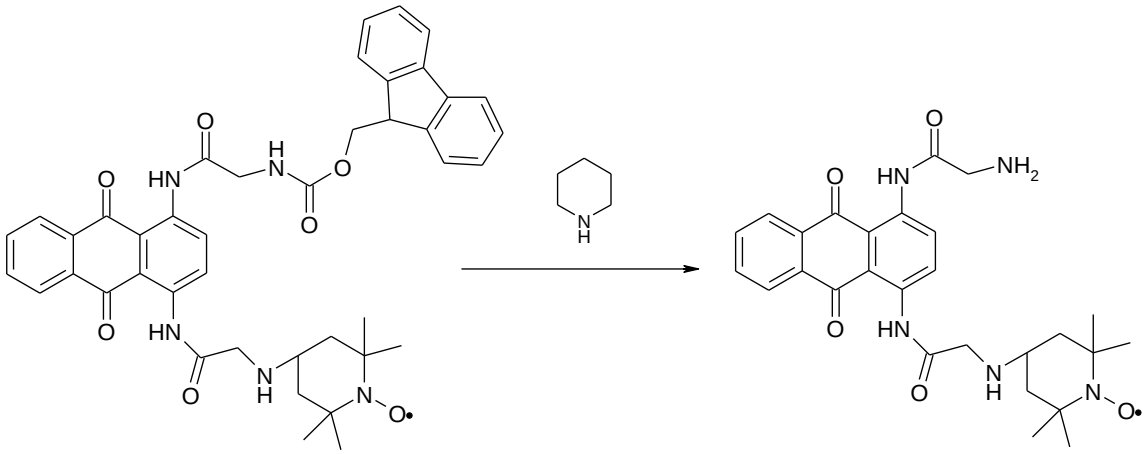

Components	Molecular formula	Molecular Weight	Volume	Weight	Density	n° of Mols
1-(FMOC-glycinamido)-4-(TEMPOamido) anthracene-9,10-dione	$C_{42}H_{42}N_5O_7$	728 g/mol		10 mg		0.014 mmol
Piperidine	$C_5H_{11}N$	85 g/mol	50 µl			

10 mg of 1-(FMOC-glycinamido)-4-(TEMPOamido)anthracene-9,10-dione were solved into 500 µl of a 10 % piperidine solution in DMF (50 µl of piperidine in 450 µl of distilled DMF). The solution was stirred at RT for 30 min during which the orange colour turn a little bit darker (once again the reaction was followed by TLC using THF as eluent). The solvent was evaporated in vacuo and the crude solid was suspended into cold Et_2O (7 ml); the suspension was placed into a centrifuge tube and centrifuged for 25 min at 2400 rpm, after which the supernatant solvent was removed. This step was repeated 5 times (the centrifugation time was reduced after the second wash to 15 min) in order to obtain 6 mg of 1-(glycinamido)-4-(2'-TEMPOaminoacetylamido)

anthracene-9,10-dione as a brilliant red solid. Yield 85%.

NOTE: Be careful during the evaporation of the piperidine/DMF solution because a concentration of piperidine could occur during the evaporation process; this could drive to the drawback cleavage reaction of the peptide bond. An attempt to avoid this process was the precipitation of the product from the starting mixture adding cold Et_2O but no precipitate was observed even after the addition of large excess of Et_2O (20 times more).

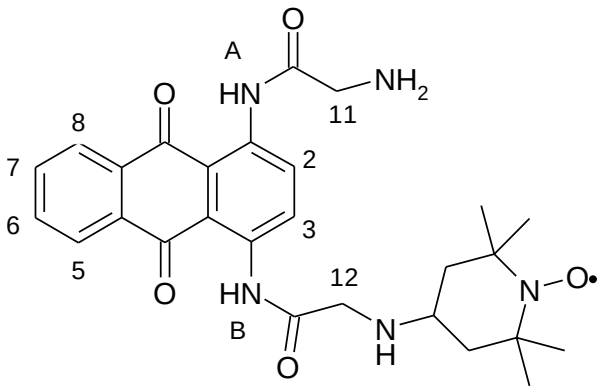

Molecular Weight	Molecular Formula
506.59 g/mol	$C_{27}H_{32}N_5O_5$

^{1}HNMR (CD_3Cl, 300MHz) δ (ppm): 12.50 (bs, 2H; $H^{A,B}$), 9.05 (bs, 1H; H^2), 8.80 (bs, 1H; H^3), 8.15 (bs, 2H; $H^{5,8}$), 7.80 (m, 1H; H^6), 7.45 (m, 1H; H^7), 3.90-3.60 (m, 4H; $H^{11,14}$)

HRMS (ESI): calcd for $C_{27}H_{33}N_5O_5$ ($M+H^+$) 507.3476, found 507.3604

SYNTHESIS SCHEME IV

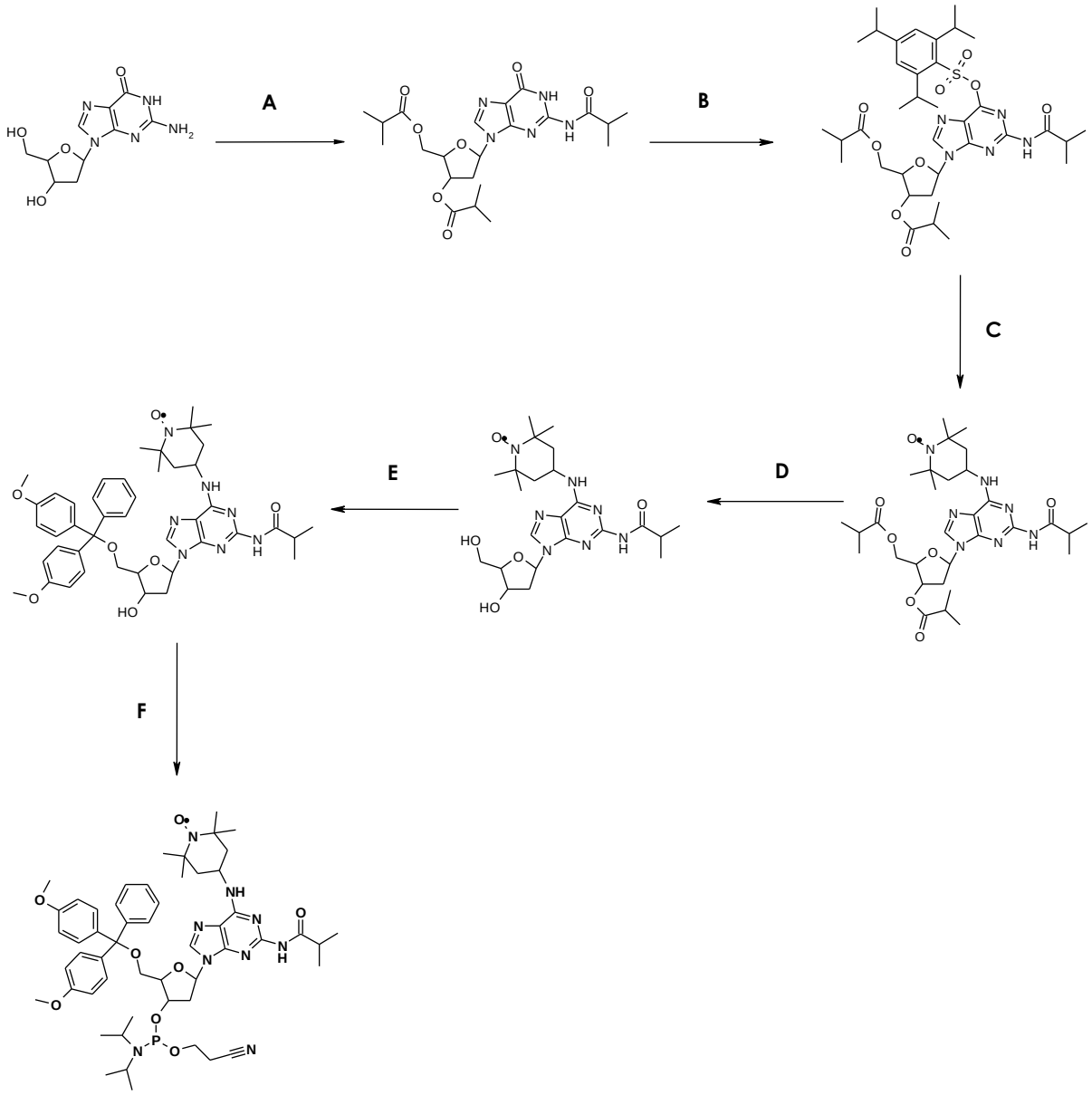

A) Isobuthyric anhydride, pyridine, DMAP, 50 °C, 24 h (Yield 89%); **B)** TPS-Cl, triethylamine, DMAP, RT, 16 h (Yield 78%); **C)** TEMPOamine, CH_2Cl_2, reflux, 16 h (Yield 55%); **D)** NH_4OH 25%, MeOH, RT, 4 h (Yield 84%); **E)** DMT-Cl, DMAP, CH_2Cl_2, RT, 16 h (Yield 83%); **F)** Bisphopsphoramidite, tetrazole, acetonitrile, RT, 2 h (Yield 72%)

Synthesis of **2,3',5'-triisobutyryl-2'-deoxyguanidine**

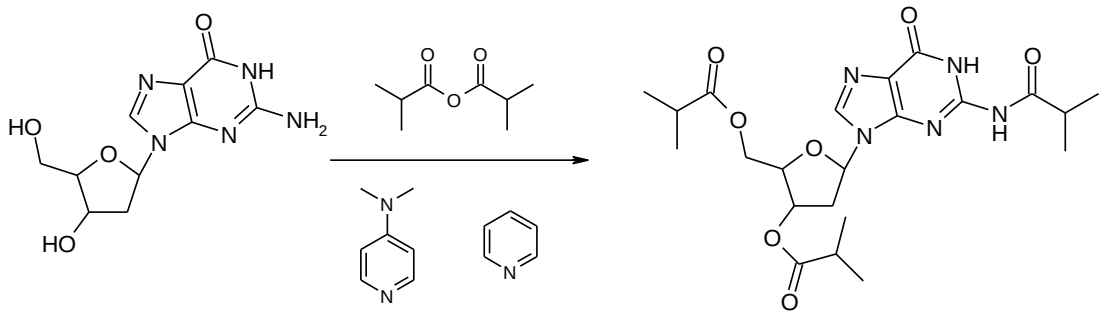

Components	Molecular formula	Molecular Weight	Volume	Weight	Density	n° of Mols
Guanidine	$C_{10}H_{13}N_5O_4$	267.2 g/mol		300 mg		1.12 mmol
Isobutyryl anhydride	$C_8H_{14}O_3$	158.2 g/mol	1.49 ml	1.42 g	0.95 g/ml	8.98 mmol
Dimethoxypyridine (DMAP)	$C_7H_{10}N_2$	122.17 g/mol		26.87 mg		0.22 mmol

A mixture of 300 mg of guanidine, 26.87 mg of DMAP and 1.49 ml of isobutyryl anhydride in 8.5 ml of pyridine was heated at 50 °C until no more starting reagent was observed by TLC (eluent EtOAc). The reaction was quenched with MeOH (1 ml) and was then cooled, concentrated to small volume and partitioned between EtOAc and H_2O. The organic phase was washed with water, dried with Na_2SO_4 and essiccated to obtain 470 mg of 2,3',5'-triisobutyryl-2'-deoxyguanidine. Yield 89%.

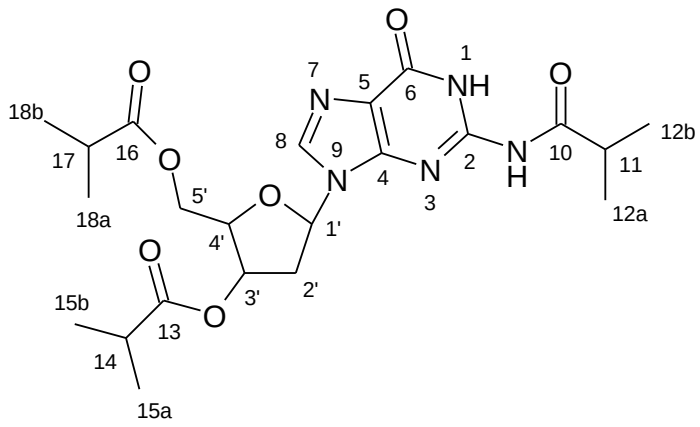

Molecular Weight	Molecular Formula
477.30 g/mol	$C_{22}H_{31}N_5O_7$

^{1}HNMR (Acetone- *d6*, 300MHz) δ (ppm): 8.01 (s, 1H; H^8), 6.32-6.27 (dd, 1H, J_1 = 8.39 Hz, J_2 = 5.99 Hz; $H^{1'}$), 5.45-5.41 (dt, 1H, J_1 = 6.26 Hz, J_2 = 1.76 Hz; $H^{4'}$), 4.37-4.30 (m, 2H; $H^{3',4'}$), 3.08-2.89 (m, 4H; $H^{2',5'}$), 2.69-2.55 (m, 3H; $H^{11,14,17}$), 1.25-1.24 (d, 3H, J_1 = 1.83 Hz; H^{18}), 1.23-1.22 (d, 3H, J_1 = 1.83 Hz; H^{18}), 1.206-1.204 (d, 3H, J_1 = 0.60 Hz; H^{15}), 1.183-1.181 (d, 3H, J_1 = 0.60 Hz; H^{15}), 1.18 (d, 3H; H^{12}), 1.11 (d, 3H; H^{12})

HRMS (ESI): calcd for $C_{22}H_{32}N_5O_7$ ($M+H^+$) 478.2296, found 478.2302

Synthesis of **2,3',5'-triisobutyryl-O⁶-[(2,4,6-triisopropylphenyl)sulfonil]-2'-deoxyguanidine**

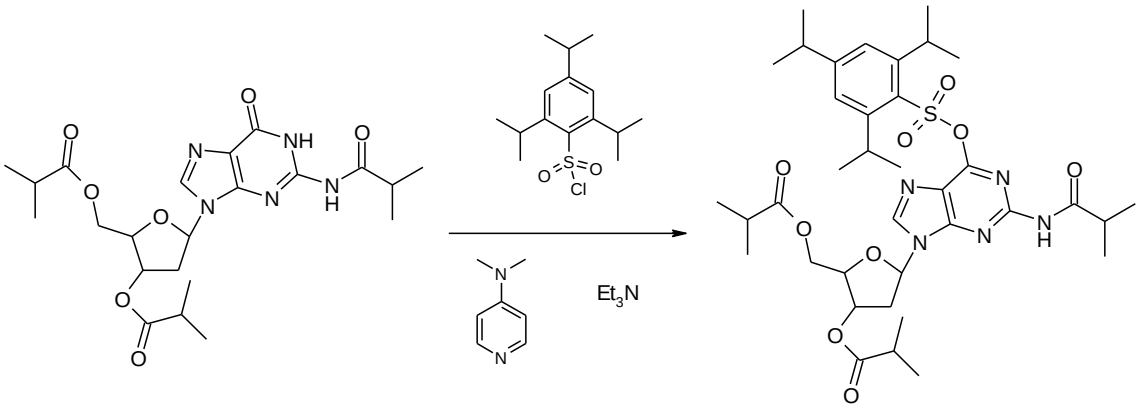

Components	Molecular formula	Molecular Weight	Volume	Weight	Density	n° of Mols
2, 3', 5'-triisobutyryl-2'-deoxyguanidine	$C_{22}H_{31}N_5O_7$	477.3 g/mol		470 mg		0.98 mmol
2, 4, 6-triisopropylbenzenesulfonil chloride (TPS-Cl)	$C_{15}H_{23}SO_2Cl$	302.86 g/mol		593.6 mg		1.96 mmol
Dimethoxypyridine (DMAP)	$C_7H_{10}N_2$	122.17 g/mol		12.21 mg		0.10 mmol

470 mg of 2,3',5'-triisobutyryl-2'-deoxyguanidine were solved in 5 ml of anhydrous CH_2Cl_2; 593,6 mg of TPS-Cl, 404 mg of triethylamine and 12,12 mg of DMAP were added to the solution and the whole was stirred at r.t. overnight. The mixture was evaporated and the residue was purified by column chromatography on silica gel (gradient from chloroform:hexane 1:1 to chloroform 100%). 680 mg of 2,3',5'-triisobutyry-O⁶-[(2,4,6-

triisopropylphenyl)sulfonil]-2'-deoxyguanidine were obtained as a white foam. Yield 78%

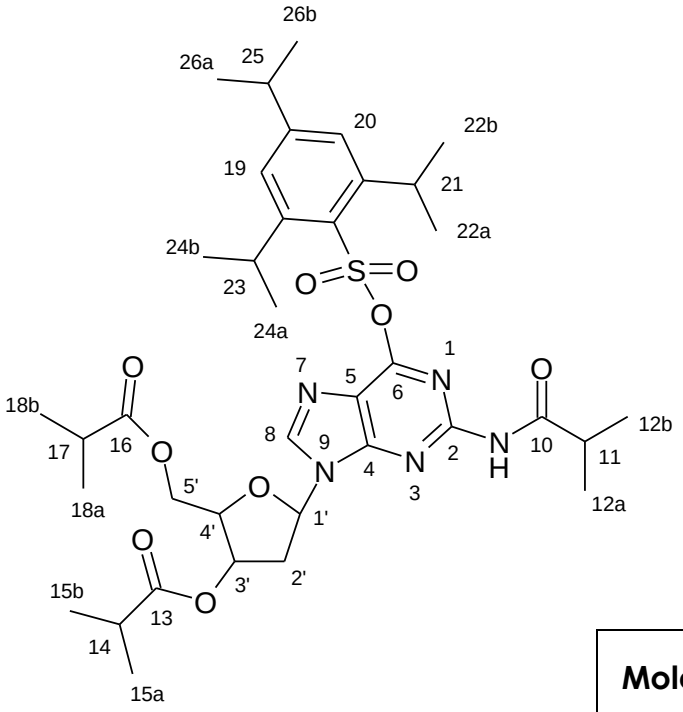

Molecular Weight	Molecular Formula
743.25 g/mol	$C_{37}H_{53}N_5O_9S$

^{1}HNMR (Acetone- *d6*, 300MHz) δ (ppm): 7.95 (s, 1H; H^8), 7.05 (s, 1H; H^{19}), 7.01 (s, 1H; H^{20}), 6.30-6.25 (dd, 1H, J_1 = 8.5 Hz, J_2 = 6.2 Hz; $H^{1'}$), 5.47-5.41 (dt, 1H, J_1 = 6.26 Hz, J_2 = 1.76; $H^{4'}$), 4.30-4.30 (m, 2H; $H^{3',4'}$), 3.15-2.93 (m, 4H; $H^{2',5'}$), 2.69-2.52 (m, 6H; $H^{11,14,17,21,23,25}$), 1.25-1.23 (d, 3H, J_1 = 1.95 Hz; H^{18}), 1.23-1.21 (d, 3H, J_1 = 1.95 Hz; H^{18}), 1.202-1.201 (d, 3H, J_1 = 0.55 Hz; H^{15}), 1.183-1.182 (d, 3H, J_1 = 0.50 Hz; H^{15}), 1.18 (d, 3H; H^{12}), 1.11 (d, 3H; H^{12}), 1.05-0.75 (m, 18H; $H^{22,24,26}$)

HRMS (ESI): HRMS (ESI): calcd for $C_{37}H_{54}N_5O_9S$ ($M+H^+$) 744.3637, found 744.3638

Synthesis of **2-3', 5'-triisobutyryl-2-isobutyramido-N⁶-(1-oxyl-2, 2, 6, 6-tetramethyl-4-piperidinyl)-2'-deoxyadenosine**

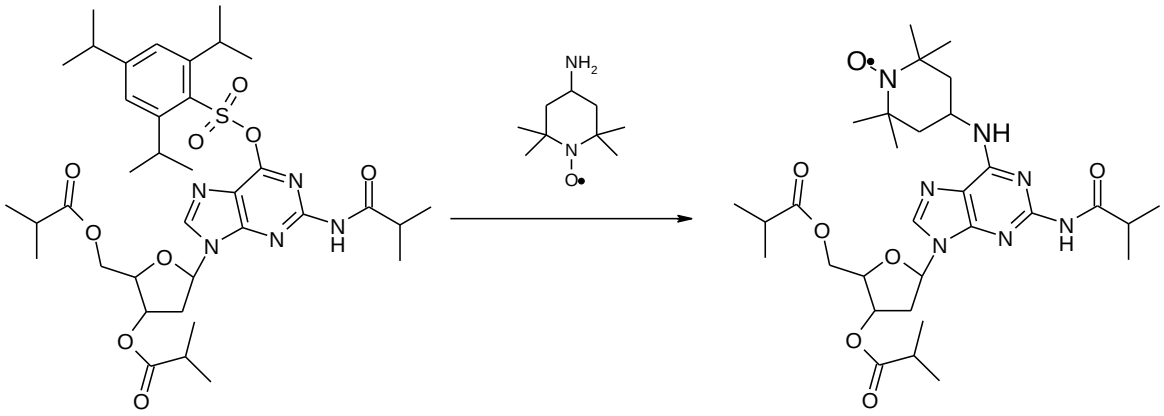

Components	Molecular formula	Molecular Weight	Volume	Weight	Density	n° of Mols
2,3',5'-triisobutyry-O⁶-[(2,4,6-triisopropylphenyl)sulfonil]-2'-deoxyguanidine	$C_{37}H_{53}N_5O_9S$	743 g/mol		486 mg		0.654 mmol
TEMPOamine	$C_9H_{19}N_2O$	171 g/mol		223 mg		1.31 mmol

2,3',5'-triisobutyryl-O⁶-[(2,4,6-triisopropylphenyl)sulfonil]-2'-deoxyguanidine (486 mg) was placed in a round bottomed flask with TEMPOamine (223 mg) and 3 ml of CH_2Cl_2. The solution was refluxed overnight after which was diluted with other 20 ml of CH_2Cl_2, washed with a saturated acqueous solution of $NaHCO_3$, with brine and with H_2O. The organic layer was thus died with Na_2SO_4, essicsated in vacuo and purified by column chromatography (eluent EtOAc:Hexane 70:30). 226.6 mg of 3',5'-diisobutyryl-2-isobutyramido-N⁶-(1-oxyl-2,2,6,6-tetramethyl-4-piperidinyl)-2'-deoxyadenosine were obtanied as a slightly red oil (last stain on column). Yield 55%.

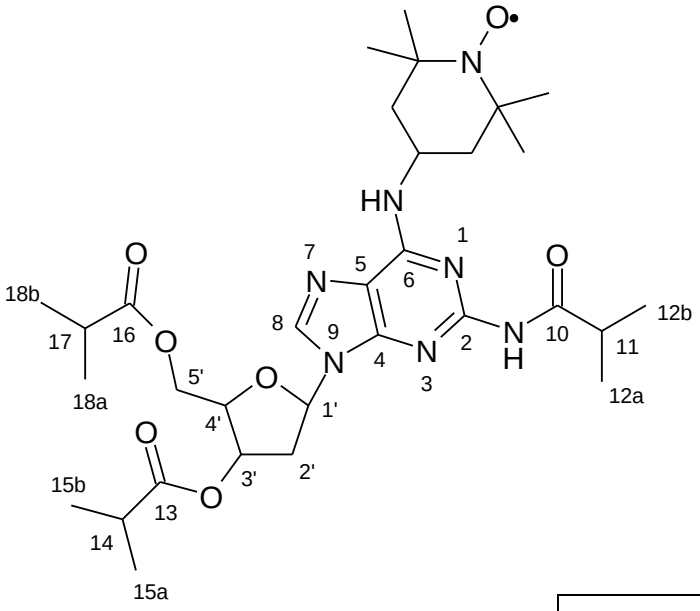

Molecular Weight	Molecular Formula
630.35 g/mol	$C_{31}H_{48}N_7O_7$

^{1}HNMR (CD_3Cl, 300MHz) δ (ppm): 7.85 (bs, 1H; H^8), 6.41 (bs, 1H; $H^{1'}$), 4.78 (bs, 1H; $H^{4'}$), 4.17 (bs, 1H; $H^{3'}$), 3.90 (m, 2H; $H^{5'}$), 2.80-2.45 (m, 5H; $H^{2',11,14,17}$), 1.40-1.20 (m, 18H; $H^{12,15,18}$), from -15 to -35 (bm, 16H; H^{TEMPO})

HRMS (ESI): calcd for $C_{31}H_{49}N_7O_7$ ($M+H^+$) 631.3687, found 631.3689; ($M+Na^+$) 653.3507, found 653.3506.

Synthesis of **2-isobutyramido-N⁶-(1-oxyl-2, 2, 6, 6-tetramethyl-4-piperidinyl)-2'-deoxyadenosine**

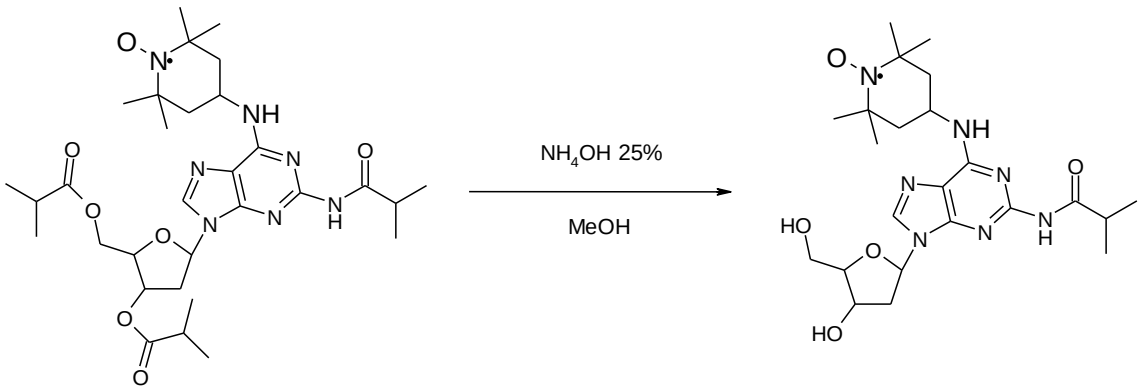

Components	Molecular formula	Molecular Weight	Volume	Weight	Density	n° of Mols
3',5'-diisobutyryl-2-isobutyramido-N⁶-(1-oxyl-2,2,6,6-tetramethyl-4-piperidinyl)-2'-deoxyadenosine	$C_{31}H_{48}N_7O_7$	630.3 g/mol		148 mg		0,22 mmol
Acqueous Ammonia 25%	NH_4OH	35 g/mol	1,1 ml	223 mg		8 mmol

In a round bottomed flask were placed 148 mg of 3',5'-diisobutyryl-2-isobutyramido-N⁶-(1-oxyl-2,2,6,6-tetramethyl-4-piperidinyl)-2'-deoxyadenosine, 1,1 ml of NH_4OH 25% and 3,3ml of MeOH. The suspension was stirred at RT for 4h after which the solvent was removed and the residue was purified by column chromatography with silica gel (eluent EtOAc:Isopropanol 98:2). One obtain 90 mg of 2-isobutyramido-N⁶-(1-oxyl-2, 2, 6, 6-tetramethyl-4-piperidinyl)-2'-deoxyadenosine as a slightly red oil. Yield 84%.

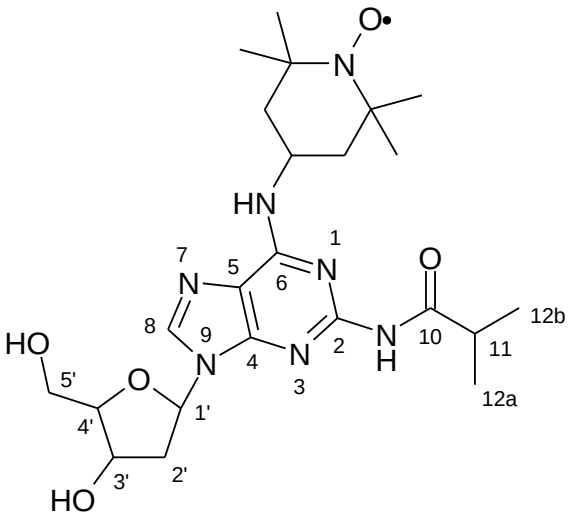

Molecular Weight	Molecular Formula
490.15 g/mol	$C_{23}H_{37}N_7O_5$

^{1}HNMR (CD_3OD, 300MHz) δ (ppm): 7.90 (bs, 1H; H^8), 6.35 (bs, 1H; $H^{1'}$), 4.78 (bs, 1H; $H^{4'}$), 4.21 (bs, 1H; $H^{3'}$), 3.92 (m, 2H; $H^{5'}$), 2.50-2.15 (m, 3H; $H^{2',11}$), 1.32-1.15 (2 bs, 6H; H^{12}), from -15 to -35 (bm, 16H; H^{TEMPO})

HRMS (ESI): calcd for $C_{23}H_{38}N_7O_5$ ($M+H^+$) 491.2851, found 491.2873.

Synthesis of **5'-dimethoxytrityl-2-isobutyramido-N^6-(1-oxyl-2,2,6,6-tetramethyl-4-piperidinyl)-2'-deoxyadenosine**

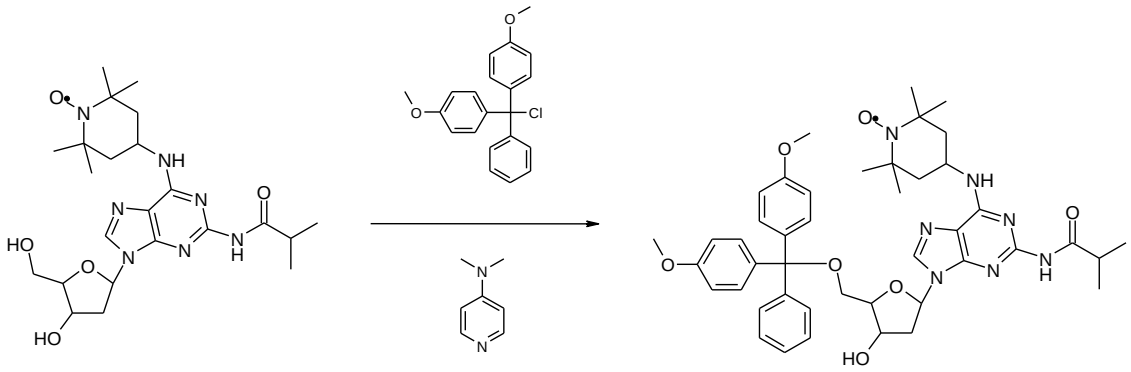

Components	Molecular formula	Molecular Weight	Volume	Weight	Density	n° of Mols
2-isobutyramido-N^6-(1-oxyl-2, 2, 6, 6-tetramethyl-4-piperidinyl)-2'-deoxyadenosine	$C_{23}H_{37}N_7O_5$	490 g/mol		220.5 mg		0.45 mmol
Dimethoxytrityl chloride	$C_{21}H_{19}ClO_2$	338.8 g/mol		183 mg		0.54 mmol
Dimethoxypyridine (DMAP)	$C_7H_{10}N_2$	122.17 g/mol		6.11 mg		0.05 mmol

220.5 mg of 2-isobutyramido-N^6-(1-oxyl-2, 2, 6, 6-tetramethyl-4-piperidinyl)-2'-deoxyadenosine were coevaporated three times with a small volume of anhydrous pyridine (~1 ml). The film thus obtained was solved with 3 ml of anhydrous pyridine and added with 183 mg of DMT-Cl and 6.11 mg of DMAP. The reaction is stirred overnight at RT under N_2 atmosphere after which the solvent was removed under vacuum. The residue was diluted with CH_2Cl_2, washed (two times) with a 5% $NaHCO_3$ watery solution and brine. The organic layer was dried and the crude product was purified by silica gel chromatography (eluent EtOAc:Methanol:TEA 97:2:1). The purified product

was finally solved into a small amount of CH_2Cl_2 and dropped into cold hexane. Centrifugation (2400 rpm, 3 min.) of the resulting suspension give 296 mg of 5'-dimethoxytrityl-2-isobutyramido-N^6-(1-oxyl-2,2,6,6-tetramethyl-4-piperidinyl)-2'-deoxyadenosine. Yield 83%.

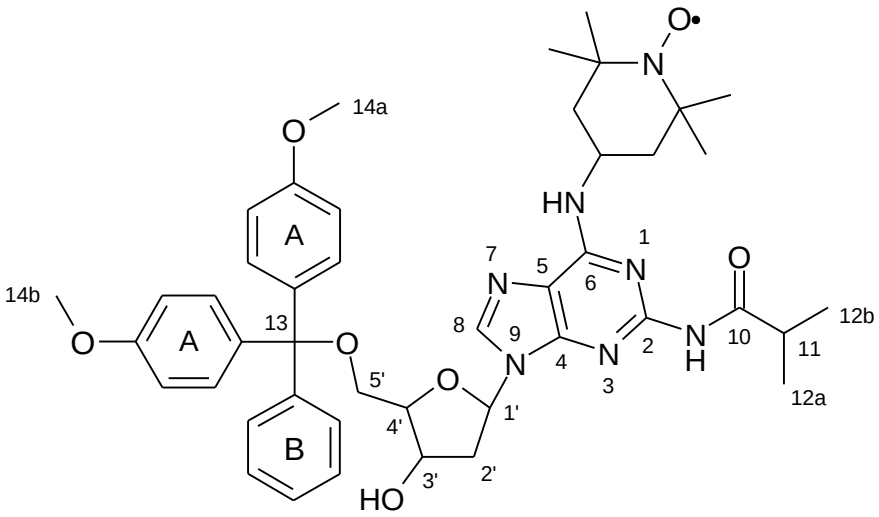

Molecular Weight	Molecular Formula
792.30 g/mol	$C_{44}H_{54}N_7O_7$

^{1}HNMR (CD_3Cl, 300MHz) δ (ppm): 7.85 (bs, 1H; H^8), 7.43 (bs, 4H; H^A), 7.30 (bs, 5H; H^B), 6.80 (bs, 4H; H^A), 6.32 (bs, 1H; $H^{1'}$), 4.71 (bs, 1H; $H^{4'}$), 4.51 (bs, 1H; $H^{3'}$), 3.79 (bs, 6H; H^{14}), 3.75-3.56 (m, 2H; $H^{5'}$), 2.64-2.43 (m, 3H; $H^{2',11}$), 1.20-1.17 (2 bs, 6H; H^{12}), from -15 to -35 (bm, 16H; H^{TEMPO})

HRMS (ESI): calcd for $C_{44}H_{55}N_7O_7$ ($M+H^+$) 793.4157, found 793.4160

Synthesis of **5'-dimethoxytrityl-2-isobutyramido-N^6-(1-oxyl-2,2,6,6-tetramethyl-4-piperidinyl)-2'-deoxyadenosine-3'-(2-cyanoethyl-N,Ndiisopropyl) phosphoramidite**

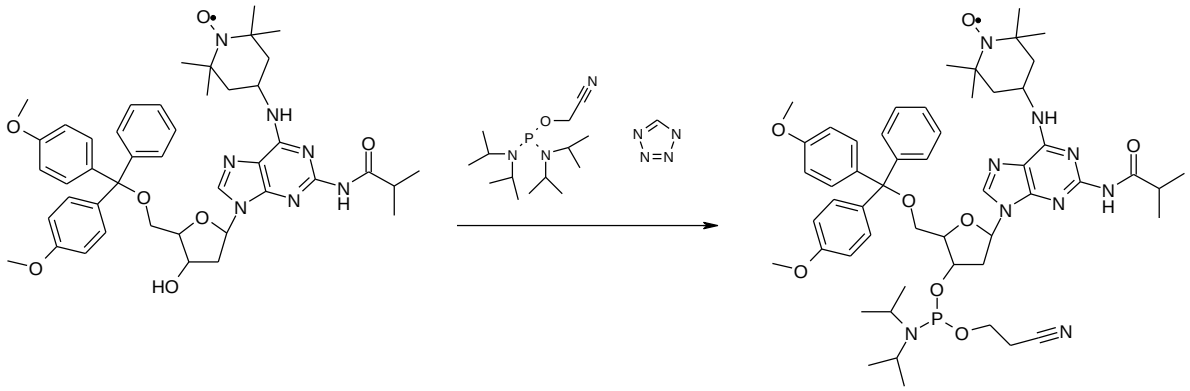

Components	Molecular formula	Molecular Weight	Volume	Weight	Density	n° of Mols
5'-dimethoxytrityl-2-isobutyramido-N^6-(1-oxyl-2,2,6,6-tetramethyl-4-piperidinyl)-2'-deoxyadenosine	$C_{44}H_{55}N_7O_7$	792.30 g/mol		174.24 mg		0.22 mmol
2-Cyanoethyl N,N,N',N'-tetraisopropyl phosphordiamidite (bisphosphoramidite)	$C_{15}H_{32}N_3OP$	301.41g/mol	139 µl	132.62 mg	0.95 g/ml	0.44 mmol
Tetrazole	CH_2N_4	70.05 g/mol		19 mg		0.27 mmol

174.24 mg of 5'-dimethoxytrityl-N^4-(1-oxyl-2,2,6,6-tetramethyl-4-piperidinyl)-2'-deoxycytidine is firstly coevaporated three times with anhydrous acetonitrile. The solid was lastly dissolved into 2 ml of anhydrous acetonitrile and to the solution were added 139 µl of bisphosphoramidite and 19 mg of sublimated tetrazole. The whole was left under Ar pressure at RT for 2 h during which the

organic salts precipitated out of the solution. Work-up of the reaction consisted in a first filtration of the suspension, as to remove the salts, followed by the removal of the solvent under vacuum. The crude mixture was dissolved in CH_2Cl_2 and washed (two times) with brine. The organic layer was dried and purified by silica gel chromatography (eluent EtOAc:MeOH:TEA gradient from 80:15:5 to 70:23:7). The purified product was solved again into a small amount of CH_2Cl_2 and dropped into cold hexane. 157.15 mg of 5'-dimethoxytrityl-2-isobutyramido-N^6-(1-oxyl-2,2,6,6-tetramethyl-4-piperidinyl)-2'-deoxyadenosine-3'-(2-cyanoethyl-N,Ndiisopropyl) phosphoramidite were obtained as a pink solid. Yield 72%.

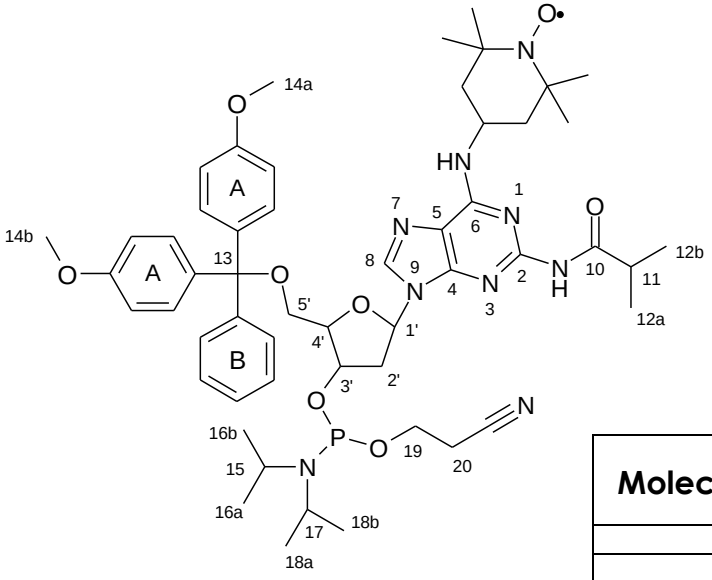

Molecular Weight	Molecular Formula
992.45 g/mol	$C_{53}H_{71}N_9O_8P$

^{1}HNMR (CD_3Cl, 300MHz) δ (ppm): 7.88 (bs, 1H; H^8), 7.41 (bs, 4H; H^A), 7.29 (bs, 5H; H^B), 6.80 (bs, 4H; H^A), 6.36 (bs, 1H; $H^{1'}$), 4.72 (bs, 1H; $H^{4'}$), 4.27 (bs, 1H; $H^{3'}$), 3.79 (bs, 6H; H^{14}), 3.77-3.56 (m, 6H; $H^{2',5',20}$), 2.82-2.43 (m, 5H; $H^{11,15,17,19}$), 1.20-1.17 (m, 18H; $H^{16,17}$), from -15 to -35 (bm, 16H; H^{TEMPO})

^{31}PNMR (CD_3Cl, 300MHz) δ (ppm): 148.94, 148.81

HRMS (ESI): calcd for $C_{53}H_{72}N_9O_8P$ ($M+H^+$) 993.5236, found 993.5236; ($M+Na^+$) 1015.5055, found 1015.5048; ($2M+H^+$) 1986.0399, found 1986.0414.

SYNTHESIS SCHEME V

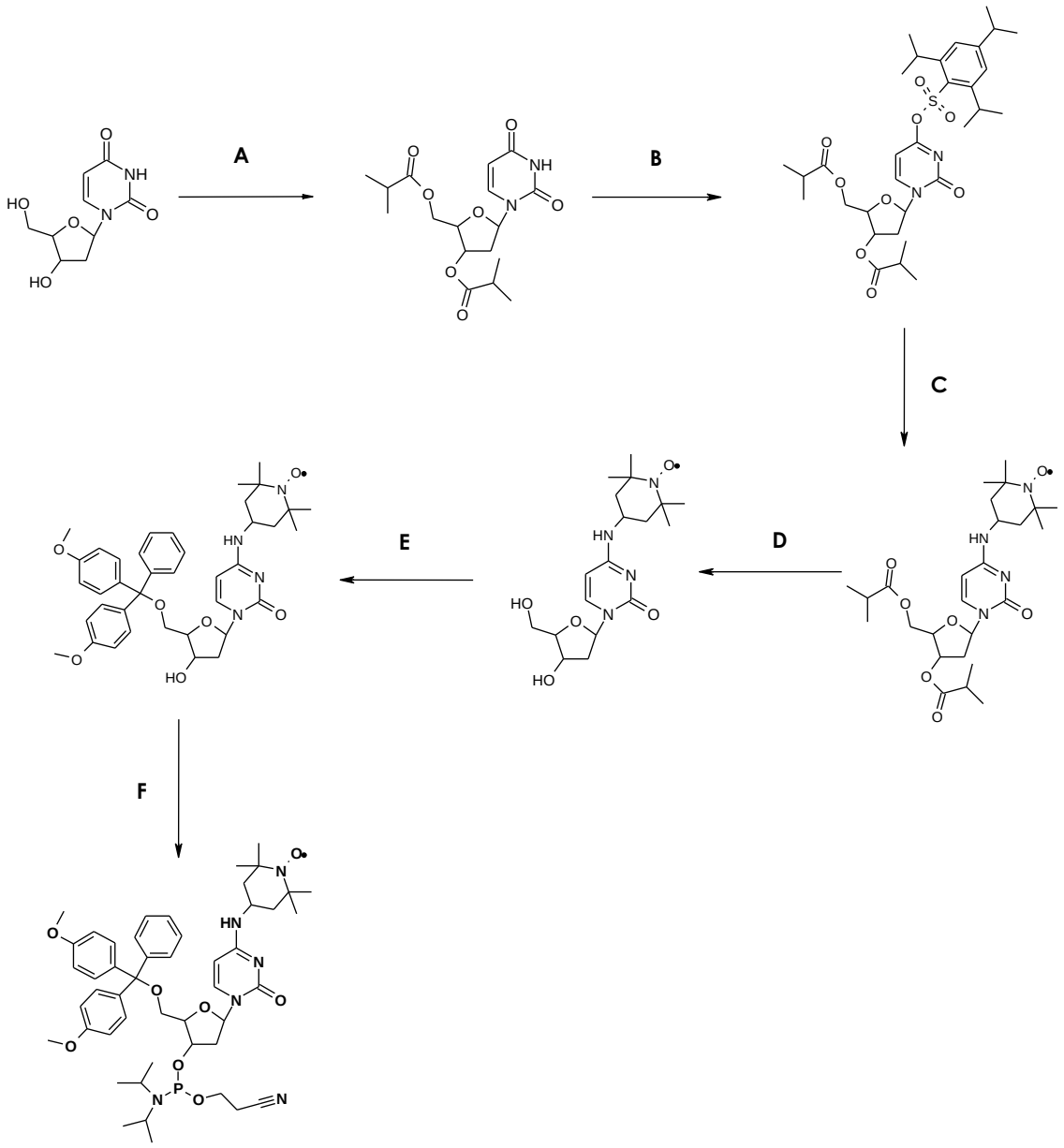

A) Isobuthyric anhydride, pyridine, DMAP, 50 °C, 24 h (Yield 91%); **B)** TPS-Cl, triethylamine, DMAP, RT, 16 h (Yield 81%); **C)** TEMPOamine, CH_2Cl_2, reflux, 16 h (Yield 59%); **D)** NH_4OH 25%, MeOH, RT, 4 h (Yield 87%); **E)** DMT-Cl, DMAP, CH_2Cl_2, RT, 16 h (Yield 81%); **F)** Bisphopsphoramidite, tetrazole, acetonitrile, RT, 2 h (Yield 75%)

Synthesis of **3',5'-diisobutyryl-2'-deoxyuridine**

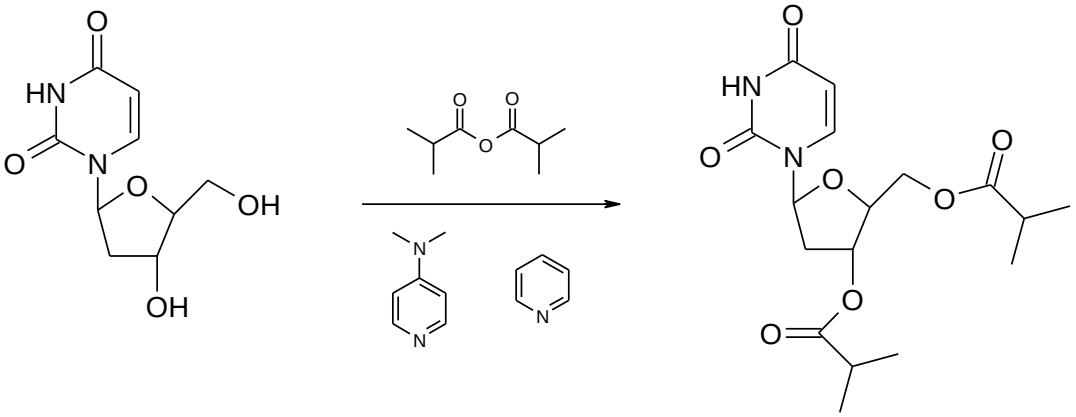

Components	Molecular formula	Molecular Weight	Volume	Weight	Density	n° of Mols
2'-deoxyuridine	$C_9H_{12}N_2O_5$	228.20 g/mol		228.20 mg		1.0 mmol
Isobutyryl anhydride	$C_8H_{14}O_3$	158.2 g/mol	666.1 µl	632.80 mg	0.95 g/ml	4 mmol
Dimethoxypyridine (DMAP)	$C_7H_{10}N_2$	122.17 g/mol		12.22 mg		0.1 mmol

A mixture of 228.2 mg of 2'-deoxyuridine, 12.22 mg of DMAP and 666.1 µl of isobutyryl anhydride in 7 ml of pyridine was heated at 50 °C until no more starting reagent was observed by TLC (eluent EtOAc). The reaction was quenched with MeOH (1 ml) and was then cooled, concentrated to small volume and partitioned between EtOAc and H_2O. The organic phase was washed with water, dried with Na_2SO_4 and essiccated to obtain 335.8 mg of 3',5'-diisobutyryl-2'-deoxyuridine. Yield 91%.

PM: 477
Molecola Formula: $C_{22}H_{31}N_5O_7$

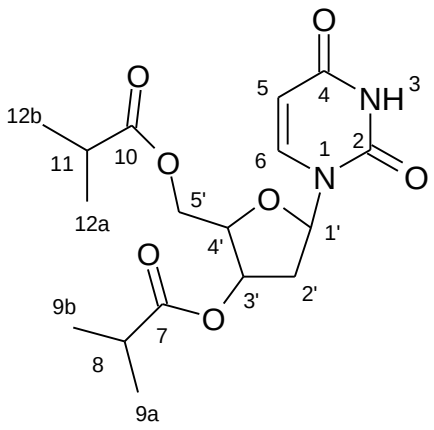

Molecular Weight	Molecular Formula
368 g/mol	$C_{17}H_{24}N_2O_7$

^{1}HNMR (Acetone-*d6* 300MHz) δ (ppm): 7.85 (s, 1H; H^6), 6.28-6.24 (dd, 1H, J_1 = 8.25 Hz, J_2 = 5.30 Hz; $H^{1'}$), 5.58 (s, 1H; H^5), 5.45-5.41 (dt, 1H, J_1 = 6.26 Hz, J_2 = 1.76 Hz; $H^{4'}$), 4.34-4.30 (m, 1H; $H^{3'}$), 3.08-2.89 (m, 2H; $H^{5'}$), 2.69-2.55 (m, 4H; $H^{8,11,2'}$), 1.25-1.24 (d, 3H, J_1 = 1.83 Hz; H^9), 1.23-1.22 (d, 3H, J_1 = 1.83 Hz; H^9), 1.206-1.204 (d, 3H, J_1 = 0.60 Hz; H^8), 1.183-1.181 (d, 3H, J_1 = 0.60 Hz; H^8)

HRMS (ESI): calcd for $C_{17}H_{25}N_2O_7$ ($M+H^+$) 369.1656, found 369.1662

Synthesis of **3',5'-diisobutyryl-O⁴-[(2,4,6-triisopropylphenyl)sulfonil]-2'-deoxyuridine**

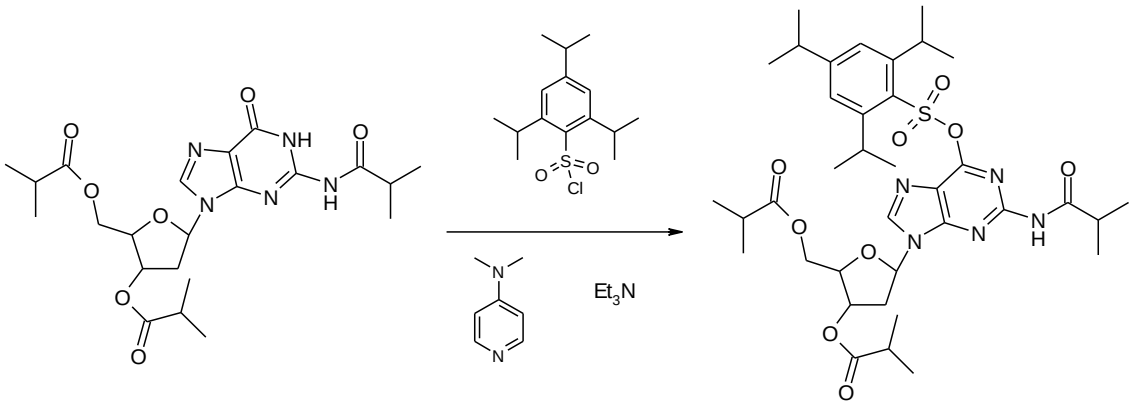

Components	Molecular formula	Molecular Weight	Volume	Weight	Density	n° of Mols
3', 5'-triisobutyryl-2'-deoxyuridine	$C_{17}H_{24}N_2O_7$	368 g/mol		295.2 mg		0,80 mmol
2, 4, 6-triisopropylbenzenesulfonil chloride (TPS-Cl)	$C_{15}H_{23}SO_2Cl$	302.86 g/mol		484.5 mg		1,60 mmol
Dimethoxypyridine (DMAP)	$C_7H_{10}N_2$	122.17 g/mol		9.77 mg		0,08 mmol

295.2 mg of 3',5'-triisobutyryl-2'-deoxyuridine were solved in 5 ml of anhydrous CH_2Cl_2; 484.5 mg of TPS-Cl, 404 mg of triethylamine and 9.77 mg of DMAP were added to the solution and the whole was stirred at r.t. overnight. The mixture was evaporated and the residue was purified by column chromatography on silica gel (gradient from chloroform:hexane 1:1 to chloroform 100%). The second stain gave 508 mg of 3',5'-diisobutyry-O⁴-[(2,4,6-triisopropylphenyl)sulfonil]-2'-deoxyuridine obtained as a white foam. Yield 81%.

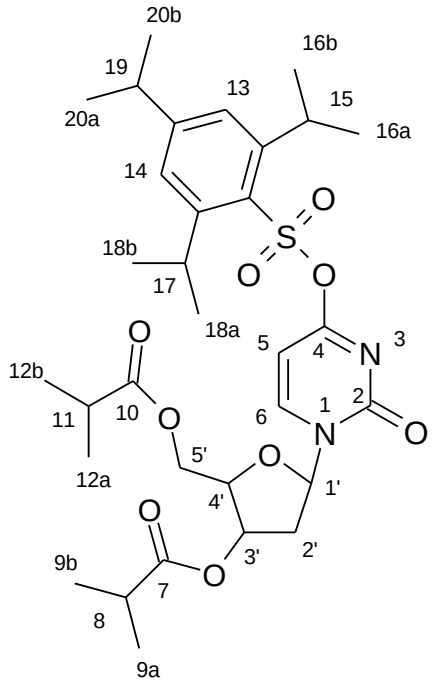

Molecular Weight	Molecular Formula
634.10 g/mol	$C_{32}H_{46}N_2O_9S$

^{1}HNMR (Acetone-*d6* 300MHz) δ (ppm): 7.90 (s, 1H; H^6), 7.10 (s, 1H; H^{13}), 7.05 (s, 1H; H^{14}) 6.26-6.20 (dd, 1H, J_1 = 8.25 Hz, J_2 = 5.30 Hz; $H^{1'}$), 5.64 (s, 1H; H^5), 5.50-5.46 (dt, 1H, J_1 = 6.26 Hz, J_2 = 1.76 Hz; $H^{4'}$), 4.33-4.28 (m, 1H; $H^{3'}$), 3.08-2.89 (m, 2H; $H^{5'}$), 2.69-2.55 (m, 7H; $H^{8,11,15,17,19,2'}$), 1.23-1.22 (d, 3H, J_1 = 1.7 Hz; H^9), 1.20-1.19 (d, 3H, J_1 = 1.7 Hz; H^9), 1.202-1.20 (d, 3H, J_1 = 0.6 Hz; H^8), 1.183-1.181 (d, 3H, J_1 = 0.6 Hz; H^8), 1.10-0.75 (m, 18H; $H^{16,18,20}$)

HRMS (ESI): calcd for $C_{32}H_{47}N_2O_9S$ ($M+H^+$) 635.2997, found 635.2998; ($M+Na^+$) 653.3507, found 653.3506.

Synthesis of **3', 5'-diisobutyryl-2-isobutyramido-N⁶-(1-oxyl-2, 2, 6, 6-tetramethyl-4-piperidinyl)-2'-deoxycitydine**

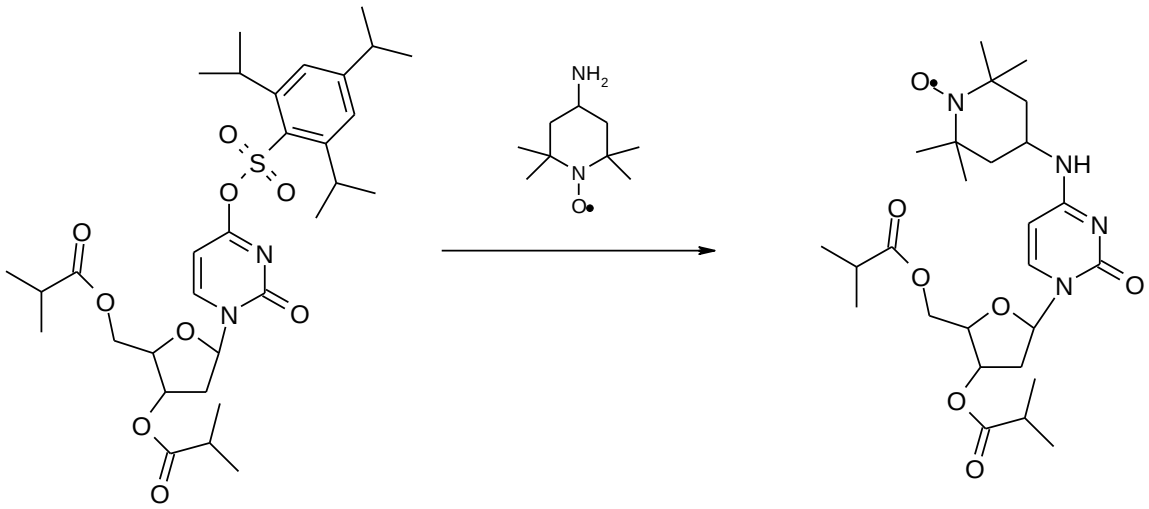

Components	Molecular formula	Molecular Weight	Volume	Weight	Density	n° of Mols
2,3',5'-triisobutyry-O⁶-[(2,4,6-triisopropylphenyl)sulfonil]-2'-deoxyguanidine	$C_{32}H_{47}N_2O_9S$	635 g/mol		381 mg		0.60 mmol
TEMPOamine	$C_9H_{19}N_2O$	171 g/mol		205.2 mg		1.20 mmol

3',5'-diisobutyryl-O⁶-[(2,4,6-triisopropylphenyl)sulfonil]-2'-deoxyuridine (381 mg) was placed in a round bottomed flask with TEMPOamine (205 mg) and 3 ml of CH_2Cl_2. The solution was refluxed overnight after which was diluted with other 20 ml of CH_2Cl_2, washed with a saturated acqueous solution of $NaHCO_3$, with brine and with H_2O. The organic layer was thus died with Na_2SO_4, essicsated in vacuo and purified by column chromatography (eluent EtOAc:Hexane 70:30). 184.43 mg of 3',5'-diisobutyryl-N⁴-(1-oxyl-2,2,6,6-tetramethyl-4-

piperidinyl)-2'-deoxycitydine were obtanied as a slightly red oil (last stain on column). Yield 59%.

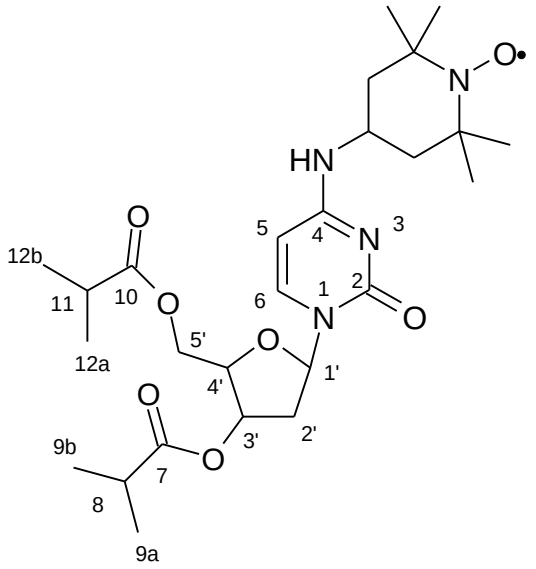

Molecular Weight	Molecular Formula
521.25 g/mol	$C_{26}H_{41}N_4O_7$

^{1}HNMR (CD_3Cl, 300MHz) δ (ppm): 7.99 (bs, 1H; H^6), 6.26 (bs, 1H; H^5), 5.82 (bs, 1H; $H^{1'}$), 4.36 (bs, 1H; $H^{4'}$), 3.93 (bs, 1H; $H^{3'}$), 3.74 (m, 2H; $H^{5'}$), 2.13-2.35 (m, 4H; $H^{2',8,11}$), 1.20-0.95 (2 bs, 12H; $H^{9,12}$), from -15 to -35 (bm, 16H; H^{TEMPO})

HRMS (ESI): calcd for $C_{26}H_{42}N_4O_7$ ($M+H^+$) 522.3048, found 522.3052.

Synthesis of **N^4-(1-oxyl-2, 2, 6, 6-tetramethyl-4-piperidinyl)-2'-deoxycytidine**

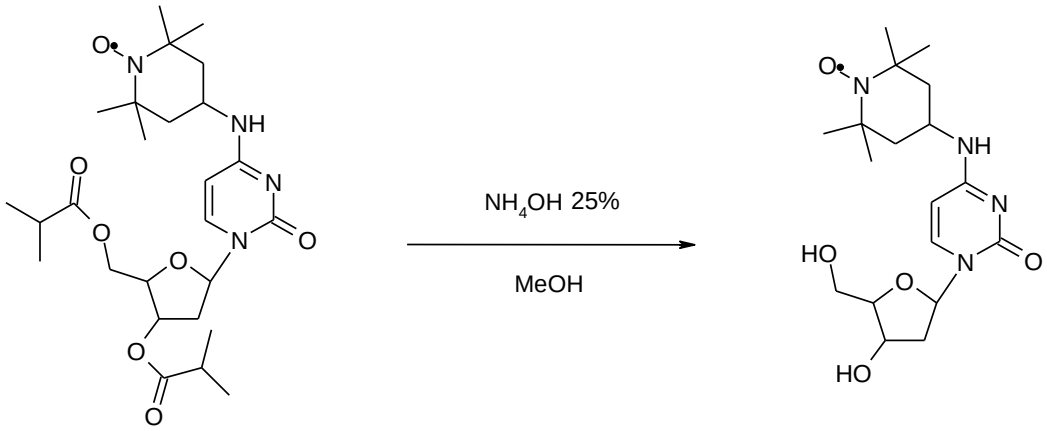

Components	Molecular formula	Molecular Weight	Volume	Weight	Density	n° of Mols
3',5'-diisobutyryl-N^4-(1-oxyl-2,2,6,6-tetramethyl-4-piperidinyl)-2'-deoxycytidine	$C_{26}H_{42}N_4O_7$	521 g/mol		156.3 mg		0,30 mmol
Acqueous Ammonia 25%	NH_4OH	35 g/mol	1,0 ml	910 mg	0.91 g/ml	6.5 mmol

In a round bottomed flask were placed 156.3 mg of 3',5'-diisobutyryl-N^4-(1-oxyl-2,2,6,6-tetramethyl-4-piperidinyl)-2'-deoxycytidine, 1 ml of NH_4OH 25% and 3 ml of MeOH. The suspension was stirred at r.t. for 4h after which the solvent was removed and the residue was purified by column chromatography with silica gel (eluent EtOAc:Isopropanol 98:2). One obtain 127.9 mg of N^4-(1-oxyl-2, 2, 6, 6-tetramethyl-4-piperidinyl)-2'-deoxycytidine as a slightly red oil. Yield 87.1%.

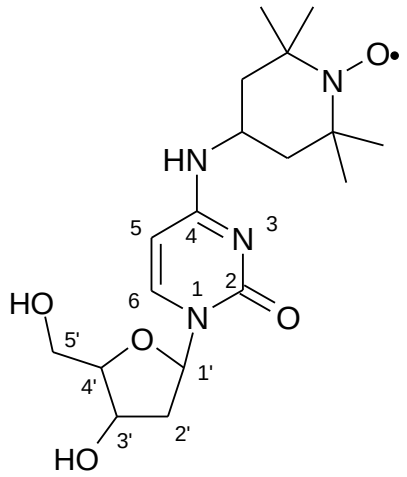

Molecular Weight	**Molecular Formula**
381.2 g/mol	$C_{18}H_{29}N_4O_5$

^{1}HNMR (CD_3OD, 300MHz) δ (ppm): 7.99 (bs, 1H; H^6), 6.26 (bs, 1H; H^5), 5.82 (bs, 1H; $H^{1'}$), 4.36 (bs, 1H; $H^{4'}$), 3.93 (bs, 1H; $H^{3'}$), 3.74 (m, 2H, $H^{5'}$), 2.13-2.35 (m, 2H; $H^{2'}$), from -15 to -35 (bm, 16H; H^{TEMPO})

HRMS (ESI): calcd for $C_{18}H_{30}N_4O_5$ ($M+H^+$) 382.2211, found 382.2274.

Synthesis of **5'-dimethoxytrityl-N^4-(1-oxyl-2,2,6,6-tetramethyl-4-piperidinyl)-2'-deoxycytidine**

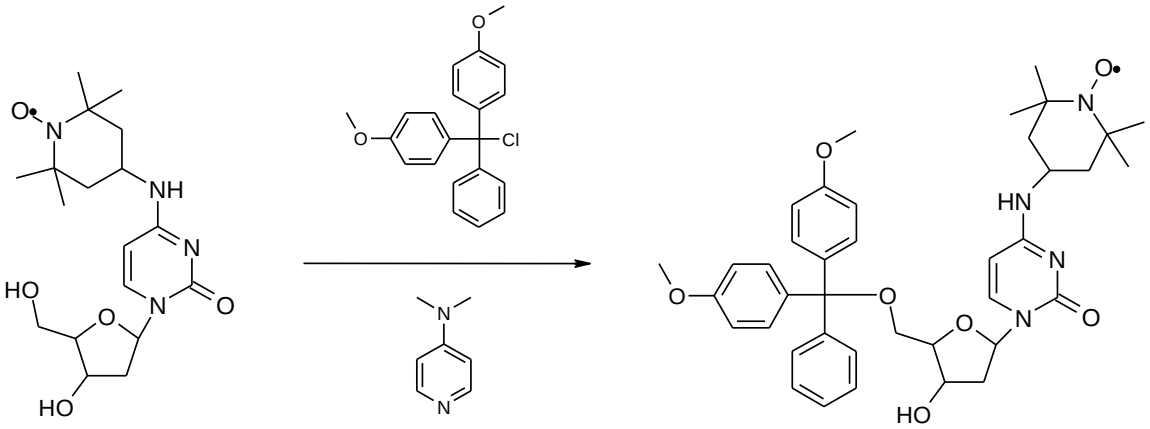

Components	Molecular formula	Molecular Weight	Volume	Weight	Density	n° of Mols
N^4-(1-oxyl-2, 2, 6, 6-tetramethyl-4-piperidinyl)-2'-deoxycytidine	$C_{18}H_{30}N_4O_5$	381 g/mol		95.25 mg		0.25 mmol
Dimethoxytrityl chloride	$C_{21}H_{19}ClO_2$	338.8 g/mol		101.64 mg		0.30 mmol
Dimethoxypyridine (DMAP)	$C_7H_{10}N_2$	122.17 g/mol		2.44 mg		0.02 mmol

95.25 mg of N^4-(1-oxyl-2, 2, 6, 6-tetramethyl-4-piperidinyl)-2'-deoxycytidine were coevaporated three times with a small volume of anhydrous pyridine (~1 ml). The film thus obtained was solved in 3 ml of anhydrous pyridine and added with 101.64 mg of DMT-Cl and 2.44 mg of DMAP. The reaction is stirred overnight at RT under N_2 atmosphere after which the solvent was removed under vacuum. The residue was diluted with CH_2Cl_2, washed (two times) with a 5% $NaHCO_3$ watery solution and brine. The organic layer was dried and the crude product was purified by silica gel chromatography (eluent EtOAc:MeOH:TEA 97:2:1). The purified product was finally solved into a small

amount of CH_2Cl_2 and dropped into cold hexane. Centrifugation (2400 rpm, 3 min.) of the resulting suspension gave 146.2 mg of 5'-dimethoxytrityl-N^4-(1-oxyl-2,2,6,6-tetramethyl-4-piperidinyl)-2'-deoxycytidine. Yield 81%.

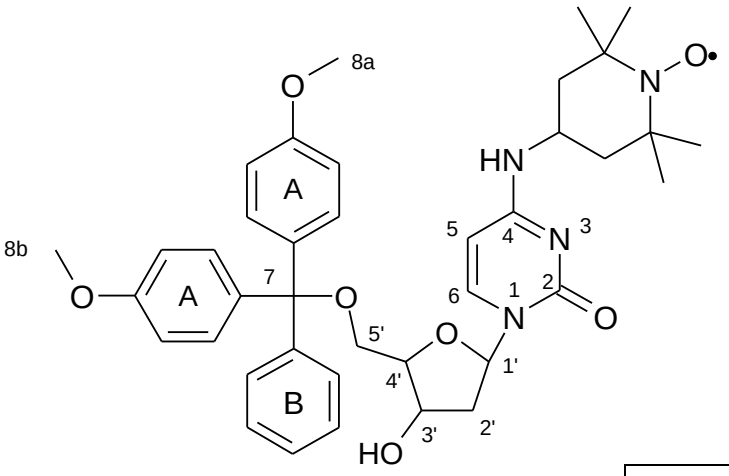

Molecular Weight	**Molecular Formula**
683.30 g/mol	$C_{39}H_{47}N_4O_7$

^{1}HNMR (CD_3OD, 300MHz) δ (ppm): 7.91 (bs, 1H; H^6), 7.40 (bs, 4H; H^A), 7.30 (bs, 5H; H^B), 6.84 (bs, 4H; H^A), 6.30 (bs, 1H; H^5), 5.43 (bs, 1H; $H^{1'}$), 4.53 (bs, 1H; $H^{4'}$), 4.06 (bs, 1H; $H^{3'}$), 3.80 (bs, 6H; H^8), 3.61 (m, 2H, $H^{5'}$), 3.48-3.39 (m, 2H; $H^{2'}$), from -15 to -35 (bm, 16H; H^{TEMPO})

HRMS (ESI): calcd for $C_{39}H_{48}N_4O_7$ ($M+H^+$) 684.3517, found 684.3528; ($M+Na^+$) 706.3336, found 706.3337; ($M+K^+$) 722.3076, found 722.3337.

Synthesis of **5'-dimethoxytrityl-N^4-(1-oxyl-2,2,6,6-tetramethyl-4-piperidinyl)-2'-deoxycytidine-3'-(2-cyanoethyl-N,N-diisopropyl) phosphoramidite**

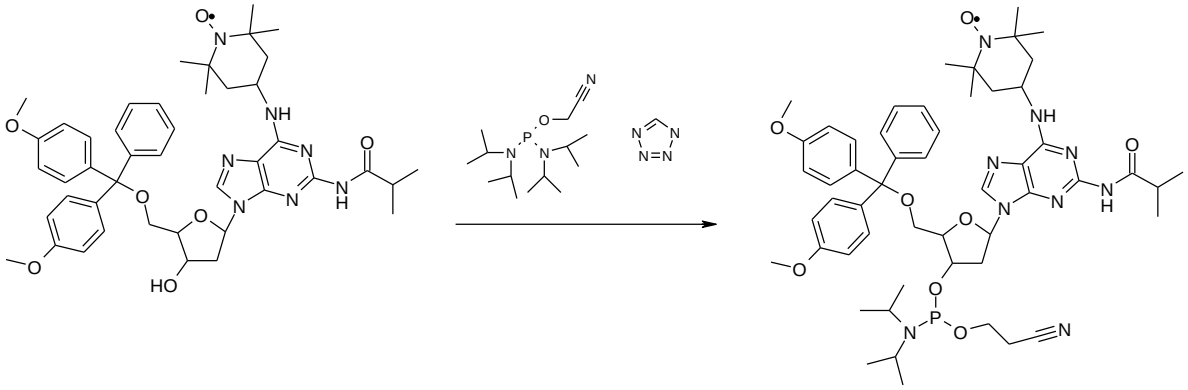

Components	Molecular formula	Molecular Weight	Volume	Weight	Density	n° of Mols
5'-dimethoxytrityl-N^4-(1-oxyl-2,2,6,6-tetramethyl-4-piperidinyl)-2'-deoxycytidine	$C_{39}H_{47}N_4O_7$	683 g/mol		136.6 mg		0.20 mmol
2-Cyanoethyl N,N,N',N'-tetraisopropyl phosphordiamidite (bisphosphoramidite)	$C_{15}H_{32}N_3OP$	301.41g/mol	127 µl	120.5 mg	0.95 g/ml	0.40 mmol
Tetrazole	CH_2N_4	70.05 g/mol		17.75 mg		0.25 mmol

136.6 mg of 5'-dimethoxytrityl-N^4-(1-oxyl-2,2,6,6-tetramethyl-4-piperidinyl)-2'-deoxycytidine is firstly coevaporated three times with anhydrous acetonitrile. The solid was lastly dissolved into 2 ml of anhydrous acetonitrile and to the solution were added 127 µl of bisphosphoramidite and 17.75 mg of sublimated tetrazole. The whole was left under Ar pressure at RT for 2 h during which the organic salts precipitated out of the solution. Work-up of the reaction consisted in a first filtration of the suspension, as to remove the salts,

followed by the removal of the solvent under vacuum. The crude mixture was dissolved in CH_2Cl_2 and washed (two times) with brine. The organic layer was dried and purified by silica gel chromatography (eluent EtOAc:MeOHl:TEA gradient from 80:15:5 to 70:23:7). The purified product was solved again into a small amount of CH_2Cl_2 and dropped into cold hexane. 132.45 mg of 5'-dimethoxytrityl-N^4-(1-oxyl-2,2,6,6-tetramethyl-4-piperidinyl)-2'-deoxycytidine-3'-(2-cyanoethyl-N,N-diisopropyl) phosphoramidite were obtained as a pink-orange solid.

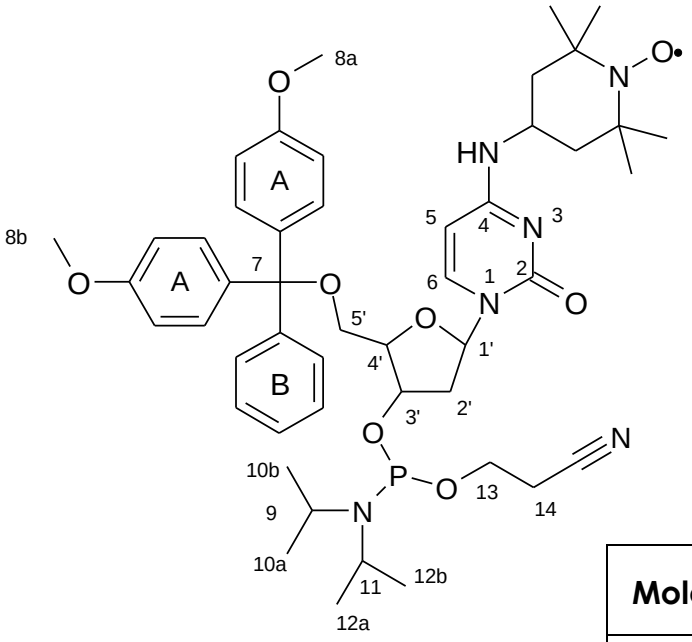

Molecular Weight	Molecular Formula
883.40 g/mol	$C_{48}H_{64}N_6O_8P$

^{1}HNMR (CD_3Cl, 300MHz) δ (ppm): 8.01 (bs, 1H; H^6), 7.43 (bs, 4H; H^A), 7.32 (bs, 5H; H^B), 6.87 (bs, 4H; H^A), 6.35 (bs, 1H; H^5), 5.49 (bs, 1H; $H^{1'}$), 4.53 (bs, 1H; $H^{4'}$), 4.15 (bs, 1H; $H^{3'}$), 3.83 (bs, 6H; H^8), 3.60-3.39 (m, 6H; $H^{5',2',13}$), 2.78-2.40 (m, 4H; $H^{9,11,14}$), 1.29-1.19 (2 bs, 12H; $H^{10,12}$), from -15 to -35 (bm, 16H; H^{TEMPO});

^{31}PNMR (CD_3Cl, 300MHz) δ (ppm): 149.25, 148.66

HRMS (ESI): calcd for $C_{48}H_{65}N_6O_8P$ ($M+H^+$) 884.4596, found 884.4592; ($M+Na^+$) 906.4409, found 906.4409; ($2M+H^+$) 1767.9116, found 1767.9116.

DNA OLIGONUCLEOTIDE SYNTHESIS SCHEME

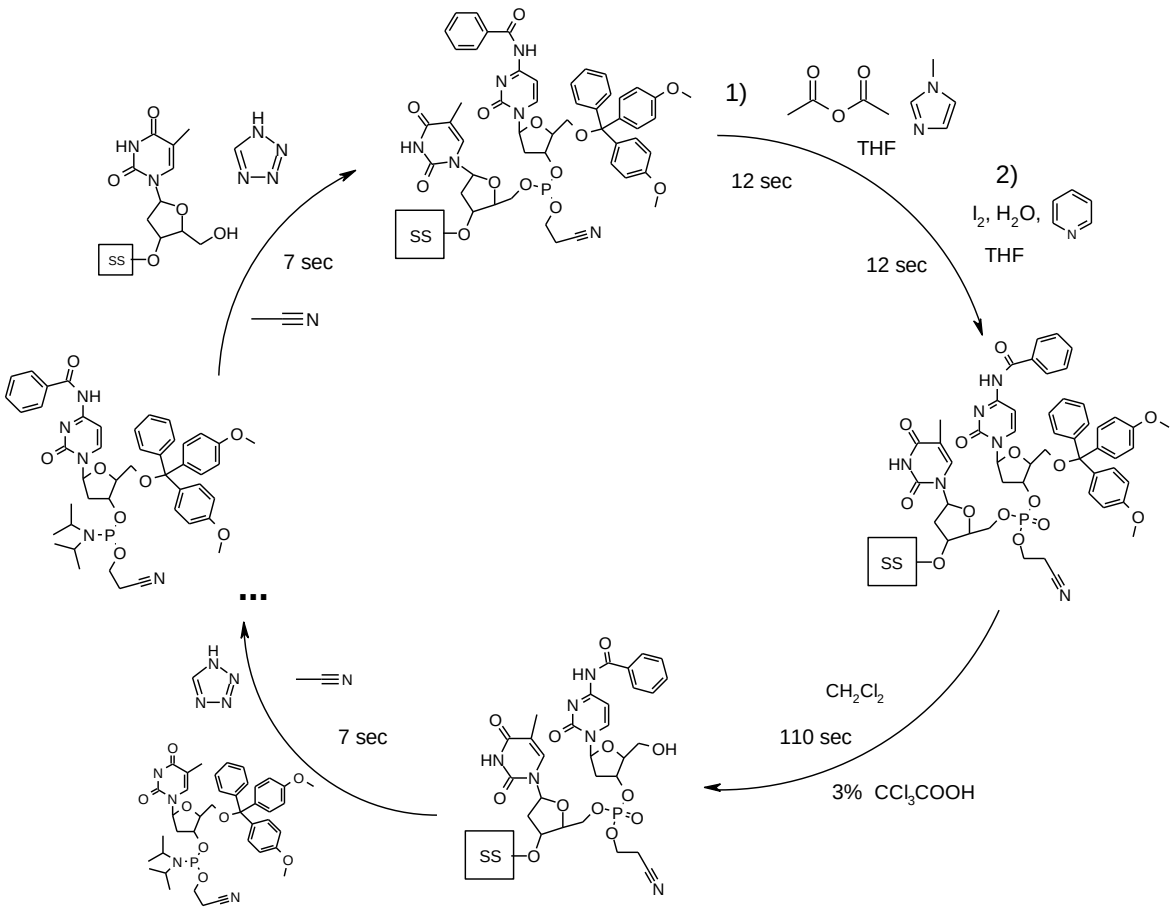

NOTE: Here is showed only the *cytidine* coupling to the solid-support-oligonucleotide strand. The same procedure was applied to all the other nucleotides coupled via automatic synthesis. For further information about reagents and condition, see the "Synthesis" part described below.

Synthesis of the **Unmodified and TEMPO-labeled Oligonucleotide strands**

The two complementary DNA strands

5' A A A A A G A C T T G G A A A A A T T T T T **3'**
3' T T T T T C T G A A C C T T T T T A A A A A **5'**

were synthesized on 1.0 µmol scale (1000 Å controlled pore glass -CPG- columns) with using standard automatic DNA oligonucleotide synthesis procedure; the instrument chosen was an Applied Biosystem 3400 DNA/RNA synthesizer. The oligo synthesis direction was always from 3' to 5'.

All the phosphoramidites used in all the synthesis were protected in the reactive groups, as to prevent secondary reactions. In particular:

- The cytidine derivative was protected at the N^6 position with a benzoyl group,
- The guanidine derivative was protected at the N^2 position with an isobutyric group,
- The adenine derivative was protected at the N^4 position with a benzoyl group.

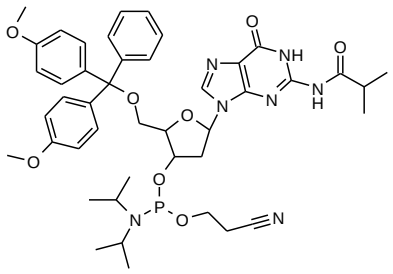

N^2-isobutyryl-guanidine

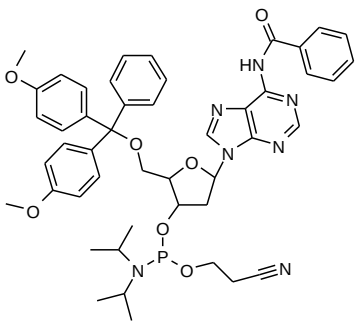

N^4-benzyl-adenine

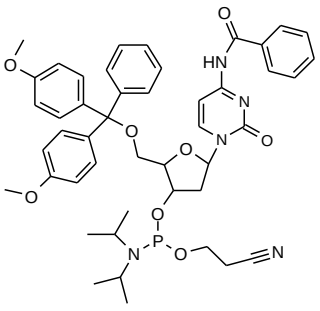

N^6-benzyl-cytidine

All the phosphoramidites were purchased from Glen Research (22825 Davis Drive, Sterling, Virginia, 20164) and were used without further purifications. The bottles were open and left under vacuum (14 mmHg) overnight before preparing the coupling solution (as to prevent moisture interference).
The synthesis route could be resumed as follow:

- Coupling of a nucleotide to the oligonucleotide strand (linked to a solid glass support) using tetrazole as catalyst

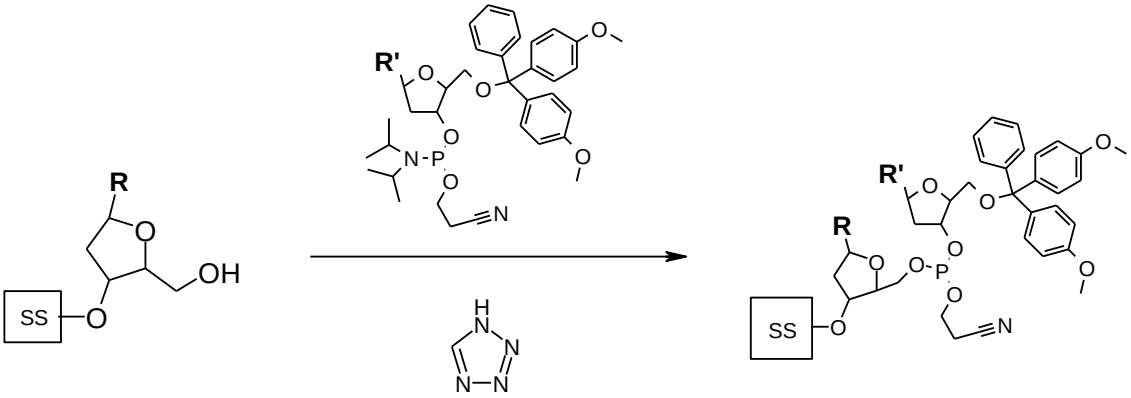

SS = solid glass support

- Capping of the unreacted 5'hydroxyl group of the oligo strand operated by acetic anhydride and N-methylimidazole as catalyst

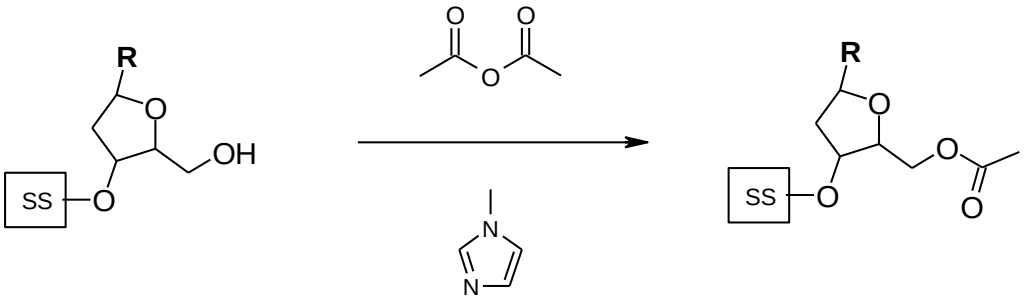

- Oxidation of the phosphite function to phosphate

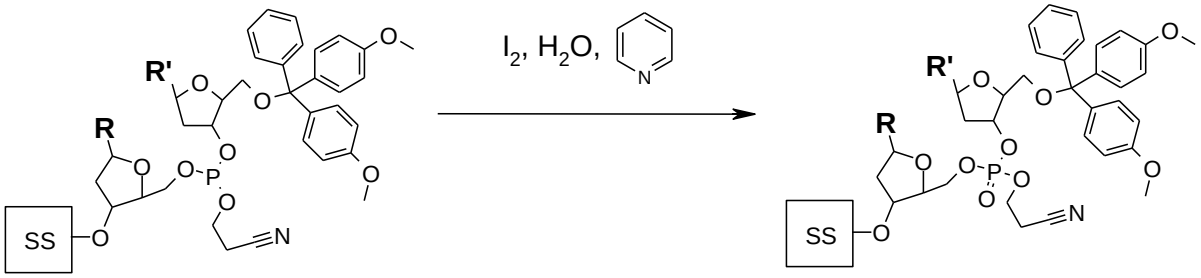

- Deprotection of the DMT group (detritylation) linked to free the 3'-hydroxyl group of the oligo for the next coupling

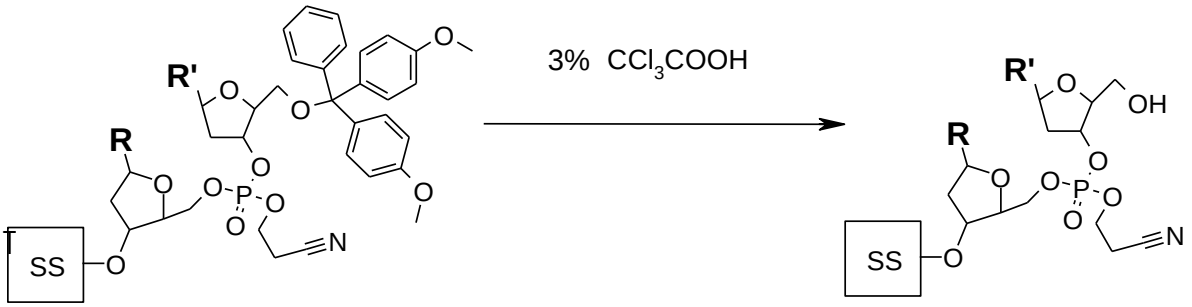

All the nucleotides solutions were constituted of a 0.1 M desired phosphoramidite into anhydrous THF and were prepared immediately before the use.

The coupling solution consisted of a 0.3 M tetrazole solution into anhydrous THF.

The capping solution was composed by two different solution, a 10% acetic anhydride solution into anhydrous THF and a 10% N-methylimidazole solution into a THF/pyridine (90/10) mixture.

The oxidation mixture was prepared mixing iodine with a mixture of pyridine, THF and H_2O with a final 0.02 M iodine concentration.
The deprotection mixture was a 3% trichloroacetic acid solution into anhydrous CH_2Cl_2.
The DNA synthesizer was firstly charged with all these solutions and all the lines were filled with the solutions before the beginning of the oligonucleotide synthesis.
This machine works with an initial pressure charge, used for delivering the solution to the glass resin, placed inside a small reactor (column). This pressure, gained from an Ar bomb, should guarantee a constant flow of 30 µl/s for each solution.
Thus, to correctly fill the lines, an initial 15 sec Ar pressure was applied to all the solution followed by 7 sec (210 µl) of oligonucleotide delivery to the waste (the column wasn't already placed) and 15 sec (450 µl) of reagent delivery to waste.
After that, the column containing CPG resin functionalised with a first nucleotide was placed into the DNA synthesizer and the first coupling was started. The coupling solution was initially delivered to the column for 1.7 sec (51 µl), followed by 7 sec (210 µl, 21 equivalents respect to the resin) of nucleotide solution delivery; to push all the activated phosphoramidite into the column, the coupling solution was delivered for a further 3.9 sec (117 µl). To ensure a good coupling result, the whole mixture was allowed to rest inside the column for 120 sec ("coupling time" or "sleep time") before washing the column with anhydrous ACN as to prepare it for the next capping step.
The capping step was accomplished delivering both the separated capping solution to the column for 12 sec (360 µl) and keeping all to react for another 6 sec. Once again, the column was washed with ACN to clean the resin from the capping reagent excess.
The oxidation step was performed with a 12 (360 µl) sec delivery of the oxidation mixture into the column followed by 12 sec of "sleep".

After washing the column with anhydrous CH_2Cl_2, the last detritylation was obtained with a 110 sec (330 µl) deprotection solution delivery to the column. Three features of this step must be underlined:

- The coupling yield is measured recording the trityl carbocation passage (freed during the acidic cleavage) into a potentiometric detector fitted inside the machine,
- This control also could stop the deprotection step before the 110 sec if the trityl value detected is under a particular cut-off value,
- To facilitate the purification step (described later in this chapter), the last DMT function wasn't removed from the oligonucleotide chain.

A last cleaning step with CH_2Cl_2 and, later, with anhydrous ACN prepare the column for the following nucleotide coupling route.

To couple the two TEMPO-labeled nucleotides, a different procedure was employed since the automatic coupling failed to give the desired product. The oligonucleotides were thus realized according to the procedure described above until the insertion of the desired TEMPO-nucleotide

A A A A T T T T T **3'**

for the TEMPOadenine and the TEMPOadenine-TEMPOcytidine oligo strands

T T G G A A A A A T T T T T **3'**

for the TEMPOcytidine oligo strand.

At this point, the spin-labeled nucleotides were inserted using the following procedure:

In a 10 ml round bottomed flask were liophylized 10 µmol of the desired TEMPO-labeled nucleotide from benzene. Meanwhile, 1 µmol of CPG resin conteining the corresponding oligonucleotide sequence was firstly dried with

argon and then under vacuum for 2,5-3 h. 9,6 mg (50 µmol) of previous dried 5-benzylthio-1H-tetrazole (BTT) and the CPG resin were placed[29] in the flask containing the phosphoramidite and the system was further equipped with a three-way exit connected to another three-way exit. The solid mixture was dried on high vacuo (two-stages pump) for 1,5 h, purged with argon and leaved under low pressure (membrane pump) overnight. After that 250 µl of dry acetonitrile were dropped into the flask and the suspension was leaved in a gentle stirring for 1,5 h. Finally, the unsoluble resin was recovered from the flask replacing it inside the column and filtering the excess of liquid (a 10 ml syringe could be used as "pump"). The solid was rinsed with acetonitrile (30 ml), dried firstly with nitrogen and then in vacuo.

To calculate the coupling yield, an analytical sample (3 mg) was taken for the quantitative analysis. It was placed inside a 10 ml volumetric flask and filled with a 70% perchloric acid solution in EtOH; 1 ml of the pink-orange solution was read with an UV spectrometer at 499 nm (the maximum absorption value of the trityl carbocation) and the concentration of the trityl was found using the Lambert-Beer equation, with ε_{499} = 71700 ("A" refers to the absorbance while "L" is the path length of the light)

$$\mathbf{A = \varepsilon_{499} \cdot L \cdot C_{(mol/L)}}$$

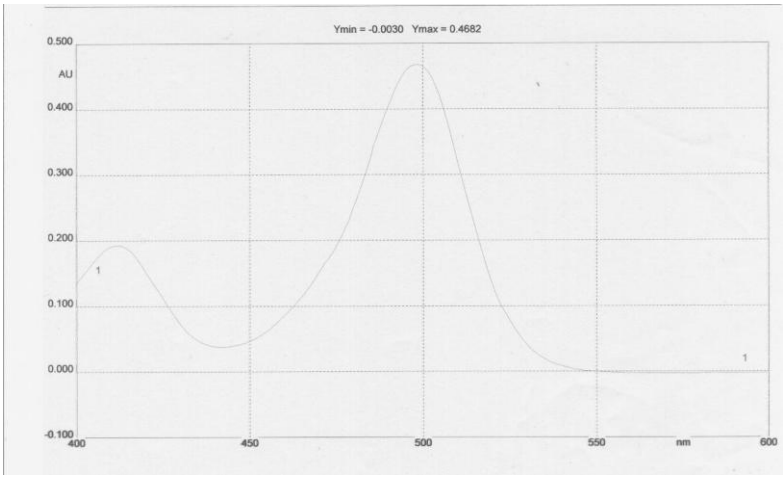

[29] Be careful during the addition of the CPG resin because of the electrostaticity it possess (when is well dried); add always the resin before the BTT (it help the resin to flow inside the flask).

From the absorption values measured for all the different TEMPOnucleotides, the following yield could be found

OLIGONUCLEOTIDE		Abs499	mg weighted	YIELD (%)
TEMPO-Adenine Single-modification		0,4682	1,5	95,5
TEMPO-Cytidine Single-modification		0,396	1	88
TEMPO-Adenine Double-modification		0,3864	1,3	92,1
TEMPO-Cytidine double-modification		0,2546	0,9	87,7

To terminate the TEMPO-labeled oligo strands, the column were replaced into the DNA synthesizer and the coupling route was restarted with some modifications of the standard procedure:

- A 1M ^{tert}Buthylhyroperoxide solution in CH_2Cl_2 was used as the oxidation solution instead of the I_2 solution,
- 3% dichloroacetic acid solution in CH_2Cl_2 was used as deprotection solution instead of 3% trichloroacetica acid solution.

The remaining strand synthesized in this manner were

5' A A A A A G A C T T G G

for the TEMPOadenine oligo strand

5' A A A A A G A

for the TEMPOcytidine oligo strand

T T G G

5' A A A A A G A

for the TEMPOadenine-TEMPOcytidine oligo strand

All the oligonucleotide strands were cleaved using roughly 1 ml of concentrated aqueous ammonia (32%) at 55 °C for 16 h for each µmol of oligo.

The purification procedure for all the oligo chains could be resumed in three section:

- Removal of the ammonia solution via *rotavapor* or *rotaflow* and purification of the resulting film was purified by reverse-phase silica gel medium-pressure-liquid-chromatography (MPLC). The flux of the system was set at 6 ml/min and the UV-VIS detector was set at 260 nm. The first of the two eluents (A) chosen for the mobile phase was a mix composed by 95% of a 0.05 M triethylamine acetate (TEAA) aqueous solution and 5% of a 50/50 ACN/H_2O solution; the second eluent (B) was a mix composed by 50% of a 0.05 M triethylamine acetate (TEAA) aqueous solution and 50% of a 50/50 ACN/H_2O solution. A first gradient starting from A_100% to A/B_50/50% was applied for 3.5 h (until the exit of the truncated oligo sequences) followed by an isocratic A/B_50/50 concentration until the exit of the desired DMT-oligonucleotide strand,
- The fractions containing the product were collected and lyophilized overnight. The resulting solid was detritylated with an acetic acid/H_2O 80/20% mixture (1 ml for each µmol) for 30 min at 0 °C; to remove the formed trityl carbocation, several (usually five) washes with Et_2O were performed, always recovering the aqueous phase,

- The watery solution was diluted to approx. 15 ml and lyophilized overnight. To check the correct deprotection and the final purity of the oligonucleotides, the resulting solid was analysed by HPLC (Water 2695 4 pumps equipped with a diode array detector). The UV-VIS detector was set at 260 nm, the two phases were: 0.05 TEAA aqueous solution for the polar eluent (A') and ACN for the apolar one (B'). A gradient starting from A'/B'_95/5% to A'/B'_40/60% was applied for all the runs.

A mass analysis was also performed to fully characterize the different products. The mass used was an Applied Biosystem Voyager System 2081 MALDI-TOF Mass Spectrometer. Each sample was prepared mixing 1 µl of the oligo solution with 1 µl of a 2-hydroxypicolinic acid (50 mg in 1 ml of a H_2O/CAN 50/50 mixture) solution and 1 µl of a 0.1 M citric acid H_2O solution.
The following results were obtained:

calcd for the 5'-AAAAATTTTTCCAAGTCAAAAA-3' sequence ($M+H^+$) 6673.4, found 6668.2
calcd for the 5'-AAAAAGACTTGGAAAAATTTTT-3' sequence ($M+H^+$) 6789.4, found 6780.2
calcd for the 5'-AAAAAGACTTGG**tA**AAAATTTTT-3' sequence ($M+H^+$) 6984.4, found 7003.3
calcd for the 5'-AAAAAGA**tC**TTGGAAAAATTTTT-3' sequence ($M+H^+$) 6969.4, found 6780.2
calcd for the 5'-AAAAAGA**tC**TTGG**tA**AAAATTTTT-3' sequence ($M+H^+$) 7146.4, found 7156.3

5. Discussion of the results

The beginning of this project was the choice of a convenient paramagnetic probe useful for our interest. The 4-aminoTEMPO was chosen for the high stability of the nitroxide moiety and for the reactivity of the primary amino group in position 4. The first property is due to the hyperconjugative effect of the 4 methyl groups surrounding the nitroxide function; in fact, even the removal of only one methyl group lead to a radical 5000 times less stable[30]. The second aspect is crucial for a implementation of the probe inside our biological system (this is, fundamentally, the key concept of SDSL).

The TEMPOamine is commercially avalaible. Nevertheless it is quite expensive, so we decided to start from a cheaper intermediate, the triacetonamine. The reported synthesis route[31] for TEMPOamine is quite straightforward (see Experimental part) except for the reduction of the oxime, which is obtained with Na in isoamilyc alchool. Instead, the use of another reducing agent, such as $LiAlH_4$, gave an easily work-up and better yield.

An interesting reaction that should be better described is the formation of the nitroxide function. The reaction is performed with H_2O_2 and Na_2WO_4 in presence of EDTA 4-Na^+ salt. The first two reagent produce *in situ* the corresponding pertungstate, a mild and selective oxidizing agent for this kind of amine. The EDTA 4-Na^+ salt[32] stabilize the hydrogen peroxide helping the formation of the peracid and avoiding secondary reaction.

[30] Rozantsev, E. G. Free Nitroxyl Radicals. *H. Ulrich ed., Plenum Pres, New York*. **(1970)**. This book is a good reference for the chemical and physical properties of the radical as well for the synthesis procedures.
[31] See ref **26**
[32] See ref **26**

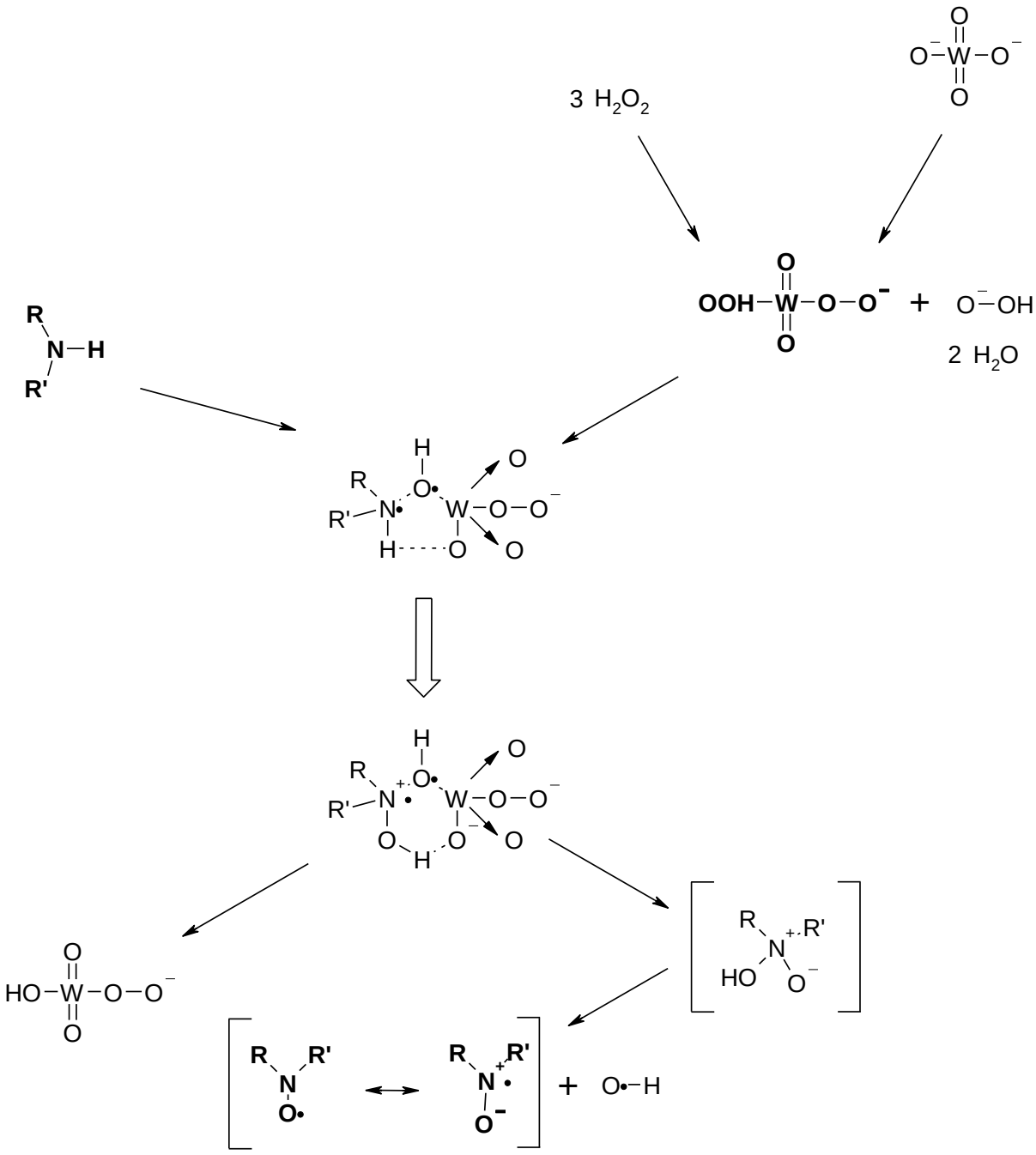

Another interesting feature of the radicals arose from the NMR spectrum. Due to faster relaxation time, all the proteon peaks of the TEMPO derivatives were broadened; all the information about coupling constant were thus lost.

Moreover, due to the proximity of the radical, the chemical shift of the TEMPO methyl and methylen hydrogens was shifted far on the right part of a spectrum; they were approximatively found in the range berween -15 and -35 ppm. This range is quite in accordance with a recent work on the calculated versus experimental chemical shift values of the TEMPO derivatives[33].

The TEMPOamine was initially inserted into different positions of the camptothecin structure. The first two derivatives synthesis started from the data obtained with *Gimatecan*[34], a 7-oximederivative of the CPT. Both derivative have the same intermediate, the 7-formylCPT, obtained through an acidic deprotection of the 7-dimethoxymethylCPT acetal. The latter was synthesized from camptothecin by a Minisci radicalic hydroxyalkylation.

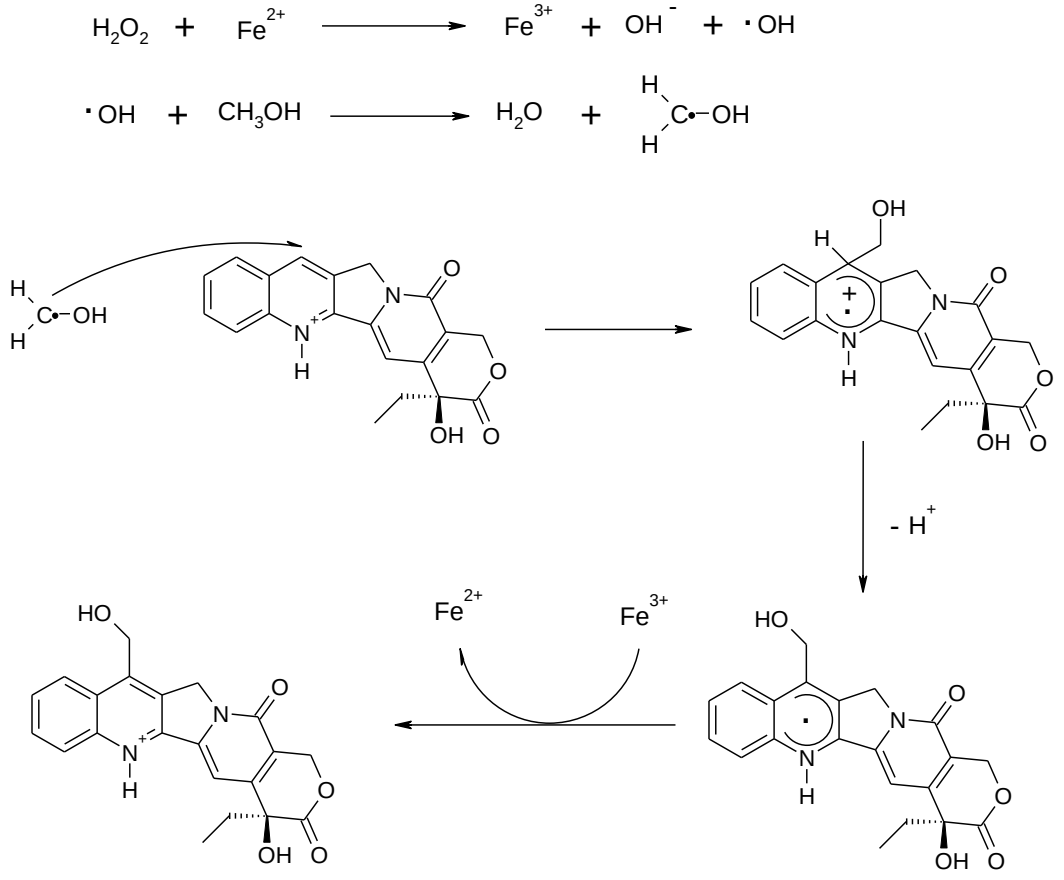

[33] Rastrelli, F.; Bagno, A. Predicting the NMR Spectra of Paramagnetic Molecules by DFT: Application to Organic Free Radicals and Transition-Metal Complexes. *Chemistry-A European Journal*. **(2008)**, 15(32)**;** 7990 - 8004

[34] See ref **19**

The 7-TEMPOiminoCPT was then obtained coupling TEMPOamine and 7-formylCPT in presence of a mild Lewis acid such as Ytterbium triflate. The product couldn't be characterized by mass since it hydrolyzed in the ESi-mass instrument (the starting reagent were detected), but it was recognized by NMR (the disappear of the formyl peak at 12 ppm and the presence of the imine peak at 9.6 ppm).

Peracid oxidation of the 7-formylCPT produce the corresponding carboxylic acid which was coupled with TEMPOamine using standard FMOC peptide synthesis. More deeply, The carboxylic acid is converted into an active hydroxyl benzotriazole ester by the action of the HBTU (the HOBT push the equilibrium to the formation of the ester) which is easily attacked by the primary 4-aminoTEMPO

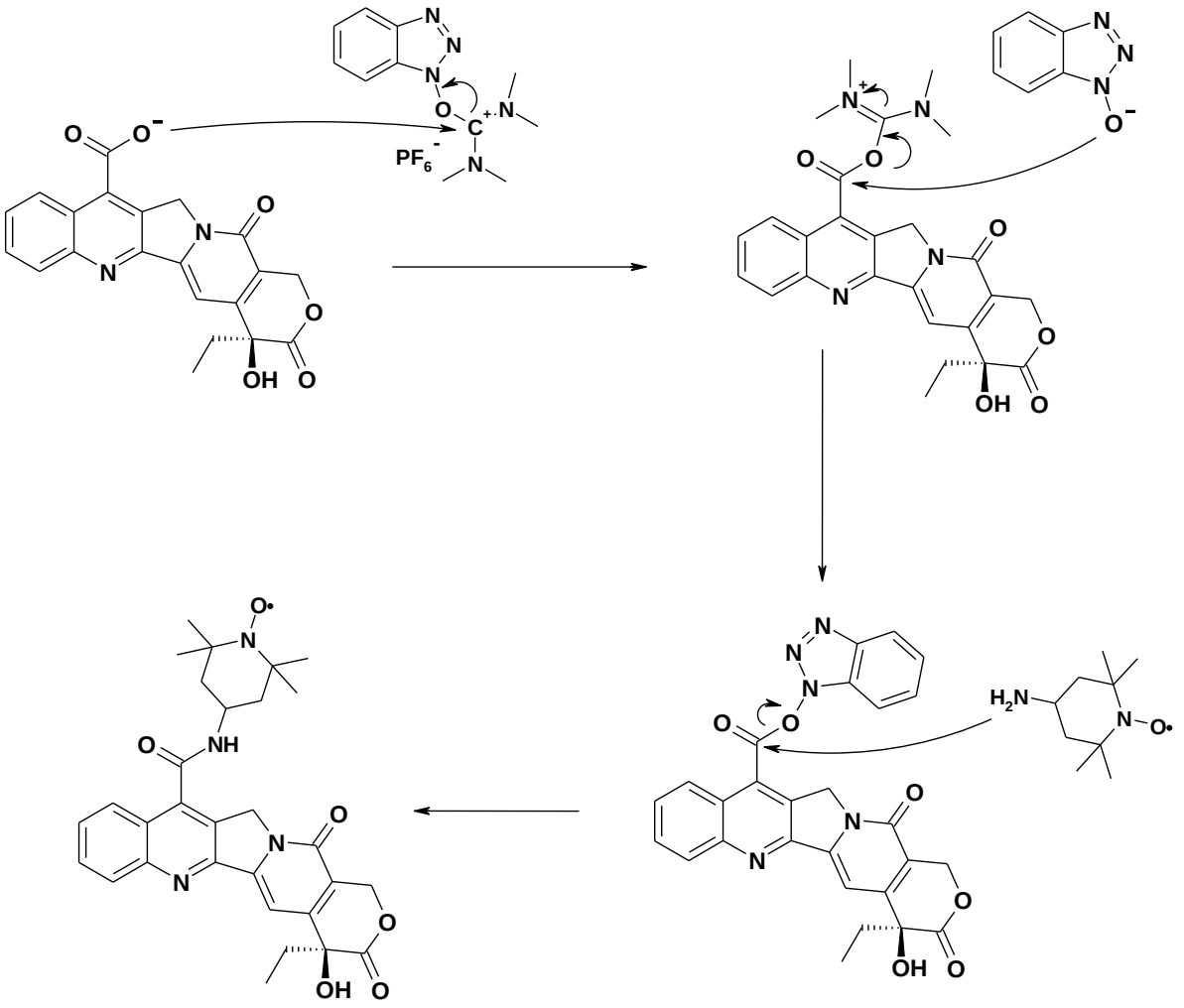

The 21-TEMPOamidoCPT was obtained through a direct nucleophylic attack at the acylic function of the 6-membered CPT lactone, while the last CPT derivative was obtained from CPT via ester formation at the 20 hydroxyl group with succinic anhydride followed by a standard peptide coupling with TEMPOamine.

To have a comparison with the EPR spectra of the CPT in presence of DNA and of the ternary complex, a 1,4-diamidoanthraquinone (with a good intercalative property) bearing the paramagnetic probe was synthesized. The harder step in the synthesis was the asymmetric substitution of the two amino groups of the anthraquinone. Thus, the first FMOC-glycine substitution was realized in a 1:1 stoichiometric ratio using DCC as reagent (the reaction mechanism is similar to the HBTU mechanism showed above). A nucleophilic acyl substitution operated by the other amino group to the bromoacetyl bromide gave the a-bromo anthraquinone derivative which was further attacked by the TEMPOamine. Last FMOC deprotection with piperidine affords the desired TEMPOanthraquine product.

The TEMPOamine was then inserted into two different nucleotides, a purine and a pyrimidine. The synthesis route was realized modifying the previous published procedure[35] especially in the last phosphitilation reaction. The synthesis was similar for both the nucleotide: a first protection of the 3' and 5' hydroxyl groups (in the guanidine was protected also the aminic function in position 2) with isobutyric anhydride allowed the activation of the carbon 4 and 6, respectively, operated by the triisopropylbenzenesulphonil chloride. This reaction transformed the oxygen atom attacked in a very good leaving group and gave the possibility to the TEMPOamine to attack the electrophilic carbon.

---

[35] Giordano, C.; Fratini, F.; Attanasio, D.; Cellai L. Preparation of Spin Labeled 2-Amino-dA , dA, dC and 5-Methyl dC Phosphoramidite for the Automatic Synthesis of EPR Active Oligonucleotides. *Synthesis* **(2001)**, 4; 565

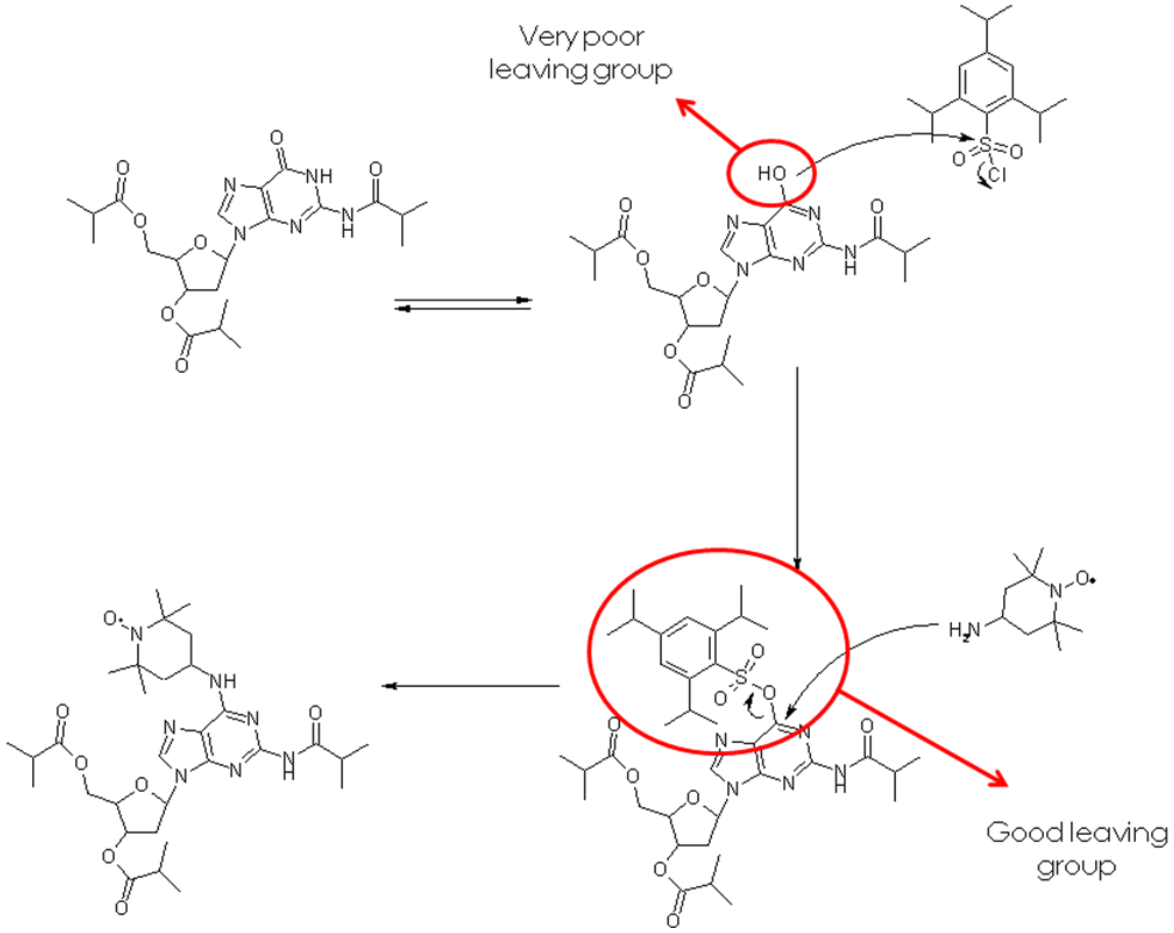

Basic catalyzed cleavage of the isobutyryl esters freed the two hydroxylic functions (but not the 2-isobutyric amide of the TEMPOadenine derivative); the 5' hydroxyl group was protected with the dimethoxytrityl moiety, a standard protective group for automatic oligonucleotide synthesis. A purification particular must be deepen: triethylamine must be added into the mobile phase during the column chromatography in order to avoid acidic DMT cleavage catalyzed by the silica stationary phase. The 3' hydroxyl function was converted to the required phosphoramidite using bisphosphoramidite and tetrazole as catalyst. This reaction was preferred to the classical reaction with chlorophosphoramidite since it didn't afford any products. The mechanism of action is summarized in the following scheme

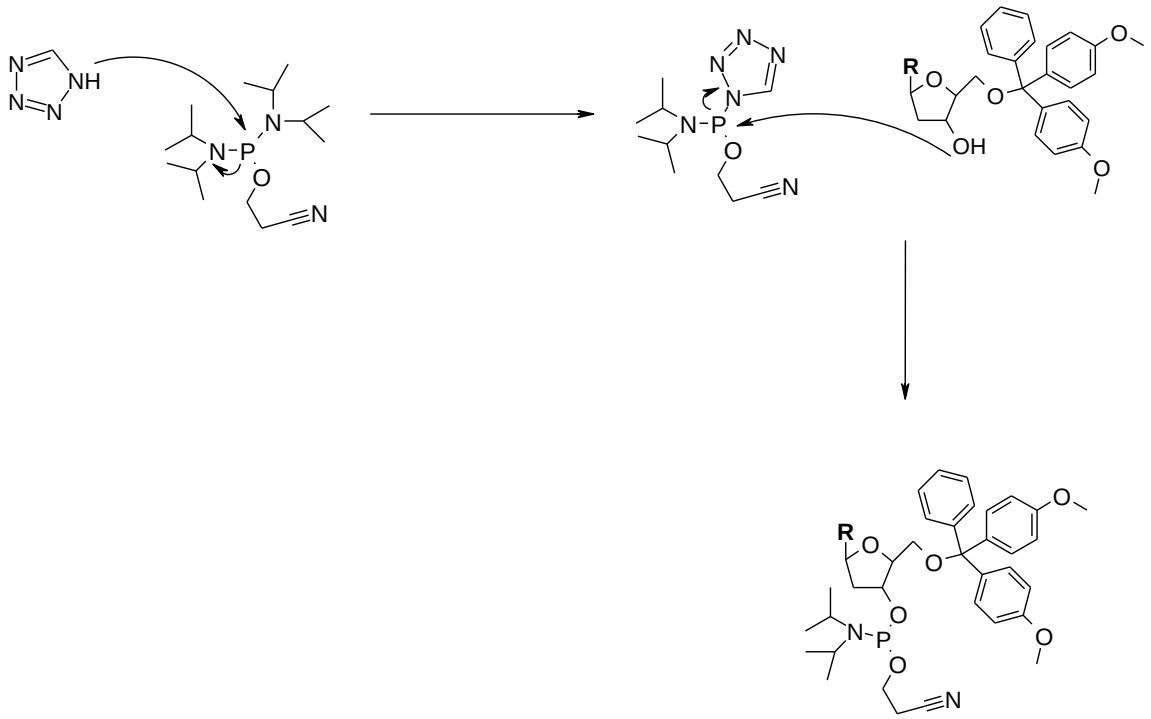

Next step was the implementation of the spin-labeled nucleotide inside an appropriate DNA oligonucleotide sequence. The following complementary ones[36]

5' A A A A A A G A **X** T T G G **Y** A A A A T T T T T **3'**

3' T T T T T C T G A A C C T T T T T A A A A A **5'**

STRAND	X	Y
Unmodified	C	A
TEMPOadenine	C	t-A
TEMPOcytidine	t-C	A
TEMPOadenine TEMPOcytidine	t-C	t-A

[36] Andersen, A. H.; Gocke, E.; Bonven, B. J.; Nielsen, O. F.; Westergaard O. Topoisomerase I has a strong binding preference for a conserved hexadecameric sequence in the promotor region of the rRNA gene from Tetrahymena pyriformis. *Nucleic Acids Res.* **(1985)**, 13**;** 1543

contain an high affinity cleavage site for the enzyme (the cleavage site is underlined in the sequence with a slash and is always in only one strand, as already mentioned in the introduction section).

The positions of the substitutions were chosen considering two aspect:

- Substitutions near the cleavage site could affect the topoisomerase I activity,
- To correctly measure the distance between two paramagnetic center, a minimum distance must be kept; usually they should be separated more than 10 Å.

Both these aspects lead to the conclusion that is not possible to substitute the nucleotides directly involved in the cleavage (the -1 and +1 nucleotides) passage.

The synthesis of the unmodified oligonucleotides was realized through a DMT-on standard DNA automatic synthesis using standard protected phosphoramidites.

The reason why the last DMT wasn't removed from the oligo strands lies in a easily removal of all the truncated sequences produced during the whole oligos synthesis (these are usually the result of an uncorrect capping procedure)

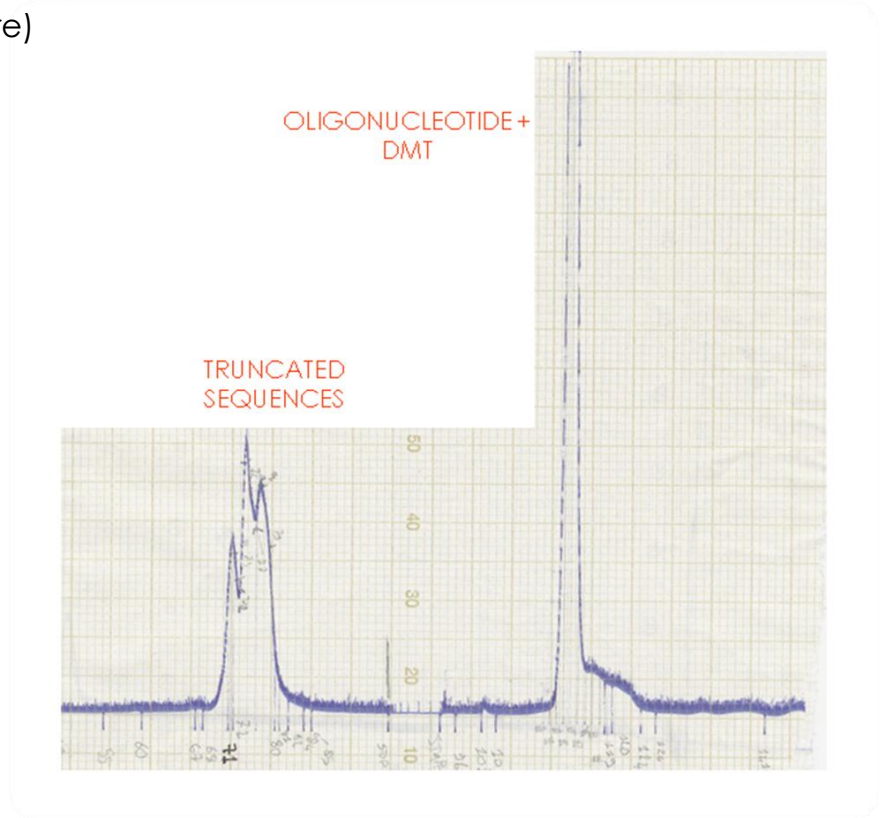

Let's now take a deeper look inside the mechanisms of action of the different steps.

The coupling step is obtained using an appropriate phosphoramidite and tetrazole as catalyst. The mechanism of action is similar to the phosphitilation process showed above

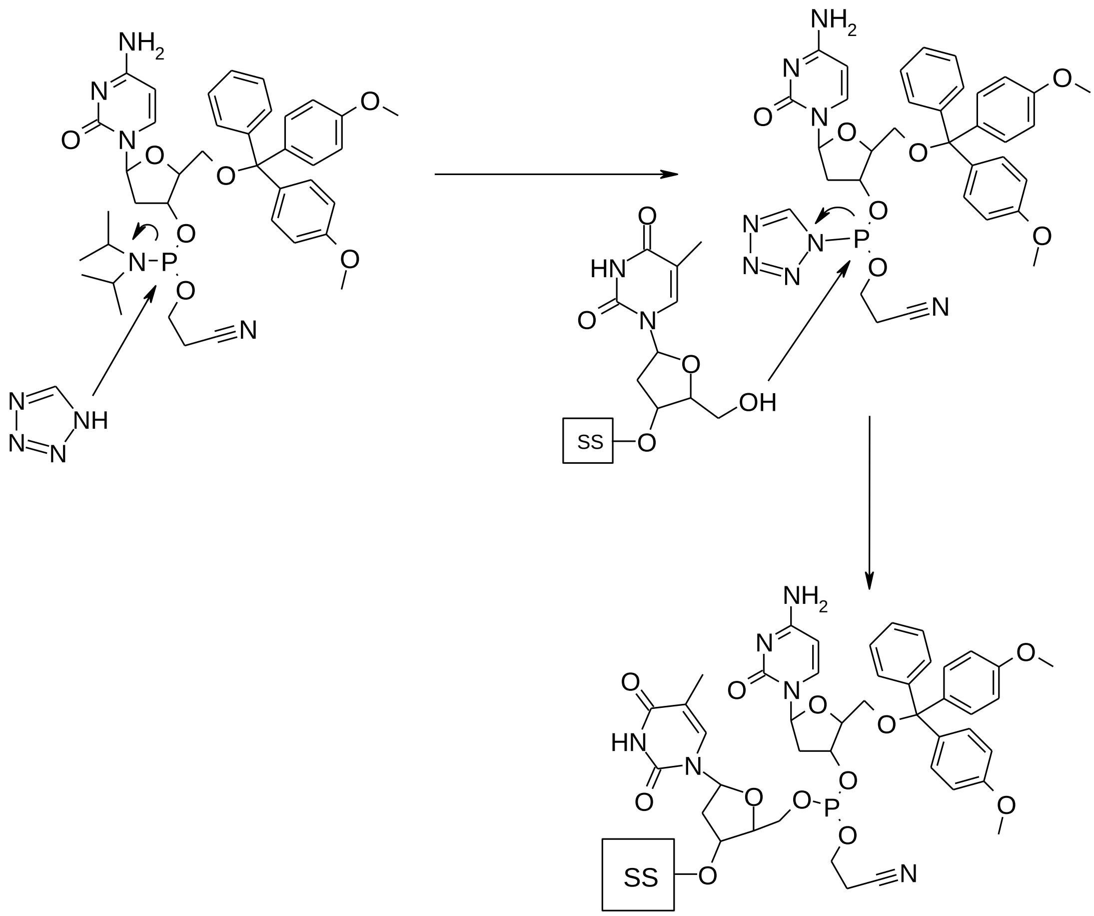

This is by far the most delicate step of the whole route. In fact, due to the low reactivity of the 5' hydroxyl group and the very low quantity involved in the reaction, all the components of the system must be completely anhydrous.

The capping reaction is a nucleophilic acyl substitution with acetic anhydride; the N-methyl imidazole activate the acetic anhydride as to push the reaction to the formation of the ester.

The oxidation step is a redox reaction where I_2 oxidize the phosphorus (III) to phosphorus (V) in presence of an oxigen donor (H_2O in this case)

The deprotection step is an acidic cleavage of the DMT group, which is a very good leaving group even in milder acidic conditions (It result stable, otherwise, in basic conditions)

A different speech must be done for the TEMPO-modified strands.

First of all, the automatic coupling failed to give the desired product; this could be explained with an harder coupling reaction due to the hindrance of the substituent or with the presence of moisture inside the nucleotide batch.

The latter explanation seems to be the correct one considering the good coupling yields obtained when the reaction was conducted under strictly anhydrous condition (see the manual coupling step in the experimental part)

A last aspect of the oligonucleotide synthesis that deserve a further deepening is the cleavage step. During the basic cleavage (see the experimental session) several group were removed; a summary of all the different reactions involved in this step could be found in the following picture

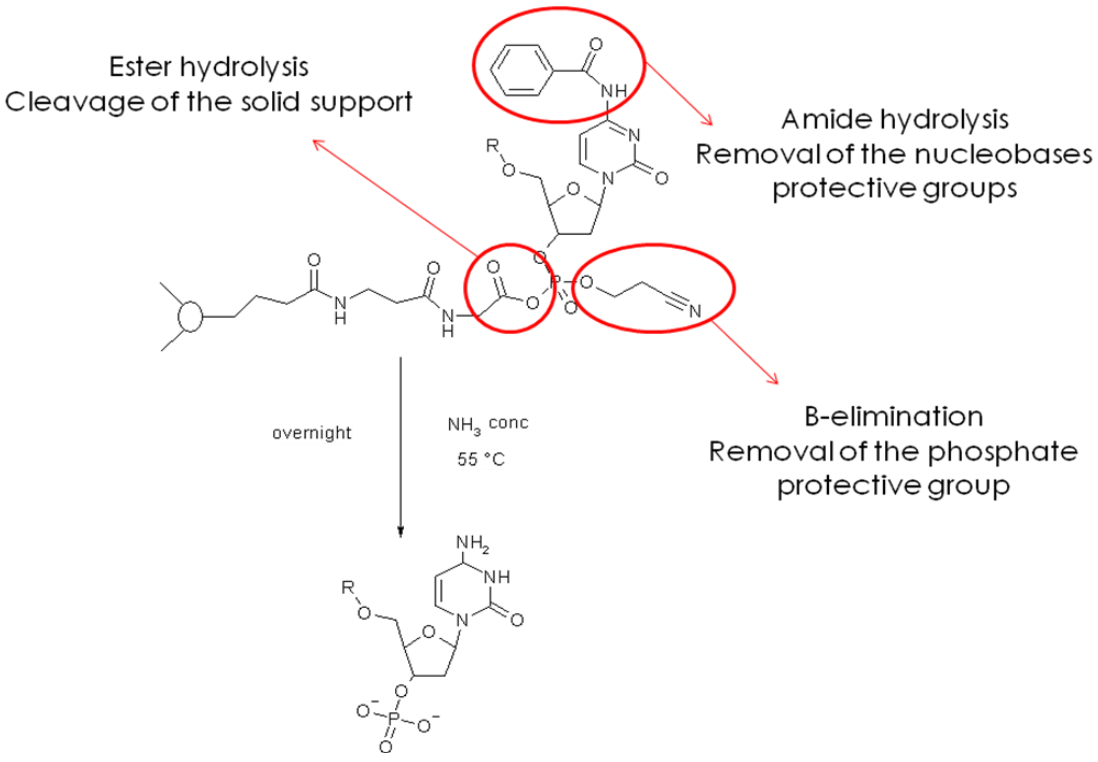

To have a general information about the secondary structure of the DNA oligos and to calculate how the TEMPO substitutions affected this value, a melting curve was calculated for all the oligos (the experiment was repeated three times for each samples). The fooliwing values were obtained:

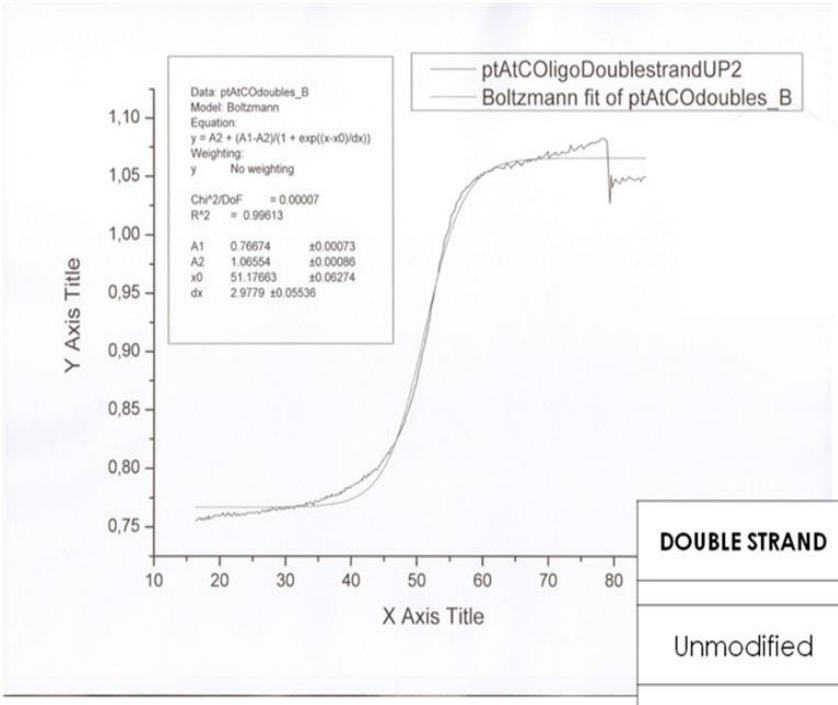

DOUBLE STRAND	MELTING TEMPERATURE
Unmodified	58.07 °C
TEMPO-adenine	54.96 °C
TEMPO-cytidine	55.10 °C
TEMPO-adenine TEMPO cytidine	51,17 °C

For each TEMPO substitution, a 3 °C loss was found; this low value suggested a B-DNA secondary structure for all the oligonucleotide strands.

Biological tests were performed for this oligo strands as to evaluate if they were recognized and processed by the Topoisomerase. All tests were performed in the laboratory of the prof. Capranico of the Biology Department of the University of Bologna. Unfortunately, two of them are completely intact

in presence of the enzyme while the other one (the TEMPOadenine strand) is only partially cleaved.

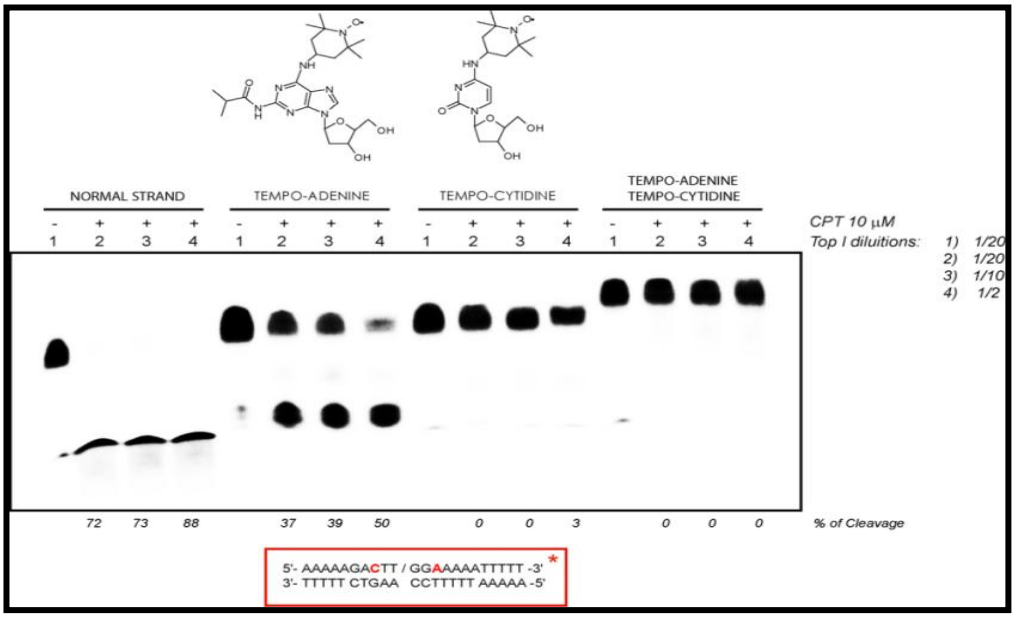

Looking at these data it is possible to suggest that substitutions in the 3'-5' direction affects, but not inhibits, the toposomerase I activity, while substitutions in the opposite direction inhibits the topo I activity. Nevertheless, none of these strands could be useful for our interest.

The CPT and anthraquinone derivatives were then characterized by EPR technique in the laboratory of the prof. Maniero of the Physical Chemistry Department of the University of Padua. As expected for a free nitroxide at room temperature, all the spectra consisted of three identical sharp lines.

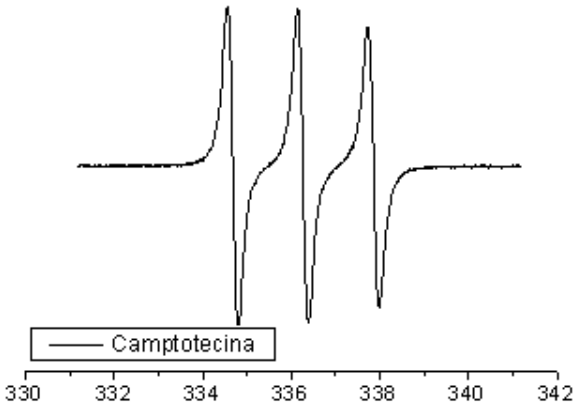

Solvente $CHCl_3$;
Temperatura 294 K
MA: 1G
CT/TC: 10/20 ms
PW: 13mW/12dB
N_{scans}: 3

As well, biological tests were carried out in order to evaluate the ability of this molecules to inhibit the topoisomerase I action.

The results showed how the two derivatives bearing the nitroxide moiety in the 7 position are able to inhibit the relegation of the DNA (in particular the 7-TEMPOiminoCPT derivative) while the other two aren't able to do it

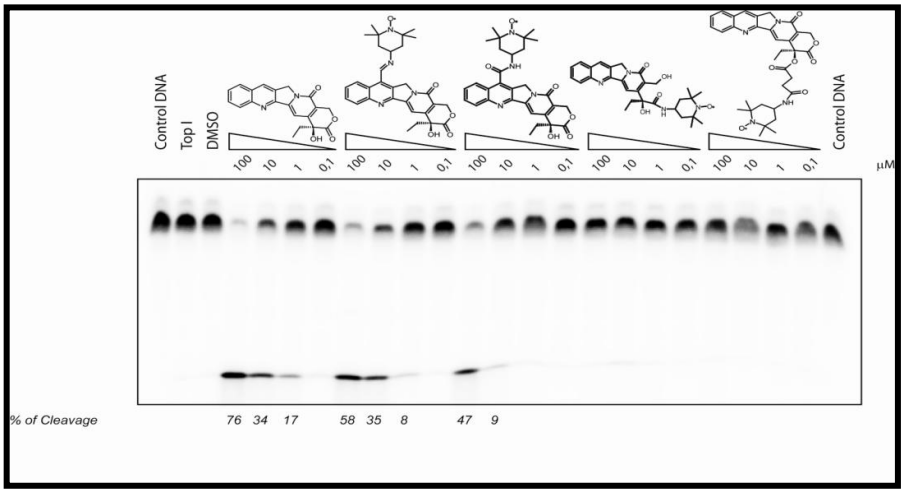

An interesting datum arise from another experiment performed in order to observe how long the binary DNA-Topo I complex could be stabilized by the inhibitor ("reversibility test"): the two active derivatives were able to stabilize it better than the camptothecin. To evaluate the effective role of the radical into this interesting aspect, another CPT derivative bearing the same chain of the 7-iminoCPT except for the nitroxide function was realized. This compound is now under biological test.

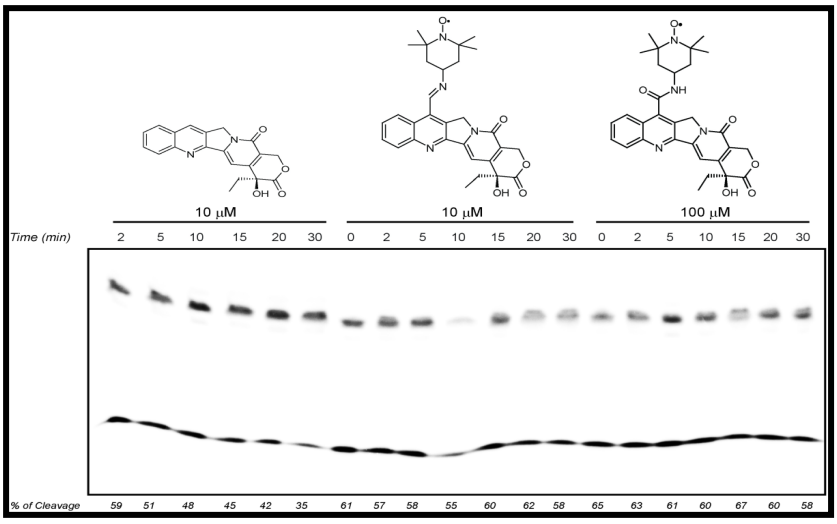

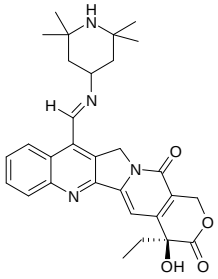

Last step for this project was the EPR experiment. Firstly was tested the capacity of the TEMPO-CPT derivatives to intercalate inside the DNA alone. As expected, none of them showed a change in the spectrum, even in higher concentration of DNA, confirming the incapacity of these molecules to intercalate (here is shown only the 7-iminoCPT).

The signal is here compared to the EPR spectrum arising from the 1,4-TEMPOamidoanthraquinone in presence of DNA

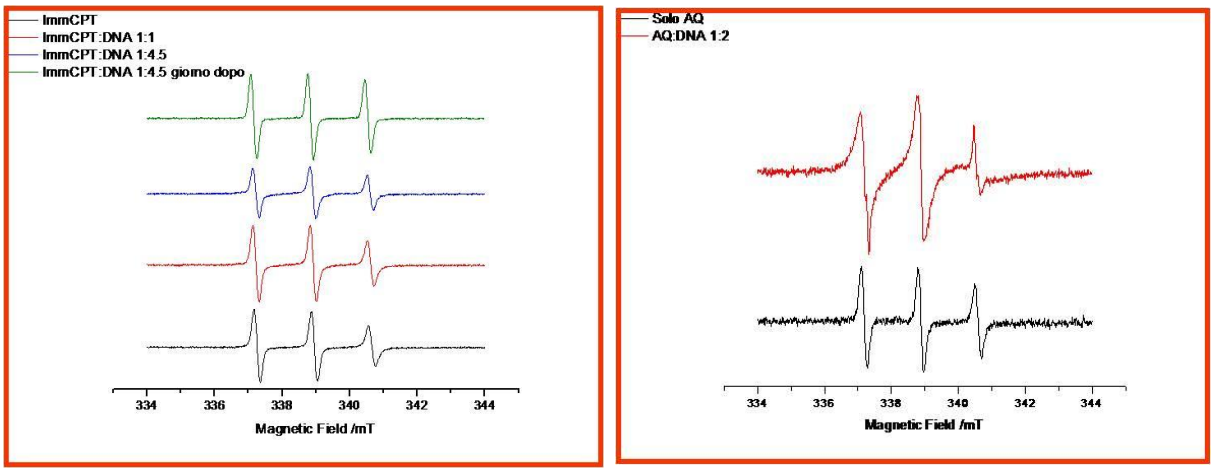

After that, a simulation of the ternary complex was built mixing the 7-iminoCPT (18 uM final concentration), the unmodified oligonucleotide strand (100 uM) and the Topoisomerase I enzyme (21 uM). The spectrum obtained (blue line) shows a different pattern compared to the spectra obtained with only CPT and DNA (red line) and only CPT and Topoisomerase I (black line)

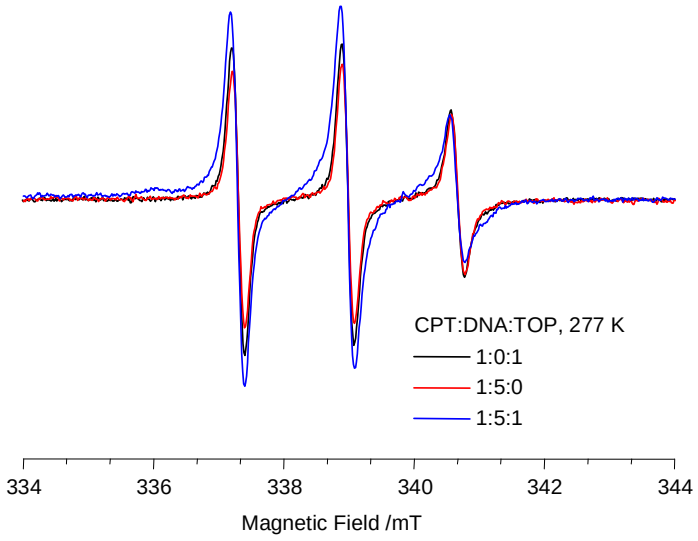

To understand the nature of the different features of this spectrum and to extrapolate informations from it, an EPR simulation was performed. Once again, the simulation was performed in the prof. Maniero laboratory.

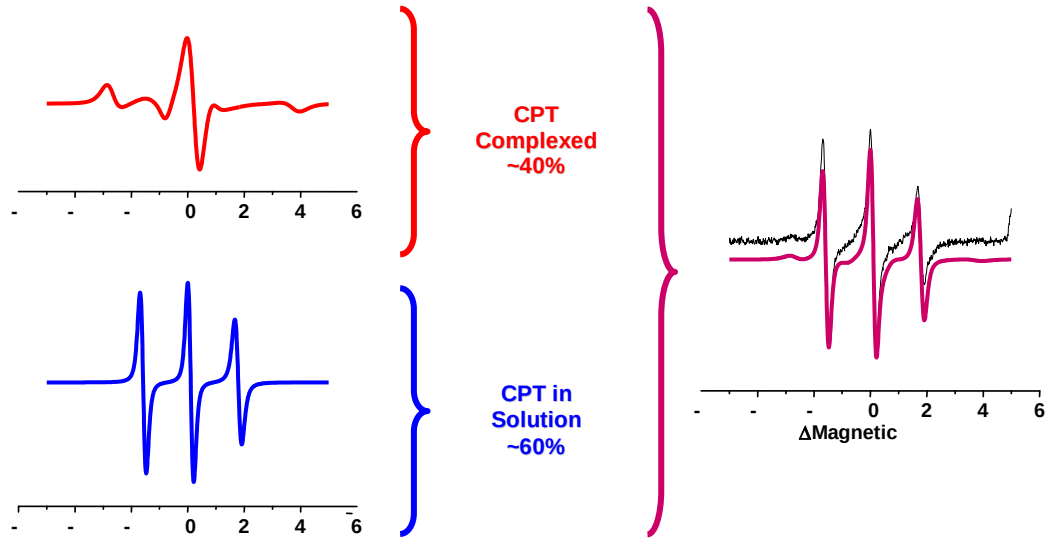

To correctly reproduce the spectrum of the ternary mixture 7-TEMPOiminoCPT:DNA:TOPI, a weighed sum of the simulations, normalized to the same number of spins, was performed. From the best fit of the experimental spectrum the relative amount of 7-TEMPOiminoCPT in the ternary complex seems to be 40±10% of the total at the steady state, while the rest is free in solution.

A final point must be focused: the presence of two individual components in the EPR experiment implies that the CPT derivative does not quickly exchange between the ternary complex and the solution, but it remain trapped inside the complex for a period surely longer than the μs scale. This datum fit with the previous one found by the Koster group (discussed in the introduction part).

B.PKA-cAMP COMPLEX

2'. Introduction

2'.1 Cyclic Adenosine 3',5'-monophosphate (cAMP) cascade

The extracellular stimuli like neurotransmitters, hormones, inflammatory stimuli, stress, epinephrine, norepinephrine, etc activate the G-proteins through receptors like GPCRs and ADR-Alpha/Beta. The major G-proteins that regulate activation of ACs are the GN-AlphaS (GN-AlphaS Complex Locus), GN-AlphaQ (Guanine Nucleotide-Binding Protein-Alpha-Q) and GN-Alphal (Guanine Nucleotide Binding Protein-Alpha Inhibiting Activity Polypeptide). Before activation these subunits are linked to other protein, GN-Beta (Guanine Nucleotide-Binding Protein-Beta) and GN-Gamma (Guanine Nucleotide-Binding Protein-Gamma) subunits; After the activation by a stimulus, the various alpha subunits convert to their GTP bound states, free the beta and gamma subunits and link the nine tmACs with distinctive regulatory features in order to regulate intracellular cAMP levels (Ref.1 & 4). GN-AlphaS and GN-AlphaQ *activate* ACs to increase intracellular cAMP levels, while GN-Alphal *decrease* intracellular cAMP levels by inhibiting ACs. GN-Beta and GN-Gamma subunits act synergistically with GN-AlphaS and GN-AlphaQ only to activate ACII, IV and VII. The rapid dephosphorilation of GTP to GDP lead to the dissociation of the GN-alpha protein from the AC and the rebonding of the beta and gamma subunits to it. The whole process drive to the inactivation of the AC activity and to the stop of cAMP formation.

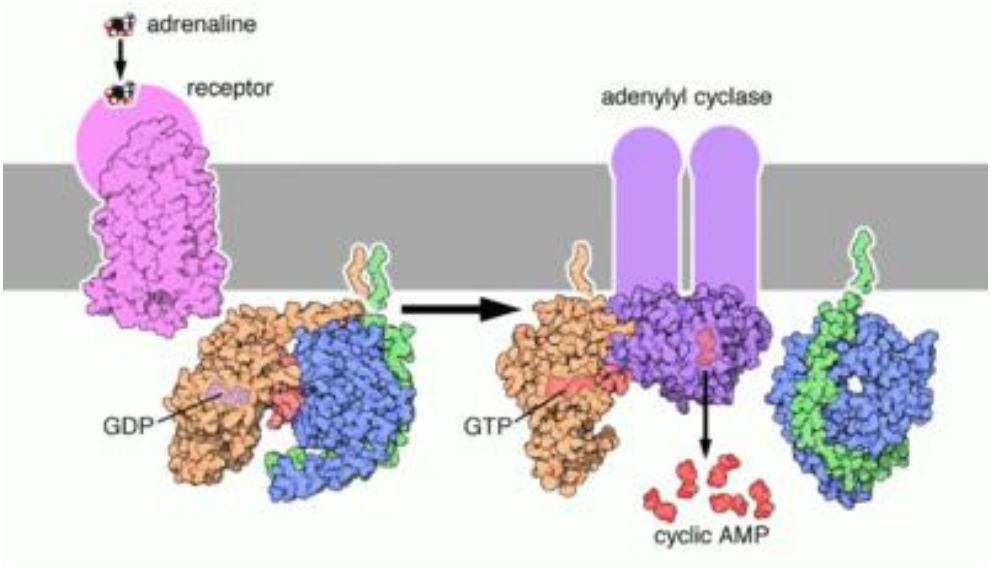

The different receptors, chiefly the GPCRs (G-Protein Coupled Receptors), Alpha and Beta-ADRs (Adrenergic Receptors), Growth Factor receptors, CRHR (Corticotropin Releasing Hormone Receptor), GcgR (Glucagon Receptor), DCC (Deleted in Colorectal Carcinoma), etc are responsible for cAMP accumulation in cells that cause different physiological outcomes, and changes in cAMP levels effects the selective activation of PKA (cAMP dependent Protein Kinase-A) isoforms. The chief source of cAMP is from ATP (Adenosine Triphosphate). In mammals, the conversion of ATP to cAMP is mediated by members of the Class-III AC (Adenylyl Cyclase)/ADCY (Adenylate Cyclase) family, which in humans comprises nine trans-membrane AC enzymes (tmACs) and one soluble AC (sAC).

tmACs are regulated by heterotrimeric G-proteins in response to the stimulation of various types of GPCRs and therefore play a key role in the cellular response to extracellular signals. sAC, in contrast, is insensitive to G-proteins. Instead, sAC is directly activated by Ca^{2+} and the metabolite HCO_3, rendering the enzyme an intracellular metabolic sensor.

The nine cloned isoforms of mammalian adenylyl cyclase share a primary structure consisting of two trans membrane regions, M1 and M2, and two

cytoplasmic regions, C1 and C2 (8) (Fig. 1). The transmembrane regions each contain six predicted membrane-spanning helices. The function of M1 and M2, aside from membrane localization, is unknown despite their topological analogy to transporters. The C1 and C2 regions are subdivided into C1a, C1b, C2a and C2b. The C1a and C2a[37] are well conserved, homologous to each other, and contain all of the catalytic apparatus. C1a and C2a domains heterodimerize with each other in solution. These domains can also form homodimers. Domains derived from different isoforms can form chimeric heterodimers. The C1b region is large (~15 kDa), variable, and contains several regulatory sites. The C2b is vanishingly short in some isoforms and lacks identified functions; hence C2 and C2a are sometimes referred to interchangeably.

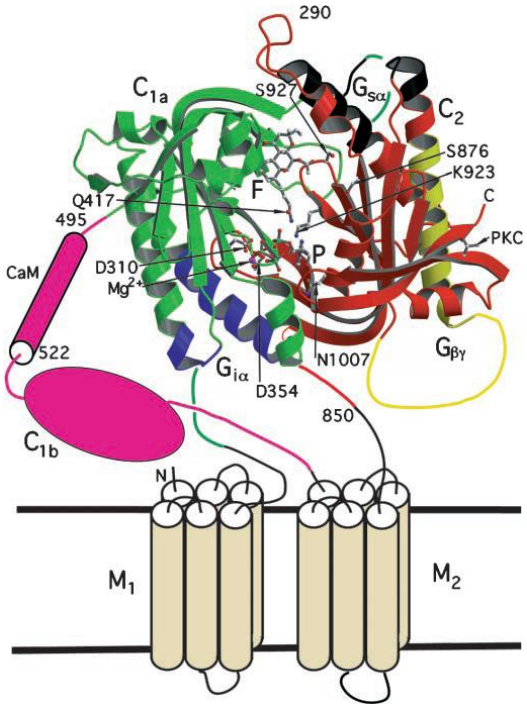

Its mechanism of action[38] can be summarized as follow:

- First deprotonation and activation of the ATP 3'-hydroxyl for nucleophilic attack and stabilization of the transition state at the a-phosphate

[37] Tang, W. J.; and Gilman, A. G. Contruction of a soluble adenylyl cyclase activated by Gs alpha and foskolin. *Science* **(1995)**, 268; 1769–1772

[1] Hurley J. H. Structure, Mechanism, and Regulation of Mammalian Adenylyl Cyclase *The Journal of Biological Chemistry* **(1999)**, *274(12)*; 7599-7602.

- Second activation of the 3'-hydroxyl through the coordination of a Mg^{2+} atom (in the figure represented as $Mg^{2+}{}_A$). A second Mg^{2+} ion (in the figure represented as $Mg^{2+}{}_B$) share with the previuos one in transition state stabilization. It has been reported that Mn^{2+} could replace the magnesium ion enhancing the activity while Ca^{2+} ion inhibits the AC activity.

Other aminoacids, Asn1007, Arg1011, and Lys1047, seems to help in the stabilization of the transition state, but their precise positions in the ATP complex and their precise roles in catalysis have yet to be determined. An important aspect that is already unknown concern the fate of the proton on the 3'-hydroxyl. It has been suggested that Asp354 in adenylyl cyclase or its counterpart in DNA polymerase could act as a general base in these reactions. Substrate-assisted catalysis could also explain the destiny of this proton.

- Attack of the activated 3'-hydroxyl group to the a-phosphate and release of the pyrophosphate leaving group.

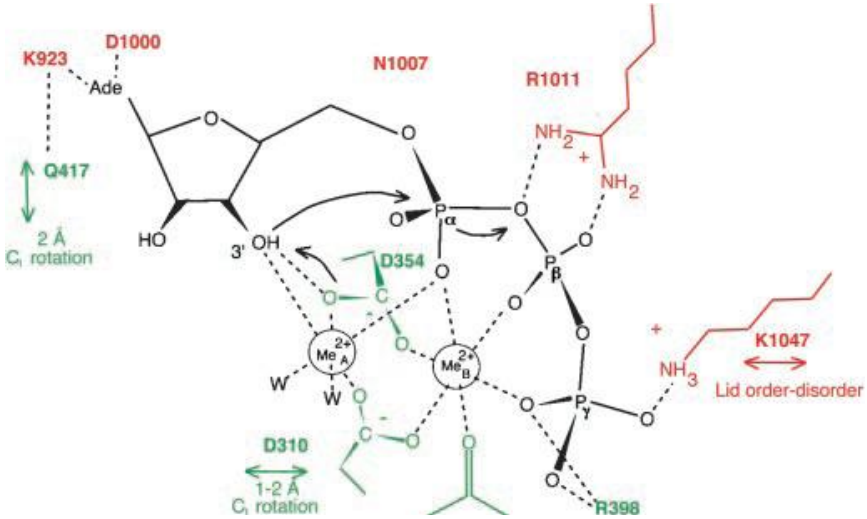

cAMP (Cyclic Adenosine 3',5'-monophosphate) is the first identified second messenger, which has a fundamental role in the cellular response to many extracellular stimuli. It was fistly discovered in 1958 by Earl. W. Sutherland[39] during his studies on the adrenalin and glucagon metabolism. Its structure is

[39] Sutherland, E.W.; Rall, T. V. Fractionalization and Characterization of a Cyclic Adenosine Ribonucleotide Formed by Tissue Particles. *J. Biological Chemistry* **(1958)**, 232; 1077-92

actually composed by an adenine nucleotide where the 3' and 5' hydroxilic functions are both bonded to the phosphate function via phosphodiesteric bond. Due to its phosphate function (with a pKa of 1.39[40]), cAMP is highly deprotonated in physiological condition. This means that it couldn't pass the cellular membrane wall through simply diffusion.

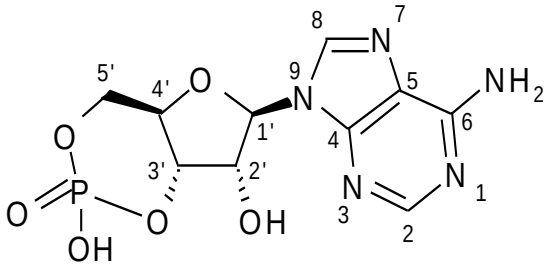

Figura 1.1b: Formula di struttura del cAMP.

The cAMP signaling pathway controls a diverse range of cellular processes through the control of different enzymes. Three main targets of cAMP are PKA, (protein kinase A), EPACs (Exchange Protein Activated by cAMP) and the CNG (Cyclic-Nucleotide Gated Ion Channel). Although cAMP directly regulates the activities of some molecules, PKA appears to be the major 'read-out' for cAMP and is the predominant cellular effector of cAMP[41]. We will describe the PKA more deeply later in the text.

Under physiological conditions, moreover, the phopshodiester bond is highly stable. So, to control and the mantain an omeostatic intracellular level of cAMP, a class of proteins, called cyclic nucleotide phosphodiesterases (PDEs), are devolved upon the hydrolysis of cyclic nucleotides[42,43] (not only cAMP).

---

[40] Kaczmarek P.; Jezowska-Bojczuk M. Coordination properties of 3',5'-cyclic adenosine monophosphate towards copper(II) ions. *Inorganica Chimica Acta* **(2005)**, *358*; 2073-2076.

[41] Malbon C.C.; Tao J.; Wang H. Y. AKAPs (A-kinase anchoring proteins) and molecules that compose their G-protein-coupled receptor signalling complexes. *Biochem. J.* **(2004)**, 379; 1-9.

[42] Mehats, C.; Andersen, C. B.; Filopanti, M.; Jin, S. L.; Conti, M. Cyclic nucleotide phosphodiesterases and their role in endocrinecell signaling. *Trends Endocrinol Metab* **(2002)**, 13; 29–35

[43] Tasken K.; Aandahl E. M. Localized effects of cAMP mediated by distinct routes of protein kinase A. *Physiol Rev,* **(2004)**, 84; 137-167

Furthermore, they also contribute to establishing local gradients of cyclic nucleotides by being localized to subcellular compartments and by being recruited into multiprotein signaling complexes. This contributes to the temporal and spatial specificity of cyclic nucleotide signaling by regulating the availability of cAMP to their effectors.

PDEs comprise a large superfamily of enzymes, and 11 families have been characterized on the basis of their amino acid sequences, substrate specificities, allosteric regulatory characteristics, and pharmacological properties (222, 305). In total, the superfamily of PDEs encompasses 25 genes in mammals giving rise to an estimate of more than 50 different PDE proteins (342). They share a modular architecture, with a conserved catalytic domain proximal to the COOH terminus, regulatory domains most often located at the NH_2 terminus and targeting domains which we are only beginning to discover (67, 110, 147). The substrate specificity of the PDEs families include cAMP-specific, cGMP-specific, and dual-specific PDEs.

2'.2 Protein Kinase-A (PKA)[44]

PKA (Protein Kinase-A) is a second messenger-dependent enzyme that has been implicated in a wide range of cellular processes, including transcription, metabolism, cell cycle progression and apoptosis. Known modulators of PKA activity include factors that either activate or inhibit AC enzyme (resulting in an increase or decrease in cAMP levels).

The enzyme occurs naturally as a four-membered structure with two regulatory (R) and two catalytic (C) subunits. Four genes encode the R subunits (RI-Alpha, RI-Beta, RII-Alpha and RII-Beta), and three encode the C subunits (C-Alpha, C-Beta and C-Gamma). Although there are major differences in the tissue distribution, biochemical and physical properties of

[44] Kim C.; Vigil D.; Anand G.; Taylor S. S. Structure and dynamics of PKA signaling protein. *European Journal of Cell Biology* (2006), 85; 651-4

the R subunit isoforms, differences between the various isoforms of the C subunit are more subtle.

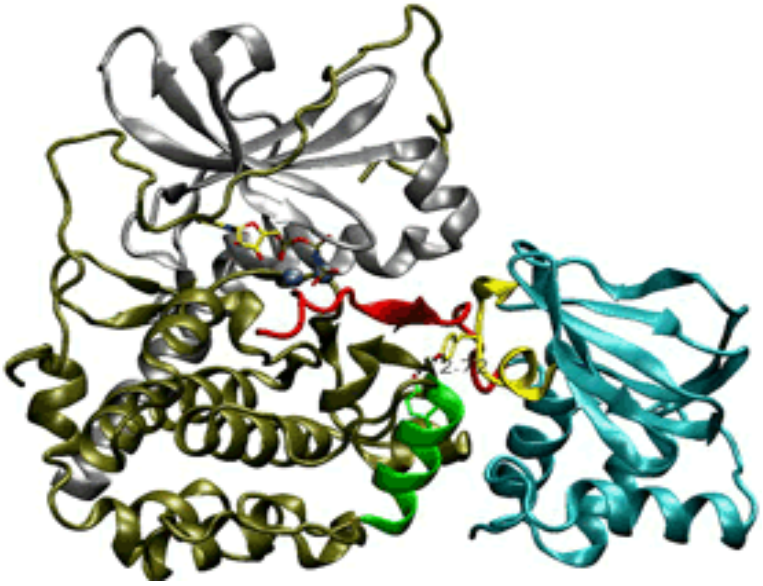

PKA is classified as a Type I or Type II enzyme depending upon the associated R subunit (i.e., RI or RII). Type I PKA is predominantly located in the cytoplasm, while Type II associates with cellular structures and organelles. Type II PKA is not a "free floating" enzyme but is anchored to specific locations within the cell by specific proteins called AKAPs (A Kinase-Anchoring Proteins). The AKAPs keep PKA localized and limit the targets that can be phosphorylated, preventing the indiscriminate phosphorylation expected from free PKA in the cytoplasm. Most AKAPs described are able to bind the RII subunits with nanomolar affinities while binding RI subunits in the micromolar range. RII-binding AKAPs range in size from 15–300kDa and are capable of binding other kinases as well as phosphatases. Anchored PKA modulates the activity of various cellular proteins, including AMPA/Kainate channels, Glutamate receptor-gated ion channels, L-type Ca2+ channels in skeletal muscle, hormone-mediated Insulin secretion in clonal beta cells, Vasopressin-

mediated translocation of Aquaporin-2 into the cell membrane of renal principal cells, motility of mammalian sperm and the sperm Acrosome reaction (Ref.1 & 2).

Regulation of PKA in the cell is related primarily to modulation of its phosphotransferase activity. The holoenzyme contains two C subunits bound to homo- or heterodimers of either RI or RII subunits. The C subunits do not interact with one another. The R subunits each have an N-terminal dimerization domain and two cAMP binding sites. Activation proceeds by the cooperative binding of two molecules of cAMP to each R subunit, which causes the dissociation and subsequent activation of each C subunit from the R subunit dimer. cAMP accumulation in cells that cause different physiological outcomes and changes in cAMP levels effects the selective activation of PKA isoforms

cAMP, once formed, serves to modulate inotropy, chronotropy and lusitropy by inducing PKA phosphorylation of contractile proteins, ion channels, enzymes of intermediary metabolism and other regulatory proteins.

PKA, once activated can phosphorylate several other substrates. The ADR-Alpha/Beta stimulation of cAMP-PKA phosphorylates several proteins related to excitation-contraction coupling like activation of RyR (Ryanodine Receptor), Pln (Phospholamban), CRP (C-Reactive Protein) but inhibits TnnI (Troponin-I). PKA phosphorylates Pln that regulates the activity of SERCA2 (Sarcoplasmic Reticulum Ca2+-ATPase-2). It leads to increased reuptake of Ca^{2+}, Cl^{-} (Chloride Ions), K^{+} (Potassium Ions), Na^{+} (Sodium Ions) and this process is affected in failing hearts.

In mammalian cells, including human, PKA regulate a huge number of processes, including growth, development, memory, metabolism, and gene expression.

Failure to keep PKA under control can have disastrous consequences, including diseases such as cancer. For this fundamental reason, great efforts are still devoted to the study of the different aspects of the cAMP-PKA system,

such as the concentration pattern of the different isoforms of PKA. An interesting study concerned this last aspect was conducted in the physiology laboratory of the Prof. Mucignat[45,46]. The work showed an abnormal distribution of the insoluble RIIa subunity in some glioma affected cerebral tissues respect to the normal ones.

Glioma[47] is a class of tumor that hits the brain and the spinal cord; it always starts from glia cells (which give the name to this cancer). It is generally uncurable and the prognosis depends on the gravity of the different gliomas.

They are usually subdivided into four classes, depending on their malignancy; the glioblastoma multiforme (GBM) is the most malignant one. The theraphy usually consists of a chirurgical removal of the solid tumor supported with a chemiotherapeutical (Temozolomide) strategy. Nevetheless, "even if you remove it surgically, the outcome is the same. The transformation of normal brain cells into tumor cells continues even after surgery"[48].

Thus, knowing the dangerousness of this pathology, different strategies could be chosen as to increase the number and the quality of the informations about gliomas. In this issue, RIIa subunity could be considered as a possible diagnostic marker for cerebral cancers or a possible target for a therapeutic strategy. In fact, the first goal is the heart of this part of my work.

[45] Mucignat-Caretta C., Caretta A. Regional variations in the localization of insoluble kinase A regulatory isoforms during rodent brain development. *Journal of Chemical Neuroanatomy*, **(2004)**, 27; 201-212.

[46] Mucignat-Caretta C.; Cavaggioni A.; Redaelli M.; Malatesta M.; Zancanaro C.; Caretta A. Selective distibution of Protein Kinase A Regulatory Subunit RIIAlpha in Rodent Gliomas *Neuro-Oncology* **(2008)**, *10*(6); 958-967.

[47] Maher, E. A.; Furnari, F. B.; Bachoo, R. M.; Rowitch, D. H.; Louis, D. N.; Cavanee, W. K.; Depinho R. A. Malgnant glioma: genetics and biology of a grave matter *Genes & Development* **(2001)**, 15; 1311-1333.

[48] Taken from an interview of Flamm, E. S. about the Senator Kennedy glioblastoma

3’ Aim of the work

Since gliomas are one of the most dangerous cancer over all the other, a very important point would be reached if it could be easily found inside the system investigated. One way to search them is *via* specific marker.

A marker is a substance with an higher affinity for the desired target; it must carry also a probe that could be easily detected even in the presence of several interference

The goal of this part of work was the realization of a marker specific for the protein kinase A (PKA) bearing a fluorescent probe in order to immediately recognize the enzyme inside the systems investigated.

To reach this goal we decided to use cyclic AMP (cAMP), since it binds preferably the PKA regulatory subunits and rhodamine as fluorescent probe, since it has a very strong fluorescence absorption/emission pattern in the visible spectrum.

The synthesis route took inspiration from previous work conducted by the researcher of the University of Parma[49] were a fluorescein probe was linked at the 8 position of the cAMP.

Furthermore, this compound was tested in gliomas affected cells as to study the effective utility of this marker.

[49] Caretta, A; Cavaggioni, A. New biologically active fluorescent cyclic nucleotides. *EP0205005* **(1985)**

4'. Experimental part

SYNTHESIS SCHEME

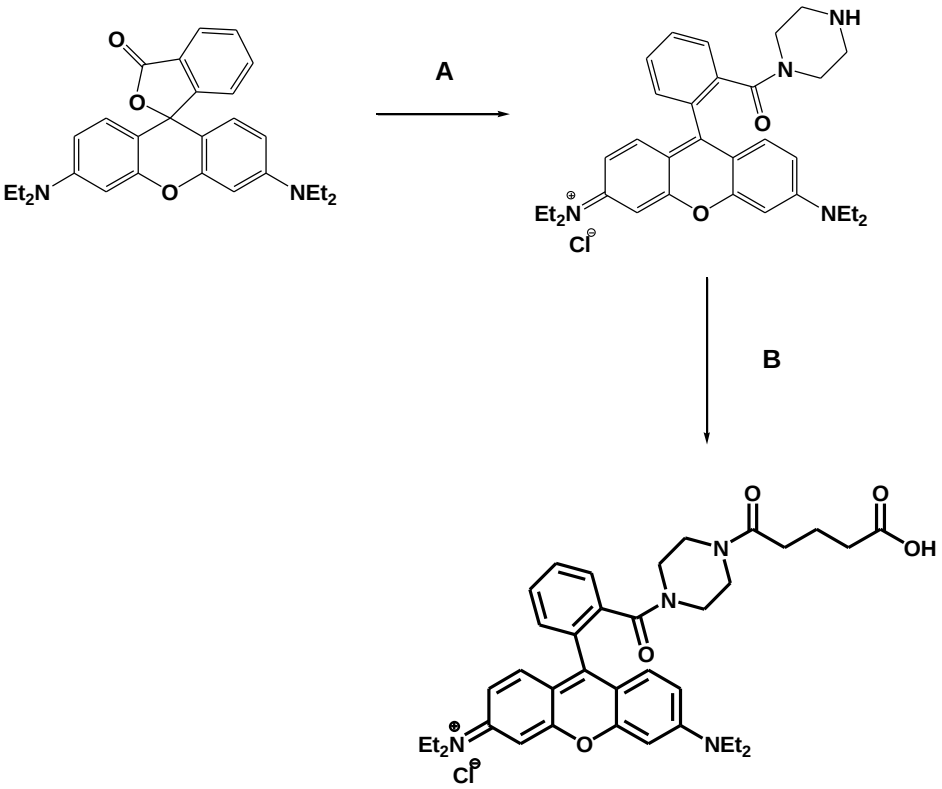

A) Piperazine, trimethylaluminium, CH_2Cl_2, 72 h, reflux (Yield 20%); **B)** Glutaric anhydride, pyridine, DMAP, 16 h, RT (Yield 60%)

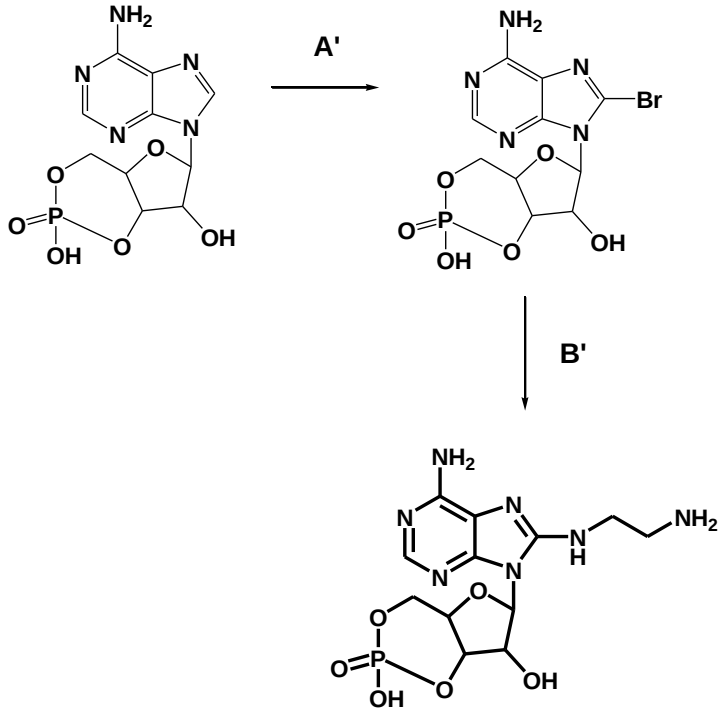

A') Br_2, sodium acetate, H_2O, 16 h, RT (Yield 64%); **B')** Ethylendiamine, 2h, 50 °C (Yield 54%)

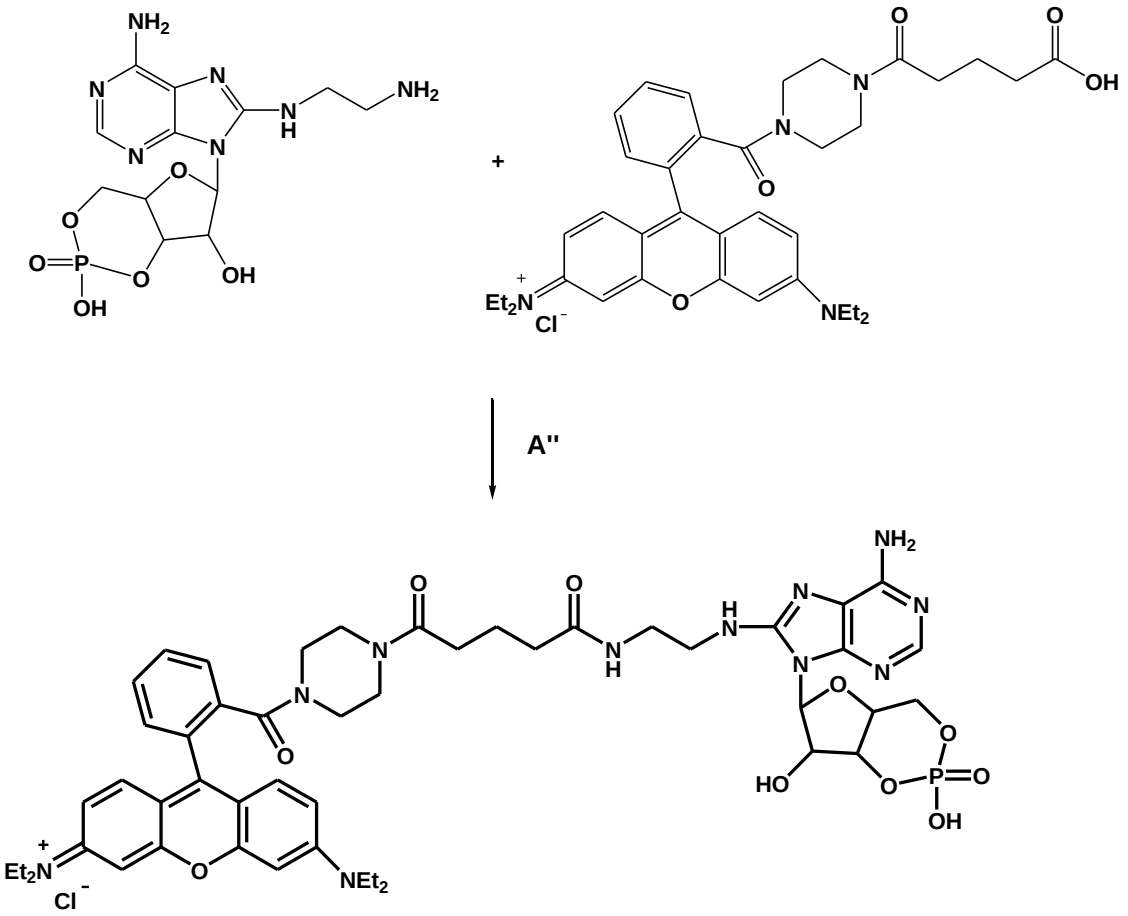

A'') Rhoda-glut, cAMP-eda, TBTU, HOBt, DIPEA, DMA, 16 h, RT (Yield 75%)

Synthesis of **Rhodamine-B-piperazine amide (Rhoda-pip)**

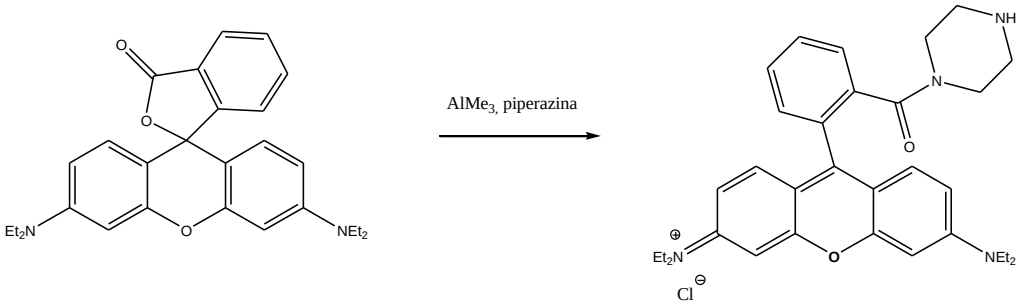

Components	Molecular formula	Molecular Weight	Volume	Weight	Density	n° of Mols
Rhodamine	$C_{39}H_{47}N_4O_7$	442.6 g/mol		6.00 g		13.56 mmol
Piperazine	$C_{15}H_{32}N_3OP$	86.14 g/mol		4.67 g		54 mmol
Trimethylaluminium	CH_2N_4	72.09 g/mol		1.96 g		27.2 mmol

In a round bottomed flask 4.67 g of piperazine were solved into 50 ml of CH_2Cl_2; 13.6 ml of a 2M trimethylaluminium solution in toluene were dropped into it. The mixture was allowed to stir at RT for 1h before the dropwise addition of a solution of 6 g of Rhodamine in CH_2Cl_2. The whole solution was refluxed for 72 h after which the precipitate obtained was filtered and washed with 100 ml of CH_2Cl_2 and with 100 ml of a CH_2Cl_2/MeOH (4/1) mixture. The organic phase was then concentrated and diluted again in EtOAc (500 ml) and washed with a saturated NH_4HCO_3 aqueous solution. The organic phase was collected while the aqueous phase was acidified with a 3 M HCl solution and extracted once again with EtOAc. The organic phase was reunite with the previous, anhydrified with Na_2SO_4 and essiccated to obtain a purple oil which was solved again into a small quantity of CH_2Cl_2. The solution was dropped

into cold Et_2O and the suspension centrifuged to obtain 1.48 g of Rhodamine-B-piperazine amide as a purple-gold solid. Yield 20%

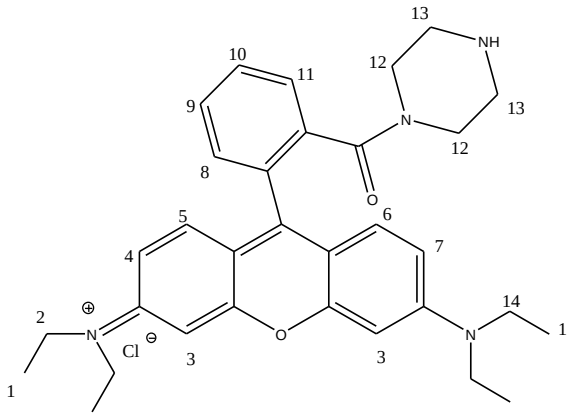

Molecular Weight	**Molecular Formula**
547.13 g/mol	$C_{32}H_{39}ClN_4O_2^+$

^{1}H-NMR ($CDCl_3$; 300 MHz) δ(ppm): 7.69 (2H, m; $H^{9,10}$), 7.58 (1H, d, J=7,1; H^{11}) 7.32 (1H, d, J=7,1; H^8), 7.18 (2H, d, J=9,2; $H^{5,6}$), 6.92 (2H, d, J=9,3; $H^{4,7}$), 6.73 (2H, s; H^3), 3.91 (4H, m; H^{13}), 3.59 (4H, m; H^{14}), 3.71 (4H, m; H^2), 3.11 (4H, m; H^{12}), 1.34 (12H, t, J=6,9; H^1)

HRMS (ESI): calcd for $C_{32}H_{39}ClN_4O_2$ ($M+H^+$) 511,3068, found 511,3015

Synthesis of **rhodamine-B-[4-(glutaryl)amide] piperazine amide (Rhoda-glut)**

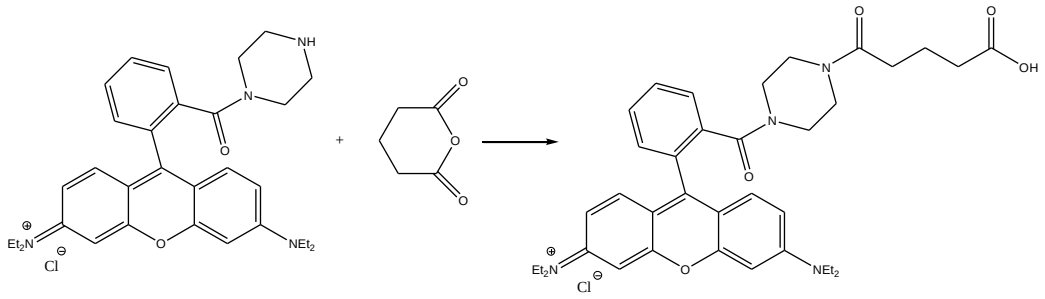

Components	Molecular formula	Molecular Weight	Volume	Weight	Density	n° of Mols
Rhoda-pip	$C_{32}H_{39}ClN_4O_2$	511.31 g/mol		500 mg		0.91 mmol
Glutaric anhydride	$C_{15}H_{32}N_3OP$	114.10 g/mol		312.63 mg		2.74 mmol
Pyridine	C_5H_5N	79.10 g/mol		361.49 mg		4.75 mmol
Dimethoxypyridine (DMAP)	$C_7H_{10}N_2$	122.17 g/mol		21.99 mg		0.18 mmol

An oven-dried round-bottomed flask was charged with 500 mg of Rhoda-pip, 312.63 mg, 361.49 mg of pyridine, 22 mg of DMAP and 50 ml of anhydrous CH_2Cl_2. The mixture was left under N_2 atmosphere at RT for 16 h; CH_2Cl_2 was later added until complete dissolution of the suspension. The organic solvent was washed firstly with a 0.5 M $NaHCO_3$ aqueous solution and then with a 0.5 M HCl solution. The organic layer was anhydrified with Na_2SO_4 and dried to obtain 360 mg of Rhoda-glut as a golden-purple solid. Yield 60%

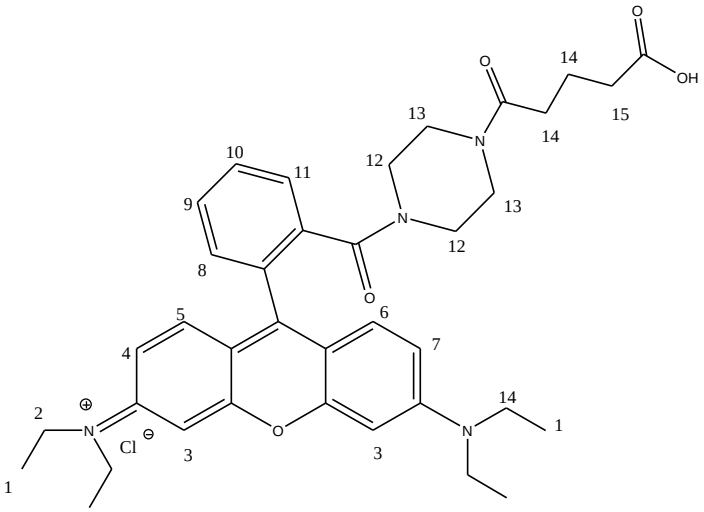

Molecular Weight	**Molecular Formula**
661.23 g/mol	$C_{37}H_{45}ClN_4O_5^+$

^{1}H-NMR ($CDCl_3$; 300 MHz) δ(ppm): 7.50-7.79 (m, 4H; $H^{8,9,10,11}$), 7.29 (2H, d, J=9,4 Hz, $H^{5,6}$), 7,07 (2H, dd, J_3=9,4 Hz, J_4=2,3 Hz, $H^{4,7}$), 6,96 (d, 2H, J_4=2,3 Hz; H^3), 3.67 (m, 8H; H^2), 2,86 (m, 8H; $H^{12,13}$), 2,31 (m, 2H; H^{13}), 2,23 (m, 2H; H^{11}),1.80 (m, 2H; H^{12}), 1.29 (12H, t, J=6,9; H^1)

HRMS (ESI): calcd for $C_{37}H_{45}ClN_4O_5^+$ ($M+H^+$) 625,3384, found 625,3143

Synthesis of 8-Br-adenosine cyclic monophosphate (8-Br-cAMP)

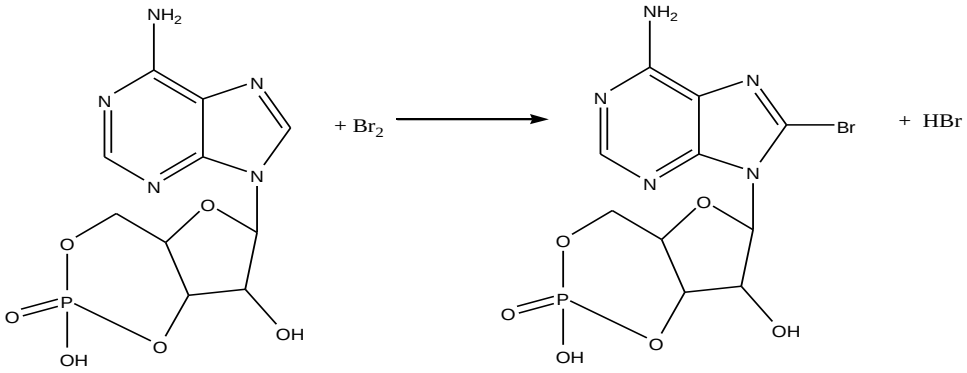

Components	Molecular formula	Molecular Weight	Volume	Weight	Density	n° of Mols
Cyclic adenosine monophosphate (cAMP)		329.23 g/mol		3 g		9.11 mmol
Sodium Acetate	$C_2H_3NaO_2$	82.04 g/mol		1.49 g		18.22 mmol
Bromine	Br_2	159.81 g/mol	470 µl	1.46 g		9.11 mmol

To a solution composed by 1.49 g of sodium acetate and 25 ml of H_2O, 3 g of cAMP were added. The solution was cooled with an ice bath and 470 µl of bromine were slowly dropped into the solution, taking care to not exceed the initial temperature. The red brown solution was left stirring at RT overnight after which a white pearl precipitate formed. A Na_2SO_3 aqueous solution was slowly added in order to remove the unreacted bromine before filter the precipitate, wash it with isopropanol and ether and dry under vacuum to obtain 2.38 g of 8-bromo-cAMP as a white solid. Yield.64%

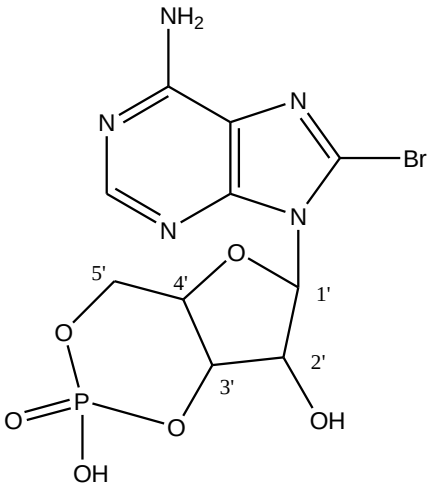

Molecular Weight	Molecular Formula
408.10 g/mol	$C_{10}H_{11}BrN_5O_6P$

^{1}H-NMR (D_2O; 300 MHz) δ(ppm): 8.22 (s, 1H; H^2), 6.16 (s, 1H; $H^{1'}$), 5.32 (m, 1H; $H^{4'}$), 5.04 (d,1H, J=5.6; $H_{3'}$), 4.48 (m, 1H; $H^{5'}$), 4.31 (m, 2H; $H^{2'}$)

HRMS (ESI): calcd for $C_{10}H_{12}BrN_5O_6P$ ($M+H^+$) 407.9703, 409.9684 found 407,9765, 409.9932

Synthesis of 8-(1',3'-diamminopropyl)-adenosine cyclic monophosphate (eda-cAMP)

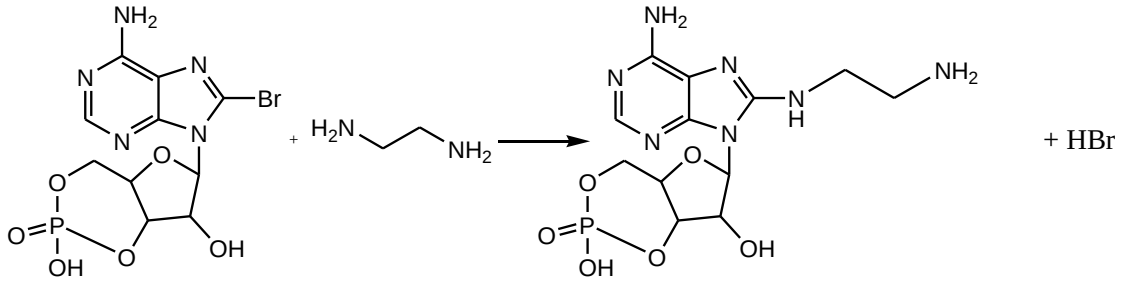

Components	Molecular formula	Molecular Weight	Volume	Weight	Density	n° of Mols
8-Br-cAMP		408.97 g/mol		500 mg		1.23 mmol
1,3-diamminopropane	$C_3H_{10}N_2$	60.10 g/mol	7.5 ml		0.899 g/ml	

500 mg of 8-Br-cAMP were solubilized in 7.5 ml of 1,3-diamminopropane and the solution was left at 50 °C under stirring. The initial blue color of the solution turn to slightly yellow after 2 h then the solution was cooled and dropped into cold Et_2O. The white precipitate formed was centrifuged (2400 rpm for 10 min) and further suspended into methanol. The suspension was added of a 0.1 M HCl aqueous solution until the complete dissolution of the solid; the solution thus obtained was dropped into cold Et_2O. The precipitate was finally crystallized into methanol to obtain 287 mg of eda-cAMP as a white solid. Yield 54%.

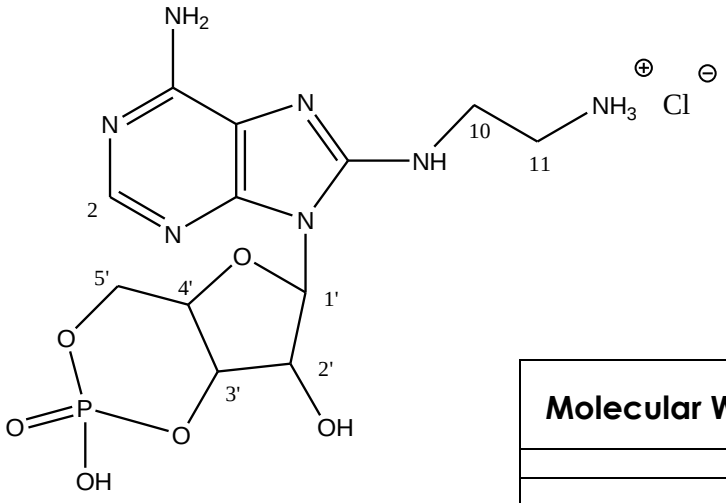

Molecular Weight	Molecular Formula
432.75 g/mol	$C_{12}H_{19}ClN_7O_6P$

^{1}H-NMR (D_2O; 300 MHz) δ(ppm): 8.26 (s, 1H; H^2), 5.92 (s, 1H; $H^{1'}$), 5.15 (m, 1H; $H^{4'}$), 5.10 (d,1H, J=5.6; $H_{3'}$), 4.47 (m, 1H; $H^{5'}$), 4.24 (m, 2H; $H^{2'}$), 3,76 (m, 2H; H^{10}), 3,38 (m, 2H; H_{11})

HRMS (ESI): calcd for $C_{12}H_{20}ClN_7O_6P$ ($M+H^+$) 388.1129, found 388.1154

Synthesis of rhodamine-B-[4-glutaryl-(8'-(1'',3''-diamminopropyl)-cAMP)-diammide] piperazine amide (cARo).

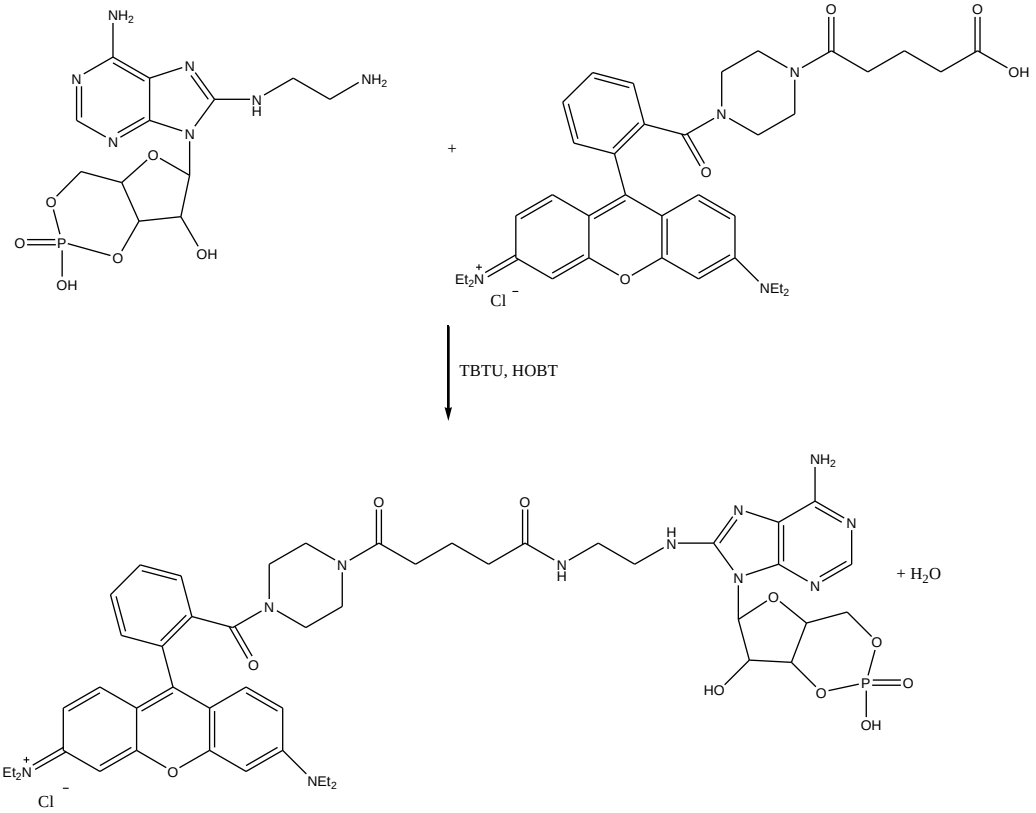

Components	Molecular formula	Molecular Weight	Volume	Weight	Density	n° of Mols
Rhoda-glut	$C_{37}H_{45}ClN_4O_5$	661.23 g/mol		156 mg		0.24 mmol
Eda-cAMP	$C_{12}H_{19}ClN_7O_6P$	423.75 g/mol		101.7 mg		0.24 mmol
Hydroxybenzotriazole tetrafluoroborate (TBTU)	$C11H_{16}BF_4N5O$	321.09 g/mol		83.48 mg		0.26 mmol
Hydroxybenzotriazole (HOBt)	$C_6H_5N_3O$	153.10 g/mol		39.81 mg		0.26 mmol
Diisopropyletylamine	$C_8H_{19}N$	129.25 g/mol	210 µl	21.99 mg	0.755 g/ml	0.18 mmol

156 mg of Rhoda-glut were solved into 5 ml of anhydrous DMA; 83.48 of TBTU, 39.81 mg of HOBt and 210 µl of DIEA were subsequently added to the solution. After 10 min 101.7 mg of eda-cAMP were added to the activated ester and the whole was left under N_2 atmosphere at RT overnight. The solution was then dropped into cold Et_2O and centrifuged (2400 rpm for 10 min) to collect the solid that was resolubilized into MeOH and dropped again into cold Et_2O. 185 mg of cARo were obtained as a golden-purple solid with a sufficient purity for the next esterification step. Yield 75%.

The samples (96% grade of purity) used for the biological test were obtained purifying it by silica column chromatography (eluent gradient CH_2Cl_2:MeOH from 90:10 to 60:40) recovering the last stain.

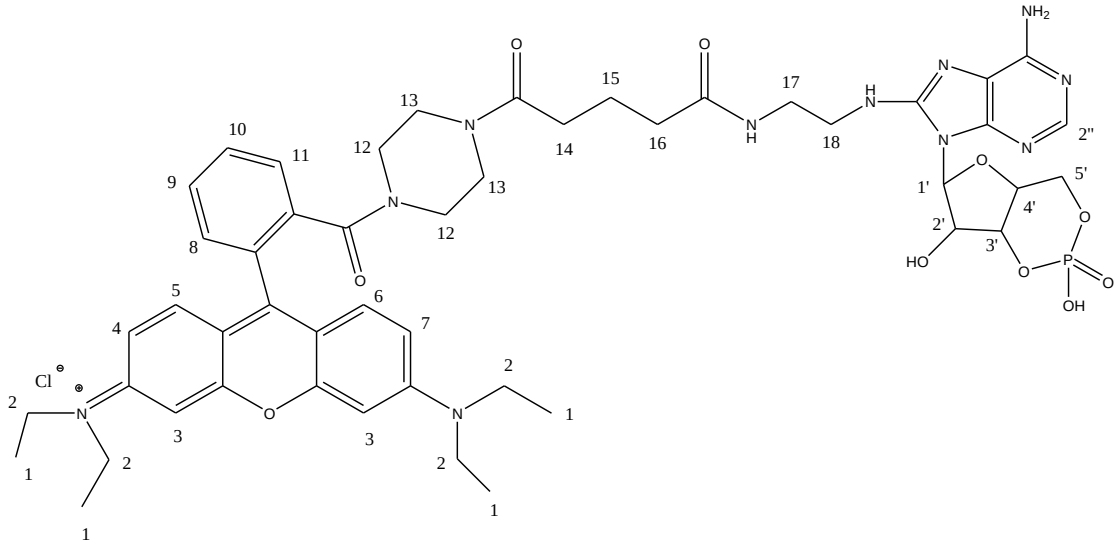

Molecular Weight	Molecular Formula
1030.5 g/mol	$C_{49}H_{61}ClN_{11}O_{10}P^+$

^{1}H-NMR ($CDCl_3$; 300 MHz) δ(ppm): 8.55 (s, 1H; $H^{2''}$), 7.58-7.87 (m, 4H; $H^{8,9,10,11}$), 7.35 (2H, d, J=9 Hz, $H^{5,6}$), 7.18 (2H, dd, J_3=9 Hz, J_4=2,5 Hz, $H^{4,7}$), 7.03 (d, 2H, J_4=2,5 Hz; H^3), 5.76 (s, 1H; $H^{1'}$), 5.23 (m, 1H; $H^{4'}$), 5.10 (m,1H; $H_{3'}$), 4.25 (m, 3H; $H^{5',2'}$), 3.87 (m, 8H; H^2), 3,48-3.55 (m, 4H; $H^{17,18}$) 2,77 (m, 8H; $H^{12,13}$), 2,31-2,23 (m, 4H; $H^{14,16}$), 1.86 (m, 2H; H^{15}), 1.19 (12H, t, J=6,9; H^1)

HRMS (ESI): calcd for $C_{49}H_{61}ClN_{11}O_{10}P^+$ ($M+2H^+$) 497.2165, found 497.7149

5’ Discussion of the results

As already described in the aim of the work of this session, the rhodamine-B-[4-glutaryl-(8'-(1'',3''-diamminopropyl)-cAMP)-diammide] piperazine amide (cARo) compound was realized starting from the fluorescein-cAMP derivarive synthetized in the University of Parma.

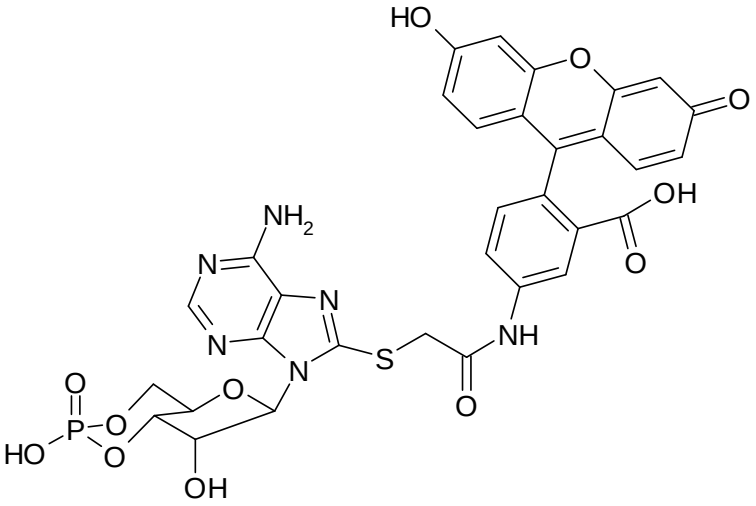

This compound showed how substitition at the 8 position didn't affect the activity of the PKA. Nevertheless, it was realized starting from fluorescein isothiocyanate, a very expensive intermediate and from 8-thio-cAMP that is hard to synthesize.

The molecule, otherwise, consists of three major component: the cAMP moiety (1), the rhodamine probe (2) and a diammidic linker.

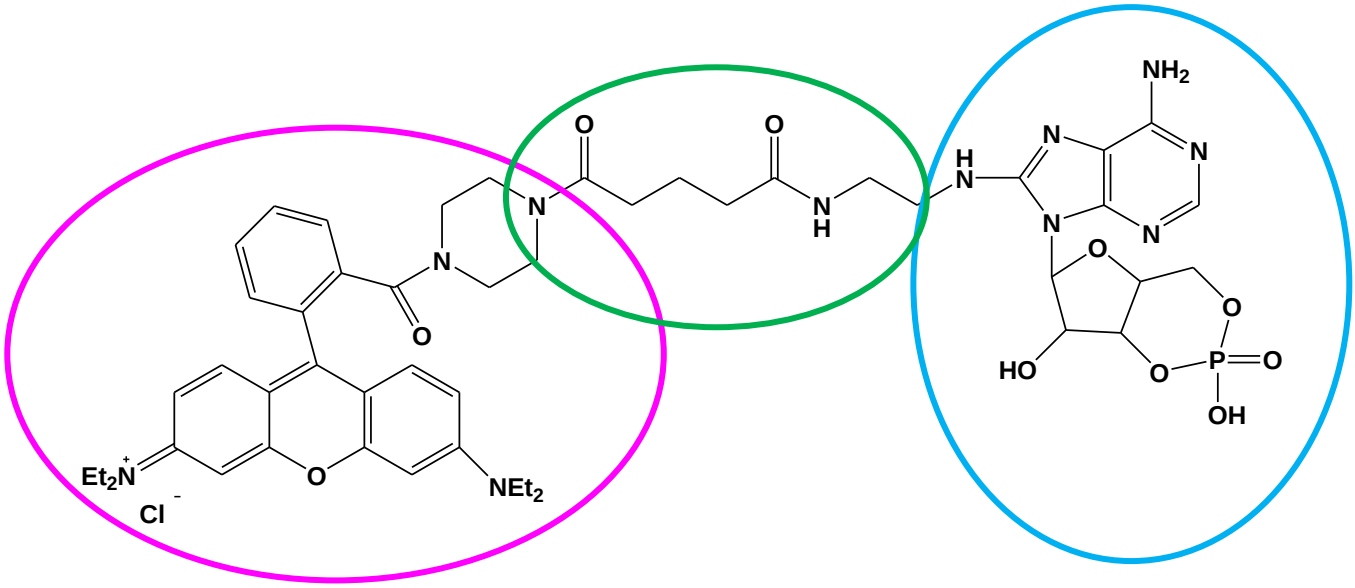

The strategy adopted for the realization of this compound was a covergent reaction between two synthons.

The first one was obtained starting from Rhodamine B base, a commercial fluorescent molecule. The reaction of this compound with piperazine was afforded using trimethylaluminium as catalyst, in order to insert a reactive amine inside the fluorescent skeleton. The mechanism of action could be the follow one:

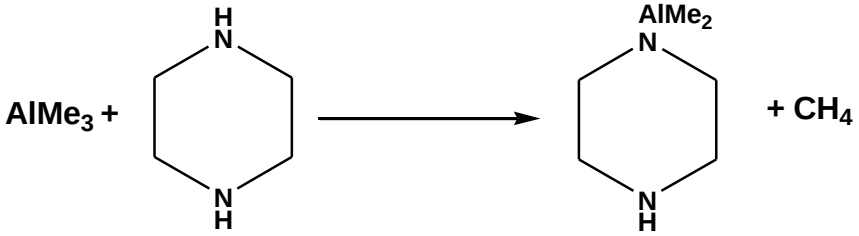

Figura 4.3a: Meccanismo di reazione proposto per l'attacco di piperazina a rodamina B.

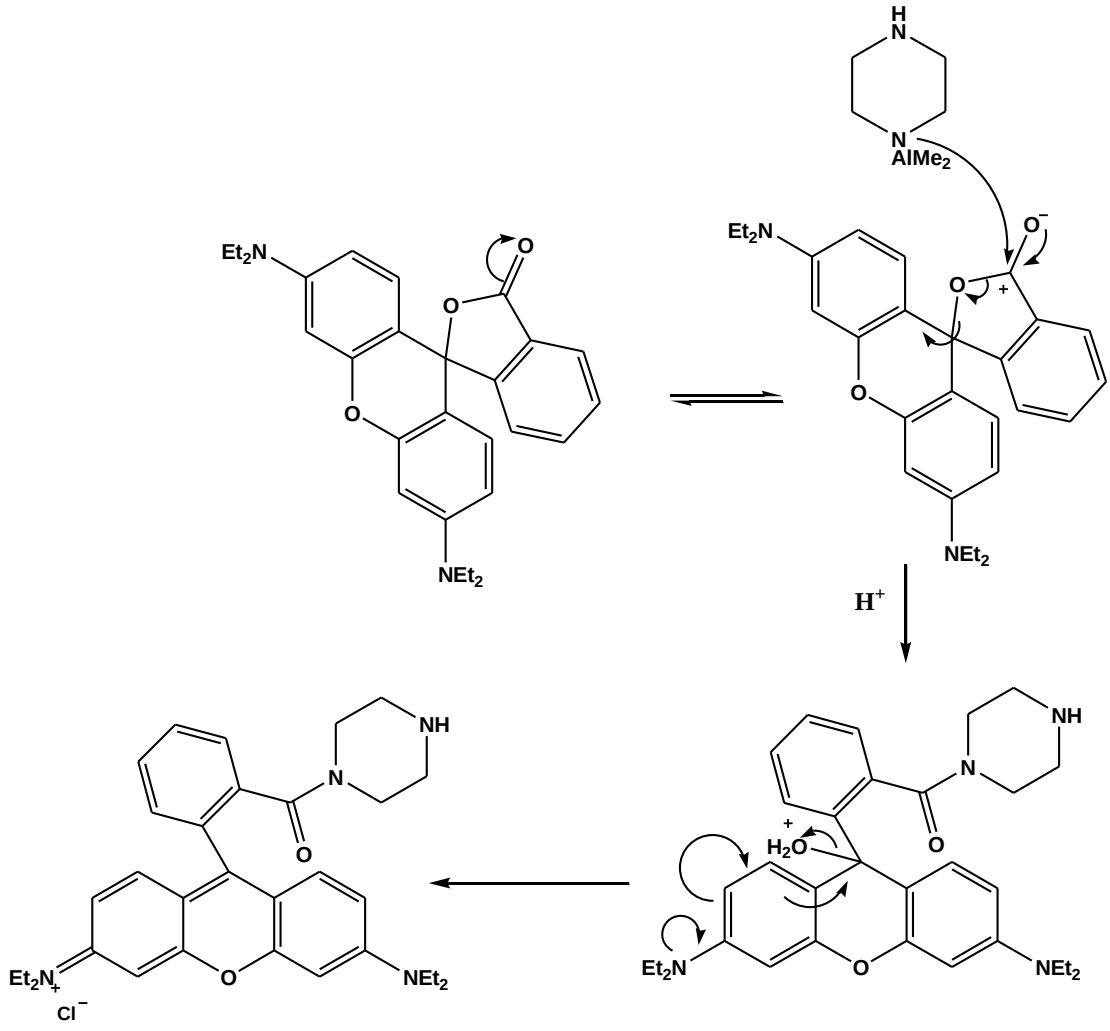

An initial attack of the trimethylaluminium to only one amino group of the piperazine give the activate intermediate able to attack the 5 member lacton as to form the desired ammido group. A subsequently acid hydrolysis of the hydroxyl function lead to the final Rhoda-pip product.
Standard FMOC peptide synthesis (via TBTU/HOBt) of this product with glutaric anhydride allow the formation of the first synthon.
The second synthon synthesis start from commercially available cyclic AMP which was initially bromurated in the 8 position using a slightly modified procedure of the Muneyama approach[50].
The 8-Br-cAMP was then substituted with 1,3-ethylendiamine (EDA) via nucleophilic aromatic substitution (S_{nAr}). The reaction was not straightforward due to the poor electrophilicity of the 8-Br-cAMP; the product was obtained in reasonable yield only when the EDA was used as solvent. The product was converted to its chlorohydrate salt to facilitate the puridication procedure and to prevent the oxidation of the primary amine.
Last step was the convergence of the two synthesized synthon. This was accomplished *via* standard FMOC peptide synthesis, using TBTU instead of HBTU (the mechanism of action is described in the discussion part of the first project).

This marker is currently under test in the laboratory of prof. Mucignat in the Department of Physiology of the University of Padua. First images obtained from rat glioma cells (F98 cell lines) and human glioblastoma cells (GLI36 cell lines) shows how this molecule is able to pass the cellular membrane and to locate into specific parts of the cytoplasm.

[50] Muneyama K.; Bauer R. J.; Shuman D. A.; Robins R. K.; Simon L. N. Adenosine 3',5'-cyclic monophosphate derivatives II. Biological activity of some 8-substituted analogs. *Biochemistry* **(1971)**, 10(12); 2390-2395.

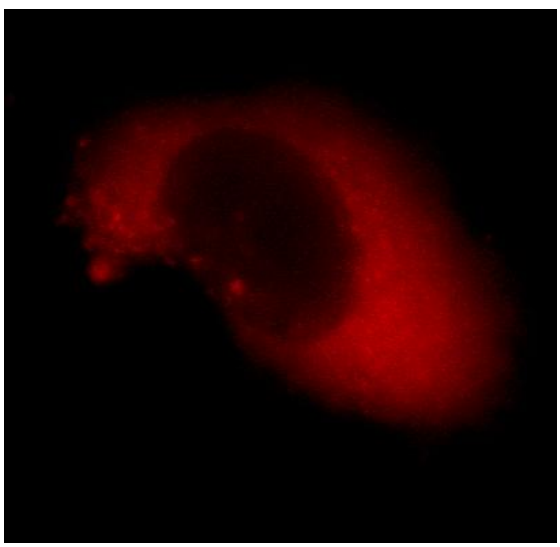

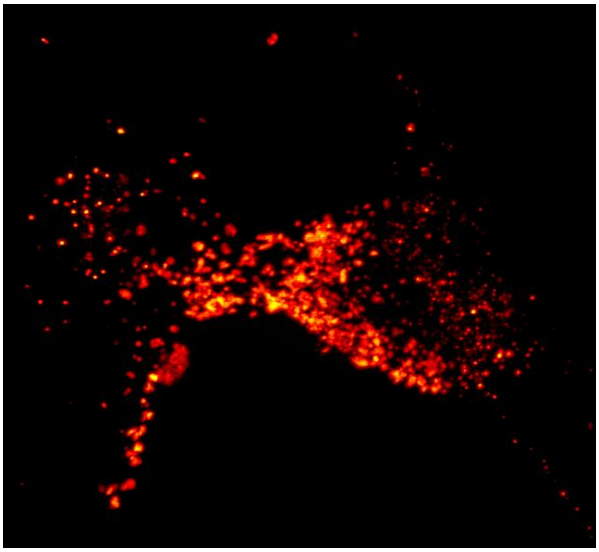

A **B**

A) GLI36 cell lines treated with a solution 500 uM of Rhodamine B
B) GLI36 cell lines treated with a solution 500 uM of cARo. The distribution of the compound inside the cell is mainly localized into specific points
C) F98 cell lines treated with a solution 500 uM of cARo.

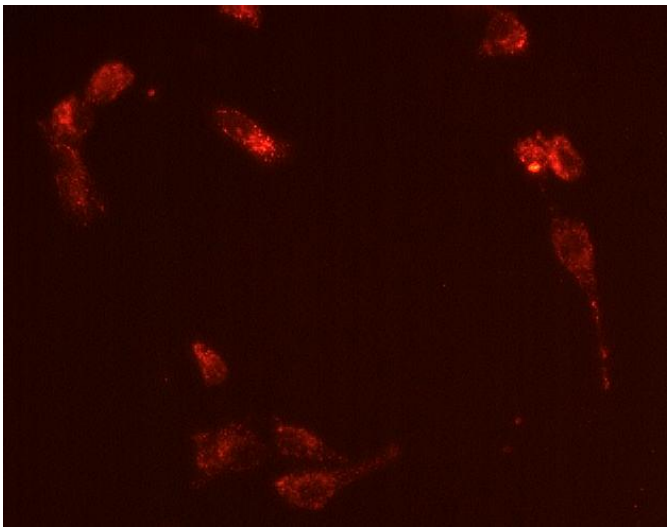

C

To act as a good diagnostic marker, it shouldn't interfere with other markers. A double staining test with cARo and a nuclear staining marker, the diaminophenylimidazole (DAPI) showed no apparent interference between

the two marker, giving another proof for the possible future utilization of the cARo molecule.

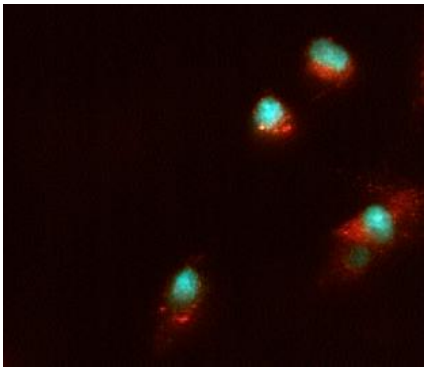

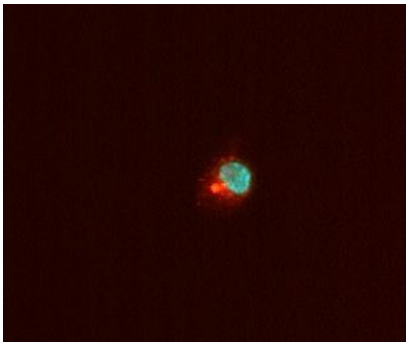

Immunoistochemical tests are currently being developed to characterize these high concentrated spots in order to understand if they could be associated with the presence of protein kinase A.